AN ANALYSIS OF THE PERFORMANCE OF A CYCLIC COUNTERCURRENT ION EXCHANGE CONTACTOR FOR PARTICLE DIFFUSION CONTROLLED REACTIONS

A thesis submitted for the degree of
DOCTOR OF PHILOSOPHY
in the Faculty of Engineering of the
University of London

by

M. M. SAIED, B.Sc. (Hons.), M.Sc., D.I.C.

Department of Chemical Engineering
and Chemical Technology,
Imperial College of Science and Technology,
London, S.W.7.

April 1971.

ABSTRACT

The principle objective of this work was to analyse the performance of a stagewise ion exchange contactor for a resin phase controlled reaction. This requires a complete knowledge of equilibrium and kinetic data for the system under investigation.

Ion exchange equilibrium data for the system sodium chloride-calcium chloride - Zeo-Karb 225 (a strong acid resin) has been obtained covering a total solution concentration range of 0.025 - 2.0 N. Of the several methods considered for the correlation of equilibrium data, the simplified Donnan equilibrium approach based on the molalities of the counterions in both phases has been found to be most satisfactory. The mean value of the Donnan equilibrium constant ($K_D = 1.3 \pm 0.19$) obtained in this study can be used to predict the equilibrium behaviour of the system under all experimental conditions.

Measurement of the resin phase diffusion coefficient for the exchange of sodium and calcium between aqueous chloride solutions and Zeo-Karb 225 at 25°C have been carried out. The results have been interpreted using Fick's Law and the Nernst-Planck model. The latter gives an interdiffusion coefficient, which is a function of resin composition, based on the trace ionic diffusion coefficients. Values of the self-diffusion coefficients, determined separately, suggest that it is also valid to predict the interdiffusion coefficient based on the self-diffusion coefficients of the individual exchanging ions.

Although, both Fick's Law (constant interdiffusion coefficient) and the Nernst-Planck model have been found

to correlate the experimental data equally well, the use of Fick's Law in the analysis of performance of a stagewise process is inadequate.

A new and simple analytical technique for the continuous measurement of the rate of approach to equilibrium, which employs Atomic Absorption Spectroscopy, has been shown to be accurate and free from interference.

A cyclic countercurrent contactor using ten stages has been employed to regenerate calcium form resin with a solution of sodium chloride (1 N) under various operating conditions. Results of the experimental runs have been analysed by considering that the exchange reaction is completely controlled by diffusion within the resin phase. A simplified theoretical model, based on the concept of a cascade of batch reactors, which take into account a variable interdiffusion coefficient and equilibrium at the bead surface in each stage has been developed to analyse the performance of the contactor.

The simplified theoretical model gives a good estimate of the number of stages required when there is partial transfer of resin and solution phases between the stages. Improved performance of the contactor with complete transfer of both phases has been confirmed experimentally and suggests the desirability of cyclic operation in countercurrent ion exchange processes.

Finally, the feasibility of a continuous ion exchange process has been assessed from a knowledge of its operating diagram.

A C K N O W L E D G E M E N T S

The author wishes to express his gratitude to Dr. M. Streat for his invaluable advice and constant encouragement throughout the course of his work. It has been a pleasure and privilege to work with him.

Thanks are also due to the technical staff in ordering items and for their help in the assembly of equipment.

Financial support from the British Council, made available in the form of a Colombo Plan Scholarship and sponsered by the Atomic Energy Commission, Pakistan, is gratefully acknowledged.

CONTENTS

C H A P T E R 1 .

ION EXCHANGE EQUILIBRIUM.

1.1. INTRODUCTION

Ion exchange resins are considered as a framework carrying a negative or a positive electric charge which is balanced by oppositely charged counterions. These counterions are mobile and exchangeable for other ions of the same sign. The exchange is stoichiometric and in general reversible.

The synthetic ion exchange resins, often a copolymer of styrene and divinylbenzene, seem to be potentially attractive as a means of separation, purification and concentration of electrolyte solutions. In order to use the resins most effectively it is necessary to understand their equilibrium behaviour when in contact with mixed electrolyte solution. Although extensive equilibrium data for the exchange of monovalent ions is available in the literature (Boyd, Schubert and Adamson 1947, Bauman and Eichhorn 1947, Bonner and Smith 1957), fewer systems involving multivalent ion exchange have been studied. Gregor, Abolafia and Gottlieb (1954) and Bonner and Smith (1957) have carried out equilibrium studies for some multivalent ion exchange systems practically all of which cover a limited range of solution concentration. One of the objectives of the present study was an accurate measurement of equilibrium properties of Zeo-Karb 225, 8% DVB (a strong acid cation exchanger manufactured by The Permutit Company Limited, London) in contact with sodium chloride - calcium chloride at various total solution concentrations.

The only published data for the system employed in this work is due to Bauman, Skidmore and Osmun (1948). Their work with Dowex 50, a cation exchanger similar to Zeo-Karb 225, showed that preference of the resin for the divalent calcium ion increases with dilution of the contacting solution. Although they covered a wide range of total solution concentrations (i.e. 0.0062 N to 6.0 N) no attempt was made to correlate the data theoretically.

It is very well known that the exchange properties of an ion exchange resin may vary from batch to batch and since reliable equilibrium data was required in subsequent work, it was decided to carry out equilibrium measurements in the concentration range from 0.025 N to 2.0 N.

A column and batch method were employed to obtain equilibrium data. In the column method resin is contacted with a continuous flow of solution of known composition until the influent and the effluent are of same composition. Resin is then washed and eluted. The eluant is analysed to obtain the resin composition. The batch method involves contacting known amounts of resin and solution and subsequent analysis of both the phases.

The column method has been employed to obtain equilibrium isotherms at various solution concentrations. This technique, in comparison with the batch method, has the obvious advantage that analysis of only resin phase is required but suffers from the disadvantage that large quantities of solution are required for equilibration. Deionised water for subsequent washing to remove sorbed electrolyte from the resin beads is also required.

In uni-divalent systems the relative amounts of the counterions in the exchanger depend upon the total solution concentration as well as on the solution composition (Subba Rao and David 1957). In the column method the resin is normally washed after equilibration with deionised water to remove any electrolyte trapped in the pores of the bed and sorbed in the beads. This small quantity of electrolyte is generally eluted during the washing step. This will alter the equilibrium distribution of the cations between the resin and solution phase. One would expect this effect to be more pronounced in cases where concentrated solutions are used for loading the resin. A comparative study using the column and the batch method for the same solution concentration confirmed that during washing of the resin in the column method the distribution of the cations alter in favour of the divalent ions.

In addition to equilibrium properties of the sodium chloride-calcium chloride-Zeo-Karb 225 system, exchange capacity and swelling weight determination of the resin in sodium and calcium ionic form have been carried out.

A further objective of the present study was an attempt to correlate the observed equilibrium data by a single valued parameter which could then be used to predict ion exchange equilibrium data in this system for any particular solution concentration. This approach is important in the design of ion exchange equipment, especially in the field of water softening.

In most earlier theoretical studies attempts to explain and correlate ion exchange equilibrium data have generally been based on adsorption theory. Empirical or semi-empirical relationships such as the Freundlich and Langmuir isotherms were employed (Helfferich 1962, p.193). This approach does not give an insight into the mechanism of the ion exchange process and is now only of historical interest.

Equilibrium between an ion exchange resin and an electrolyte solution has also been explained on the basis of the Donnan membrane equilibrium theory (Bauman and Eichhorn 1947 and Subba Rao and David 1957). In this approach the resin phase is assumed to be homogeneous consisting of concentrated electrolyte solution in which only one ion is mobile. The Donnan theory is derived for a system in equilibrium with respect to the thermodynamic identity of the electrochemical potential of the exchanging ions between the two phases.

Bauman and Eichhorn (1947) were the first to apply Donnan's theory to a number of ion exchange systems. Good correlation of the data was obtained for dilute solution concentrations. In their treatment they assumed that the activities of counterions can be represented by their molar concentrations.

Subba Rao and David (1957) refined this approach by including the activity coefficients of the counterions in the solution as well as in the resin phase. They assumed that the resin phase activities can be defined as the activities of a solution of the same concentration as that of the resin phase. They showed that ion exchange data for sodium chloride-copper chloride - Dowex 50W system for various solution concentrations can be correlated to give a single valued parameter using the Donnan membrane equilibrium theory.

The most widely used concept for the representation of equilibrium data is to consider that ion exchange is a chemical reaction between an external solution and the resin phase. For this argument, the Law of Mass Action can be applied to describe equilibrium between the components taking part in the reaction. Here again, resin is considered as a homogeneous phase consisting of a concentrated electrolyte solution. Using classical thermodynamics it is possible to derive a relationship similar to the Law of Mass Action for an ion exchange system at equilibrium.

Simplified forms of the Law of Mass Action have been employed by Boyd, Schubert and Adamson (1947), Kressman and Kitchener(1949), Duncan and Lister (1949) and Ekedaht et al (1950). Their findings, usually at one solution concentration, show that the thermodynamic equilibrium constant based on the Law of Mass Action varies with the ionic composition of the resin phase. In the calculation of the thermodynamic equilibrium constant the activity of each reacting component in the resin phase was expressed in terms of ionic composition. Composition of the exchanging ions was expressed as mole fraction, molarity and equivalent fraction. In the case of the solution phase, activities if used, were those of the pure electrolytes instead of the activities of the mixed electrolytes.

Three groups of investigators; Ekedaht et al (1950), Bonner et al (1952) and Gaines and Thomas (1953)

have treated the ion exchange resin as a solid resinate. This abstract thermodynamic approach differs from the classical thermodynamic treatment in the sense that resin and solution phase activity coefficients can be expressed on two different concentration scales.

In the present study, molal concentration units have been chosen to correlate the experimental data since this is considered more appropriate. In published literature the activity coefficients of various electrolytes are usually presented a s mean molal activity coefficients. In addition the activity coefficients of mixed electrolytes, determined from Harned's rule, have been employed to correlate the observed data using various forms of Donnan and thermodynamic equilibrium theory.

1.2. THEORY

1.2.1. Interpretation of Ion Exchange Equilibria

1.2.1.A. Law of Mass Action

The Law of Mass Action states that 'for a homogeneous system, the rate of a chemical reaction is proportional to the active masses of the reacting components'.

As suggested by Bauman, Schubert and Adamson (1947) ion exchange may be regarded as a chemical reaction between a resin phase and an external electrolyte solution. In this approach the resin is considered as a solid solution and homogeneous in a physical sense. Consider an ion exchange reaction,

$$z_B\, A^{zA} + z_A \bar{B}^{zB} \rightleftharpoons z_B \bar{A}^{zA} + z_A B^{zB} \qquad (1)$$

where A and B are the reacting components, z is the valence of a component. A bar on a symbol indicates resin phase. According to the Law of Mass Action, the rates of reaction in the forward and reverse direction are:

$$\text{Forward rate} \quad \alpha \left[a_A\right]^{z_B} \left[\bar{a}_B\right]^{z_A} \qquad (2A)$$

$$\text{Reverse rate} \quad \alpha \left[a_B\right]^{z_A} \left[\bar{a}_A\right]^{z_B} \qquad (2B)$$

where a is the activity of a component. Here, the active mass has been identified as the activity of the reacting species. At equilibrium, the rates of reaction in the forward and reverse direction are equal;

$$k_f \left[a_A\right]^{z_B} \left[\bar{a}_B\right]^{z_A} = k_r \left[\bar{a}_A\right]^{z_B} \left[a_B\right]^{z_A} \qquad (3)$$

where k_f, k_r are the rate constants for forward and reverse reactions respectively. Rewriting equation (3), it becomes

$$\frac{\left[\bar{a}_A\right]^{z_B}\left[a_B\right]^{z_A}}{\left[\bar{a}_B\right]^{z_A}\left[a_A\right]^{z_B}} = \frac{k_f}{k_r} = K_c \qquad (4)$$

where K_c is defined as the chemical equilibrium constant for the reaction (1). It may be said that the Law of Mass Action is obeyed, if the appropriate values of activities when substituted into Equation (4) give a constant value of K_c, independent of the composition, for an ion exchange system. The assumption of considering the resin as a solid solution is justified by the fact that ions in the resin phase substitute freely for one another during an exchange process. This fact is further supported by X-ray diffraction measurements carried out on cation exchanger similar to Zeo-Karb - 225 which showed a random distribution of counterions throughout the resin (Boyd, Schubert and Adamson, 1947).

Classical thermodynamics has been used to treat the problem of chemical equilibrium. It is possible, for example, to thermodynamically define the condition of equilibrium and by use of heat content and enthalpy data the actual state of chemical equilibrium can be determined.

For a system in equilibrium at constant temperature and pressure, the change in free energy of the system may be expressed as follows:

$$(\partial G)_{P,T} = (\partial G)_{P,T,(\text{Products})} - (\partial G)_{P,T,(\text{Reactants})} \qquad (5)$$

where ∂G is the partial molal free energy of a component at constant temperature T and constant pressure P. The partial molal free energy of a component is also expressed as μ - chemical potential of a species. Thus Equation (5) can be written as

$$\partial G_{P,T} = \Sigma\mu_{P,T}\ (\text{Products}) - \Sigma\mu_{P,T}\ (\text{Reactants}) \qquad (6)$$

Defining molal activity of component i as

$$\mu_i = \mu^o_i + RT \ln a_i \tag{7}$$

where μ^o_i is the chemical potential of component i in the standard state, R is gas constant, T is absolute temperature and a_i is molal activity of component i. Substitution of Equation (7) in Equation (6) gives

$$(\partial G)_{P,T} = \Sigma(\mu^o_i + RT \ln a_i)_{P,T,\text{Products}} - \Sigma(\mu^o_j + RT \ln a_j)_{P,T,\text{Reactants}} \tag{8}$$

For a reaction of the type

$$z_A\bar{B}^{z_B} + z_B A^{z_A} \rightleftharpoons z_B\bar{A}^{z_A} + z_A B^{z_B} \tag{1}$$

Equation (8) defining equilibrium state becomes

$$\partial G = \left[z_B(\bar{\mu}^o_A + RT \ln \bar{a}_A) + z_A(\mu^o_B + RT \ln a_B)\right] - \left[z_B(\mu^o_A + RT \ln a_A) + z_A(\bar{\mu}^o_B + RT \ln \bar{a}_B)\right] = 0 \tag{9}$$

On simplification Equation (9) becomes

$$\Delta G^o + RT \ln \frac{\bar{a}_A^{z_B} a_B^{z_A}}{a_A^{z_B} \bar{a}_B^{z_A}} = 0 \tag{10}$$

where ΔG^o is the standard free energy change

or

$$\frac{\bar{a}_A^{z_B} a_B^{z_A}}{a_A^{z_B} \bar{a}_B^{z_A}} = e^{-\Delta G^o/RT} \tag{11}$$

Since the R.H.S. of Equation (11) consists of all constant values, it may be written as

$$\frac{\bar{a}_A^{z_B} a_B^{z_A}}{a_A^{z_B} \bar{a}_B^{z_A}} = \text{Constant} = K_a \tag{12}$$

where K_a is the thermodynamic equilibrium constant.

In the above derivation for the thermodynamic equilibrium constant, the components of the system have been taken as counterions. As a rule, in a rigorous thermodynamic treatment, ions do not represent components. In Gibb's thermodynamics a system consists of independent components which are accessible in an isolated state. Ions, because of their charge, must be accompanied by ions of opposite charge and hence cannot be isolated.

In abstract thermodynamics, the individual quantities referring to the ionic species are undefined and fictitious. The quantities like partial molal volume or activity cannot be measured by thermodynamic means. Nevertheless, the use of individual ionic activities does not invalidate the rigour of thermodynamic treatment as they combine or cancel of necessity in such a way that they can equally well be expressed in terms of truely Gibbsian components.

Substituting the activities in Equation (12) by molalities according to

$$a_i = m_i \gamma_i \tag{13}$$

where γ_i is the molal activity coefficient of ionic species i,

$$K_a = \frac{\bar{m}_A^{z_B} m_B^{z_A} \bar{\gamma}_A^{z_B} \gamma_B^{z_A}}{\bar{m}_B^{z_A} m_A^{z_B} \bar{\gamma}_B^{z_A} \gamma_A^{z_B}} \tag{14}$$

Equation (14) cannot be evaluated as such, because it contains quantities like ionic activity coefficients which cannot be measured and are thermodynamically ill defined. In cases where both the coions and the ionogenic groups are monovalent the ionic activity coefficients can be replaced by the mean activity coefficients which are measurable quantities. Thus Equation (14) can be written

as

$$K_a = \frac{\bar{m}_A^{z_B} m_B^{z_A} (\bar{\gamma}_{AR}^{\pm z_A+z_R})^{z_B} (\gamma_{BY}^{\pm z_B+z_Y})^{z_A}}{\bar{m}_B^{z_A} m_A^{z_B} (\bar{\gamma}_{BR}^{\pm z_B+z_R})^{z_A} (\gamma_{AY}^{\pm z_A+z_Y})^{z_B}} \qquad (15)$$

where R represents the ionogenic group of the resin, Y refers to the coion. For a uni-divalent exchange reaction this reduces to

$$K_a = \frac{\bar{m}_A m_B^2 \bar{\gamma}_{AR}^{\pm 3} \gamma_{BY}^{\pm 4}}{\bar{m}_B^2 m_A \bar{\gamma}_{BR}^{\pm 4} \gamma_{AY}^{\pm 3}} \qquad (16)$$

by substituting $z_A = 2, \quad z_B = 1$ (17A)

$z_R = 1, \quad z_Y = 1$ (17B)

Equation (15) represents the general expression for the thermodynamic equilibrium constant for a chemical reaction in a homogeneous phase.

If the ratio of the activity coefficients in the resin phase is assumed to be unity, Equation (15) reduces to

$$K_a = \frac{\bar{m}_A^{z_B} m_B^{z_A} (\gamma_{BY}^{\pm z_B+z_Y})^{z_A}}{m_A^{z_B} \bar{m}_B^{z_A} (\gamma_{AY}^{\pm z_A+z_Y})^{z_B}} \qquad (18)$$

Similarly, when the ratio of activity coefficients in both the phases is considered unity, Equation (15) reduces to its simplest form;

$$K_a = \frac{\bar{m}_A^{z_B} \, m_B^{z_A}}{m_A^{z_B} \, \bar{m}_B^{z_A}} \qquad (19)$$

For the appropriate activity coefficients to be applied, Harned's rule must be used to correct for the activity coefficients in a mixture of electrolytes. Activity coefficients in the resin phase are not available and pose a problem. It has been customary to ignore the resin phase activity coefficients (Boyd, Schubert and Adamson 1947, Bauman and Eichhorn 1947, Duncan and Lister 1949 and Ekedaht et al 1950). If it may be assumed that the activity coefficients for the cations in the resin phase are proportional to the activity coefficients of these same cations in an aqueous solution of the same ionic strength as that in the resin phase, Equation (16) can be evaluated to determine K_a. It then requires only the activity coefficients in the aqueous phase.

To increase the rigour of the thermodynamic treatment for ion exchange reactions a new approach has been suggested by Ekedaht et al (1950), Bonner et al (1952) and Gaines and Thomas (1953). In this treatment, the resin is considered as a mixture of resinate AR and BR. The standard and the reference states for the resinates are assumed to be such as when

$$\bar{N}_{AR} = 1, \quad \bar{a}_{AR} = 1, \quad \bar{f}_{AR} = 1 \qquad (20A)$$

$$\bar{N}_{BR} = 1, \quad \bar{a}_{BR} = 1, \quad \bar{f}_{BR} = 1 \qquad (20B)$$

and $$\bar{N}_{BR} + \bar{N}_{AR} = 1 \qquad (20C)$$

where $\bar{N}_{AR}$ is the mole fraction of resinate AR and $\bar{f}_{AR}$ is the rational activity coefficient.

With these conventions the corresponding thermodynamic equilibrium constant has been termed the Rational Thermodynamic Equilibrium constant and can be defined by

$$n_{K_a} = \frac{\bar{a}_{AR}^{z_B} \; a_{BY}^{z_A}}{\bar{a}_{BR}^{z_A} \; a_{AY}^{z_B}} \tag{21}$$

$$= K \frac{\bar{\varepsilon}_{AR}^{z_B}}{\bar{\varepsilon}_{BR}^{z_A}} \tag{22}$$

where K is defined as the equilibrium quotient (Bonner and Smith 1957) and is equal to

$$\frac{a_{BY}^{z_A} \; \bar{N}_{AR}^{z_B}}{a_{AY}^{z_B} \; \bar{N}_{BR}^{z_A}} \tag{23}$$

Application of the Gibbs-Duhem equation to the ion exchange resin phase gives

$$\bar{N}_{AR} \; d \ln \bar{\varepsilon}_{AR} + \bar{N}_{BR} \; d \ln \bar{\varepsilon}_{BR} = 0 \tag{24}$$

Combining Equations (20), (22) and (24), for a uni-divalent exchange system, one obtains

$$\ln {}^{n}K_a = \int_0^1 \ln K \; d \bar{N}_{AR} \tag{25}$$

The rational thermodynamic equilibrium constant can be determined by graphical integration from a plot of $\bar{N}_{AR}$ and ln K. Alternatively, as suggested by Reichenberg (1966) it may be evaluated as

$$n_{K_a} = K \left[\bar{N}_{AR} = 0.5 \right] \tag{26}$$

1.2.1.B Donnan Membrane Equilibrium

When a cation exchange resin is brought in contact with an electrolyte solution some of the cations and anions penetrate the resin phase. In order to maintain electroneutrality, the number of entering cations must be balanced either by an equivalent number of anions entering the resin phase or by expulsion of an equivalent number of cations from the resin phase into the external solution. The first possibility leads to electrolyte sorption whilst the second represents an ion exchange process between resin phase and the external electrolyte solution.

For the distribution of a single salt, consider a cation exchange resin in contact with a dilute solution of a strong electrolyte. The resin phase is usually more concentrated than the external solution. In order to equalize the concentration in the two phases, the resin phase counterions tend to diffuse into the external solution. Similarly, the anions being more concentrated in the external electrolyte solution tend to diffuse into the resin phase. Since the ions are charged, an accumulation of positive charge in the solution and a negative charge on the resin takes place. As a result a potential difference is established at the interface. This electrical potential difference termed the 'Donnan potential' pulls anions back into the positively charged solution and cations into the negatively charged resin. The result is exclusion of coions from the resin phase. At equilibrium the tendency of the ions to level out the concentration differences is balanced by the action of the electrical field in order to maintain electroneutrality in each phase.

The efficiency of the exclusion of coions depends on the magnitude of the Donnan potential, and so is a function of the ion concentration and charges in the two phases.

The ensuing equilibrium may be treated as Donnan membrane equilibrium, if the resin phase is regarded as a concentrated aqueous solution separated from the external solution by a hypothetical membrane. This treatment was considered by Bauman and Eichhorn (1947) and Subba Rao and David (1957) who studied ion exchange equilibria using Dowex 50.

Thermodynamics can be employed for the derivation of a relationship representing Donnan membrane equilibrium between the resin and the solution phase. Consider an ion exchange reaction of the type;

$$z_B\, A^{z_A} + z_A\, \bar{B}^{z_B} \rightleftharpoons z_B\, \bar{A}^{z_A} + z_A\, B^{z_B} \qquad (1)$$

For a system in equilibrium the electrochemical potential of the ionic species must be the same in both the phases;

$$\eta_A = \bar{\eta}_A \quad , \quad \text{and} \quad \eta_B = \bar{\eta}_B \qquad (27)$$

where η_i is the electrochemical potential of ionic species i and is defined as

$$\eta_i = \mu_i + \varphi z_i \mathcal{F} \qquad (28)$$

where μ_i is the chemical potential of ionic species i, $\mathcal{F}$ is Faraday's constant and φ is the electrical potential. Equation (28), in terms of activities of the ionic species as defined by Equation (7), may be written as

$$\eta_i = \mu^{o}_i + RT \ln a_i + \varphi z_i \mathcal{F} \qquad (29)$$

Combining the two Equations (29) for ion i in each phase, the Donnan potential is equal to

$$E_{DON} = \bar{\varphi} - \varphi = \frac{1}{z_i \mathcal{F}} RT \ln \frac{a_i}{\bar{a}_i} \qquad (30)$$

Combining two Equations (30) for both the cations A and B, it becomes

$$\frac{a_A^{z_B}}{\bar{a}_A^{z_B}} = \frac{a_B^{z_A}}{\bar{a}_B^{z_A}} \tag{31}$$

or

$$\frac{\bar{a}_A^{z_B} \; a_B^{z_A}}{a_A^{z_B} \; \bar{a}_B^{z_A}} = 1 \tag{32}$$

The above equations describe ion exchange equilibrium in terms of activities of counterions in the resin and solution phase.

In the above treatment of the Donnan membrane equilibrium, the components considered are counterions only. Though they are thermodynamically ill-defined, they do exist physically and provide valid reasoning.

For the evaluation of Equation (32) if it may be assumed that the activity coefficients for the cations in the resin phase are proportional to the activity coefficients of the same cations in a solution of the same ionic strength as that in the resin phase, one obtains

$$\frac{\bar{m}_A^{z_B} \; m_B^{z_A} \; \bar{\gamma}_A^{z_B} \; \gamma_B^{z_A}}{m_A^{z_B} \; \bar{m}_B^{z_A} \; \gamma_A^{z_B} \; \bar{\gamma}_B^{z_A}} = K_D \tag{33}$$

where K_D is the Donnan equilibrium constant. γ_A refers to molal activity coefficient of ionic species A and m_A is the molality of A.

Other forms of the Donnan equilibrium equations have been reviewed by Helfferich (1962). The form of the equation depends on the model chosen to represent the ion exchange process. In the derivation of Equation (32) the

effects of changes in swelling and pressure on ion exchange equilibrium are implicit in the activity terms. Various simplified forms of Equation (33) have been employed in the literature in an attempt to determine K_D.

If the ratio of the activity coefficients of ion A and B in the resin phase is assumed to be unity, Equation (33) becomes

$$K_D = \frac{\bar{m}_A^{z_B} \; m_B^{z_A} \; \gamma_B^{z_A}}{m_A^{z_B} \; \bar{m}_B^{z_A} \; \gamma_A^{z_B}} \tag{34}$$

and if the ratio of the activity coefficients of ion A and B in both the phases is assumed to be unity, Equation (33) simplifies to

$$K_D = \frac{\bar{m}_A^{z_B} \; m_B^{z_A}}{m_A^{z_B} \; \bar{m}_B^{z_A}} \tag{35}$$

K_D can, therefore, be determined from the composition of the resin and solution in equilibrium.

1.3. FACTORS INVOLVED IN CATION EXCHANGE EQUILIBRIA

In section 1.2. ion exchange between a resin phase and an electrolyte solution has been regarded as a stoichiometric exchange reaction of counterions. In fact when an ion exchange resin is brought in contact with an electrolyte solution, the following processes may take place;

a) Stoichiometric ion exchange depending upon the 'selectivity' of the resin for one of the counterions.
b) Sorption or desorption of water by the ion exchanger as free or unbound water of hydration of the ions. This phenomenon is called 'swelling'.
c) Sorption or desorption of undissociated electrolyte and is termed 'sorption'.

These factors must be considered when computing an equilibrium constant for an ion exchange process, especially when the batch method is used.

1.3.1. Selectivity

All cation exchangers are in general selective but to different extents. The important factors which effect selectivity of a resin for a counterion are the degree of crosslinking, the valence and hydrated ionic volume of the counterion. Of these, the most important factor is the ionic valence, and this is well explained by Donnan theory. The Donnan potential, a purely electrostatic effect, is proportional to the ionic charge and its valence. Therefore, a counterion of higher valence will be more strongly attracted and preferred by the resin. The Donnan theory also predicts that the preference of counterions with higher valence increases with the dilution of the external solution.

For cations of the same valence, it has been found that the selectivity for an ion decreases with increase in its hydrated ionic volume (Helfferich, P.159. 1962). For example the order of preference for alkali metals is

$$Cs > Rb > K > Na > Li$$

which is the same sequence as that of their increasing hydrated ionic volume. In a highly crosslinked resin, where the hydration is incomplete, the above sequence may alter or even take a reverse order. In concentrated solutions, hydration of the ions by water may be replaced by complexing with the coions or resin fixed ionic groups; in such cases selectivity of the resin for an ion cannot be explained by the arguments presented above.

The following empiricalexpressions are generally used to express the selectivity of a resin for a counterion;

$$Q_r = \frac{\bar{x}_A^{z_B} \; x_B^{z_A}}{x_A^{z_B} \; \bar{x}_B^{z_A}} \qquad (36)$$

$$Q_m = \frac{\bar{m}_A^{z_B} \; m_B^{z_A}}{m_A^{z_B} \; \bar{m}_B^{z_A}} \qquad (37)$$

and

$$Q_m' = \frac{\bar{m}_A^{z_B} \; m_B^{z_A} \; \pm^{z_A}\gamma_{BY}}{m_A^{z_B} \; \bar{m}_B^{z_A} \; \pm^{z_B}\gamma_{AY}} \qquad (38)$$

where Q_r, Q_m and Q_m' represent rational, molal and corrected molal selectivity coefficients. These values are not constants and depend on the experimental conditions.

1.3.2. Swelling

When partially dried resin is placed in water, it takes up water and consequently swells but only to a limited extent. Ionic species, due to their charge density, have a tendency to hydrate themselves by attracting water molecules around them. The swelling of the resin is opposed by the rigid crosslinked structure of the resin matrix. An equilibrium is established when the tendency of the ionic species in the resin to hydrate and thus to

expand the matrix is equal to the resulting tension set up in the matrix structure of the resin. The contractive forces of the stretched matrix result in an increase in pressure on the pore liquid within the exchanger. The pressure difference between the pore liquid and the external solution is called the 'swelling pressure' and is defined as

$$\pi = \bar{P} - P$$

where $\bar{P}$ is pressure in the resin phase, and P is pressure in the external solution.

Swelling can also be attributed to the dilution of the concentrated interior of resin phase or as the electrostatic repulsion of the resin fixed ionic groups when the counterions become mobile on hydration.

The extent to which a resin can swell depends upon the degree of crosslinking. The number and nature of the ionic species in the resin phase. Generally, swelling of a resin is stronger when the degree of crosslinking and concentration of the external solution is low, the hydrated ionic volume and valence of the counterion is high and specific interactions like complexing of counterions with coions or resin ionogenic groups is negligible.

For an ion exchange process at equilibrium,when a swelling change due to net transfer of solvent has taken place, the general equation representing the change in free energy for an ion exchange process, may be written as

$$\partial G_{P,T} = \Sigma \mu_{P,T}(\text{Products}) - \Sigma \mu_{P,T}(\text{Reactants}) \qquad (6)$$

$$\partial G = (\mu_A + \bar{\mu}_B + \mu_S) - (\mu_A + \mu_B + \bar{\mu}_S) \qquad (39)$$

where μ_S represents the chemical potential of solvent. The corresponding Equation (16) for the thermodynamic equilibrium constant becomes

$$K_a = \left(\frac{\bar{a}_A}{a_A}\right)^{z_B} \left(\frac{a_B}{\bar{a}_B}\right)^{z_A} \left(\frac{\bar{a}_S}{a_S}\right)^{h} \qquad (40)$$

where h is the number of moles sorbed by the exchanger during the ion exchange process. It may be pointed out that in the definition of activity by Equation (7), the effect of pressure appears implicitly. For the same reason, Equation (33) for Donnan membrane equilibrium theory, in which changes in the ionic hydrated volume are considerable, have been treated by Helfferich, 1962, p.170).

1.3.3. Sorption

When an ion exchanger is immersed in an electrolyte solution, it does sorb some of the electrolyte. The extent to which this sorption of electrolyte occurs depends on the magnitude of Donnan potential. This electrolyte can be almost entirely removed by thorough washing with deionised water.

In ion exchange systems where sorption of electrolyte is considerable, it is important to analyse both phases for each counterion. Considerable error may be introduced if only one of the ions is analysed and the other one is calculated from a material balance.

Generally, the sorption of an electrolyte is favoured by high concentration of the external solution, low capacity and low crosslinking of the resin, high valence of the counterion, low valence of the coion and small molal volume of the electrolyte. In addition, interactions like complex formation may also lead to sorption of electrolyte.

Consider an ion exchange process with the sorption of g moles of electrolyte AY, the general expression for the thermodynamic equilibrium constant becomes

$$K_a = \left(\frac{\bar{a}_A}{a_A}\right)^{z_B} \left(\frac{a_B}{\bar{a}_B}\right)^{z_A} \left(\frac{\bar{a}_{AY}}{a_{AY}}\right)^{g}$$

where a_{AY} is the mean molal activity of electrolyte AY. In the above treatment swelling effects have been assumed to be negligible.

If the equilibrium studies are carried out by the batch method, swelling changes due to sorption of water or the exchange of a smaller hydrated ion for a larger one and sorption of electrolyte may lead to changes in the total solution concentration. Obviously, measurement of one ion in solution or of both the ions in the solution phase alone are not sufficient to determine the extent of exchange and thus the equilibrium constant for the process.

Hence, in order to avoid consideration of such complicating factors the equilibrium composition of both the phases must be determined. Such data can then be used to compute the equilibrium constants.

1.4. METHODS OF OBTAINING ION EXHANGE EQUILIBRIUM DATA

Ion exchange equilibrium data may be obtained by a batch or by a column method.

In the batch method a sample of resin is contacted with a fixed volume of solution of known composition. The equilibrium distribution of the competing ions is determined by analysing the solution and / or resin phase.

If the sorption of the electrolyte and swelling changes during the equilibration process are negligible then this method offers several advantages.

Firstly, only solution phase analysis is necessary for one equilibrium point on an isotherm since resin phase composition can be calcualted by mass balance.

Secondly, more than one equilibrium point can be determined with the same sample of resin by converting the resin stagewise from one ionic form to the other by successive equilibrations with new solution.

Thirdly, less time and less solution is required.

There are, however, several disadvantages in this method when electrolyte sorption and swelling changes are considerable. Analysis of one phase alone may lead to errors in the computation of the equilibrium constant. Since sorption and swelling changes would both effect the total solution concentration, it is necessary in such cases to analyse resin as well as the solution for all the components. Any values obtained from a mass balance may not give the correct amount of the components present in the system. Another disadvantage is that the solution composition for the equilibrium point cannot be fixed beforehand since it changes during equilibration. The column method has been devised to overcome some of these shortcomings.

In the column method, the resin sample is contacted with a flowing solution of known composition until the

effluent has the same composition as the influent. The resin and solution are then considered to be at equilibrium. The resin is then washed with deionised water to remove any interstitial electrolyte. If electrolyte sorption is considerable, centrifugation is alternatively used. The washed resin is then eluted with a solution containing a third counterion which is more strongly preferred by the resin. The amount of the two exchanging ions is determined by analysing this eluant. Usually the choice of the third counterion is such that it does not interfere with analysis of the other two.

The disadvantages of this method are that considerable time and feed solution are required for each equilibrium. Also, since the resin is eluted by removing the exchanging ions only one equilibrium point can be determined for any one resin sample at a time. Finally if sorption is considerable, washing of the resin may introduce changes in the resin composition. This may happen in systems where the relative amounts of exchanging ions are dependent on the total solution concentration (for example, uni-divalent ion exchange). During washing, the small amount of sorbed electrolyte that leaves the resin, produces a very dilute solution of the salts originally used for loading. This may lead to a change in the resin composition since in dilute solution the divalent ion is more preferred than the univalent ion.

1.5. EXPERIMENTAL

1.5.1. Equilibrium

The cation exchange resin used in this study was Zeo-Karb 225, 8% DVB; a sulphonated styrene-divinylbenzene copolymer manufactured by 'The Permutit Company Limited,' (London). A batch of the resin of 14-52 B.S.S. mesh size was thoroughly washed with deionised water and methanol respectively. It was then converted to the required form by cyclic conversions.

Equilibrium isotherms for the sodium chloride-calcium chloride-Zeo-Karb 225 system were obtained using a column method. The total solution concentrations employed were 0.025, 0.110, 0.20, 0.60, 1.0 and 2.0 N.

An accurately measured volume of the prepared resin in sodium form was placed in a glass column of internal diameter 2.5 cm. The column was fitted with a sintered glass disc at the bottom to retain the resin beads. A solution, containing sodium chloride and calcium chloride, of known concentration and composition was passed through the column at a rate of about 0.50 ml/min always ensuring an excess of the solution ($C_o V \gg \bar{C}\bar{V}$) was used. When the feed and effluent solution compositions were identical, it was assumed that equilibrium had been reached. The solution flow was discontinued and the column was allowed to drain. Any excess solution in the resin pores or in the sintered glass disc was removed by drying on tissue paper.

The resin sample was then washed with deionised water until the washings were free from the exchanging counterions. The resin in the column was then eluted by passing hydrochloric acid (1.0 N) at about 0.50 ml/min. A total of 250 ml of eluant was collected from each run. The eluant was analysed to give the resin phase composition.

Several experimental runs were carried out to determine an equilibrium isotherm for the sodium chloride-

calcium chloride-Zeo-Karb 225 system using a batch method. The purpose of this determination was to check if there was any difference in the isotherms obtained be the two methods. The difference in the two, if any, would give the extent to which sorption of electrolyte takes place and the effect of washing on the equilibrium distribution of counterions. The total solution concentration for these runs was 1.0 N since this data was required in subsequent work.

An accurately weighed quantity of dry resin was contacted with deionised water and allowed to swell. It was then filtered and the water adhering to the beads was removed by drying the resin beads between two sheets of blotting paper. The resin was brought in contact with a mixture of sodium chloride and calcium chloride solutions of known composition. A shaking time of 15-20 hours was employed for these equilibrations.

Duplicate runs were carried out for each point on the isotherm. After equilibrium had been established, resin was filtered, centrifuged and eluted using hydrochloric acid (1.0 N). The eluant and solution from each run was analysed to get resin and solution phase composition.

In both methods, the eluted resin was washed with deionised water and titrated against standard sodium hydroxide in the presence of excess sodium chloride. This gave the total mequiv. of cations on the resin for each run. Other properties of Zeo-Karb 225; exchange capacity and swelling weight, are given in Appendix 1.

1.5.2. Chemical Analysis

The analysis of sodium and calcium in aqueous solution was carried out using a SP-90 Atomic Absorption Spectrophotometer (AAS). This uses an acetylene-air flame and employs a combination of slits and mirrors with a Littrow type monochromator to isolate the radiation

being determined (see Appendix 2). The signal from the photomultiplier is amplified and rectified before passing to the output meter.

In emission spectroscopy the solution is introduced into the flame in the form of small droplets. At the flame temperature most of the sample is dissociated into an atomic state. A small proportion of the resulting atoms are then also excited to a higher energy state which decay to the ground state emitting radiation of a wavelength characteristic of the element concerned. The light emission from the excited atoms is proportional to the concentration in the solution.

In atomic absorption spectroscopy the measurement is based on the number of atoms which remain in the ground state. This consists of passing a beam of light through the flame of exactly the same wavelength as that emitted by the excited atoms of the element in question. The intensity of this beam is measured both before and after it has been passed through the absorbing ground state atoms, and the amount of energy absorbed is directly proportional to the number of atoms present. The beam of light with correct characteristics is obtained by a hollow cathode discharge lamp (see Appendix 2.).

The choice of method depends on its sensitivity and lack of interference by other elements. As there are, in general, more atoms left in the ground state than in the excited state, analysis by the atomic absorption method is more sensitive. Also, the degree of absorption is almost independent of flame temperature while in the case of emission its intensity varies greatly with temperature. For the alkaline earth metals atomic absorption spectroscopy has been found most suitable for analysis. Sodium has been determined in this study by an emission technique because of its high emission sensitivity (Elwell and Gidley 1961).

1.5.2.A. Sodium Analysis

For the analysis of sodium the solutions were diluted so that they fell in the range of 1-5 p.p.m. (parts per million). Since the elements contained a high concentration of hydrochloric acid, all the standard solutions and the sample solutions were prepared such that they contained 25% (v/v) hydrochloric acid (IN). This avoided errors due to interference or suppression from high concentrations of hydrochloric acid in the sample solutions. In aqueous solutions, deionised water was used for the preparation of sample solutions and standard solutions. Deionised water was used as blank. Details of the sodium analysis by the emission method and a typical calibration curve are given in Appendix 2.

1.5.2.B. Calcium Analysis

The absorption method was used for the determination of calcium. All the eluants and solutions were diluted so that they fell in the range of 1-10 p.p.m. Again, as in the case of sodium, standard and sample solutions contained 25% (v/v) hydrochloric acid (IN) to avoid any suppression or interference due to the high concentration of hydrochloric acid in the eluants. Details of the analysis of calcium by the absorption method and a typical calibration curve are given in Appendix 2.

1.6. RESULTS

1.6.1. Capacity

The exchange capacity of Zeo-Karb 225, 8% DVB resin was determined as by the method described in Appendix 1. Both the volume and weight exchange capacities are given in Tables 1 and 2. The exchange capacity of the resin, including electrolyte sorption, was calculated from the results of each batch equilibrium measurement. The results are shown in Table 2. The average exchange capacity of the resin is 4.524 m.eq/gm of dry sodium form and 4.589 m.eq/gm of dry calcium form resin. The volume exchange capacity has been determined to be 2.00 m.eq/ml of (bulk) resin.

1.6.2. Electrolyte Sorption

The effect of electrolyte sorption from a 1.0 N solution of varying composition are given in Table 3. It is expressed as a difference between the total mequivalents of cations from the analysis of eluant by AAS and the total mequivalents of hydrogen on the resin by titration in the equilibrium studies using a batch method. In the case of calcium form resin, electrolyte sorption is 4.01% of the total exchange capacity per gm. In the case of sodium form resin it is 2.52%. The volume (bulk) exchange capacity inclusive of electrolyte sorption has been found to be 2.08 m.eq /ml of resin in either form.

1.6.3. Equilibrium

Equilibrium data for the system sodium chloride-calcium chloride-Zeo-Karb 225, 8% DVB resin is presented in Table 4. Figure 1 gives exchange isotherms for various total solution concentrations. The equivalent fraction of each ion in

the resin and in the solution phase was calculated from the analysis performed using the Atomic Absorption Spectrophotometer.

All the isotherms are drawn as smooth curves through the experimental points. The data from these isotherms have been used in the calculation of various selectivity coefficients and equilibrium constants. Figure 2 shows isotherms for total solution concentration of 1.0 N obtained from the column and the batch method respectively.

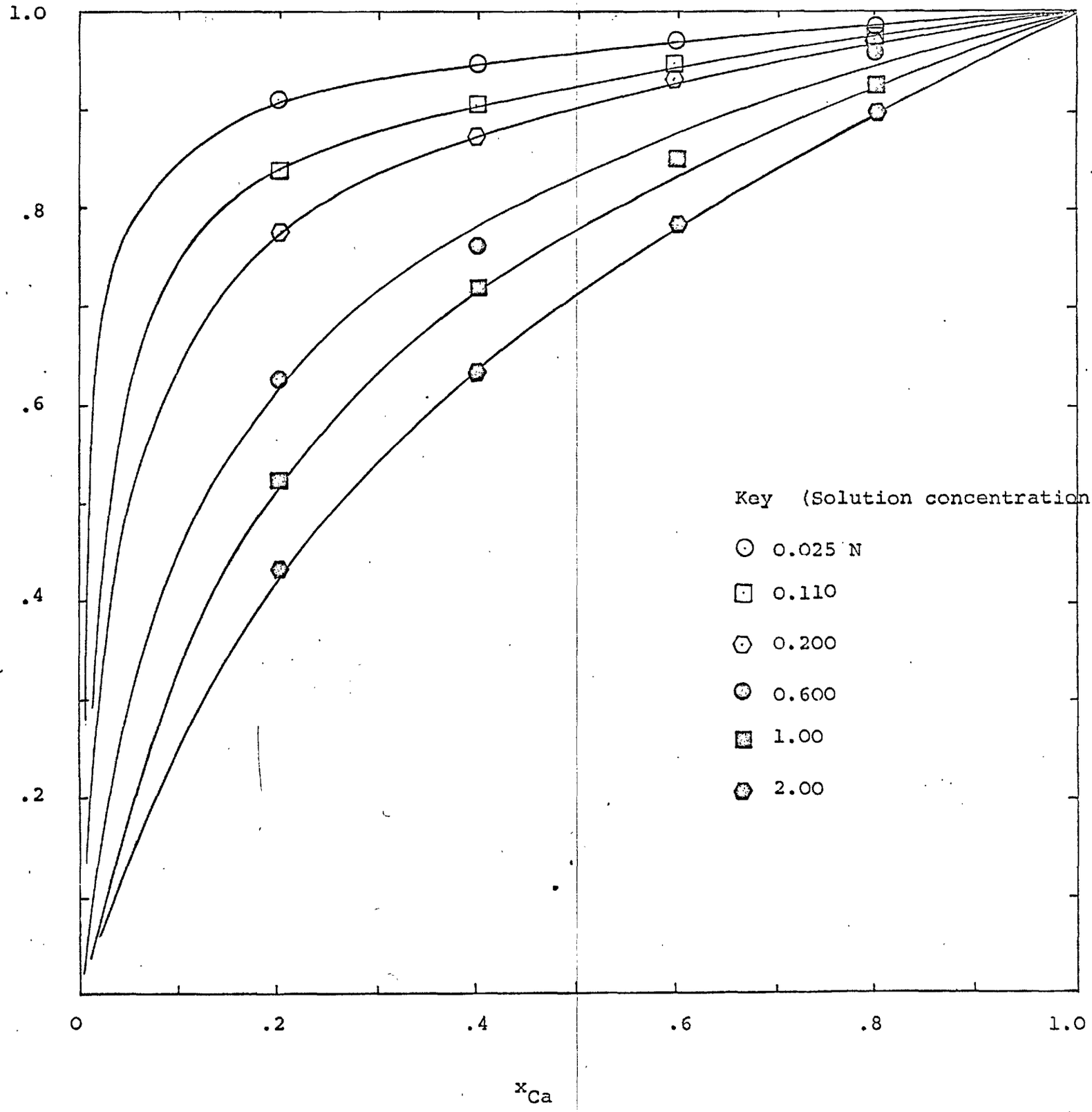

Figure 1. Equilibrium isotherm for the system NaCl - $CaCl_2$ Zeo-Karb 225 8% DVB resin ($25^{o}C$)

Table 1. Total weight exchange capacity* of Zeo-Karb 225, 8% DVB resin using the Column method.

No.	Ionic Form	Weight of Resin gm	m.equiv/gm		Average m.equiv/gm
			AAS method	Titration method	
1	Na^+	1.1793	4.527	4.527	
2	Na^+	1.1608	4.523	4.520	
3	Na^+	1.1722	4.519	4.526	
					4.524
1	Ca^{++}	1.1250	4.587	4.588	
2	Ca^{++}	1.1965	4.597	4.582	
3	Ca^{++}	1.2100	4.592	4.591	
					4.589

* An average volume exchange capacity of the resin in either form has been determined to be 2.00 mequiv/ml.

Table 2. Total weight exchange capacity of Zeo-Karb 225, 8%, DVB resin inclusive of sorbed electrolyte (C_o = 1N)

No.	Ionic Form	Weight of Resin gm	m.equiv/gm		% Sorption
			AAS method (No washing)	Titration method (Washing)	
1	Na^+	1.212	4.7050	4.592	
2	Na^+	1.117	4.7052	4.590	
3	Na^+	0.985	4.7046	4.584	
4	Na^+	0.970	4.7049	4.580	
					2.52
1	Ca^{++}	1.052	4.7052	4.520	
2	Ca^{++}	1.020	4.7058	4.529	
3	Ca^{++}	1.534	4.7065	4.525	
4	Ca^{++}	0.970	4.7060	4.524	
					4.011

Table 3. Amount of sorbed electrolyte on Zeo-Karb 225, 8% DVB resin in contact with sodium chloride-calcium chloride solution (C_o = 1N)

Resin Composition $\bar{x}_{Ca}$	0	0.06	0.095	0.28	0.82	0.85	1.0
% Sorption	2.52	2.55	2.65	3.00	3.70	3.81	4.01

Table 4. Equilibrium Composition of sodium and calcium on Zeo-Karb 225, 8% DVB resin using column method (25°C)

Solution Normality C_o	Solution Composition x_{Ca}	Resin Composition $\bar{x}_{Ca}$
0.025	0.2	0.909
	0.4	0.946
	0.6	0.968
	0.8	0.983
0.110	0.2	0.840
	0.4	0.903
	0.6	0.947
	0.8	0.976
0.20	0.2	0.775
	0.4	0.874
	0.6	0.932
	0.8	0.973
0.60	0.2	0.625
	0.4	0.761
	0.6	0.834
	0.8	0.961
1.0	0.2	0.522
	0.4	0.716
	0.6	0.846
	0.8	0.925
2.0	0.2	0.432
	0.4	0.631
	0.6	0.780
	0.8	0.895

Solution Normality C_o	Solution Composition x_{Ca}	Resin Composition $\bar{x}_{Ca}$
1.0*	0.060	0.25
	0.095	0.33
	0.280	0.585
	0.310	0.615
	0.578	0.790
	0.620	0.825
	0.640	0.830
	0.820	0.920
	0.852	0.935
	0.922	0.960

*Batch method.

1.7. CORRELATION OF DATA AND DISCUSSION

1.7.1. Capacity

The exchange capacity of Zeo-Karb 225, 8% DVB resin in hydrogen form has been reported by Helfferich (1962) to be 2.10 m.eq /ml and 4.80 m.eq /gm. The exchange capacity of this batch of resin in hydrogen form can be calculated from the observed capacity in sodium form as follows:

When a gm of resin in the sodium form is converted into hydrogen form, the weight of the resin decreases according to the following relationship;

$$W_H = W_{Na} - \bar{C}_o \left[\text{Eq.(Na)} - \text{Eq.(H)} \right] \qquad (42)$$

where W_H is the weight of resin in hydrogen form, Eq.(A) refers to the equivalent weight of ionic species A.

or $W_H = 1.0 - 4.524 \left[0.023 - 0.001 \right]$

$= 0.9004$ gm

Thus exchange capacity in hydrogen form would be

$4.524/0.9004 = 5.028$ m.eq/gm.

As stated earlier the exchange properties of resin may vary from batch to batch; the batch of resin used in this study had a higher capacity than the one quoted in literature.

The above mentioned relationship when used for the determination of exchange capacity of resin in calcium form gives

$4.524/(1-4.524(0.023-0.020)) = 4.596$ m.eq/gm.

This value differs from the observed value for calcium form of resin by 0.152%,

$$\left[(4.596 - 4.589) \,/\, 4.589 \right] \times 100 = 0.152\%$$

The small difference in the theoretical and observed value reflects the accuracy of experimental determinations.

1.7.2. Sorption

The sorption of electrolyte has been found to vary with the ionic form of the resin; it is greater when the resin is in the calcium form, smaller in the sodium form. This is not unexpected on the basis of the Donnan theory. As stated in section 1.3 the Donnan potential is smaller when the valence of the counter ion is higher and the electrolyte exclusion is less efficient.

Electrolyte sorption data is important for a design engineer; it can be used to determine the size of the washing section of a continuous ion exchange process and in cases where valuable material is being recovered it would determine the loss of material in the washing section and whether it is worth recovering.

1.7.3. Equilibrium Data

The experimental results for the sodium chloride-calcium chloride-Zeo-Karb 225, 8% DVB resin system are presented in Figure 1. Equivalent fractions are used as co-ordinates, since cation exchange is essentially a constant normality process and data presented in this form is useful for design purposes.

In section 1.3. it was stated that one of the most important factors affecting the selectivity of an ion exchange resin is the valence of the counterions. This has been verified in this study. Zeo-Karb 225 is selective for the divalent calcium ion in preference to sodium; characteristic of uni-divalent exchange. The results are

in accord with those of the previous investigators of uni-divalent exchange reactions (Boyd, Schubert and Adamson 1947, Subba Rao and David 1957, Bauman, Skidmore and Osmun 1948). This can be understood from considering the Donnan potential. As stated in section 1.3.1. the magnitude of the Donnan potential acting on an ion is proportional to the valence of the counterion. Hence the counterion of higher valence is more strongly attracted and preferred by the ion exchanger. Similarly, the tendency of the anions to diffuse into the resin and cations to diffuse into the external solution phase is enhanced when the counterion concentration differences are large. The Donnan potential and therefore preference of counterions of higher valence increases with the dilution of the external solution.

Figure 2 depicts two exchange isotherms for the same total solution concentration but obtained by two different methods; the batch and the column method. The difference between them is due to the washing step which is employed in the case of the column method. It seems that during washing, sorbed electrolyte leaves the resin beads and forms a very dilute solution. The presence of this dilute solution of mixed electrolyte changes the equilibrium composition of the resin in favour of the divalent ion. This difference will be expected to be more pronounced for a case where the equilibrium distribution of counterions on the resin is very sensitive to the total solution concentration.

In order to correlate the experimental data obtained for the sodium chloride-calcium chloride-Zeo-Karb 225 system, a computer programme was written to calculate the rational selectivity coefficient Q_r, and the molal selectivity coefficient Q_m (see Appendix 3).

The values of the Donnan membrane equilibrium constant, thermodynamic equilibrium constant based on the Law of Mass Action and the rational thermodynamic equilibrium

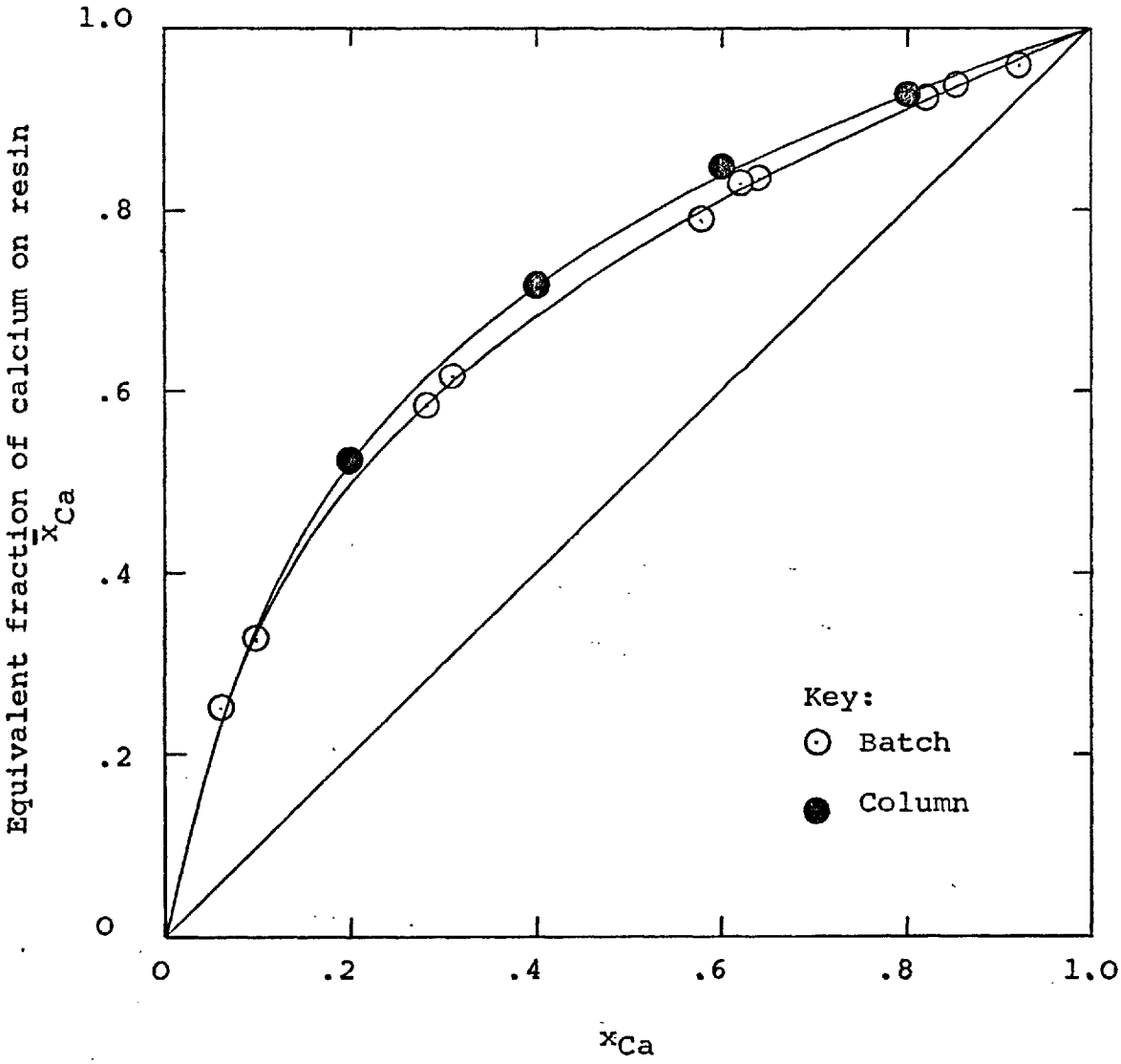

Figure 2. Equilibrium isotherms for NaCl-$CaCl_2$-Zeo-Karb 225, 8% DVB resin (C_o = 1.0, 25°C).

constant have also been calculated. Table 6 gives the computed results as a function of resin composition.

Table 5 gives a list of the various factors used for the correlation of the data obtained in this study.

The rational selectivity coefficient defined by Equation (36) has been applied to correlate the experimental data obtained for the sodium chloride-calcium chloride-Zeo-Karb 225 system. The equivalent ionic fractions in each phase were calculated from the smooth curves drawn through the experimental data points for an isotherm. Writing Equation (36) for uni-divalent exchange reaction;

$$Q_r = \frac{\bar{x}_A \, (1-x_A)^2}{x_A \, (1-\bar{x}_A)^2} \qquad (43)$$

where x_A is the equivalent fraction of ionic species A, Q_r is the rational selectivity coefficient.Figure 3 shows the values of rational selectivity coefficient as a function of resin phase composition for various total solution compositions. Table 6 gives values of Q_r computed for all the isotherms.

As previously stated in the definition of Q_r, it is not a constant quantity but is a function of experimental conditions. The results show that Q_r varies slightly with the resin composition and also decreases with an increase in the solution normality. The value of Q_r, calculated from the data given by Bauman, Skidmore and Osmun (1948) for sodium chloride-calcium chloride-Dowex 50W resin, comes to 4.30 for an isotherm at total solution concentration of 1.71N. This value is in good agreement with 4.10 of this study for an isotherm at total solution concentration of 2.00N.

Substitution of experimental data in Equation (37) which represents molal selectivity coefficient and also simplified forms of Donnan membrane and thermodynamic

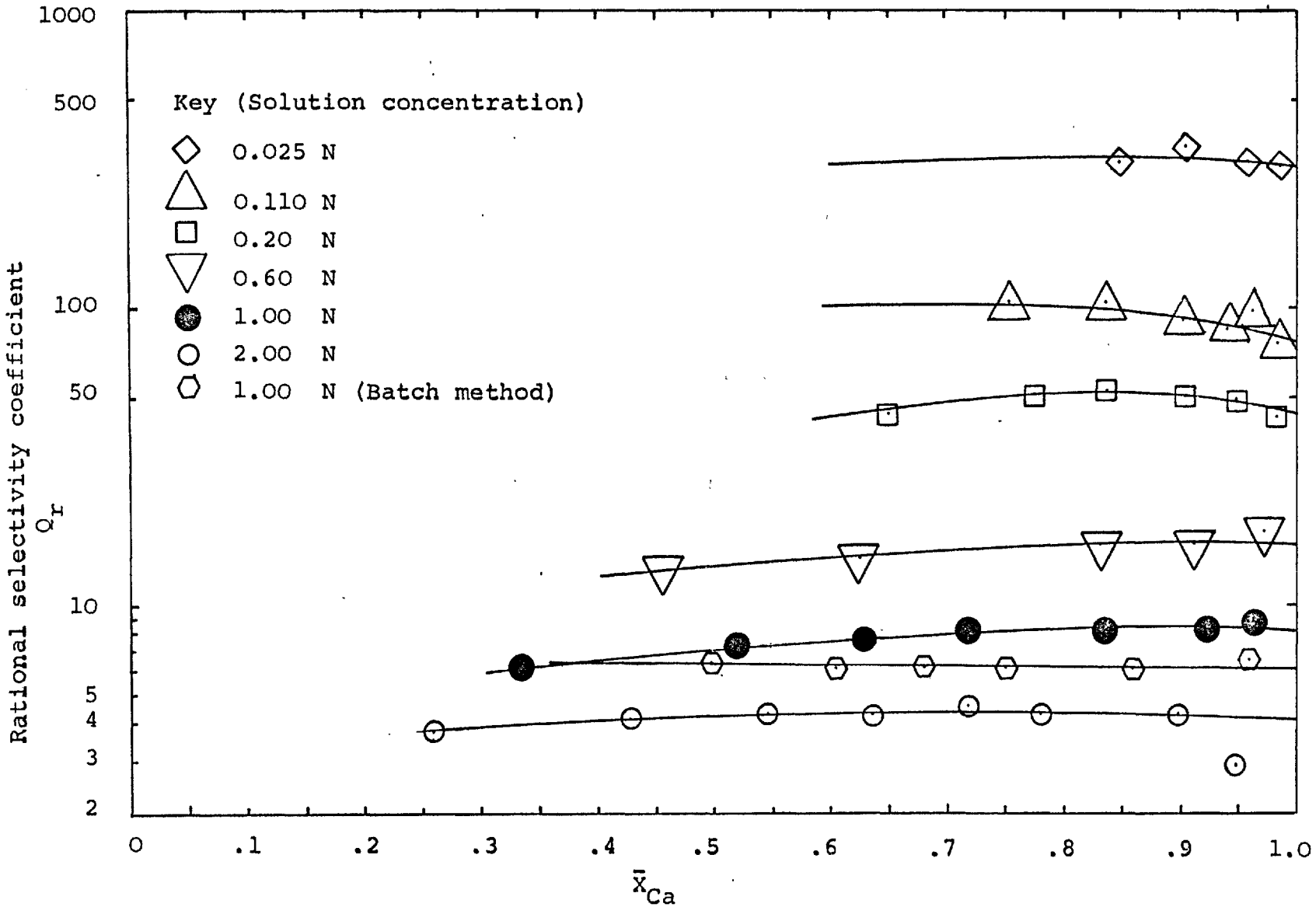

Figure 3. Dependence of rational selectivity coefficient on resin composition and total solution concentration

$$Q_r = \frac{\bar{x}_{Ca} \; x^2_{Na}}{\bar{x}_{Na}^2 \; x_{Ca}} = (K_D) = (K_a)$$

Table 5. Various factors employed for the correlation of experimental data obtained in this study.

Symbol	Factor	Definition	Remarks
Q_r	Rational selectivity coefficient	$Q_r = \frac{\bar{x}_{Ca}}{x_{Ca}} \frac{x^2_{Na}}{\bar{x}^2_{Na}}$	An empirical relation.
Q_m	Molal selectivity coefficient	$Q_m = \frac{\bar{m}_{Ca}}{m_{Ca}} \frac{m^2_{Na}}{\bar{m}^2_{Na}}$	An empirical relation. Also represents the simplified form of K_D, K_a, K_c when ratio of activity coefficients in both phases is assumed to be unity.
Q'_m	Corrected molal selectivity coefficient	$Q'_m = \frac{\bar{m}_{Ca}\, m^2_{Na}\, \gamma^{\pm 4}_{NaCl}}{\bar{m}^2_{Na}\, m_{Ca}\, \gamma^{\pm 3}_{CaCl_2}}$	An empirical relation. Also represents the simplified form of K_D, K_a, K_c when the activity coefficients ratio in the resin phase is unity.
K_c	Chemical equilibrium constant	$K_c = \frac{\bar{a}_{Ca}}{a_{Ca}} \frac{a^2_{Na}}{\bar{a}^2_{Na}}$	Based on Law of Mass Action, similar to K_a. Resin phase considered as electrolyte solution.
K_D	Donnan membrane equilibrium constant	$K_D = \frac{\bar{m}_{Ca}\, m^2_{Na}\, \gamma^{\pm 4}_{NaCl}\, \gamma^{-3}_{CaCl_2}}{\bar{m}^2_{Na}\, m_{Ca}\, \bar{\gamma}^{\pm 4}_{NaCl}\, \gamma^{\pm 3}_{CaCl_2}}$	Based on Donnan membrane equilibrium
K_a	Thermodynamic equilibrium constant	$K_a = \frac{\bar{a}_{Ca}}{a_{Ca}} \frac{a^2_{Na}}{\bar{a}^2_{Na}}$	Based on the concept of free energy change in a chemical reaction. Resin phase considered as homogeneous and (solid) electrolyte solution.

Symbol	Factor	Definition	Remarks
$^{n}K_{a}$	Rational thermodynamic equilibrium constant	$\ln {}^{n}K_{a} = \int_{0}^{1} \ln K \, d\bar{N}_{Ca}$	Same as K_{a}, but resin considered as resinate, and different scale of activity coefficients in both phases.
K	Equilibrium quotient	$K = \frac{a^{2}_{Na} \; \bar{N}_{Ca}}{a_{Ca} \; \bar{N}^{2}_{Na}}$	

TABLE 6. Computed values of rational selectivity coefficient, molal selectivity coefficient, corrected molal selectivity coefficient, Donnan membrane equilibrium constant and thermodynamic equilibrium constant for sodium chloride - calcium chloride - Zeo-Karb 225, 8% DVB resin system.

$$Q_r = \frac{\bar{x}_{Ca}}{x_{Ca}} \cdot \frac{x^2_{Na}}{\bar{x}^2_{Na}}$$

$$Q_m = \frac{\bar{m}_{Ca}}{m_{Ca}} \cdot \frac{m^2_{Na}}{\bar{m}^2_{Na}}$$

$$K_a = K_D = Q'_m = \frac{\bar{m}_{Ca}}{m_{Ca}} \cdot \frac{m^2_{Na}}{\bar{m}^2_{Na}} \cdot \frac{\gamma^4_{NaCl}}{\gamma^3_{CaCl_2}}$$

$$K_a = K_D = \frac{\bar{m}_{Ca}}{m_{Ca}} \cdot \frac{m^2_{Na}}{\bar{m}^2_{Na}} \cdot \frac{\gamma^4_{NaCl}}{\bar{\gamma}^4_{NaCl}} \cdot \frac{\bar{\gamma}^3_{CaCl_2}}{\gamma^3_{CaCl_2}}$$

Solution concentration C_o	x_{Ca}	$\bar{x}_{Ca}$	$\frac{\bar{x}_{Ca} \cdot x^2_{Na}}{x_{Ca} \cdot \bar{x}^2_{Na}}$	m_{Ca}	$\bar{m}_{Ca}$	m_{Na}	$\bar{m}_{Na}$	Q_m	Q'_m	$Q'_m \frac{\gamma^{-3}_{CaCl_2}}{\gamma^4_{NaCl}}$
0.025	.100	.850	306.000	.001	.023	2.814	.993	1.157	2.475	108.63
	.200	.908	343.289	.003	.020	3.011	.610	1.296	2.781	92.669
	.300	.932	329.210	.004	.018	3.093	.451	1.242	2.451	63.310
	.400	.947	303.418	.005	.015	3.144	.352	1.144	2.283	61.650
	.500	.960	300.000	.006	.013	3.189	.266	1.131	2.026	52.390
	.600	.970	287.407	.008	.010	3.223	.199	1.083	1.979	49.070
	.700	.978	259.799	.009	.008	3.250	.146	.979	1.780	42.950
	.800	.987	292.012	.010	.005	3.281	.086	1.100	2.039	46.870
	.900	.995	442.222	.011	.003	3.308	.033	1.665	2.631	52.890
0.110	.100	.752	99.037	.006	.099	2.483	1.638	1.657	4.692	299.15
	.200	.837	100.809	.011	.088	2.770	1.079	1.682	4.842	223.26
	.300	.878	96.350	.017	.077	2.909	.809	1.606	4.413	163.39
	.400	.905	90.249	.022	.066	3.001	.630	1.503	4.146	137.18
	.500	.926	84.551	.028	.055	3.073	.491	1.407	3.663	109.44
	.600	.945	83.306	.033	.044	3.138	.365	1.386	3.483	98.02
	.700	.964	95.635	.039	.033	3.202	.239	1.590	4.208	107.68
	.800	.977	92.344	.044	.022	3.247	.153	1.535	3.050	73.49
	.900	.988	76.235	.050	.011	3.284	.080	1.267	3.592	81.45
0.2	.100	.652	43.609	.010	.181	2.147	2.291	1.333	3.902	457.81
	.200	.776	49.490	.020	.161	2.564	1.480	1.508	4.547	220.92
	.300	.838	52.154	.030	.141	2.774	1.072	1.586	4.747	217.81

/...

	.400	.875	50.400	.040	.121	2.899	.828	1.531	4.368	167.32
	.500	.905	50.139	.050	.101	3.001	.630	1.522	4.227	139.60
	.600	.930	50.612	.060	.081	3.086	.465	1.535	4.205	125.98
	.700	.950	48.857	.070	.060	3.155	.332	1.481	3.795	102.09
	.800	.968	47.266	.081	.040	3.216	.213	1.432	3.526	87.29
	.900	.984	42.708	.091	.020	3.271	.106	1.293	2.989	70.25
0.60	.100	.458	12.629	.030	.546	1.500	3.549	1.170	2.992	823.85
	.200	.624	14.124	.061	.486	2.053	2.474	1.303	3.809	183.93
	.300	.720	15.000	.091	.425	2.375	1.847	1.380	3.759	94.66
	.400	.784	15.123	.121	.364	2.591	1.428	1.389	3.683	52.71
	.500	.835	15.335	.152	.304	2.764	1.092	1.406	3.830	42.60
	.600	.878	15.731	.182	.243	2.909	.809	1.441	3.847	31.64
	.700	.913	15.509	.213	.182	3.028	.577	1.420	3.829	24.58
	.800	.945	15.620	.243	.121	3.138	.365	1.429	3.158	16.45
	.900	.975	17.333	.273	.061	3.240	.166	1.584	3.524	15.80
1.0	.100	.336	6.173	.051	.914	1.096	4.333	.960	1.703	996.72
	.200	.520	7.222	.102	.812	1.706	3.149	1.118	2.085	575.81
	.300	.630	7.516	.152	.711	2.073	2.435	1.160	2.244	341.86
	.400	.720	8.265	.203	.610	2.375	1.847	1.273	2.530	217.33
	.500	.785	8.491	.254	.508	2.594	1.421	1.305	2.670	176.76
	.600	.835	8.179	.305	.407	2.764	1.092	1.256	2.692	138.90
	.700	.882	8.144	.356	.305	2.923	.782	1.249	2.677	107.99
	.800	.925	8.222	.407	.203	3.069	.498	1.260	2.671	106.96
	.900	.965	8.753	.458	.102	3.206	.233	1.340	2.902	78.50
2.0	.100	.258	3.796	.103	1.847	.840	4.831	1.197	0.6068	525.19
	.200	.427	4.162	.205	1.643	1.397	3.749	1.307	0.764	316.28

/...

	.300	.545	4.300	.308	1.439	1.789	2.987	1.346	0.879	195.08
	.400	.635	4.290	.411	1.234	2.090	2.402	1.341	1.083	161.29
	.500	.718	4.514	.515	1.029	2.368	1.860	1.409	1.145	105.91
	.600	.780	4.298	.618	.824	2.577	1.454	1.340	1.244	76.07
	.700	.842	4.337	.722	.618	2.787	1.046	1.350	1.388	58.34
	.800	.898	4.316	.825	.413	2.977	.676	1.343	1.636	59.95
	.900	.949	4.054	.929	.206	3.151	.339	1.260	1.166	35.74
1.0*	.100	.329	5.919	.051	.914	1.073	4.378	.921	1.400	818.20
	.200	.498	6.324	.102	.812	1.632	3.291	.979	1.566	439.20
	.300	.602	6.207	.152	.711	1.979	2.617	.959	1.576	240.15
	.400	.682	6.070	.203	.610	2.247	2.096	.936	1.655	141.50
	.500	.752	6.113	.254	.508	2.483	1.638	.941	1.640	108.71
	.600	.812	6.126	.305	.407	2.686	1.244	.941	1.710	96.22
	.700	.862	5.820	.356	.305	2.855	.914	.893	1.700	68.90
	.800	.912	5.888	.407	.203	3.025	.584	.903	1.66	66.60
	.900	.960	6.667	.458	.102	3.189	.266	1.021	1.875	50.75

*Batch method

equilibrium constant, produces the results as shown in Figure 4. Equation (37) when applied to a uni-divalent exchange reaction becomes;

$$Q_m = \frac{\bar{m}_A \; m_B^2}{m_A \; \bar{m}_B^2} \tag{44}$$

A very good correlation of the data is obtained. The molal selectivity coefficient Q_m shows an average variation of 16.4% and a maximum variation of 40% from the average value of 1.30. All the computed values are given in Table 6. A sample calculation in Appendix 3 explains the calculation of Q_m from resin composition, swelling weight and its exhange capacity.

Rewriting Equation (44) in terms of equivalent fractions of the exchanging ions in each phase, it becomes

$$Q_m = \frac{\bar{x}_A \; (1-x_A)^2}{x_A \; (1-\bar{x}_A)^2} \; \frac{C_E}{\bar{C}_E} \tag{45}$$

where x_i is the equivalent fraction of ion i, C_E is the total equivalents per 1000 gm of water.

or $$Q_m = Q_r \frac{C_E}{\bar{C}_E} \tag{46}$$

Since C_E is the total mequiv per 1000 gm of water and not normality of the solution, it varies with the composition of the mixed electrolyte solution. C_E is, however, a function of the normality of the solution according to the following relationship:

$$C_E = \frac{(x_A + x_B)\; C_o \times 1000}{1000\;(x_A \rho_A + x_B \rho_B) - \left[x_A \times \text{Eq.(A)} + x_B \times \text{Eq.(B)}\right] C_o} \tag{47}$$

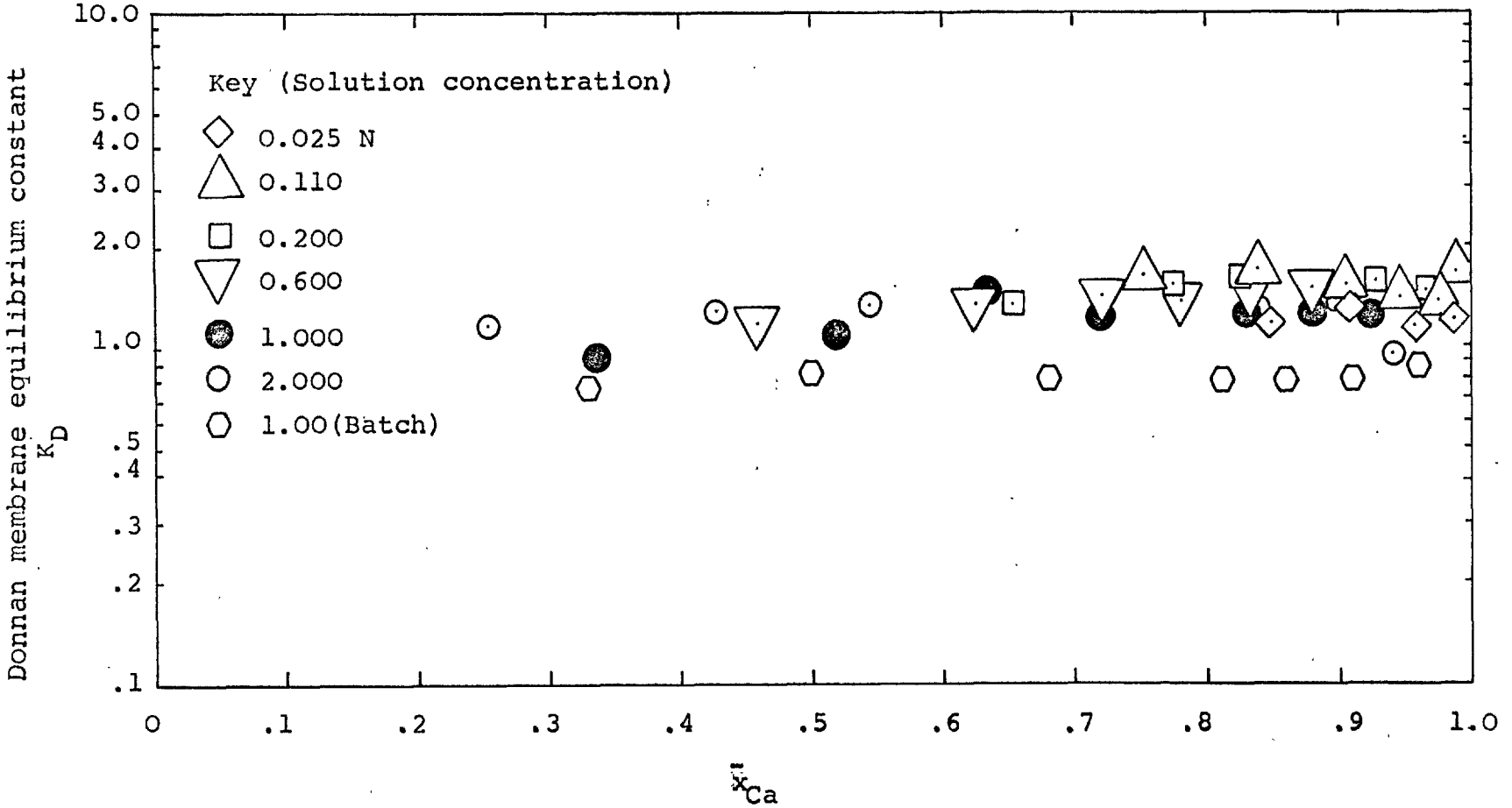

Figure 4. Correlation of data

$$K_D = \frac{\bar{m}_{Ca}\, m^2_{Na}}{m_{Ca}\, \bar{m}^2_{Na}} = (K_a) = (Q_m)$$

where ρ_i is the density of the solution containing electrolyte iY of normality C_o. In dilute solutions both the C_o and C_E may be taken as similar.

Similarly, $\bar{C}_E$, the total number of ionic equivalents in the resin phase per 1000 gm of water may not be constant; particularly in cases where the swelling weight (gm of water/gm of dry resin) varies with composition. Fortunately, in the system sodium-calcium ions the swelling weight change is very small (See Appendix 1) and value of $\bar{C}_E$ can be taken as constant.

If it may be assumed that C_E can be approximated to C_o (solution normality) then both $\bar{C}_E$ and C_E become constant for a particular exchange isotherm. With these assumptions it is possible to calculate the variation of $\bar{x}_i$ with x_i for various values of C_E by substituting a mean value of Q_m (obtained from Figure 4) and $\bar{C}_E$ in Equation (45). This has been shown in Figure 5, which compares the experimental data with the theoretical isotherms. A good agreement between the theoretical isotherms and the experimental points establishes the fact that the single valued parameter i.e. Q_m may be used to predict the behaviour of this ion exchange system.

In the above treatment the molal selectivity coefficient also represents the simplified form of the Donnan and thermodynamic equilibrium constant. The assumption being that the ratio of the activity coefficients of both ions in each phase is unity. Therefore it may be said that the ion exchange data for the system used in this study can be formulated according to either the Donnan membrane equilibrium or the thermodynamic equilibrium constant based on the Law of Mass Action.

Application of the Donnan membrane equilibrium (Equation 34) and an identical equation representing the thermodynamic equilibrium (Equation 18) inclusive of solution phase activity coefficients for an uni-divalent reaction gives:

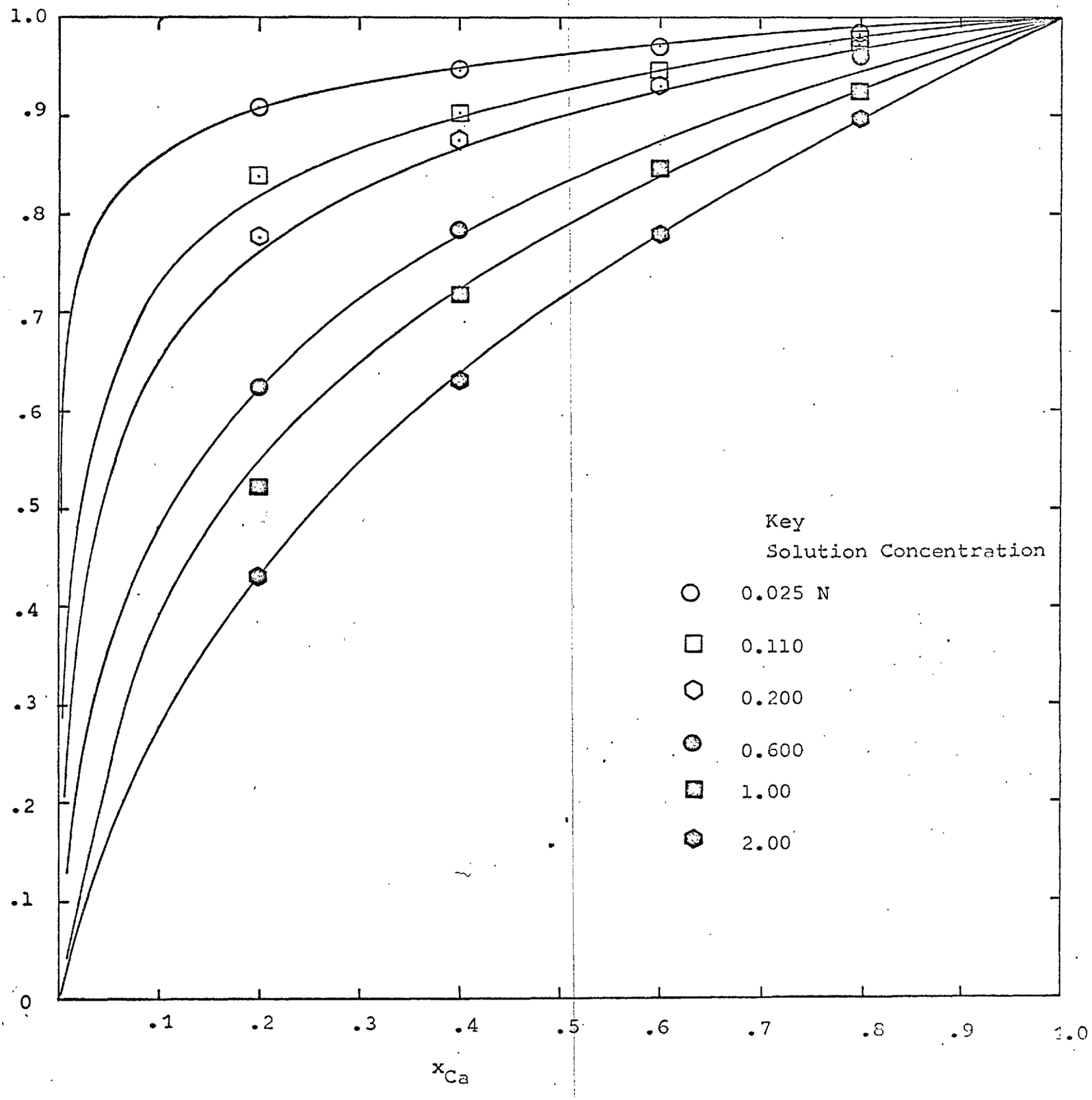

Figure 5. Comparison of experimental and theoretical data. The curves are computed with K_D = 1.3.

$$K_D = K_a = \frac{\bar{m}_A}{m_A} \frac{m_B^2}{\bar{m}_B^2} \cdot \frac{\gamma_{\bar{BY}}^{\pm 4}}{\gamma_{\bar{AY}}^{\pm 3}} = Q_m' \qquad (48)$$

where Q_m' has been defined as a corrected molal selectivity coefficient, $\gamma_{\bar{iY}}^{\pm}$ is mean molal activity coefficient of an electrolyte iY in mixed electrolyte solution.

The activity coefficients for the solution phase may be obtained from Parsons (1951). For the activity coefficient of one electrolyte in a mixture, Harned's rule may be applied;

$$\log \gamma_{\bar{BY}\ (mix)}^{\pm} = \log \gamma_{\bar{BY}\ (pure)}^{\pm} - \alpha_{12} I_2 \qquad (49)$$

where $\gamma_{\bar{BY}\ (mix)}^{\pm}$ is the mean molal activity coefficient of BY in a mixture at total ionic strength I_T, $\gamma_{\bar{BY}\ (pure)}^{\pm}$ is the mean molal activity coefficient of BY in a pure aqueous solution at I_T, α_{12}, is a constant represented by the slope in a plot of log $\gamma_{\bar{BY}\ (mix)}^{\pm}$ against I_T (See Figure 8), and I_2 represents the ionic strength of A^Y. A similar relationship holds for $\gamma_{AY\ (mix)}$.

Values of α_{12} and α_{21} have been taken from Moor and Ross (1965) and activity coefficients for pure electrolytes have been taken from the tables given by Parsons (1951). Figure 7 shows the activity coefficients of sodium chloride and calcium chloride as a function of solution molality. For the determination of ionic strength of an electrolyte the following relationship holds:

$$I_{iY} = \tfrac{1}{2} \Sigma\, m_i\, z_i^2 \qquad (50)$$

where I_{iY} is the ionic strength of an electrolyte iY and m_i is the molality of ionic species i.

The calculated values of Q_m' which represent also K_D and K_a in their simplified form are given in Table 6. Figure 6 shows the variation of Q_m' with the resin composition.

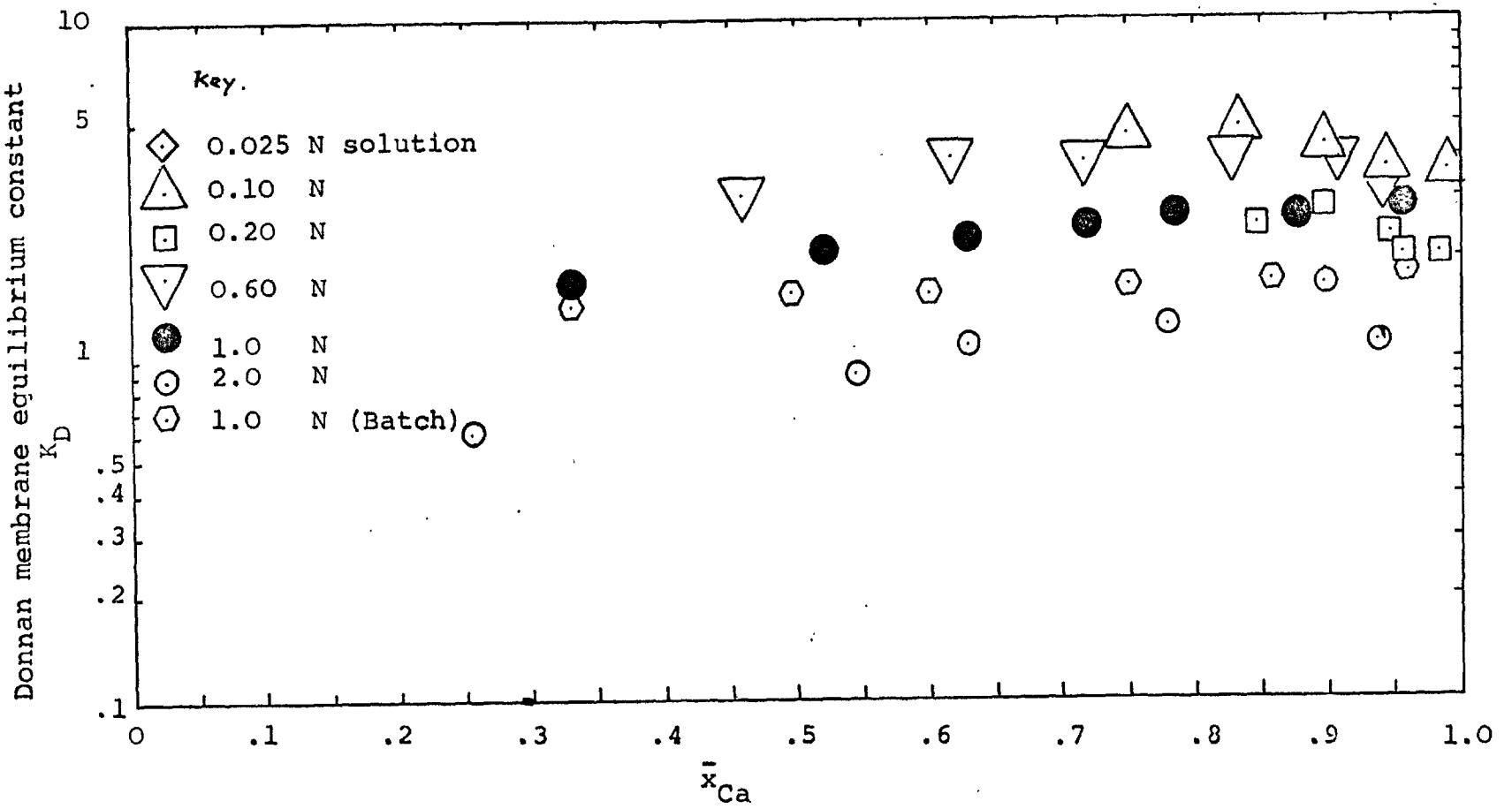

Figure 6. Correlation of data

$$K_D = \frac{\bar{m}_{Ca}}{m_{Ca}} \frac{m^2_{Na}}{\bar{m}^2_{Na}} \frac{\gamma^{\pm 4}_{\bar{}NaCl}}{\gamma^{\pm 3}_{\bar{}CaCl_2}} = (K_a) = (Q'_m)$$

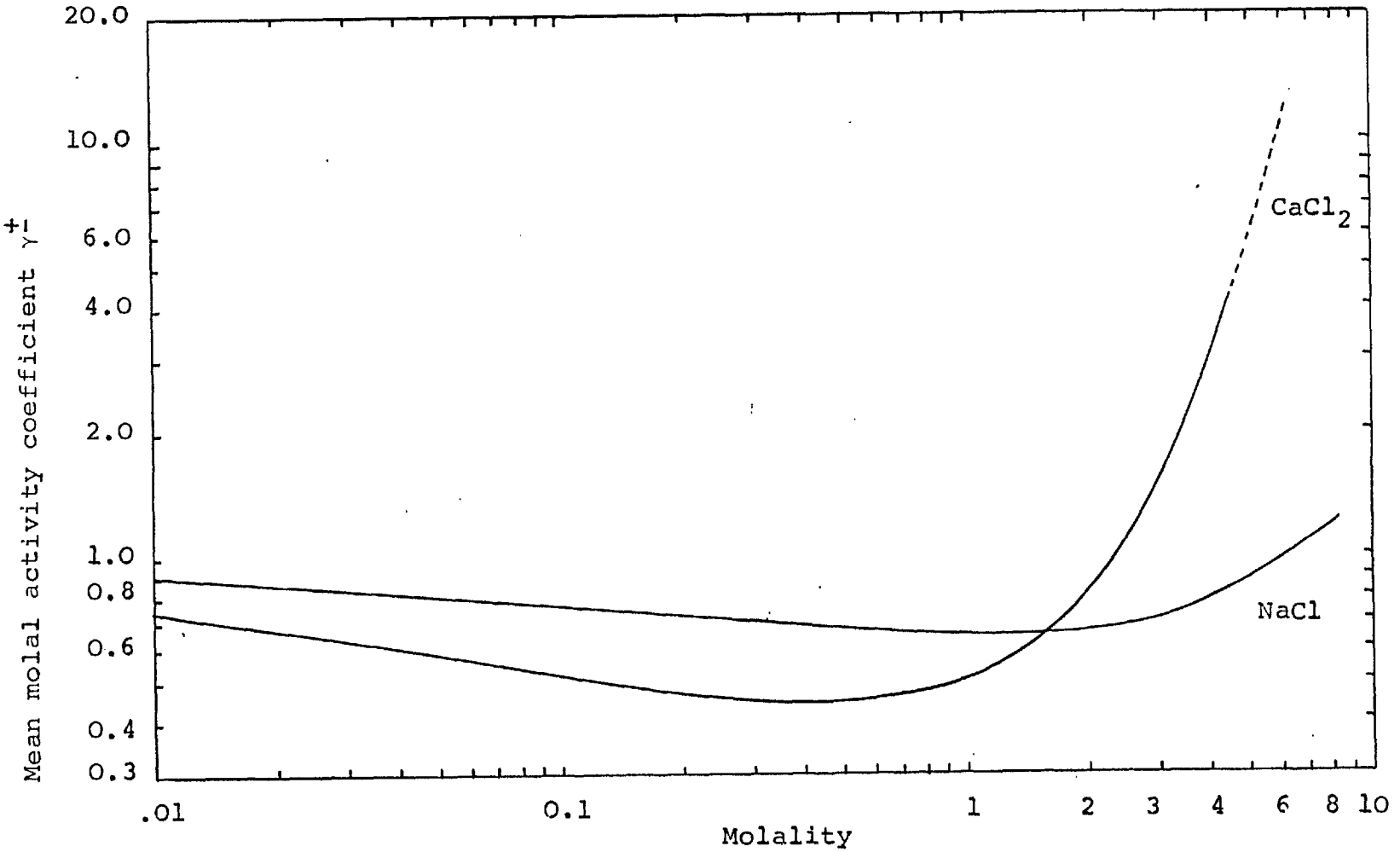

Figure 7. Mean molal activity coefficients used in data correlation

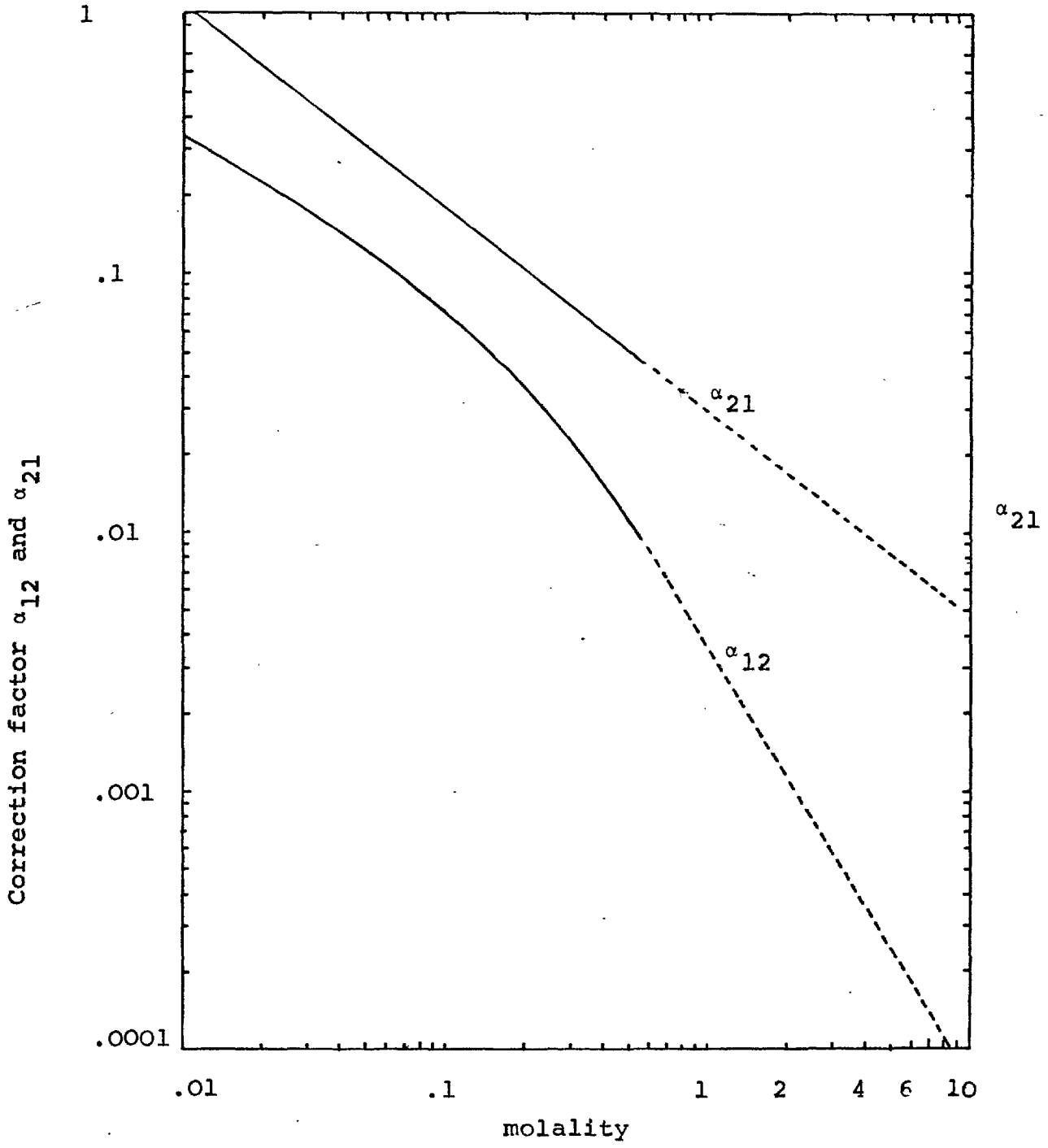

Figure 8. Relation of α_{12} and α_{21} to total molality of calcium chloride-sodium chloride solution

This approach would be expected to give a better correlation than the one represented by K_D and K_a in which the ratio of the activity coefficients in both phases is considered as unity but comparison of Figures (6) and (4) shows that the scatter in the data has infact increased. One may conclude that the ion exchange data for the system employed here cannot be interpreted according to the Donnan membrane equilibrium or the thermodynamic equilibrium based on Law of Mass Action where the activity coefficients of the aqueous phase are also considered in the formation of an expression representiing K_D or K_a.

In an attempt to increase the rigour of the treatment given above, Equation (33) representing the Donnan membrane equilibrium as well as the thermodynamic equilibrium constant was applied to correlate the experimental data. Equation (33) for a uni-divalent exchange system becomes

$$K_D = K_a = \frac{\bar{m}_A \; m_B^{\,2} \; \gamma_{\pm BY}^{\,4} \; \bar{\gamma}_{\pm AY}^{\,3}}{m_A \; \bar{m}_B^{\,2} \; \bar{\gamma}_{\pm BY}^{\,4} \; \gamma_{\pm AY}^{\,3}} \qquad (51)$$

The solution phase activities were obtained as described above. For the resin phase activity coefficients it was assumed that the activity coefficient in the resin phase may be represented by the activity coefficient of these same cations in an aqueous solution which is of the same ionic strength as that in the resin phase. It may be pointed out that molalities in the resin phase occured as high as 6.55, for which the corresponding activity coefficients were obtained by extrapolating the data of Moor and Ross (1965) for α_{12} and α_{21}.

The computed values of Equation (51) are given in Table 6. Figure 9 gives the variation of K_D or K_a with resin composition. The value of K_D or K_a in this

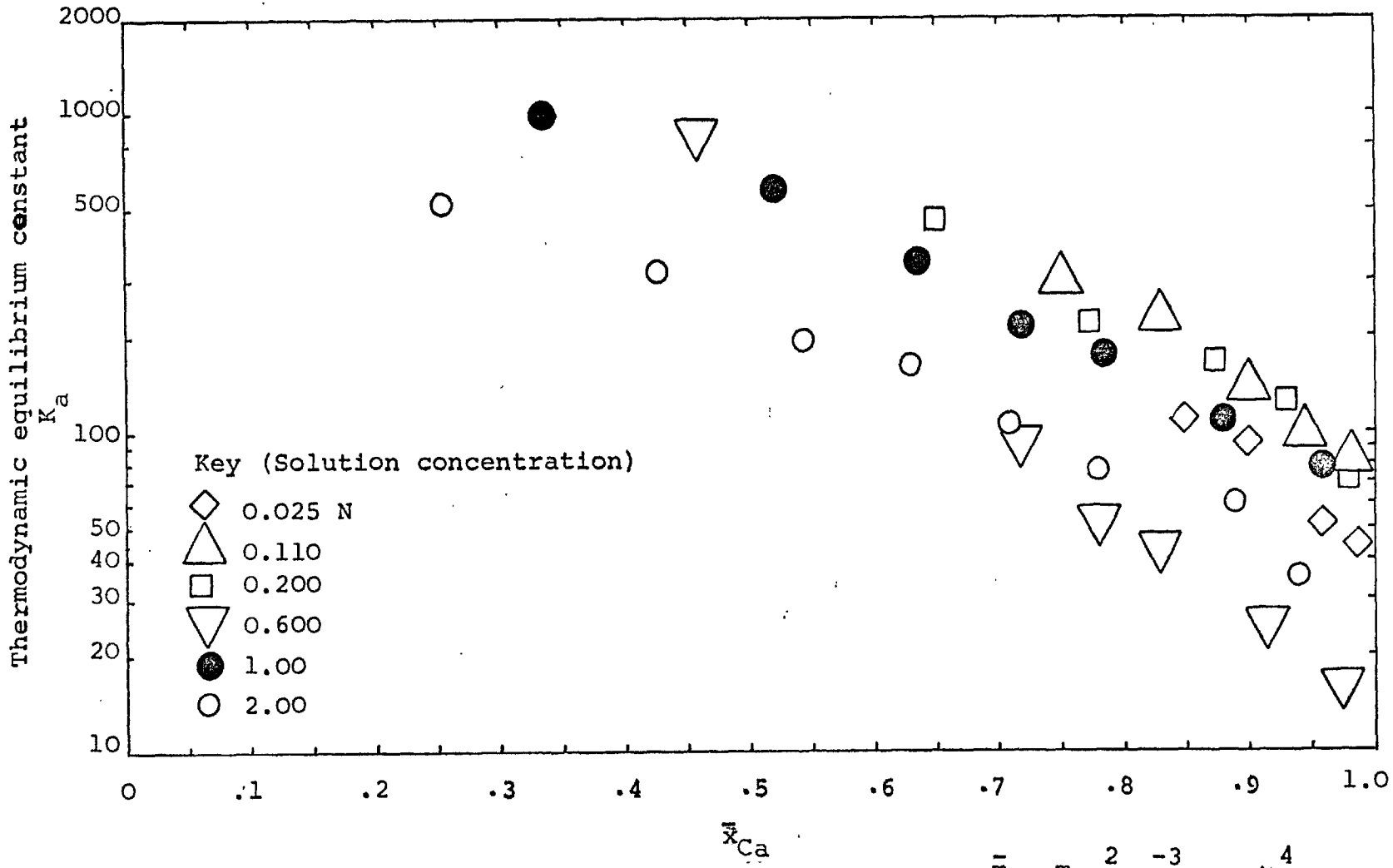

Figure 9. Correlation of data

$$K_a = \frac{\bar{m}_{Ca}\, m_{Na}^{\,2}}{m_{Ca}\, \bar{m}_{Na}^{\,2}} \; \frac{\gamma_{CaCl_2}^{-3}\, \gamma_{NaCl}^{4}}{\gamma_{CaCl_2}^{3}\, \gamma_{NaCl}^{-4}} = (K_D)$$

case shows a much greater variation. It is not a constant as one might expect but decreases with an increase of calcium in the resin phase. This approach seems to fail in correlating the data for the system under consideration and shows that the assumption made to calculate the resin phase activity coefficients is probably invalid.

Finally, Equation (25) representing the rational thermodynamic equilibrium constant was applied to correlate the data.

Value of ${}^{n}K_{a}$ for the sodium chloride-calcium chloride-Zeo-Karb 225, 8% DVB system have been obtained at various total solution concentration from a plot of

$$\log {}^{n}K_{a} = \int_{0}^{1} \log K \, d\bar{N}_{Ca} \qquad (25)$$

using the simple approximation as suggested by Reichenberg (1966);

$${}^{n}K_{a} = K\left[\bar{N}_{Ca} = 0.5\right] \qquad (26)$$

where $\bar{N}_{Ca}$ is the mole fraction of calcium in the resin phase and K is the equilibrium quotient defined by Equation (23).

Figure 10 shows that ${}^{n}K_{a}$ is nearly constant for one isotherm over the whole of resin composition, but changes with the total solution concentration.

Table 7. Values of rational thermodynamic equilibrium constant ${}^{n}K_{a}$ obtained from Figures 10.A and 10.B

No.	Total Solution Concentration N	${}^{n}K_{a} = K\left[\bar{N}_{Ca}=0.5\right]$
1	0.0110	17.60
2	0.200	17.60
3	0.600	16.50
4	1.00	10.30
5	2.00	4.90
6 (Bonner & Smith)	0.066-0.10	13.42

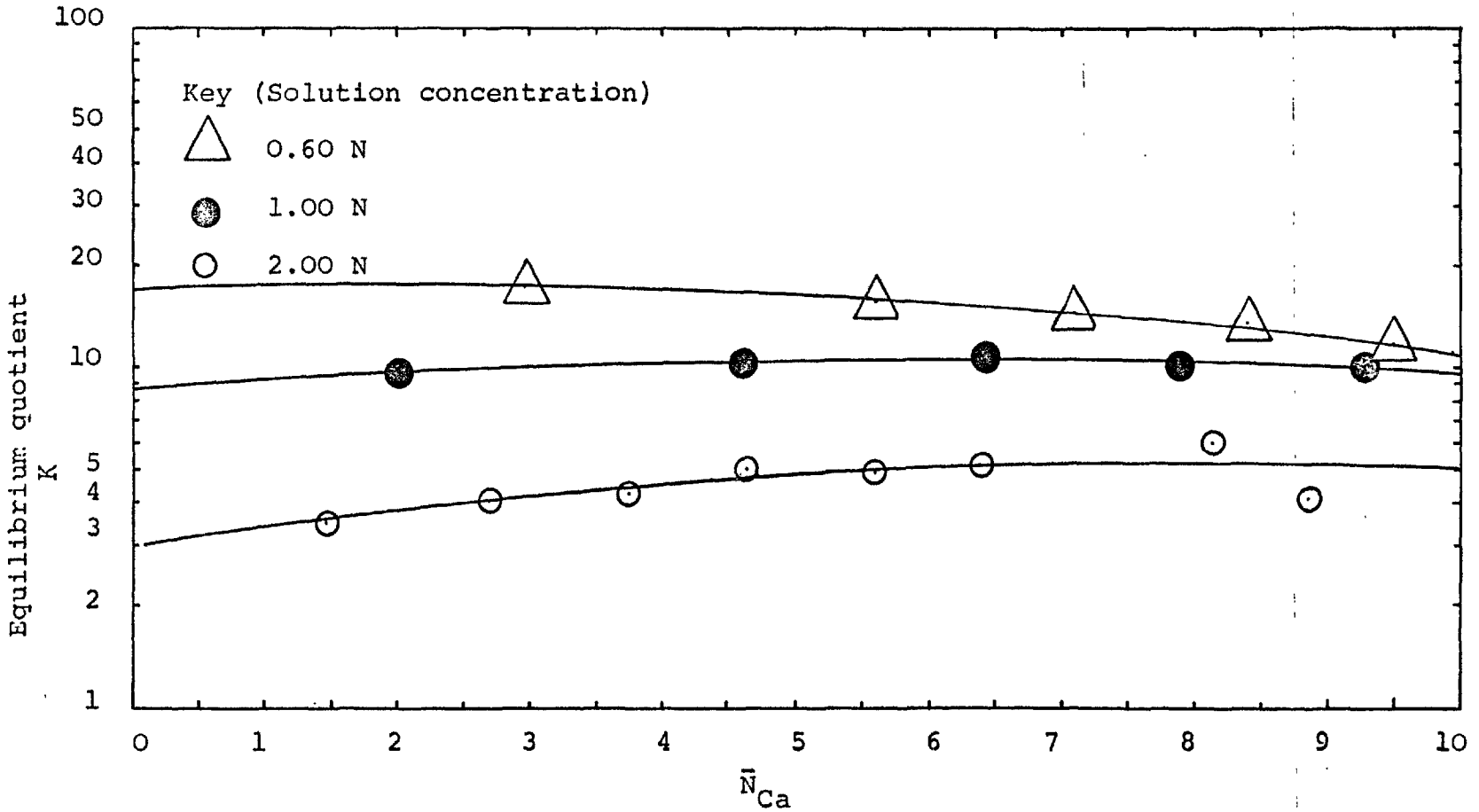

Figure 10.A Correlation of data for rational thermodynamic equilibrium constant

$$n_{K_a} = K\left[\bar{N}_{Ca} = 0.50\right]$$

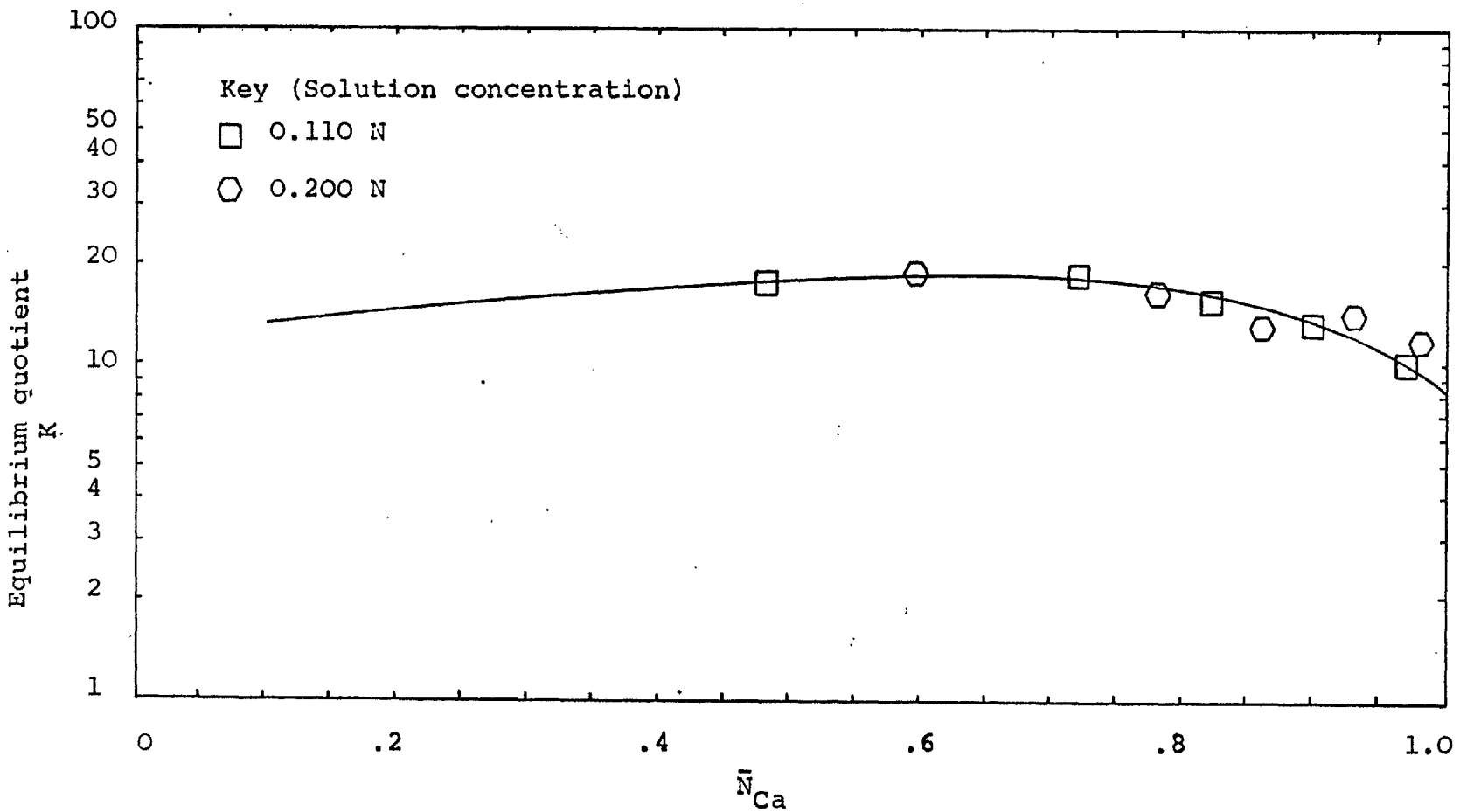

Figure 10.B Correlation of data for rational thermodynamic equilibrium constant

$$^{n}K_{a} = K\left[\bar{N}_{Ca} = 0.50\right]$$

The only value of ${}^{n}K_a$ available in literature for the system employed here is from Bonner and Smith (1957). They represented a uni-divalent exchange by the relation.

$$\tfrac{1}{2}AY + \bar{B} \rightleftharpoons BY + \tfrac{1}{2}\bar{A}$$

and the rational thermodynamic equilibrium constant was defined as

$${}^{n}K_a = \frac{m_B \; \bar{N}_A^{\frac{1}{2}} \; \gamma_{BY}^{2} \; \bar{\gamma}_{AR}^{3/2}}{m_A^{\frac{1}{2}} \; \bar{N}_B \; \gamma_{AY}^{3/2} \; \bar{\gamma}_{BY}^{2}} \qquad (52)$$

A comparison of Equations (21) and (52) would show that their ${}^{n}K_a$ is the square root of the ${}^{n}K_a$ as defined in the present work. Therefore, their value of ${}^{n}K_a$ has been calculated according to Equation (21) and compared with those obtained here (see Table 7). For example, the value of ${}^{n}K_a$ is

$${}^{n}K_a \text{ (Ca-Na)} = \frac{{}^{n}K_a \text{ (Ca-Li)}}{{}^{n}K_a \text{ (Na-Li)}} = \frac{(5.16)^2}{1.98} = 13.42 \qquad (53)$$

which is comparable with the value obtained in the present work. It may be pointed out that the value from the work of Bonner and Smith (1957) is for a solution of 0.1M (Ionic strength) which for a uni-divalent mixed electrolyte would correspond to 0.066 N to 0.1N depending upon the solution composition.

1.8. CONSLUSION

Equilibrium data for the system sodium chloride-calcium chloride-Zeo-Karb 225, 8% DVB resin has been obtained and correlated.

Various forms of the Donnan equilibrium theory and Law of MassAction have been applied to interpret the observed data. It has been found that the simplified form of the Donnan equilibrium constant defined as

$$K_D = \frac{\bar{m}_{Ca} \; m_{Na}^2}{\bar{m}_{Na}^2 \; m_{Ca}} \qquad (19)$$

gives the best approach to a single value parameter to predict ion exchange data for this system over a range of solution concentration. A close agreement between the experimental data and the theoretically predicted (for $K_D = 1.30$) has been obtained. The value of K_D obtained here is in agreement with the results calculated from the data of Bauman et al (1948) in their case K_D is 1.49 for about 1.71 N solution whilst for 0.030 N it is 1.13.

No improvement in the correlation could be achieved when activity coefficients of the species in the solution phase were included as a refinement. Inclusion of resin phase activities of the exchanging cations resulted in further scatter of the data. The assumption that resin phase activities can be represented by activities in a solution of the same cation and of the same ionic strength must be regarded with suspicion.

It has been shown that the column method and batch method give different equilibrium isotherms due to electrolyte sorption when washing is employed in the former method. In the design of a continuous ion exchange process the use of an isotherm obtained by the column method may lead to a considerable error when dealing with concentrated solutions.

The analytical technique of Atomic Absorption Spectroscopy has proved satisfactory and free from interference for the analysis of sodium-calcium solutions.

CHAPTER 2

DIFFUSION COEFFICIENT WITHIN ZEO-KARB 225

2.1. INTRODUCTION

Ion exchange is an interfacial mass transfer process. Ions diffuse from within a resin phase to a solution whilst an equivalent number of ions diffuse in the opposite direction. The rate of exchange may be controlled by either interdiffusion of counterions within the ion exchange bead (particle diffusion) or interdiffusion of counterions in the liquid film adhering to the particle (film diffusion) or by the rate of chemical exchange reaction. The latter is true for resins with chelating groups which form sluggish reacting complexes whereas for ordinary ion exchange resins particle diffusion and film diffusion are the potential rate determining steps. Generally, both mechanisms affect the rate of ion exchange but under special conditions the overall rate may be controlled by either of them. Ion exchange reactions in systems with small size beads and dilute solutions ($M < 0.03$) may be controlled by film diffusion (e.g., water softening) whereas particle diffusion is the controlling step in systems with large size beads and concentrated solutions ($M > 0.10$) as is usually the case in regeneration processes (Boyd, Schubert and Adamson 1947)

The rate of exchange in dilute solutions can often be represented by rate laws which incorporate an overall mass transfer coefficient which is itself expressed in terms of the diffusion coefficients of the exchanging ions in the aqueous phase. The diffusion coefficients of various ions in the solution phase have been measured for a large number of electrolytes (Robinson and Stokes 1950). They can also be predicted, for very dilute solutions from ionic conductance data.

Diffusion of ions in the resin phase is rather complex since the counterions have to diffuse through the pore liquid within the interior of a heterogeneous resin bead. The crosslinked polymer chains as well as specific interactions between the charged ions and the matrix due

to electrostatic attraction act as a barrier to the free movement of ionic species. So far ion exchange theories have assumed that the resin can be treated as a quasi-homogeneous phase. Such a simplifying assumption permits the use of an 'effective' diffusion coefficient within the resin phase which may be used in deriving apparent rate laws of ion exchange. Unlike the film diffusion coefficient, the diffusion coefficient within the resin phase cannot be predicted from first principles. However, attempts have been made to correlate the resin phase diffusion coefficient ($\bar{D}_i$) with the diffusion coefficient of the same ion in solution phase (D_i). Wheeler's (1951) and Mackie's (1955) models are based on the pore volume (tortuosity of the diffusion path) and do not consider the electrostatic interactions. Boyd's model (1947a) on the other hand is more rigorous and considers interactions but neglects the tortuosity of the diffusion path. In view of the lack of reliability in predicting the diffusion coefficient within the resin phase from first principles, accurate values are generally determined experimentally.

In the theoretical treatment ion exchange rates may be expressed by two models: Fick's Law and the Nernst-Planck model. The former is based on a constant interdiffusion coefficient $\bar{D}_{AB}$ and is strictly true for isotopic exchange or the exchange of counterions with equal diffusion coefficients. The Nernst-Planck model considers a variable interdiffusion diffusion coefficient $\bar{D}_{A-B}$ which depends on the trace ionic diffusion coefficients, valence and the relative amounts of the counterions within the resin. The trace ionic diffusion coefficient ($\bar{D}_A$) is defined as the self diffusion coefficient ($\bar{D}_{AA}$) of ion A when resin contains ion A in trace quantity and B as a major counterion. Fick's Law when applied to the exchange of counterions with unequal diffusion coefficient leads to two constant interdiffusion coefficients; $\bar{D}_{AB}$ and $\bar{D}_{BA}$ for the exchange reaction in the forward and reverse direction respectively. The Nernst-Planck model, however, gives a variable interdiffusion coefficient $\bar{D}_{A-B}$ which is independent of the

direction of exchange. Both the models have been widely tested for typical ion exchange reactions. It has been shown by Hering and Bliss (1963), James Kuo and David (1963) and Morig and Gopala Rao (1965) that both models are valid for the prediction of exchange reactions in which the resin is completely converted from one form to the other. However, for fractional conversions (stagewise contact) the use of Fick's Law with a constant interdiffusion coefficient is not valid and use of a variable interdiffusion coefficient is essential. The objective of the present study was, therefore, to determine the variable interdiffusion coefficient for the system sodium chloride-calcium chloride - Zeo-Karb 225, 8% DVB at various resin compositions.

It has been shown theoretically by Helfferich and Plesset (1958) and verified experimentally by Turner et al (1966) that $\bar{D}_{A-B}$ may be predicted from the knowledge of the valence, and trace ionic diffusion coefficients of the counterions for various resin compositions using the Nernst Planck model. This treatment assumes the constancy of the trace ionic diffusion coefficient in which case it may be replaced by the self-diffusion coefficient $\bar{D}_{AA}$ (Here $\bar{D}_{AA}$ is defined as the diffusion coefficient with which ion A^* on the resin exchanges with its isotope A in the solution phase). This simplifying assumption makes the situation simpler since the self-diffusion coefficient $\bar{D}_{AA}$ is easy to determine by isotopic redistribution technique whilst the determination of trace ionic diffusion coefficient requires special analytical techniques. Boyd and Soldano (1954) have shown that this assumption may not be true particularly in highly crosslinked resins (16% DVB), where $\bar{D}_{AA}$ is itself a function of resin composition.

From the preceeding paragraph it is evident that to predict the interdiffusion coefficient it is necessary to determine the trace ionic diffusion coefficient of the individual ions in the system. A series of experimental runs were therefore carried out to determine the trace

ionic diffusion coefficients of sodium and calcium in Zeo-Karb 225 resin. Self-diffusion coefficients of calcium and sodium ions within the resin phase have also been determined using the radiotracer technique. The comparison of the trace ionic diffusion coefficient ($\bar{D}_A$) and the self-diffusion coefficient ($\bar{D}_{AA}$) gives the variation of the latter with resin composition. In case the variation of $\bar{D}_{AA}$ with resin composition is negligible, self-diffusion coefficients can also be used to predict the interdiffusion coefficient as a function of resin composition employing the Nernst-Planck model.

2.2. THEORY

Ion exchange is a diffusion controlled process and to describe the rate of exchange it is necessary to write flux equations for each of the diffusing species and integrate under the appropriate initial and boundary conditions.

2.2.1. Isotopic Exchange

The driving force for the flux of an ionic species within the resin phase consists of the concentration gradient of the species and the gradient of the electrical potential. The latter may be neglected in the case of isotopic exchange.

Consider an ion exchange reaction between resin in A^* form and solution containing the counterion A. Here A^* refers to an isotope of A. The flux equation for the exchange can be written as

$$J_A = -\bar{D}_{AA} \nabla \bar{C}_A \qquad (54)$$

where J_A is the flux of ion A (moles/sec. cm^2)

$\bar{C}_A$ is the concentration of ion A within the resin phase (moles/cm^3)

$\bar{D}_{AA}$ is the self-diffusion coefficient of ion A within the resin phase (cm^2/sec)

∇ represents the vector differential operator.

The rate of change of resin phase composition is related with the flux through the equation of Law of conservation of mass, also known as continuity equation;

$$\frac{\partial \bar{C}_A}{\partial t} = -\nabla J_A \qquad (55)$$

$$= -\bar{D}_{AA} \nabla^2 C_A \qquad \text{(Fick's Law)} \qquad (56)$$

where t is time in seconds.

Combination of Equations (54) and (56) for systems with spherical geometry and assuming constant $\bar{D}_{AA}$ gives

$$\frac{\partial \bar{C}_A}{\partial t} = -\bar{D}_{AA} \left(\frac{\partial^2 \bar{C}_A}{\partial r^2} + \frac{2}{r} \frac{\partial \bar{C}_A}{\partial r} \right) \qquad (57)$$

where r is radial space coordinate.
The above equation has been solved analytically for both the constant boundary (Barrer 1941) and variable boundary (Patterson 1947) conditions, and can be employed for the interpretation of experimental rate data from isotopic exchange or exchange of ions of equal diffusion coefficient within the resin phase.

2.2.2. Ion Exchange

The fluxes of the ions are coupled for exchange reactions involving two ions with markedly different diffusion coefficients in the resin phase. Such reactions cannot be rigorously represented by Equation (54). In addition, other factors such as the selectivity of the ion exchanger, specific interactions, electrolyte sorption and changes in swelling pressure complicate the situation.

Consider a system where the diffusion coefficient of the exchanging ions within the resin phase are not equal;

$$z_A B^{z_B} + z_B \bar{A}^{z_A} \rightleftharpoons z_B A^{z_A} + z_A \bar{B}^{z_B} \qquad (1)$$

The flux of ion A and B due to concentration gradient is

$$J_A = -\bar{D}_A \nabla \bar{C}_A \qquad (58)$$

and $$J_B = -\bar{D}_B \nabla \bar{C}_B \qquad (59)$$

where $\bar{D}_A$ and $\bar{D}_B$ are the trace ionic diffusion coefficients

of ion A and B respectively. It has been shown by Helfferich and Plesset (1958) that counterdiffusion of ions with different diffusion coefficients will generate electric potential gradients in the resin. These potential gradients are generated due to the tendency of the faster ions to diffuse at a higher rate than the slower counterions. To maintain electroneutrality in the system, the electric field generated by the diffusion process retards the diffusion of the faster ion and accelerates the slower ion such that the net fluxes of the counterions remain equivalent to one another.

The effect of the electric potential gradient generated can be accounted for by applying the Nernst-Planck equation for the fluxes of the two ions;

$$J_A = (J_A)_{diff.} + (J_A)_{el.} \tag{60}$$

where $(J_A)_{diff.}$ is the flux of ion A due to concentration gradient. $(J_A)_{el.}$ is flux of ion A due to electrical potential gradient and J_A is the net flux of ion A. For an ionic species A the flux due to electric potential gradient is

$$(J_A)_{el.} = -u_A z_A \bar{C}_A \nabla \varphi \tag{61}$$

where u_A is the mobility of the ion A and is related to the diffusion coefficient of the species by the Nernst-Einstein equation.

$$u_A = \frac{\bar{D}_A \mathcal{F}}{RT} \tag{62}$$

Combination of Equations (58), (60), (61) and (62) gives for ion A

$$J_A = -\bar{D}_A \left(\nabla \bar{C}_A + z_A \bar{C}_A \frac{\mathcal{F}}{RT} \nabla \varphi\right) \tag{63}$$

where $\mathcal{F}$ is Faraday constant, R is gas constant and T is absolute temperature. Similarly for ion B

$$J_B = -\bar{D}_B \left(\nabla \bar{C}_B + z_B \bar{C}_B \frac{\mathcal{F}}{RT} \nabla \varphi\right) \quad (64)$$

Electroneutrality for the system requires

$$z_A \bar{C}_A + z_B \bar{C}_B = \text{constant} \quad (65)$$

and in the absence of any electric current

$$z_A J_A + z_B J_B = 0 \quad (66)$$

Hence combining the two Equations (63) and (64) for counterions and eliminating the electric potential by use of Equations (65) and (66);

$$J_A = -\left[\frac{\bar{D}_A \bar{D}_B \left(z_A^2 \bar{C}_A + z_B^2 \bar{C}_B\right)}{\bar{D}_A z_A^2 \bar{C}_A + \bar{D}_B z_B^2 \bar{C}_B}\right] \nabla \bar{C}_A \quad (67)$$

The quantity in square brackets is termed the interdiffusion coefficient $\bar{D}_{AB}$ and is dependent not only on the trace ionic diffusion coefficients of the counterions, but also on their relative concentrations. Thus Equation (67) may be written as

$$J_A = -\bar{D}_{AB} \nabla \bar{C}_A \quad (68)$$

which when combined with the material balance Equation (55), for spherical geometry becomes

$$\frac{\partial \bar{C}_A}{\partial t} = \frac{1}{r^2} \frac{\partial}{\partial r} \left(r^2 \bar{D}_{AB} \frac{\partial \bar{C}_A}{\partial r}\right) \quad (69)$$

Equation (69) is non-linear and has so far not been solved analytically. A computer programme originally developed by Helfferich (1964) has been extended in this study to solve it numerically for various boundary conditions (For details of the programme see Appendix 5).

The method of numerical solution of Equation (69) is almost identical with the theoretical treatment of unsteady state heat transfer by conduction within a sphere which is heated on the outer surface by convection (Mickley, Sherwood and Reed 1957). Contrary to the situation in heat transfer the interface composition between the two phases is not equal but related by the equilibrium isotherm. The numerical solution gives theoretical exchange rate as a function of time for given values of $\bar{D}_A/\bar{D}_B$ and z_A/z_B. A matching technique using both the theoretical and the experimental rate curves, has been employed to calculate the diffusion coefficient of an ion within the resin phase.

In the derivation of Equation (67) it has been assumed that the $\bar{D}_A$ and $\bar{D}_B$ (trace ionic diffusion coefficients of ion A and B) remain constant, there is no sorption and swelling changes during exchange are negligible. However, for real systems deviations from ideal behaviour can be expected.

2.3. TECHNIQUES FOR THE DETERMINATION OF THE DIFFUSION COEFFICIENT IN THE RESIN PHASE

The experimental techniques for the determination of the diffusion coefficient of a counterion within the resin phase involves contacting a known amount of resin in A form with a solution BY of known concentration. Two methods are usually employed.

In the batch method the rate of exchange as a function of time can be obtained by measuring the change in the composition of either the resin or the solution phase in a well stirred vessel. The latter, being more convenient, is generally employed (Boyd, Schubert and Adamson 1947, Turner et al. 1966). The ratio of the total number of equivalents of counterions in each phase i.e. $\bar{C}_o\bar{V}/C_oV$ determines the boundary conditions which exist during the exchange process. Here $\bar{V}$ refers to the volume of the resin (ml) and $\bar{C}_o$ is the exchange capacity (meq/ml). In the case of finite solution volume the boundary conditions for the resin beads change as the exchange progresses. When the solution volume is infinite ($\bar{C}_o\bar{V} \ll C_oV$) it corresponds to constant boundary conditions.

An alternative method involves the shallow bed technique; an excess of solution volume of known concentration containing BY is passed through a shallow bed of resin beads in A form. The rate of change of effluent composition is recorded. It corresponds to the infinite solution volume condition provided the solution is passed through the bed at a steady high flow rate to maintain constant boundary conditions. The experimental conditions are maintained such that resin phase diffusion controls the exchange rate. Large size beads, high rate of stirring and concentrated solution (greater than 0.03M) provide such conditions (Boyd, Schubert and Adamson 1947).

Two analytical techniques have been widely used for the analysis of the solution phase. Measurement of the change in conductivity of the aqueous solution in contact with resin is accurate and convenient. The only drawback is that

ionic conductivity is extremely sensitive to temperature variation and thus requires careful temperature control. The technique has been employed successfully, however, for batch as well as for continuous measurements (for example Turner et al 1966) but is limited to systems in which the counterions have markedly different mobilities in solution e.g.systems containing hydrogen and other cations are feasible. For systems containing counterions of similar ionic conductance, this technique does not offer any advantage over the alternative radiotracer method.

In the radiotracer technique, the change in composition of the solution phase is obtained by measuring the change in radioactivity of the solution phase. Usually, an isotope is released by the resin during the exchange reaction. This measurement can be performed in two ways; either continuously by passing the solution through a suitable counter or by drawing aliquots of solution for subsequent radiometric analysis. The latter method is accurate and more easily achieved (Boyd and Soldano 1954) and has been employed in this work. The continuous method is much less accurate since the integration time for counting is usually small resulting in poor statistical accuracy in the data unless relatively large amounts of radioactivity are employed. In the batch method the counting time of each sample can be varied to minimize statistical errors.

In view of the desirability of a continuous analytical technique and because of the limitations in the aforementioned methods a new experimental technique was developed for the measurement of trace elements in solution.

2.4. DEVELOPMENT OF A NEW ANALYTICAL TECHNIQUE

Solutions containing trace quantities (up to 20 mg/litre) of sodium or calcium were analysed using a Unicam SP-90 atomic absorption spectrophotometer (AAS). The operation and the principles of the instrument have already been described (Section 1.5.2.).

The technique was adapted for continuous recording of the change in solution composition with time. A solution sample was continuously drawn into the flame of the instrument through a fine capillary immersed in the reaction vessel and the output signal recorded on a Y-t plotter. The curve gave light absorption as a function of time. This can be transposed to a concentration-time curve using the appropriate calibration curve.

Individual samples were also taken by batch sampling during an exchange run and analysed separately using AAS.

In the continuous runs the solution contained trace quantities of A in the presence of a large (1N) excess of ion B. All the standard solutions for the calibration curve were, therefore, prepared in 1N solution of B which was also used as the blank solution. A typical output signal recording is shown in Figure 11.

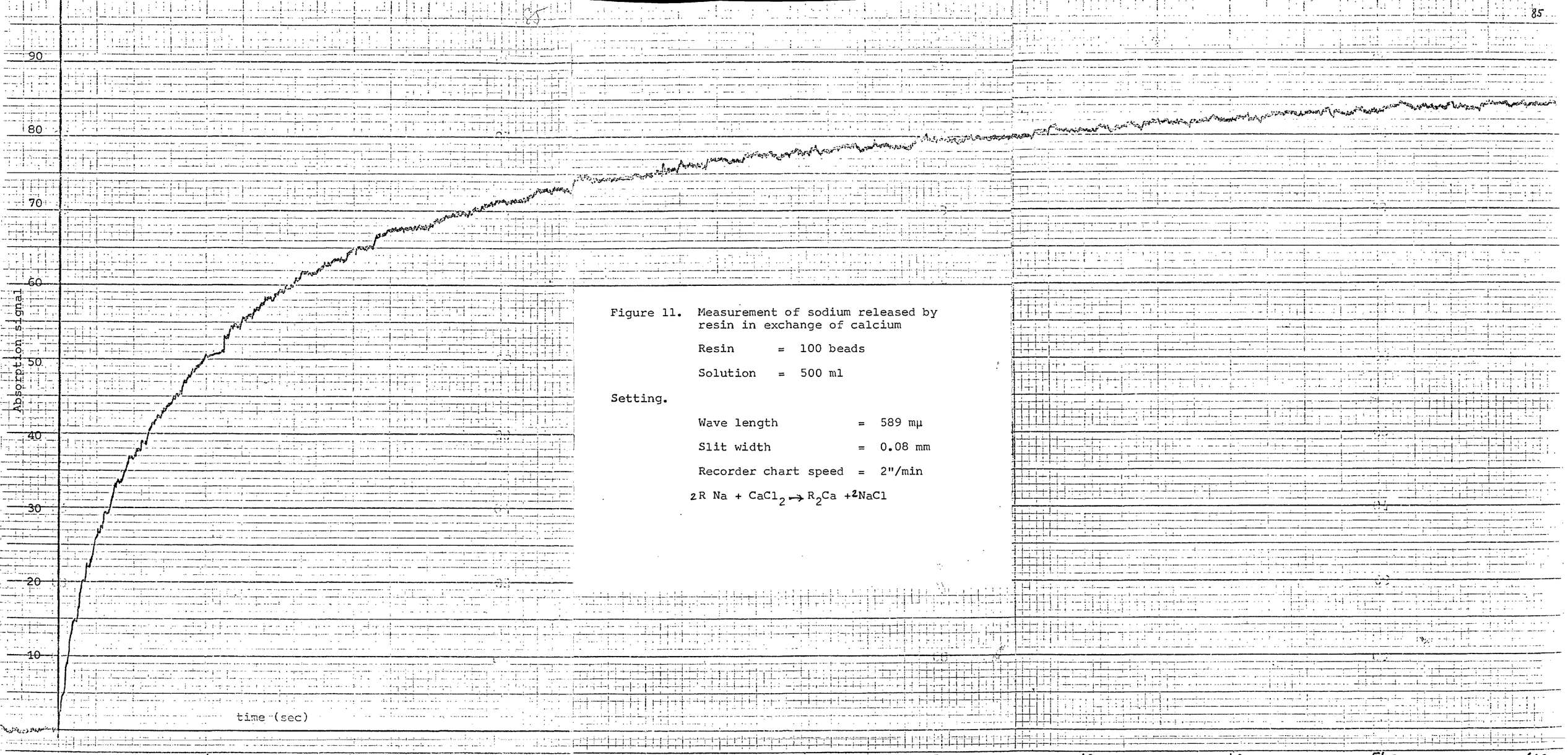

Figure 11. Measurement of sodium released by resin in exchange of calcium

Resin = 100 beads

Solution = 500 ml

Setting.

Wave length = 589 mμ

Slit width = 0.08 mm

Recorder chart speed = 2"/min

$$2R\,Na + CaCl_2 \rightarrow R_2Ca + {}^{2}NaCl$$

2.5. EXPERIMENTAL

2.5.1. Resin Preparation

Diffusion in the resin phase is highly dependent on bead size and thus it was necessary to obtain a fine cut of uniformly sized spherical beads for the experimental work. This was done by fluidizing a narrow size range of the resin sample in a glass column of 2.5 cm. internal diameter using tap water at a flow rate of about one lit/min. Small beads were elutriated by the fluidizing stream of water and were discarded whilst the remaining beads were collected for use. Two such batches were prepared one in sodium form and the other in calcium and stored under water for experimental runs. Measurement of the average radius of the wet beads from each batch was done on a microscope using a magnification of X50. About 400 beads from each batch were measured. Size distribution and calculation of an average size of the bead is shown in Appendix 4 .

2.5.2. Apparatus

The experimental apparatus used in this study is shown in Figure 12. It consists of a beaker and a stirrer arrangement fitted with a thermometer. The whole set-up as shown in Figure 12 was kept in a water bath maintained at 25^{o}C. A paddle stirrer was employed to mix the contents of the beaker. During the continuous runs solution was drawn through a capillary tube from a glass tube surrounded with a nylon mesh bag at the end which was immersed in the solution. This avoided the withdrawal of resin beads and the formation of a central vortex and improved mixing of the solution.

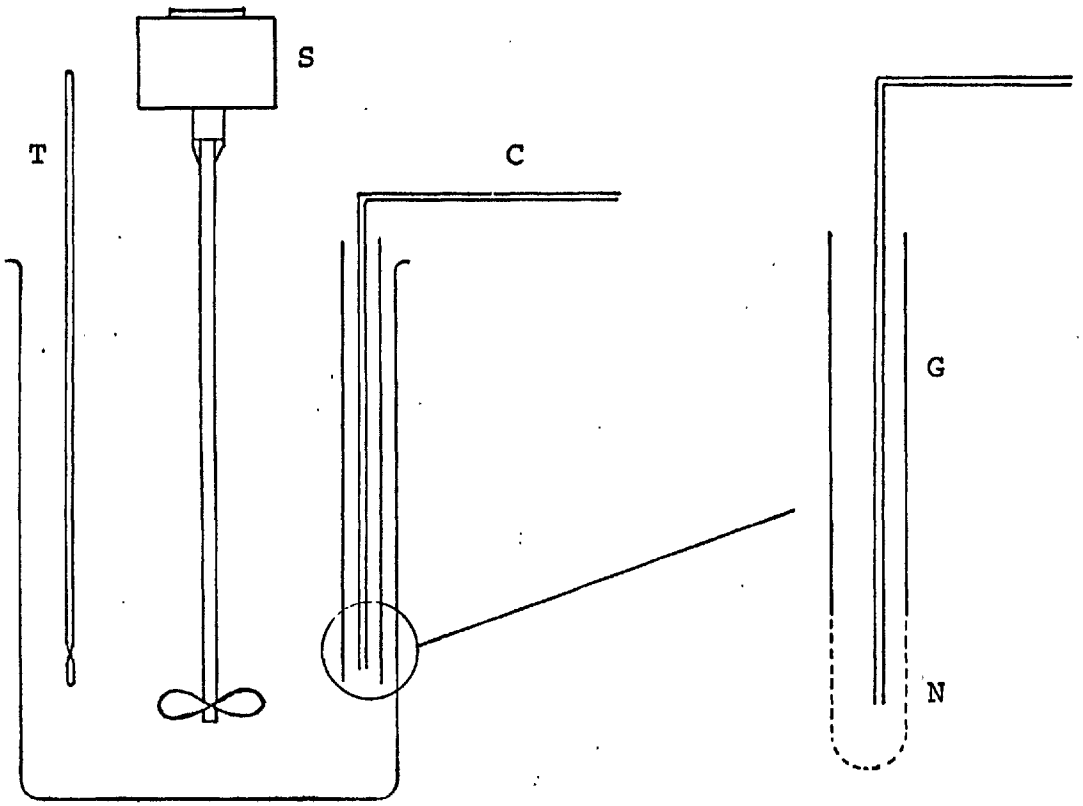

Figure 12 Apparatus used in this study

C - Capillary to draw sample into the AAS
S - Stirrer, T - Thermometer, G - Glass tube, N - Nylon mesh.

2.5.3. Ion Exchange Runs

2.5.3.A. Finite Solution Volume (Batch Method)

For each run, 5.0 ml. of Zeo-Karb 225, 8% DVB resin of known composition was accurately measured and centrifuged to remove interstitial water. The resin was then placed in a beaker containing 20.0 ml of deionised water, stirred at 750 r.p.m. and allowed to reach isothermal equilibrium in a water bath maintained at 25°C. The exchange reaction was initiated by rapidly adding 20.0 ml. of an electrolyte solution (2N) to the beaker, ensuring that this solution was also at 25°C. The total solution concentration after mixing was 1.0 N. The reaction zero time was taken when half of the electrolyte had been added. The total time taken for addition of electrolyte was about 2-3 seconds.

Aliquots of 0.10 ml. were drawn from the beaker at predetermined times, using a syringe. The time taken for each sampling was about 1-2 seconds. At the end of the run all the samples were analysed by AAS for both sodium and calcium after appropriate dilution. From the analysis of the samples a plot of fractional approach to equilibrium as a function of time was obtained.

2.5.3.B. Infinite Solution Volume (Continuous Method)

In the case of infinite solution volume ($\bar{C}\bar{V} \ll CV$), the measurement of solution concentration was carried out continuously.

About 0.1 ml. (100 beads) of Zeo-Karb 225, 8% DVB resin of known composition was taken in a beaker with 375 ml. of demineralised water at 25°C, and fitted with a stirrer. After thermal equilibrium had been attained, 125 ml. of electrolyte solution (4N) was rapidly added to the beaker, ensuring that this solution was also at 25°C. The recorder chart attached to the atomic absorption

spectrophotometer was started when half of the solution had been added. Solution was continuously withdrawn by a capillary and the flame absorption was recorded as a function of time (see Figure 11). The total time for a complete run varied from 800 to 1500 seconds. Continuous recording was carried out for the first 600-720 seconds since longer times resulted in the partial blockage of the flame head. The samples for the latter part of the run were than analysed by withdrawing aliquots at known intervals of time and separately measuring their composition. From an analysis of the solution at the end of each run a plot between fractional approach to equilibrium as a function of time was obtained using a calibration chart for the ion under consideration. A calibration curve and a plot between F and t are shown in Figures 13 and 14, for the reaction.

$$2NaR + CaCl_2 \longrightarrow CaR_2 + 2NaCl$$

2.5.4. Isotopic Exchange Finite Solution Volume (Batch Method)

For the determination of the self-diffusion coefficient of calcium and sodium in Zeo-Karb 225, 8% DVB resin the apparatus and the procedure was similar to the one described in Section 2.5.3.A.

The resin sample, loaded with the radiotracer was contacted with a solution of the same cation and of known concentration. Aliquot s of 50 µl were withdrawn from the /the solution in/beaker at predetermined time intervals and analysed by nucleonic counting.

2.5.5. Radiometric Analysis

2.5.5.A. Calcium

The low energy beta particle from Ca-45 was measured using a liquid scintillation β-counter. The scintillant was prepared in the laboratory by mixing toluene and

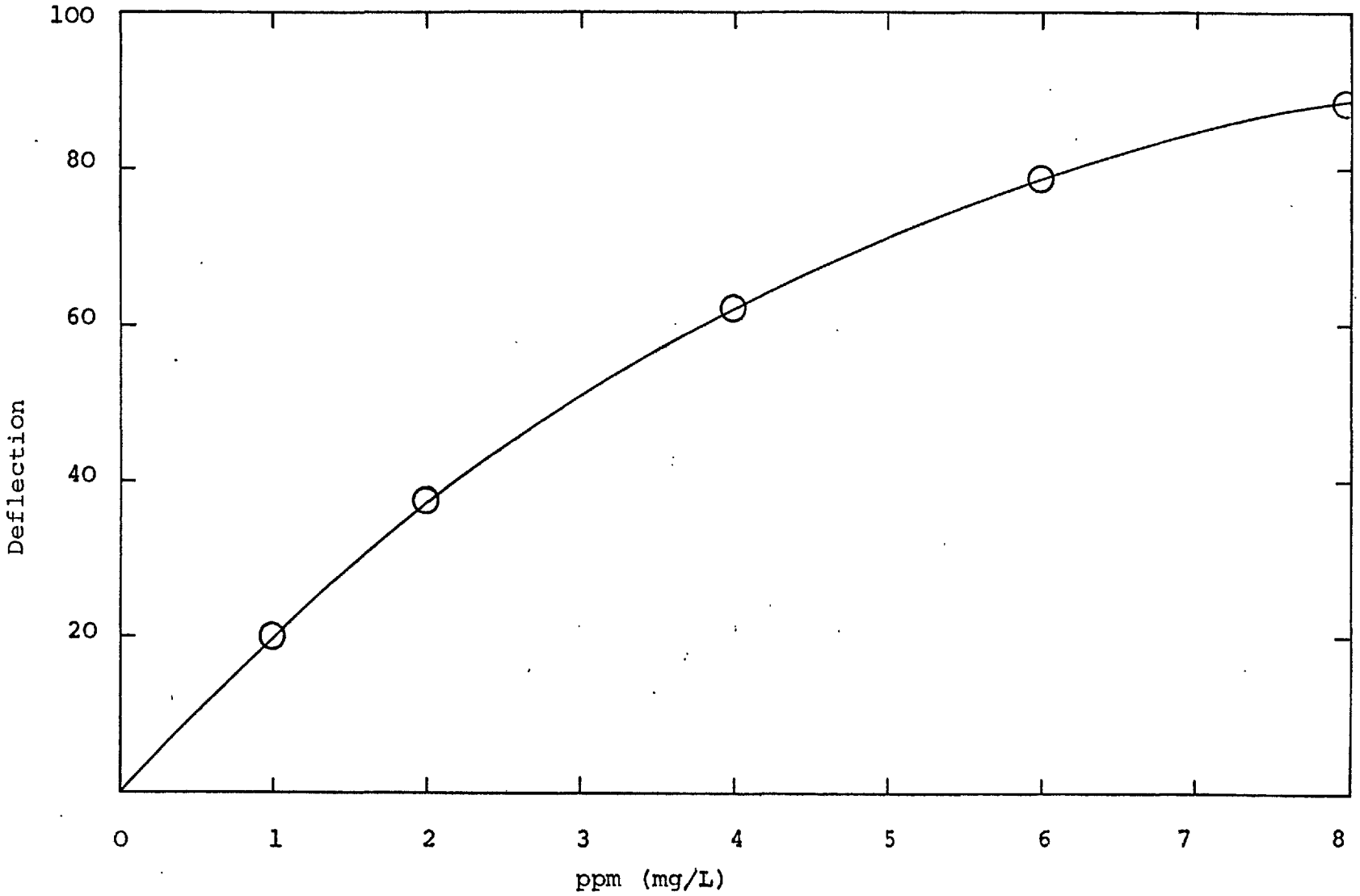

Figure 13. Calibration curve for sodium

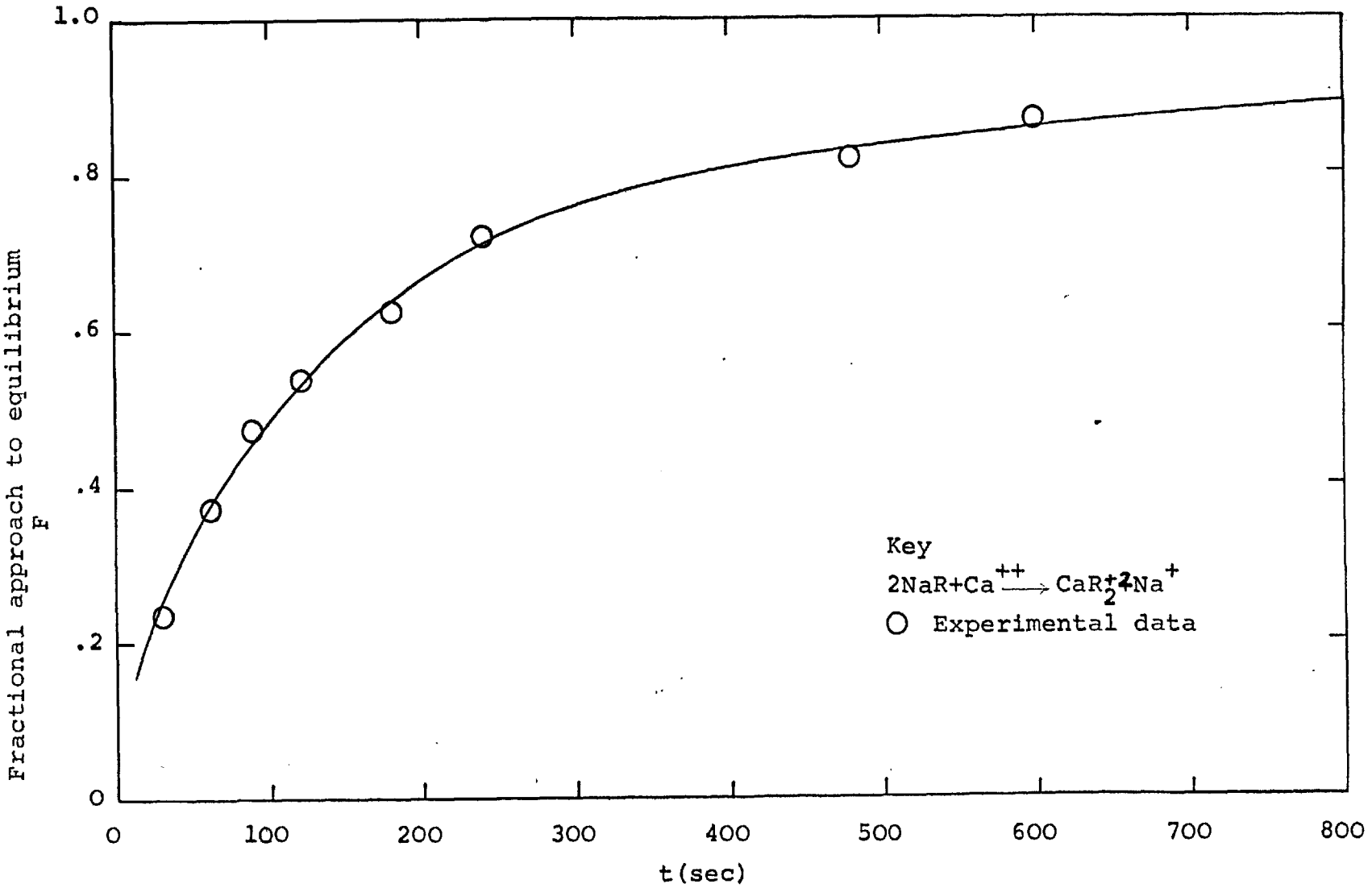

Figure 14. Representation of experimental data obtained from Figure11.

Triton X-100 (See footnote)*in the ratio of 2:1 (V/V) and followed by the addition of 0.4% (W/V) of PPO (2,5 - Diphenyloxazole). The scintillant, first used by Patterson and Green (1965), gave a clear emulsion when 4 ml. of it was used for each sample.

The beta particles of 250 keV energy emitted by Ca-45 excite the scintillant which returns to the ground state by emitting light photons. These photons cause an avalanche of electrons through the photomultiplier tube giving a voltage pulse. The number of pulses is dependent on the number of disintegrations of the active sample. Since the half life of Ca-45 is 165 days and the total time of each run was about 120min. no decay correction was applied.

2.5.5.B. Sodium

In the case of sodium the γ-activity of sodium (1.37 MeV, 2.75 MeV) was measured employing a 4 $\bar{\Lambda}$ - geometry scintillation counter with a solid state Lithium drifted germanium detector. The last sample from each run was counted between every two consecutive samples withdrawn during that run. An average of the count rate of the last sample obtained before and after each sample was used to calculate the fractional approach to equilibrium for that particular sample. This technique avoided any decay correction which would otherwise be required.

* Iso-octyl phenoxy polyethoxy ethanol containing 10 moles of ethlene oxide.

2.6. CORRELATION OF THE EXPERIMENTAL DATA

2.6.1. Average Radius of the Resin Beads

The average radius of the resin beads in the sodium form was derived from an analysis of resin size distribution obtained by microscopic measurement. An arithmetic average resin bead radius of 396 beads was found to be 0.04702 cm. The second batch of resin, used for experiments in which resin sample was initially in calcium from, gave an average radius of 0.050 cm. Preliminary studies of size measurement of resin in different ionic forms revealed that a very small change in radius of the bead occurs with a change in its ionic form. The resin bead radius increases by 1.2% when the calcium form is converted to sodium form. Therefore, no correction has been applied for this change in the bead size.

2.6.2. Calculation of the Self-Diffusion Coefficient

The experimental results of the isotopic diffusion runs were interpreted using Fick's Law (Equation 56). The following procedure was used in order to determine $\bar{D}_{Na-Na}$ and $\bar{D}_{Ca-Ca}$.

1. All the experimental data was plotted as F (t) vs t where F represent the fractional approach to equilibrium;

$$F(t) = \frac{A(t)}{A(\infty)} \qquad (70)$$

where A(t) refers to the radioactivity of the solution withdrawn at time t and A(∞) the radioactivity of the solution withdrawn at the end of the run.
A smooth curve was drawn through these data points and fitted to a polynomial of the form,

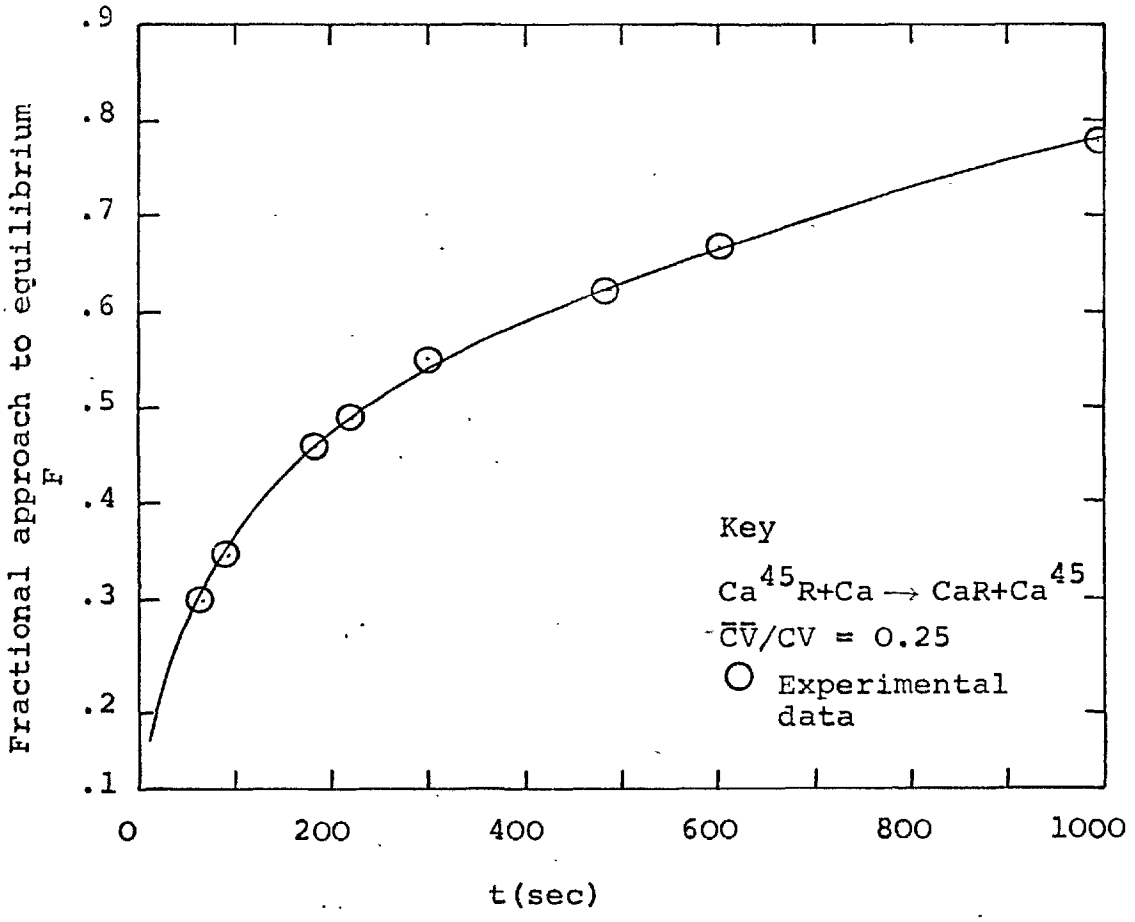

Figure 15.A Experimental rate curve for isotopic exchange

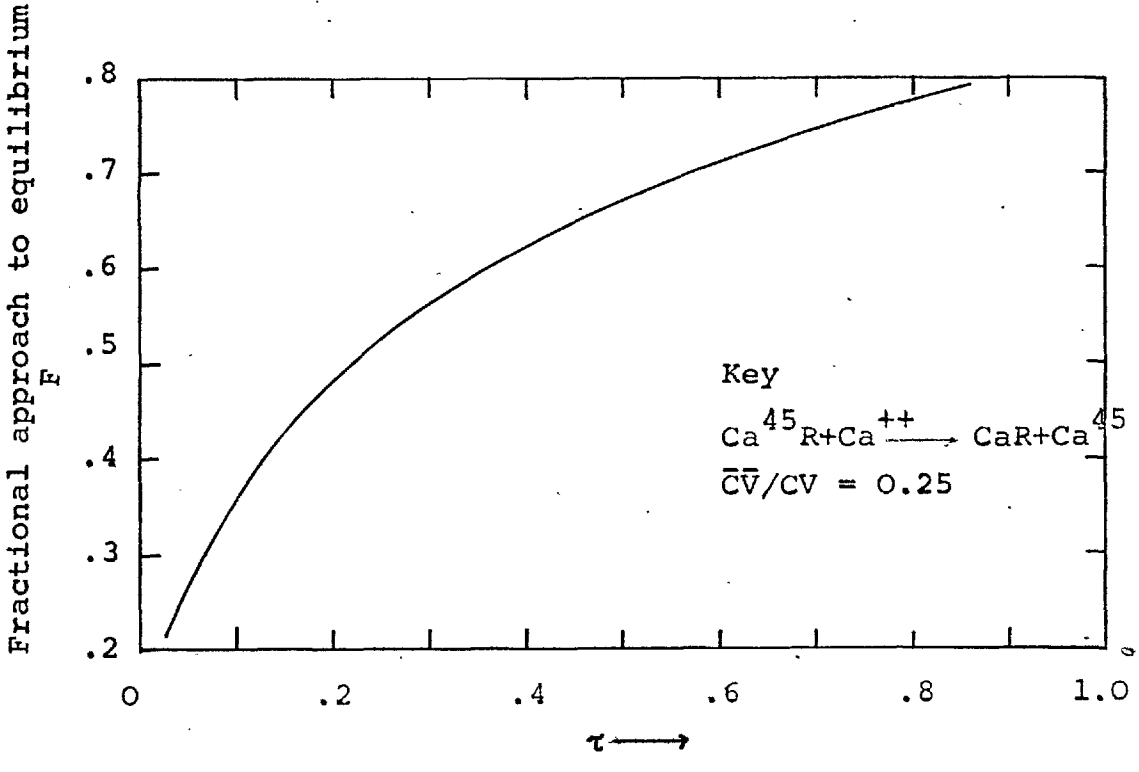

Figure 15.B Theoretical rate curve for isotopic exchange

$$t = AF^{n} + BF^{n-1} + \cdots + P \qquad (71)$$

using a least square analysis of the data points on the curve. A standard subroutine POLYFIT, obtainable from the computer library of the department, was employed for this purpose (See Figure 15A).

2. The theoretical rate curves for the isotopic exchange for variable boundary condition were obtained from the numerical solution of Equation (57). Here Helfferich's general computer programme (1964) which solves Equation (69) for variable diffusion coefficient was adapted with appropriate values of z_A, z_B and for $\bar{D}_A/\bar{D}_B = 1$ in which case equations (57) and (69) become identical. The computed results have been found in agreement with the published data (Helfferich 1962, p.585) based on the analytical solution of Equation (57) (See Figure 15.B)

3. The general computer programme was extended by subroutine CROSPLOT to calculate the self-diffusion coefficient of the ion under consideration by matching the values of observed time 't' and the computed time 'τ' for the same value of F (See Appendix 5 for CROSPLOT subroutine). The dimensionless time 'τ' is defined as

$$\tau = \bar{D}_{AA}\, t/r^2 \qquad (72)$$

where r is the radius of the bead. The self-diffusion coefficient was then obtained by substituting the value of r, t and τ in the Equation (72). The values of the self-diffusion coefficients obtained as described above are

$$\bar{D}_{Na\text{-}Na} = 8.848 \times 10^{-7} \quad cm^2/sec$$

$$\bar{D}_{Ca\text{-}Ca} = 2.26 \times 10^{-7} \quad cm^2/sec$$

4. Finally a comparison between the experimental data and the theoretical rate curves for sodium and calcium based on these values of the self-diffusion coefficients are shown in Figures 16 and 17, Tables 8 and 9.

2.6.3. Calculation of the Trace Ionic Diffusion Coefficient

The following procedure was employed for the calculation of the trace ionic diffusion coefficient of sodium and calcium from an interpretation of experimental data obtained for mutual exchange under constant boundary conditions.

From the recorder chart shown in Figure 11 and the analysis of the solution at the end of a run, a plot between F and t was obtained. Here F refers to the fractional approach to equilibrium and is defined as

$$F(t) = C_A(t)/C_A(\infty) \qquad (73)$$

where $C_A(t)$ is the concentration of ion A in solution at time t and $C_A(\infty)$ is the concentration of ion A in solution at equilibrium.

The rate curve thus obtained was fitted to a polynomial. For the computation of the theoretical rate curve between F and τ, the Nernst-Planck model represented by Equation (69) with variable interdiffusion coefficient was employed.

The numerical solution of Equation (69) can proceed by a finite difference method if the values of z_A/z_B and $\bar{D}_A/\bar{D}_B$ are specified for a given set of boundary conditions. Assuming that the trace ionic diffusion coefficients are constant for complete exchange in forward and reverse directions (Hering and Bliss 1963) it is possible to evaluate $\bar{D}_A$ and the ratio $\bar{D}_A/\bar{D}_B$ by a cross-plot technique.

Consider the exchange reaction:

$$z_B A^{z_A} + z_A \bar{B}^{z_B} \rightleftharpoons z_A B^{z_B} + z_B \bar{A}^{z_A}$$

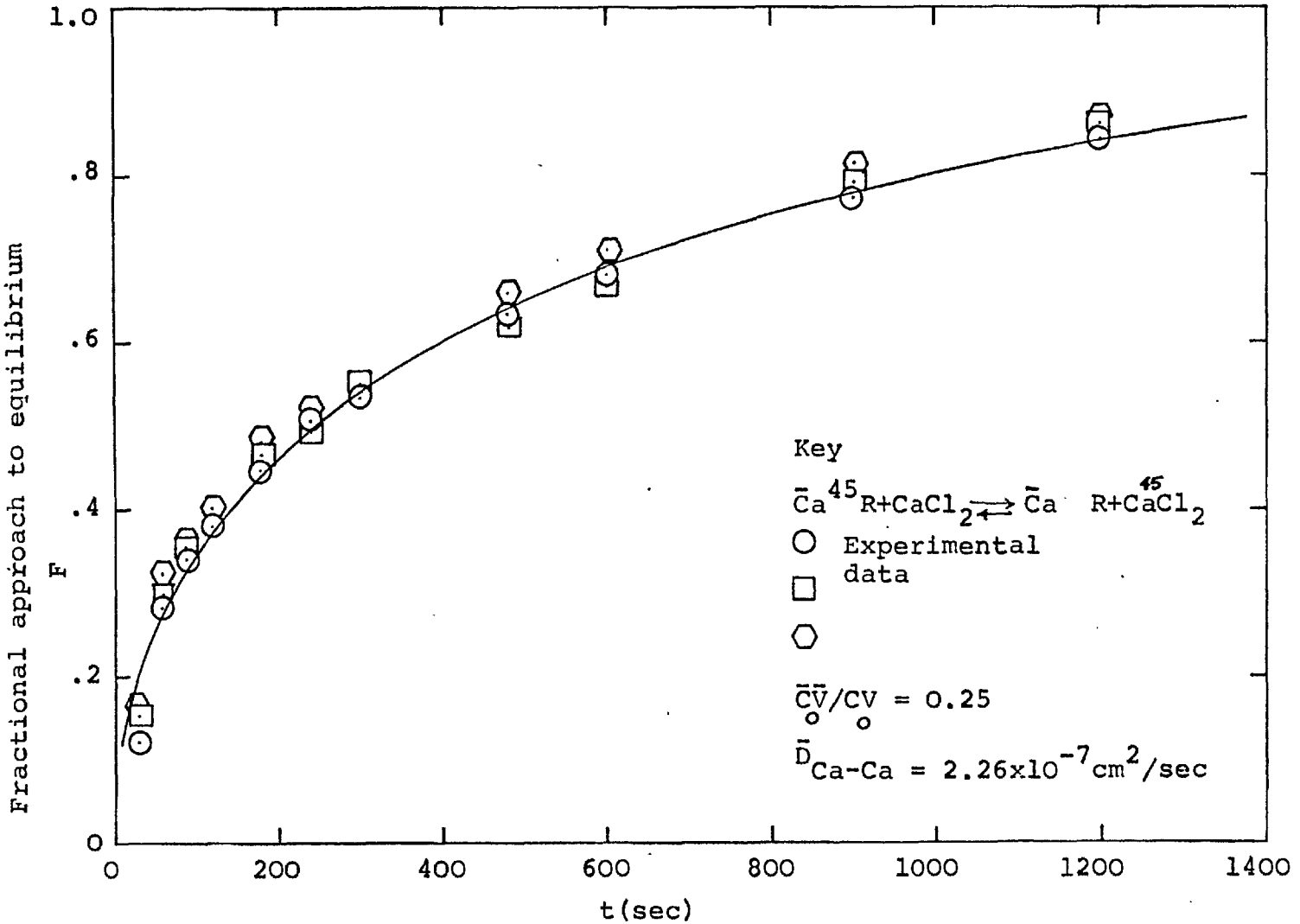

Figure 16. Correlation of data. Isotopic exchange of calcium on Zeo-Karb 225, 8% DVB

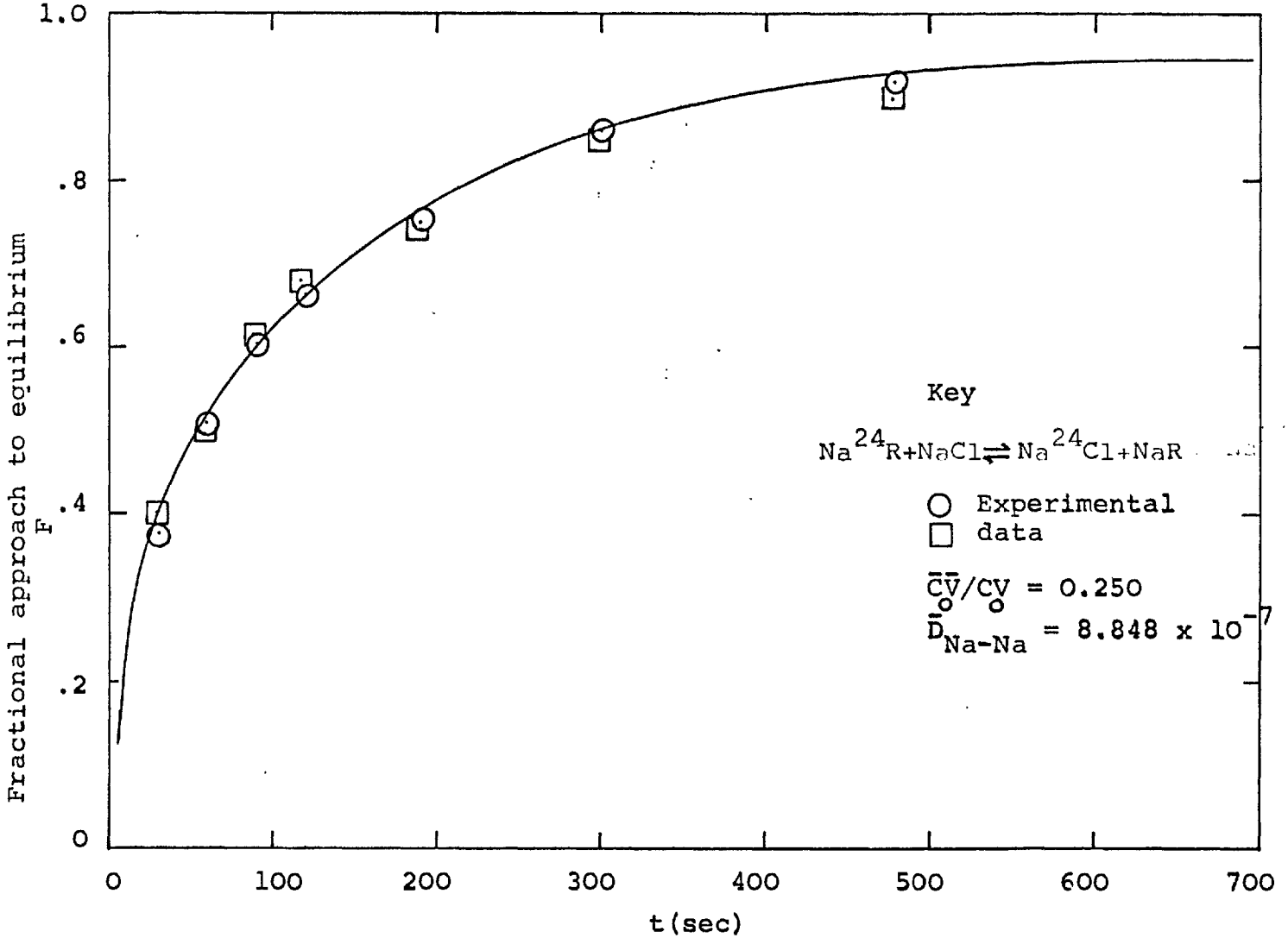

Figure 17. Correlation of data. Isotopic exchange of sodium on Zeo-Karb 225, 8% DVB

Table 8. Fractional approach to equilibrium vs Time
Isotopic exchange of Sodium

r = 0.0470 cm.

Fick's Law

$\bar{C}\bar{V}/C_oV = 0.25$

t = 25°C

F	τ	$t_{obs.}$ sec	$\bar{D}_{Na} \times 10^{-7}$ cm^2/sec	$*t_{cal.}$ sec
0.263	0.00473	11.80	8.85	11.80
0.355	0.00946	24.30	8.60	23.60
0.420	0.01419	36.50	8.57	35.40
0.472	0.01893	48.50	8.65	42.00
0.514	0.02366	59.50	8.80	58.80
0.551	0.02839	70.00	8.94	71.00
0.583	0.03310	81.30	9.02	82.50
0.611	0.03780	92.50	9.05	94.00
0.637	0.04250	104.00	9.03	106.00
0.660	0.04740	115.00	9.00	118.00
0.735	0.06630	165.00	8.83	166.00
0.789	0.0852	213.00	8.83	212.00
0.832	0.1041	258.00	8.89	259.00
0.865	0.1230	306.00	8.88	307.00
0.891	0.1420	360.00	8.73	354.00
0.912	0.1610	420.00	8.49	402.00

Average 8.848

* $t = \frac{\pi^2 \tau}{\bar{D}_{Na}}$ where $\bar{D}_{Na\text{-}Na} = 8.848 \times 10^{-7}$ cm^2/sec

Table 9. Fractional approach to equilibrium vs Time
Isotopic exchange of Calcium

R = 0.050

Fick's Law

$\bar{C}\bar{V}/C_oV_o = 0.25$

t = 25°C

F	τ	$t_{obs.}$ sec	$\bar{D}_{Ca} \times 10^{-7}$ cm^2/sec	$*t_{cal.}$ sec
0.263	0.00473	40.50	2.92	52.30
0.355	0.00946	81.00	2.92	104.50
0.420	0.01419	158.10	2.24	156.50
0.472	0.01893	211.20	2.24	208.50
0.514	0.02366	270.80	2.18	261.20
0.551	0.02839	320.00	2.21	312.80
0.583	0.03310	379.50	2.18	366.55
0.611	0.03780	431.50	2.19	417.45
0.637	0.04250	490.00	2.17	470.10
0.660	0.04740	547.05	2.16	523.75
0.735	0.06630	760.00	2.18	732.50
0.789	0.08520	979.20	2.17	942.80
0.832	0.10410	1152.45	2.25	1150.00
0.865	0.12300	1439.35	2.14	1366.00
0.891	0.14200	1600.00	2.22	1572.00
0.912	0.16100	1835.75	2.20	1784.45
Average			2.26	

$*t = a^2.\tau/\bar{D}_{Ca}$ where $\bar{D}_{Ca-Ca} = 2.26 \times 10^{-7}$ cm^2/sec

Two experimental curves of F (fractional approach to equilibrium) against t (time in seconds) were obtained for the forward and reverse reaction. This data was fitted to a polynomial function using the subroutine POLYFIT.

Equation (69) was solved for the values $z_A/z_B = 2/1$ and for values of α ($\bar{D}_A/\bar{D}_B$) arbitrarily chosen as 1, 1/3.5 and 1/10. Tables of F against τ were obtained, where $\tau = \bar{D}_A t/r^2$ (See Table 10, 11). Using a curve matching technique, average values of $\bar{D}_A$ could be calculated for each value of α in both the forward and reverse direction using subroutine CROSPLOT. Plotting $\bar{D}_A$ against α yielded a cross-plot with an intersection at the appropriate value of $\bar{D}_A$ and α if the underlying assumptions are justified (See Figure 18). The values of $\bar{D}_A$, $\bar{D}_B$ and α obtained for the mutual exchange of sodium and calcium under constant boundary conditions are

$$\bar{D}_{Na} = 8.54 \times 10^{-7} \quad cm^2/sec$$

$$\bar{D}_{Ca} = 2.252 \times 10^{-7} \quad cm^2/sec$$

and $\alpha = 3.8$

Finally a comparison of the experimental data and the theoretical rate curve for $\alpha = 3.8$ was made to check the variable diffusion coefficient model (Figures 19, 20 and Tables 12 and 13).

The same procedure as described above was employed to calculate the trace ionic diffusion coefficient of sodium and calcium for the mutual exchange under variable boundary conditions. The computed values of $\bar{D}_{Na}$, $\bar{D}_{Ca}$ and α are

$$\bar{D}_{Na} = 7.96 \times 10^{-7} \quad cm^2/sec$$

$$\bar{D}_{Ca} = 2.11 \times 10^{-7} \quad cm^2/sec$$

and $\alpha = 3.8$

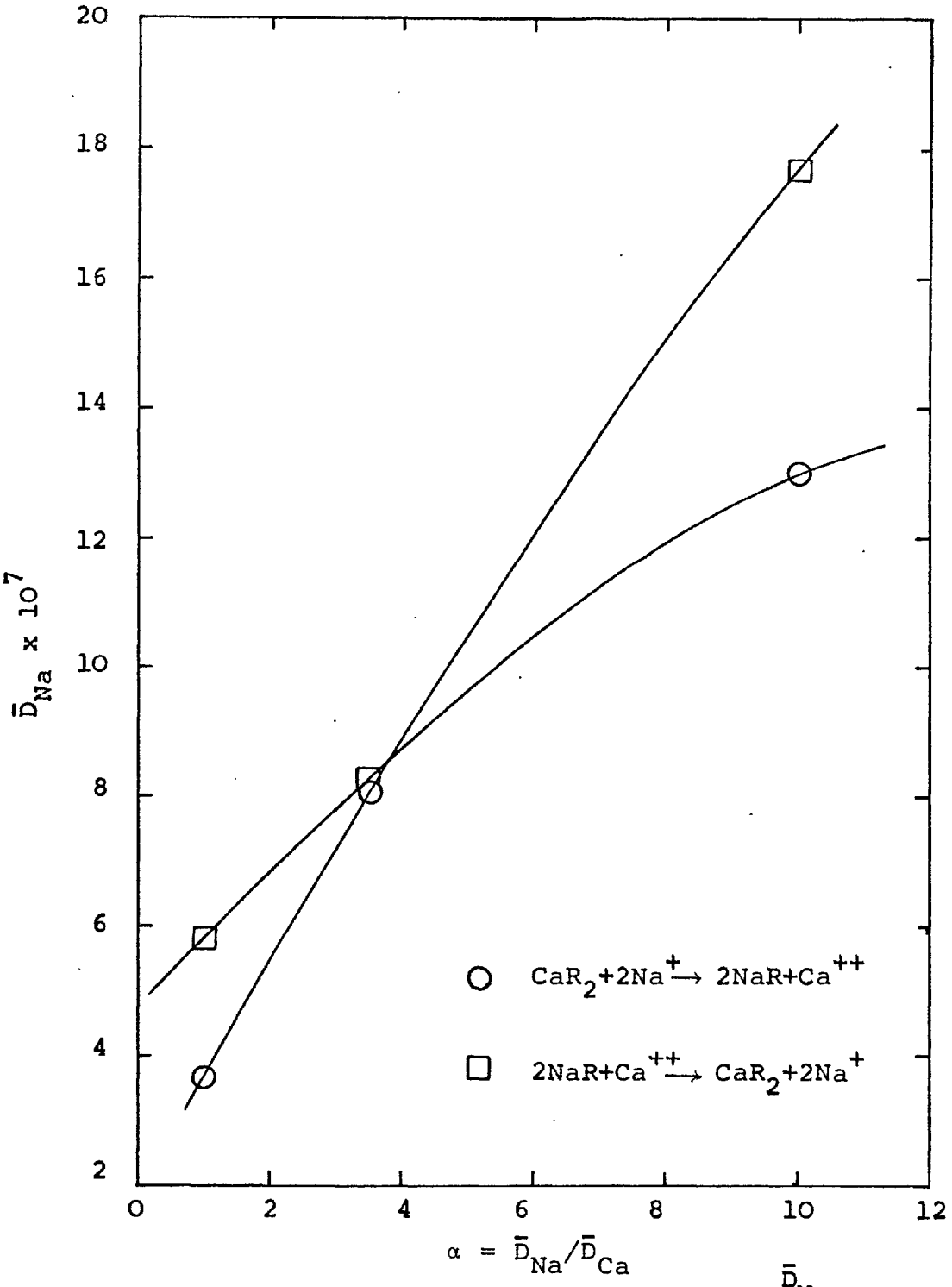

Figure 18. Variation of $\bar{D}_{Na}$ with $\left(\frac{\bar{D}_{Na}}{\bar{D}_{Ca}}\right)$ for forward and reverse exchange under constant boundary conditions

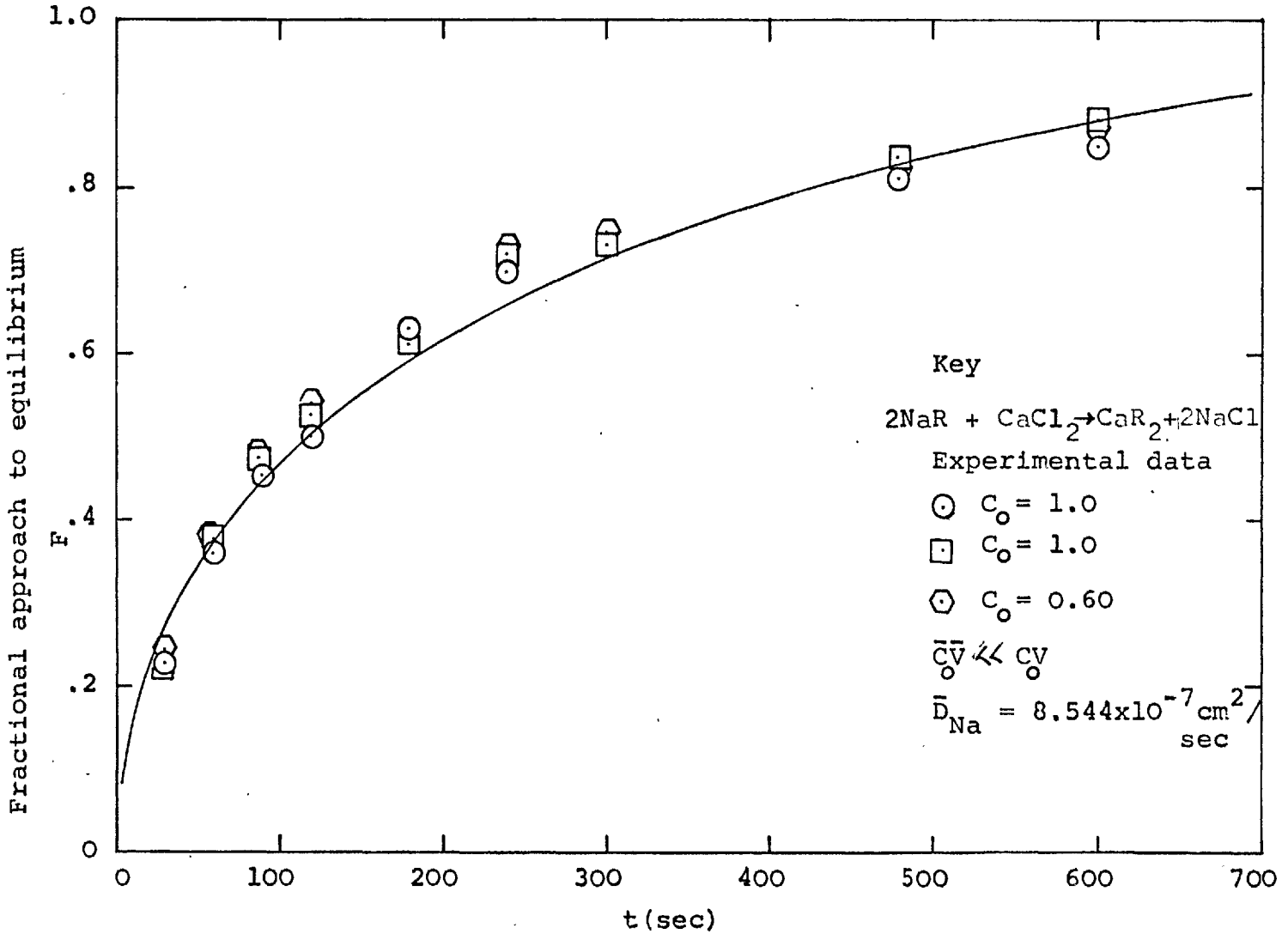

Figure 19. Correlation of data, Nernst Planck Model for complete conversion

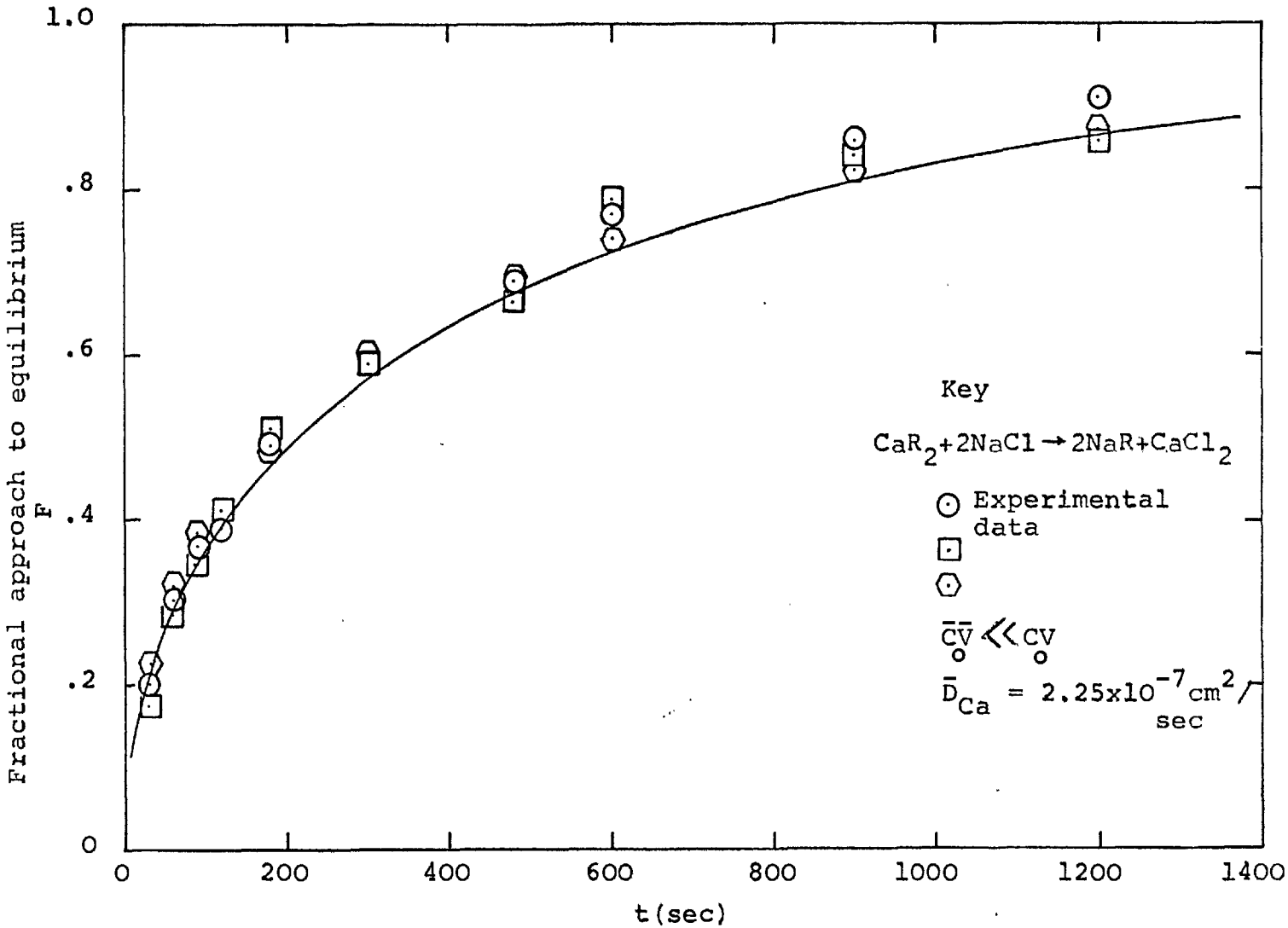

Figure 20. Correlation of data, Nernst Planck Model, complete conversion

Table 10. Fractional approach to equilibrium vs dimensionless time: Nernst Planck Model

$z_A/z_B = \frac{1}{2}$

r = 0.047 cm.

Constant boundary conditions

Resin initially in sodium form, complete conversion to calcium form.

F	$\bar{D}A/\bar{D}B$ $\frac{1}{\tau}$	$\bar{D}_{Na}$ x10^7cm^2/sec	F	$\bar{D}A/\bar{D}B$ $\frac{3.5}{\tau}$	$\bar{D}_{Na}$ x10^7cm^2/sec
0.219	0.00473	3.69	0.181	0.00473	5.15
0.301	0.00946	4.93	0.251	0.00946	6.12
0.361	0.01419	5.62	0.302	0.01419	7.36
0.409	0.01893	5.72	0.344	0.01893	8.15
0.450	0.02366	5.70	0.380	0.02366	8.42
0.485	0.02839	5.78	0.412	0.02839	8.44
0.516	0.03312	5.96	0.440	0.03312	8.40
0.545	0.03794	6.21	0.466	0.03785	8.41
0.637	0.05687	7.07	0.489	0.04258	8.50
0.704	0.07580	6.78	0.511	0.04731	8.67
0.759	0.09509	6.06	0.532	0.05214	8.89
0.887	0.17080	5.72	0.602	0.07106	9.90
0.947	0.24650	6.73	0.658	0.08999	10.23
			0.705	0.10892	9.70
			0.746	0.12821	8.86
			0.858	0.20392	7.54
			0.924	0.27962	8.24
Average		5.84			8.29

* $\tau = \bar{D}_A \times t/d^2$

Table 10. Fractional approach to equilibrium vs dimensionless time: Nernst Planck Model

$z_A/z_B = \frac{1}{2}$

r = 0.0470 cm.

Constant boundary conditions

Resin initially in sodium form, complete conversion to calcium form

F	$\frac{\bar{D}A/\bar{D}B}{10^{\tau}}$	$\bar{D}_{Na}$ x10^7cm^2/sec
0.142	0.00473	7.83
0.242	0.01419	9.63
0.307	0.02366	12.04
0.358	0.03312	13.31
0.400	0.04258	13.50
0.454	0.05678	13.38
0.470	0.06151	13.41
0.499	0.07097	13.61
0.513	0.07570	13.78
0.574	0.09945	15.00
0.615	0.11838	15.84
0.651	0.13730	16.10
0.712	0.17516	14.93
0.822	0.27016	11.67
0.925	0.42156	12.02
Average		12.98

Table 11. Fractional approach to equilibrium vs dimensionless time: Nernst Planck Model

$z_A/z_B = 2$

r = 0.050 cm.

Constant boundary conditions

Resin initially in calcium form, complete conversion to sodium form.

F	$\bar{D}A/\bar{D}B$ 1 τ	$\bar{D}_{Ca}$ x10^{7}cm^2/sec	F	$\bar{D}A/\bar{D}B$ 3.5 τ	$\bar{D}_{Ca}$ x10^{7}cm^2/sec
0.219	0.00473	3.03	0.153	0.00135	1.38
0.301	0.00946	3.60	0.211	0.00268	1.80
0.36115	0.01419	3.70	0.254	0.00400	2.04
0.409	0.01893	3.69	0.290	0.00533	2.17
0.450	0.02366	3.66	0.320	0.00665	2.24
0.485	0.02839	3.65	0.346	0.00798	2.27
0.516	0.03312	3.66	0.370	0.00931	2.28
0.545	0.03794	3.68	0.392	0.01063	2.28
0.637	0.05687	3.78	0.412	0.01196	2.28
0.704	0.07580	3.84	0.431	0.01330	2.28
0.759	0.09509	3.88	0.448	0.01464	2.28
0.887	0.17080	3.82	0.465	0.01599	2.28
0.947	0.24650	3.68	0.481	0.01736	2.28
			0.496	0.01874	2.29
			0.510	0.02013	2.29
			0.524	0.02158	2.30
			0.572	0.02720	2.35
			0.614	0.03306	2.39
			0.652	0.03918	2.44
			0.686	0.04573	2.49
			0.718	0.05275	2.53
			0.748	0.06051	2.57
			0.833	0.09066	2.67
			0.891	0.12528	2.72
			0.933	0.16811	2.76
Average		3.67			2.31

Table 11. Fractional approach to equilibrium vs dimensionless time: Nernst Planck Model

$z_A/z_B = 2$

r = 0.050 cm.

Constant boundary conditions

Resin initially in calcium form, complete conversion to sodium form

F	$\bar{D}A/\bar{D}B$	$\bar{D}_{Ca}$
	$10\frac{}{\tau}$	$x10^7 cm^2/sec$
0.147	0.00095	1.02
0.203	0.00187	1.33
0.262	0.00327	1.58
0.294	0.00420	1.67
0.321	0.00514	1.72
0.346	0.00610	1.74
0.369	0.00712	1.76
0.391	0.00812	1.75
0.411	0.00918	1.76
0.450	0.01147	1.77
0.469	0.01270	1.77
0.487	0.01401	1.78
0.505	0.01539	1.79
0.547	0.01903	1.83
0.607	0.02553	1.90
0.664	0.03343	1.98
0.716	0.04294	2.07
0.815	0.07021	2.24
0.914	0.12974	2.40
0.948	0.17229	2.48
Average		1.77

Table 12. Fractional approach to equilibrium vs time
Comparison of experimental data with theoretical based on Nernst Planck Model

$z_A/z_B = \frac{1}{2}$

$\bar{D}_{Na} = 8.544 \times 10^{-7}$ cm^2/sec $\qquad \bar{D}_A/\bar{D}_B = 3.80$

$r = 0.0470$

Constant boundary conditions

Resins initially in sodium form, complete conversion to calcium form

F	$\mathcal{T}$	$t_{obs.}$	$t_{cal.}$
0.178	0.00473	19.690	12.30
0.247	0.00946	33.47	24.46
0.298	0.01419	41.79	36.69
0.339	0.01839	50.04	48.93
0.375	0.02366	60.18	61.16
0.406	0.02839	71.91	73.39
0.434	0.03312	84.26	85.620
0.460	0.03785	96.34	97.86
0.483	0.04285	107.54	110.090
0.505	0.04310	117.58	122.32
0.525	0.05214	126.63	134.69
0.595	0.07106	155.27	183.72
0.651	0.08999	188.16	232.65
0.697	0.10890	237.66	281.58
0.737	0.22780	303.61	330.51
0.772	0.14711	380.34	380.40
0.872	0.22202	634.09	576.13
0.931	0.29800	777.07	771.85

Table 13. Fractional approach to equilibrium vs time comparison of experimental data with theoretical based on Nernst Planck Model

$z_A/z_B = 2$

$\bar{D}_{Ca} = 2.252 \times 10^{-7}$ $cm^2 sec^{-1}$ $\quad \bar{D}_{Ca}/\bar{D}_{Na} = 1/3.8$

$r = 0.050$ cm

Constant boundary conditions

Resin initially in calcium form, complete conversion to sodium form

F	I	$t_{obs.}$	$t_{cal.}$
0.149	0.00125	23.60	13.82
0.206	0.00247	35.77	27.37
0.248	0.00369	46.97	40.93
0.282	0.00491	58.36	54.48
0.312	0.00613	70.35	68.04
0.338	0.00735	82.97	81.60
0.361	0.00850	96.11	95.16
0.383	0.00979	109.64	108.73
0.402	0.01102	123.42	122.34
0.421	0.0122	137.35	136.01
0.438	0.01340	151.35	149.75
0.454	0.01470	167.37	163.59
0.470	0.01590	179.36	177.56
0.484	0.01720	193.33	191.69
0.498	0.01850	207.25	205.99
0.512	0.01980	221.13	220.48
0.525	0.02120	235.33	235.55
0.572	0.02650	288.52	294.18
0.612	0.03190	340.54	354.27
0.648	0.03770	395.60	418.60
0.682	0.04390	451.40	487.84
0.714	0.05000	511.60	562.00
0.743	0.05800	577.27	644.14
0.828	0.08600	828.10	965.00
0.886	0.12000	1122.40	1366.64
0.930	0.16200	1491.77	1799.69

The calculation of average trace ionic diffusion coefficients for various values of α are presented in Tables 14, 15 and Figure 21 shows the corresponding cross-plot for this case.

Finally a comparison between the experimental data and the theoretical rate curve for $\alpha = 3.8$ has been shown in Figures 22, 23 and Tables 16 and 17.

Table 14. Fractional approach to equilibrium vs dimensionless time: Nernst Planck Model

$z_A/z_B = \frac{1}{2}$

$\bar{C}_V/\bar{C}_{V_o} = 0.25$

r = 0.047 cm.

F	$\bar{D}_A/\bar{D}_B$=1 1 τ	$\bar{D}_{Na}$ x10^{7}cm^2/sec	$\bar{D}A/\bar{D}B$ 2	$\bar{D}_{Na}$ x10^{7}cm^2/sec	$\bar{D}A/\bar{D}B$ 3.8 τ	$\bar{D}_{Na}$ x10^{7}cm^2/sec
0.10	0.00				0.00123	6.680
0.20	0.0031	4.02	0.0037	4.80	0.0050	6.500
0.30	0.0077	5.32	0.0092	6.35	0.0120	8.300
0.40	0.0150	5.91	0.0182	7.17	0.0235	9.260
0.50	0.0258	5.83	0.0316	7.12	0.0400	9.050
0.60	0.0410	5.770	0.0500	7.05	0.0630	8.860
0.70	0.0630	5.15	0.0780	6.39	0.0990	8.100
0.80	0.0980	5.10	0.1160	6.04	0.1500	7.800
0.90	0.1700	4.85	0.1900	5.42	0.2500	7.140
1.00						
Average		5.24		6.30		7.960

F	$\bar{D}A/\bar{D}B$ 5 τ	$\bar{D}_{Na}$ x10^{7}cm^2/sec	$\bar{D}A/\bar{D}B$ 10 τ	$\bar{D}_{Na}$ x10^{7}cm^2/sec
0.10	0.0014	7.60	0.0019	10.65
0.20	0.0056	7.28	0.0079	10.28
0.30	0.0134	9.25	0.0192	13.26
0.40	0.0260	10.25	0.0375	14.80
0.50	0.0450	10.15	0.0650	14.65
0.60	0.0740	10.40	0.1030	14.50
0.70	0.1140	9.41	0.1600	13.10
0.80	0.1720	8.85	0.2450	12.75
0.90	0.2800	8.00	0.4000	11.40
Average		9.021		12.82

Table 15. Fractional approach to equilibrium vs dimensionless time: Nernst Planck Model

$z_A/z_B = 2$

$\bar{C}\bar{V}/C_oV_o = 0.25$

$r = 0.05$ cm.

F	$\bar{D}A/\bar{D}B$ 1 / τ	$\bar{D}_{Ca}$ x10^7cm^2/sec	$\bar{D}A/\bar{D}B$ ½ / τ	$\bar{D}_{Ca}$ x10^7cm^2/sec	$\bar{D}A/\bar{D}B$ 1/3.5 / τ	$\bar{D}_{Ca}$ x10^7cm^2/sec
0.10	0.00034	4.010	0.00029	3.420	0.00019	2.242
0.20	0.00165	2.680	0.00124	1.940	0.00092	1.440
0.30	0.00410	2.770	0.00300	2.030	0.00230	1.555
0.40	0.00830	2.050	0.00500	2.130	0.00452	1.660
0.50	0.01500	3.470	0.01040	2.410	0.00780	1.810
0.60	0.02570	4.070	0.01720	2.720	0.01320	2.090
0.70	0.0410	4.660	0.02800	3.180	0.02220	2.520
0.80	0.0660	5.320	0.04550	3.670	0.03420	2.760
0.90	0.1120	5.830	0.08000	4.170	0.06100	3.180
Average		3.984		2.852		2.139

F	$\bar{D}A/\bar{D}B$ 1/5 / τ	$\bar{D}_{Ca}$ x10^7cm^2/sec	$\bar{D}A/\bar{D}B$ 1/10 / τ	$\bar{D}_{Ca}$ x10^7cm^2/sec
0.10	0.00017	2.005	0.00013	1.536
0.20	0.00082	1.280	0.00064	1.000
0.30	0.00209	1.410	0.00167	1.126
0.40	0.00410	1.510	0.00325	1.190
0.50	0.00720	1.670	0.00575	1.330
0.60	0.01160	1.8350	0.00980	1.550
0.70	0.01900	2.160	0.01600	1.820
0.80	0.03100	2.500	0.02550	2.060
0.90	0.05200	2.710	0.04500	2.340
Average		1.896		1.550

Table 16. Fractional approach to equilibrium vs time

Fick's Law

$\bar{D}_{Ca-Na} = 3.980 \times 10^{-7}$ cm^2/sec

Nernst Planck Model

$\bar{D}_{Ca} = 2.110 \times 10^{-7}$ cm^2/sec

r = 0.050 cm. $\bar{\bar{C}}\bar{V}_o/CV_o = 0.25$

$\bar{D}_{Ca}/\bar{D}_{Na} = 1/3.80$

F	τ(FL)	τ(NP)	$t_{obs.}$	$t_{cals.(FL)}$	$t_{cal.(NP)}$
0.10	0.00034	0.00018	2.12	2.14	2.21
0.20	0.00165	0.00090	16.00	10.20	10.70
0.30	0.00410	0.00228	37.00	25.69	26.90
0.40	0.00830	0.00450	68.00	52.50	53.00
0.50	0.01500	0.00770	108.00	94.00	90.70
0.60	0.02570	0.01280	158.00	161.00	151.01
0.70	0.04100	0.02200	220.00	257.00	259.00
0.80	0.06600	0.03400	310.00	420.00	402.00
0.90	0.11200	0.06000	480.00	705.00	707.00

Table 17. Fractional Approach to equilibrium vs time
Fick's Law

$\bar{D}_{Na-Ca} = 5.24 \times 10^{-7}$ cm^2/sec

r = 0.0470 $\quad \bar{D}_{Na}/\bar{D}_{Ca} = 3.80$

$\bar{D}_{Na} = 7.960 \times 10^{-7}$cm^2/sec $\quad \bar{C}_o\bar{V}/C_oV = 0.25$

F	τ(FL)	τ(NP)	$t_{obs.}$	$t_{cal.(FL)}$	$t_{cal.(NP)}$
0.10			4.00		3.44
0.20	0.0031	0.0050	17.00	13.00	14.00
0.30	0.0077	0.0120	32.00	32.50	33.60
0.40	0.0150	0.0235	56.00	63.20	65.80
0.50	0.0258	0.0400	98.00	109.00	112.10
0.60	0.0410	0.0630	157.00	173.00	176.40
0.70	0.0630	0.0990	270.00	268.00	278.00
0.80	0.0980	0.1500	425.00	412.00	420.00
0.90	0.1700	0.2500	775.00	715.00	700.00

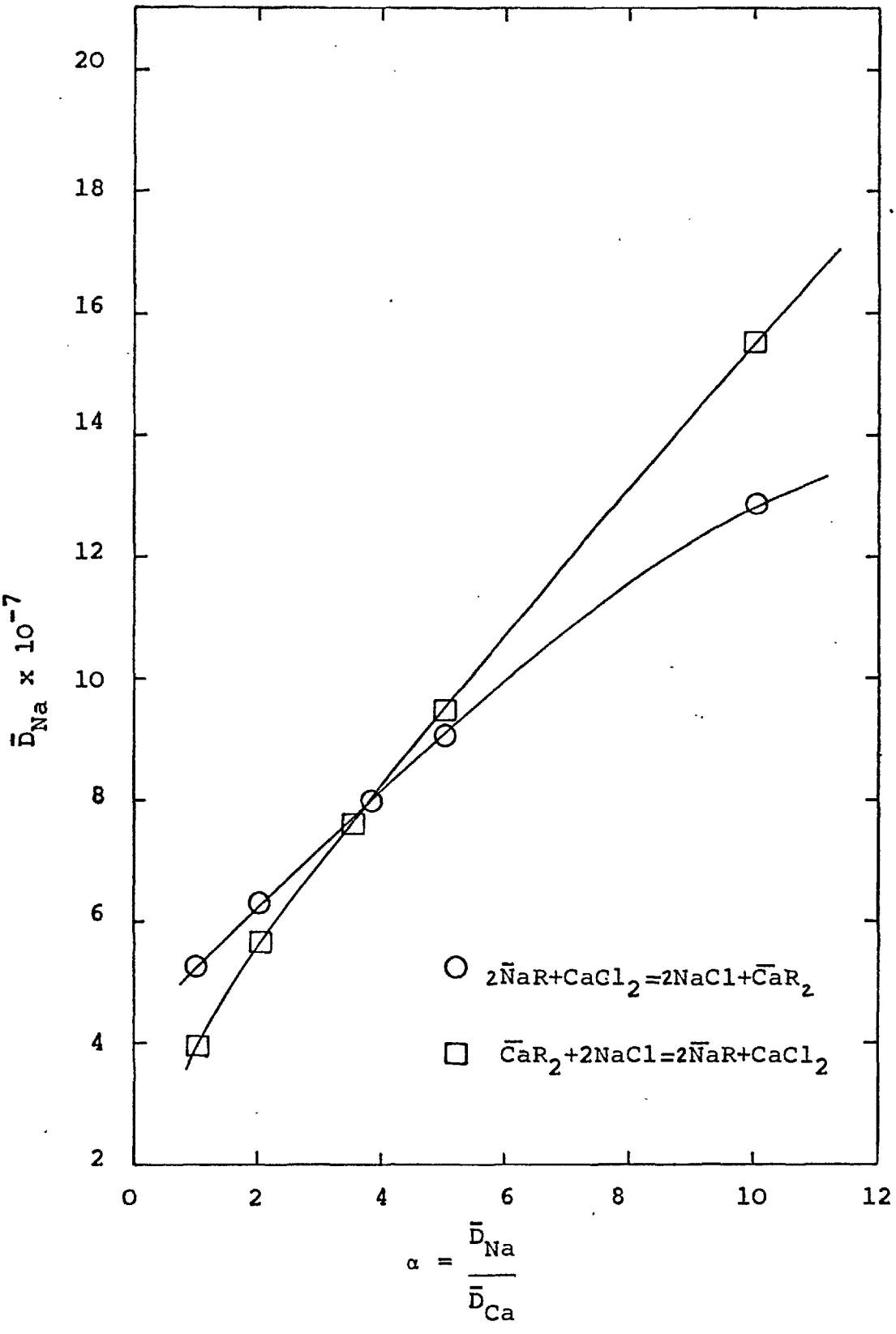

Figure 21. Variation of $\bar{D}_{Na}$ with $(\bar{D}_{Na}/\bar{D}_{Ca})$ for forward and reverse exchange under variable boundary conditions $(\bar{C}\bar{V}/C_oV = 0.25)$

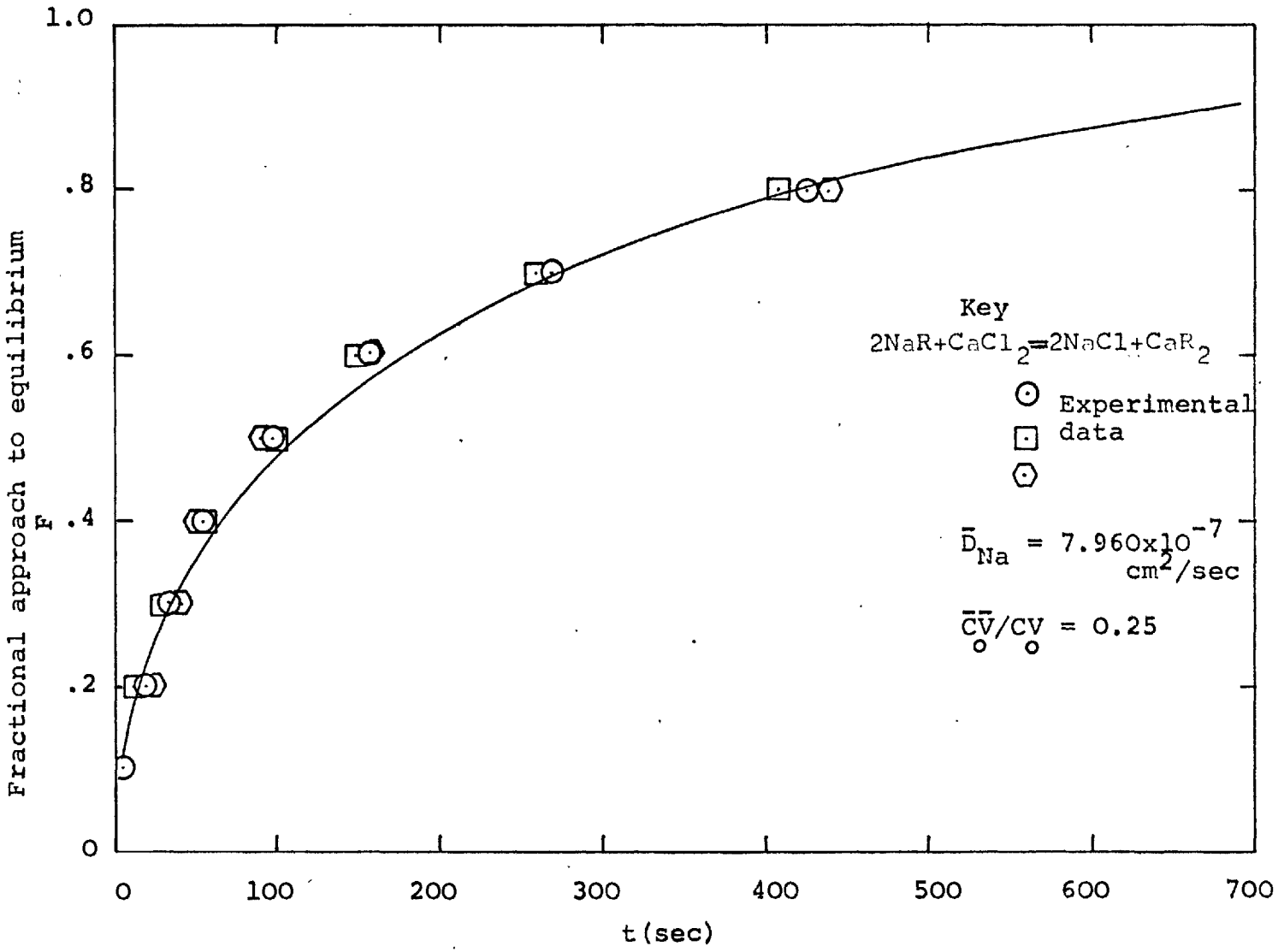

Figure 22. Correlation of data, Nernst Planck Model $\bar{D}_{Na}/\bar{D}_{Ca}$ = 3.8

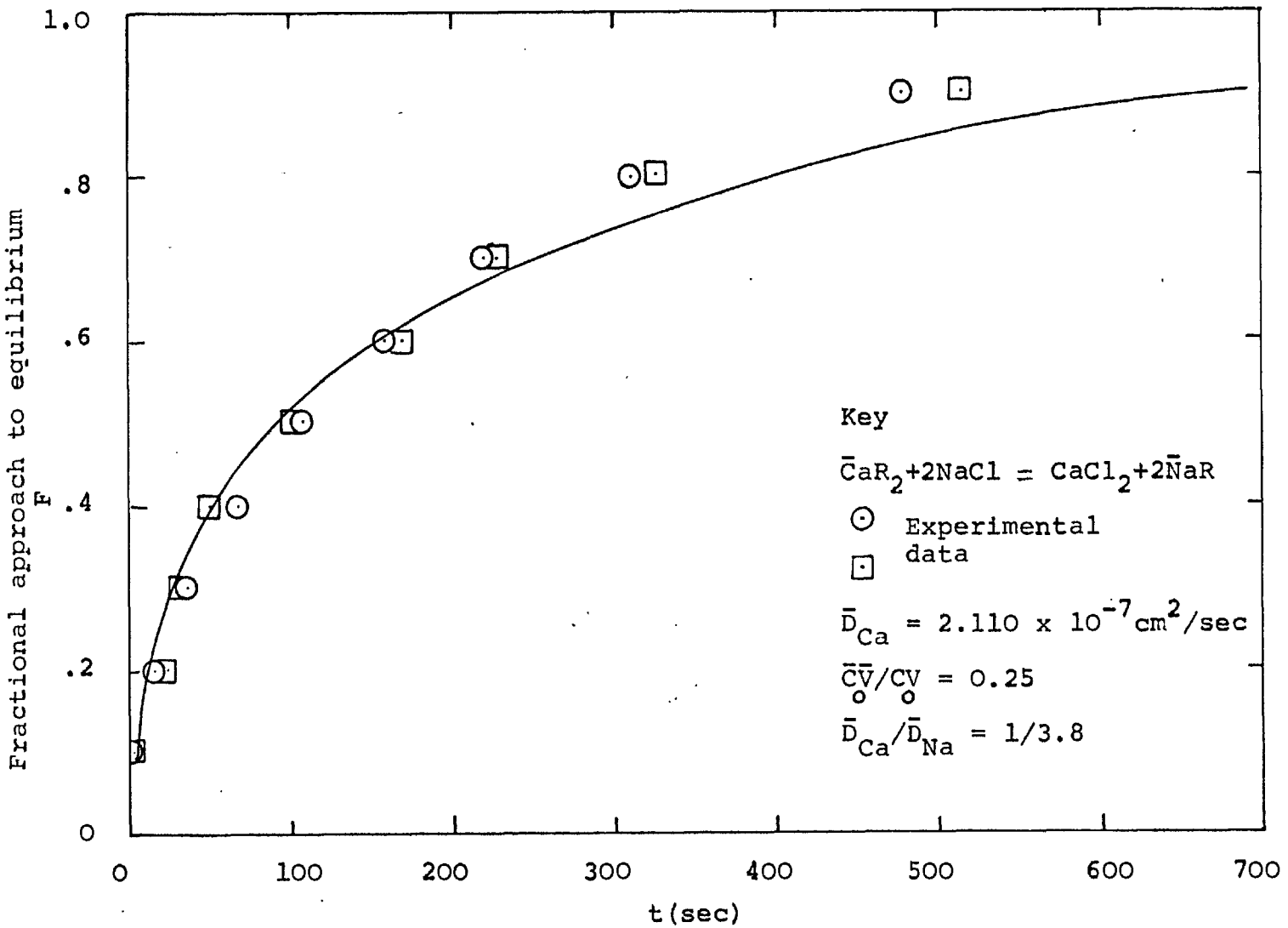

Figure 23. Correlation of data, Nernst Planck model

2.7. RESULTS AND DISCUSSION

Table 18 shows all the experimental results obtained in the present study. The self-diffusion coefficient of sodium in Zeo-Karb 225, 8% DVB resin has been determined to be 8.848×10^{-7} cm^2/sec and that of calcium 2.26×10^{-7} cm^2/sec.

Table 19 shows results for the self-diffusion coefficient of sodium within a similar cation exchanger and these values may be compared with the value obtained here. It may be noted that the value of $\bar{D}_{Na-Na}$ obtained here is in good agreement with the value of 9.44×10^{-7} cm^2/sec obtained by Boyd and Soldano (1954). The comparison with other results in Table 19 shows that there is almost a factor of two between them. This may be due to slight differences in the degree of crosslinking of different resins. It has been shown by Boyd and Soldano (1954) that $\bar{D}_{Na-Na}$ decreases from 9.44 to 2.4×10^{-7} when the degree of crosslinking of the resin is increased from 8.6% to 16%. It is always difficult to compare different resins from different sources. It is quite likely that the resin batch used in this study has a slightly different degree of crosslinking than the nominal value of 8% as reported by the manufacturer.

The value of $\bar{D}_{Ca-Ca}$ could not be compared with similar values due to lack of data in the literature. Table 20 shows the comparison of the self-diffusion coefficients of calcium obtained in this study with the self-diffusion coefficients of other divalent cations within a similar cation exchanger. It is surprising that the self-diffusion coefficients of divalent ions decreases in the same order as their hydration number. Generally, the reverse is true (Helfferich 1962, p.106).

Figures 19 and 20 show the rate curves for the exchange of sodium and calcium under constant boundary conditions. The forward and the reverse exchange rates are markedly different, as expected according to the Nernst Planck model, which considers a variable interdiffusion coefficient

Table 18. Summary of experimental data

Nature of exchange	Reaction	Boundary conditions	$\bar{D}_{Na-Na} \times 10^7$	$\bar{D}_{Ca-Ca} \times 10^7$	$\bar{D}_{Na} \times 10^7$	$\bar{D}_{Ca} \times 10^7$	$\bar{D}_{Na-Ca} \times 10^7$	$\bar{D}_{Ca-Na} \times 10^7$	$\alpha = \bar{D}_{Na} / \bar{D}_{Ca}$
			Isotopic		NP		FL		
Isotopic	NaCl+NaR	$\bar{C}_o\bar{V}/C_oV=0.25$	8.848						3.91
Isotopic	$CaCl_2+CaR_2$	$\bar{C}_o\bar{V}/C_oV=0.25$		2.260					
Ion Exchange	$CaCl_2$+NaR	$\bar{C}_o\bar{V}/C_oV=0.25$			7.96		5.24		
Ion Exchange	$2NaCl+CaR_2$	$\bar{C}_o\bar{V}/C_oV=0.25$				2.11		3.98	3.8
Ion Exchange	$CaCl_2$+NaR	Constant			8.54		5.84		
Ion Exchange	$2NaCl+CaR_2$	Constant				2.25		3.67	3.8

Units of $\bar{D}_i$ are cm^2/sec.

Table 19. Self-Diffusion coefficient of sodium in cation exchange resins (25°C)

$\bar{D}_{Na-Na}$ x10^{7}cm^2/sec	Resin	Solution Equil/Lit	Reference	Reported by
15.80	Dowex-50 8% DVB	0.10 NaCl	Morig and Rao (1965)	
18.00	Dowex 50 8%DVB	0.50 NaCl	Morig and Rao (1965)	
11.00	Dowex 50 8% DVB	1.00 NaCl		Turner et al (1966)
9.440	Dowex 50 8% DVB	0.22 NaCl	Boyd and Soldano (1954)	
8.848	Zeo-Karb 225 8% DVB	1.00 NaCl	This study	

Table 20. Self-Diffusion Coefficients of divalent ions in cation exchange resins (25°C)

Ion	Self-Diffusion coefficient x10^{7}cm^2/sec	Resin	Hydration number*	Reference
Calcium	2.260	Zeo-Karb 225 8% DVB	5.20	This study
Strontium	1.260	Dowex 50W 8% DVB	4.70	Morig and Rao (1965)
Barium	0.792	Dowex 50W 8% DVB	2.0	James Kuo and David (1963)
Zinc	0.630	Dowex 50W 8% DVB	-	Soldano and Boyd (1954)

* Helfferich (1962, P.106)

for an exchange reaction between ions of different diffusion coefficient within the resin phase. Fick's Law model which considers a constant interdiffusion coefficient is unable to explain this effect. A resin diffusion run was also carried out with 0.6N $CaCl_2$ solution and has been included in Figure 19. The results from the runs under variable boundary conditions are shown in Figures 22 and 23.

Comparison of the observed rates with those predicted by Nernst-Planck model are generally in good agreement. Exact quantitative agreement cannot be expected since the simplifying assumptions of the theory namely, the absence of coions, negligible swelling changes and constant trace ionic diffusion coefficient of the exchanging ions are not completely satisfied. It would be highly speculative to attribute this deviation to specific physical causes. Possibly, contrary to the assumption of the theory, the internal coion concentration is higher which may lead to a retardation of the exchange rate especially at the start of a run as has been observed in this study. Since no coions are present in the resin at the start of a run, coions from the external solution will tend to diffuse into the exchanger and tend to effect the kinetics as equilibrium is approached. The net effect of this may well be the lowering of the experimental rates.

In the foregoing theoretical treatment it has been assumed that the trace ionic diffusion coefficients of the exchanging ions are constant. This may not be the case. Evidence in the literature (Soldano and Boyd 1954) indicates that the trace ionic diffusion coefficient of an ion may vary with the composition of the resin. In such a case the ratio of the two diffusion coefficients, $\bar{D}_A$ and $\bar{D}_B$, cannot be taken as a constant. This variation must then be considered in the computation of exchange rates for any system. Figure 24 shows the two values of α obtained in this study. Although there is close agreement, this discrepency may cast doubt on this simplifying assumptions.

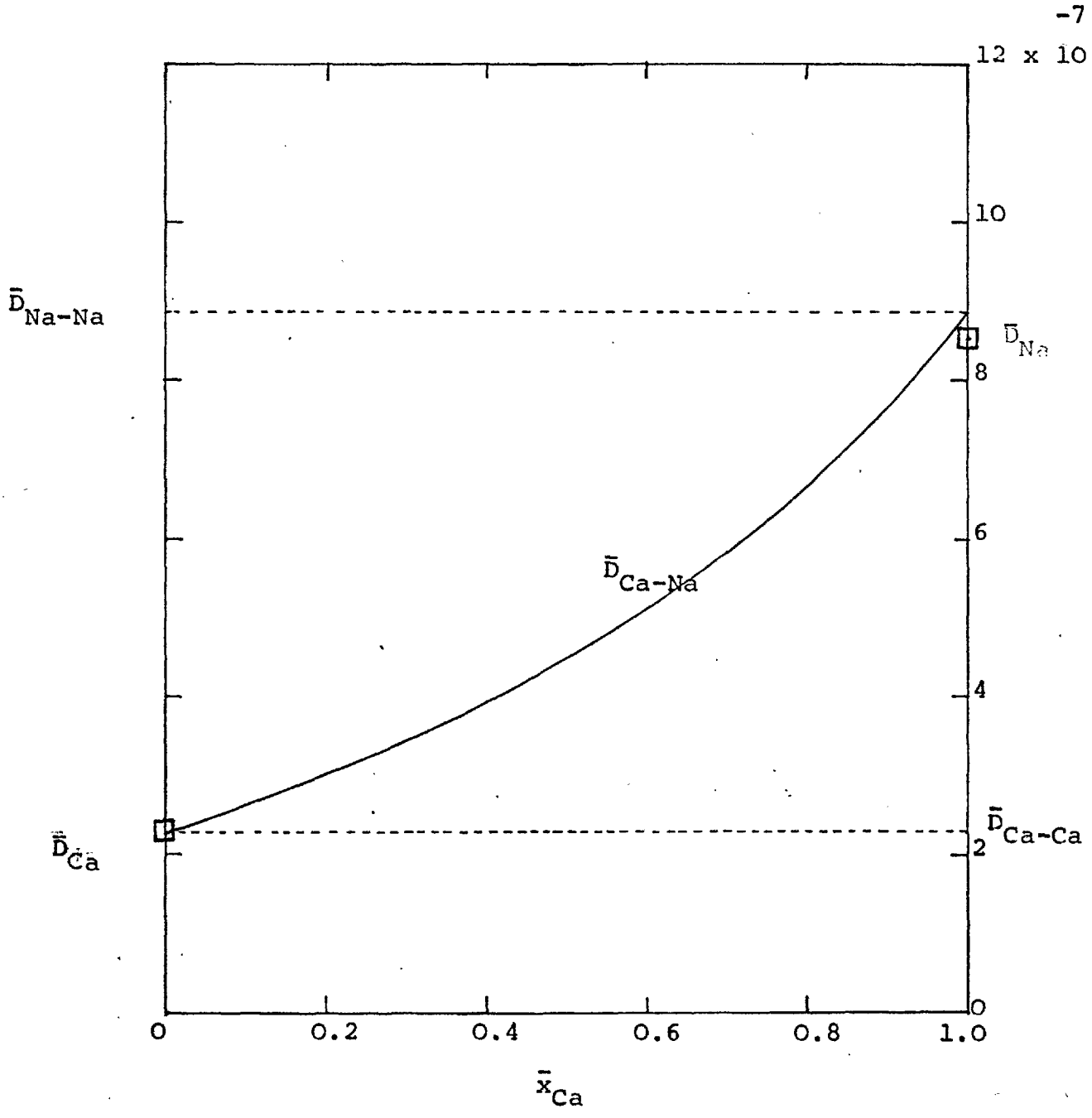

Figure 24. Interdiffusion coefficient $\bar{D}_{Ca-Na}$ as a function of resin phase composition (based on self-diffusion coefficients).

In order to check the validity of using the self-diffusion coefficients instead of the trace ionic diffusion coefficients in the Nernst-Planck model an analysis of the experimental data from the literature, for other uni-divalent exchange reactions, has been carried out. Only those systems have been analysed for which the mutual exchange data and isotopic exchange data had been obtained in one study e.g. Na^+- Sr^{++} (Morig and Rao 1965) and Na^+- Ba^{++} (James Kuo and David 1963) Data for Na^+- Zn^{++} system (Her ing and Bliss 1963) was obtained from two different sources and thus the result in Table 21for this system is apparently misleading.

The mutual exchange rate curves for these systems were reproduced on graph paper and the numerical data was obtained in the form of F as a function of time 't'. Applying the cross-plot technique, as used in the present study, to this data, values of the trace ionic diffusion coefficients for Sr^{++} and Ba^{++} were computed. Table 21 shows all the computed values of trace ionic diffusion coefficients and self-diffusion coefficients along with their α values respectively. Unfortunately, the experimental data for Na^+ - Ba^{++} system did not prove to be sufficient to obtain a cross-plot and, therefore, $\bar{D}_{Na}$ and $\bar{D}_{Ba}$ could not be computed. However, for Na^+- Ca^{++} and Na^+- Sr^{++} it may be noted that the trace ionic diffusion coefficient of the faster ion decreases slightly whereas the effect on the slower ion is less significant.

Next, these values of the trace ionic diffusion coefficients along with their α values were used to back calculate the rate curves for the forward as well as the reverse exchange reactions using the Nernst-Planck model. A comparison of the experimental and the computed rate curves has been shown in Figures 25 and 26. The two curves for each reaction are based on the trace ionic diffusion coefficients and the self-diffusion coefficients respectively. It may be noted that both curves represent the experimental data adequately and equally well, which suggests that the

Table 21. Comparison of the self diffusion coefficient and the Trace ionic diffusion coefficient of various uni-divalent ion exchange systems (25°C)

System A	System B	$\bar{D}_{AA}$ x10^7cm^2/sec	$\bar{D}_{BB}$ x10^7cm^2/sec	α	$\bar{D}_A$ x10^7cm^2/sec	$\bar{D}_B$ x10^7cm^2/sec	α	Ref.
Na	Ca	8.848	2.26	3.91	8.54	0.25	3.8	This study
Na	Sr	18.00	1.26	14.13	16.15	0.955	16.95	Morig and Rao (1965)
Na	Ba	16.00	0.792	20.01				James Kuo and David (1963)
Na	Zn	9.44	0.630	14.90	20.30	2.310	8.80	Soldano and Boyd (1954) Hering and Bliss (1963)

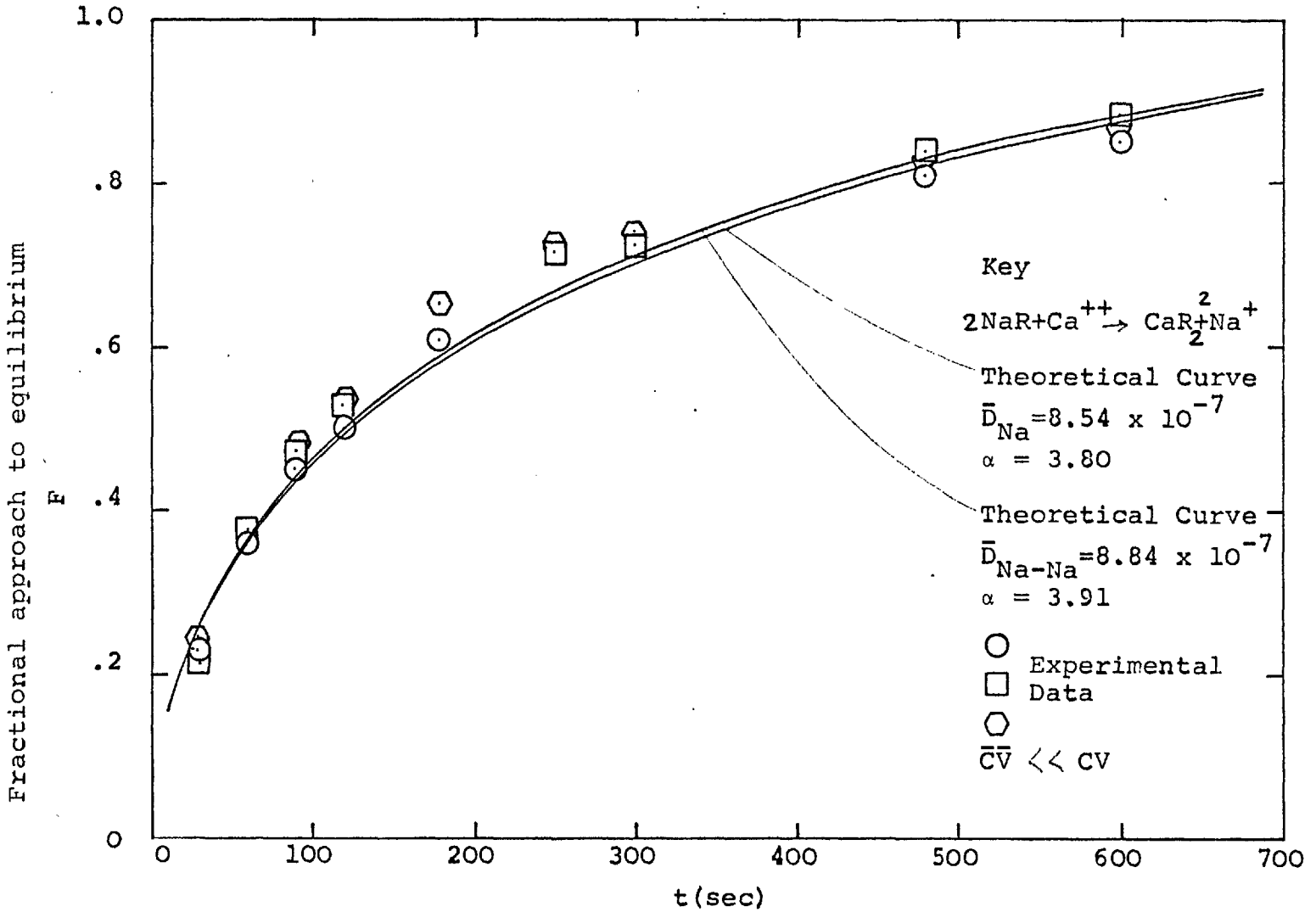

Figure 25. Comparison of the experimental and theoretical rate curves for Ca^{++}/Na^+ system.

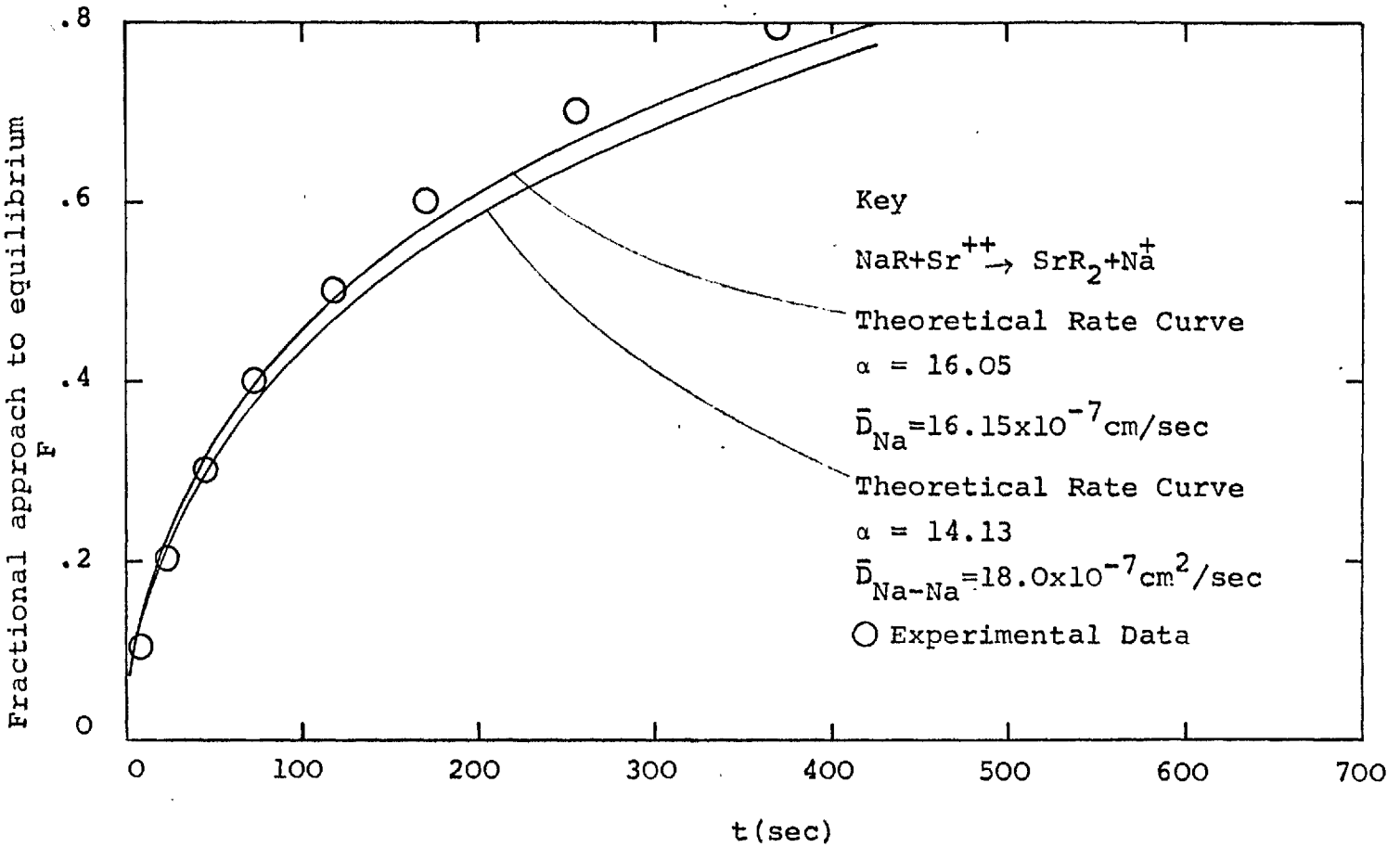

Figure 26. Comparison of the experimental and theoretical rate curve for Sr^{++}/Na^{+} system (Data from Morig and Rao).

self-diffusion coefficients and their ratio can be safely used to interpret the mutual ion exchange reaction rates. This in turn, simplifies the situation since determination of the self-diffusion coefficient is much simpler than that of the trace ionic diffusion coefficients which requires special analytical techniques. Also for the calculation of the variable interdiffusion coefficient the use of the self-diffusion coefficients of the exchanging ion will be adequate. Such a plot of $\bar{D}_{Na-Ca}$ vs $\bar{x}_{Ca}$ is shown in Figure 24.

Finally, the experimental data for ion exchange with variable boundary conditions has also been interpreted by assuming a constant interdiffusion coefficient ($\bar{D}_A = \bar{D}_B$) employing Fick's Law. Tables 16 and 17 show that an equally good correlation is obtained with this approach. In the light of the Nernst-Planck model which includes the electric potential gradient in addition to concentration gradient, it might appear that the use of a constant interdiffusion coefficient (Fick's Law) in this case is strictly an empirical approach and must not be generalised.

2.8. CONCLUSION

The self-diffusion coefficients and the trace ionic diffusion coefficients of sodium and calcium have been determined. The experimental data was interpreted by means of the Nernst-Planck model and Fick's Law model.

The self-diffusion coefficients and their ratio α can be used to calculate the interdiffusion coefficient which controls the exchange rate between ions of different mobility within the resin phase. This obviates the need to determine the trace ionic diffusion coefficient of the exchanging ions separately. However, further study of self-diffusion in heteroionic exchangers is required to confirm this.

The interpretation of the mutual exchange runs shows that both theoretical models, namely, Fick's Law and Nernst Planck represent the results of this study equally well. However, the Nernst Planck model is theoretically more meaningful since it takes into account the effect of electrical potential gradi ent of the diffusing ions.

It may also be concluded from the present study that it is perfectly adequate to use a constant interdiffusion coefficient (Fick's Law) for the analysis of the performance of an ion exchange unit where complete conversion of resin from one ionic form to another takes place. However, this may lead to considerable error if the change in the resin composition is only fractional as in the case of a continuous countercurrent stagewise process. Here, the exchange rate is controlled by the interdiffusion coefficient (Nernst-Planck model) which may vary from stage to stage depending upon the composition of the resin.

The experimental equipment and the analytical technique using Atomic Absorption Spectroscopy, developed in this study, proved a simple and accurate means of determining the trace ionic diffusion coefficients.

CHAPTER 3

ANALYSIS OF THE PERFORMANCE OF CLOETE-STREAT CONTACTOR FOR A PARTICLE DIFFUSION CONTROLLED ION EXCHANGE REACTION

3.1 INTRODUCTION

Ion exchange has been widely used in the fields of hydro-metallurgy, water treatment and more generally in the chemical process industries for the concentration, purification and separation of ionic species in solution. Ion exchange is traditionally a fixed bed process operated in a batchwise manner. This has tended to detract from its value as a chemical engineering unit operation and thus in recent years there has been a serious attempt to develop continuous process equipment. Consequently, a large number of sophisticated plant designs have been developed but only a few have as yet been successful on a commercial scale.

The fixed bed is intrinsically simple and operates as follows.
A solution is passed in down flow through a packed bed of resin particles until the resin is exhausted or leakage becomes serious. The solution flow is stopped and the resin is regenerated using a carefully controlled quantity of regenerant. Regeneration is usually incomplete in order to avoid poor regeneration efficiencies. The resin is washed to remove the regenerant from the voids of the bed and the adsorption cycle is repeated. Regeneration may be performed in downflow (cocurrent) or upflow (countercurrent). The latter is usually preferred. In either case the resin remains stationary in the column as a packed bed.

The fixed bed technique has much to commend it, since it is simple in concept and easy to operate. It involves only one major piece of equipment and because there is no movement of the resin particles, attrition losses due to mechanical breakage of resin beads are negligible. A fixed bed column can claim reasonably high volumetric throughputs without channelling and good chemical efficiency. Despite these advantages there are certain drawbacks which have prompted the chemical engineer to attempt to develop continuous countercurrent equipment.

The intrinsic inefficiency of the fixed bed technique with respect to resin utilisation is obvious, due to batchwise operation which always leads to a product stream of non-uniform composition. At any instant in time, only a part of the bed is being used for useful ion exchange, since the rest of the bed is either exhausted or waiting to be exhausted. In the case of cocurrent operation, the resin at the bottom of the bed which is partially exhausted at the end of the adsorption cycle will be completely exhausted by the ions which move downward during cocurrent regeneration. High ionic leakage in the next adsorption cycle will result unless a large excess of regenerant chemical is used. This can be largely avoided by operating the regeneration cycle in upflow (countercurrent). Here, the bottom of the bed is completely regenerated, pushing contaminating ions towards the top of the bed. Excessive leakage is thus avoided at the start of the adsorption cycle.

A fixed bed column is normally confined to the treatment of clear liquors and to maintain the operating performance a backwash cycle is always required. Expensive filtration steps are required if it is necessary to process unclarified liquors containing suspended solids e.g. uranium ore pulps. Although it is possible to operate a fixed bed column at high throughput, this is usually at the expense of increased pressure drop which will involve a gradually increasing energy cost. Flow rates of about 20 gal/min ft^2 are almost universally accepted as an adequate compromise between throughput, performance and energy consumption. Also, of course high throughputs must of necessity involve more expensive column design and construction, since pressure vessel construction will be necessary. Similarly, there is an upper limit to column diameter in fixed bed equipment since liquid distribution and product collection can become a serious problem. For this reason, individual fixed columns rarely exceed 6 ft in diameter. Duplicate columns, often in parallel would be used to overcome this restriction.

3.1.1 Development of Continuous Ion Exchange Equipment

Multiple Fixed Bed Cascade

A single ion exchange column is strictly a batch contactor and would result in an interrupted flow of product solution. This is rarely used in practice. More commonly, two or more fixed bed columns in series are employed. The cascade is operated such that one column is on the adsorption cycle, whilst another is being regenerated. In this way a continuous product stream is possible though cyclic variation in composition of the product solution still exists. The use of several fixed bed columns involves a large inventory of resin and the use of several large storage vessels to conserve regenerant solutions, as well as expensive automatic values and controllers. However, the principle of switching of liquid flow from column to column whilst keeping the resin beds stationary is widely used. A good example of this is the treatment of clear uranium leach liquors which employs three columns in series (Arden 1957).

3.1.2. Moving Bed Techniques

a. Complete Transfer of Resin Bed.

In a more sophisticated design the concept of moving the resin particles between the columns was introduced by Porter and Arden (1956) as an innovation in the uranium industry. The process can be explained by reference to Figure 27. The system consists of an array of three adsorption columns and operates automatically. Consider a bank of three adsorption columns. As the resin in the leading column (A) is loaded, the flow is diverted to the other two columns (B and C). The loaded resin from column A is hydraulically transfered to another column where it is backwashed to remove the leach liquor from the voids. The empty column A is then refilled with fully regenerated resin from the leading column of the elution bank. The flow system is then changed so that column A, containing

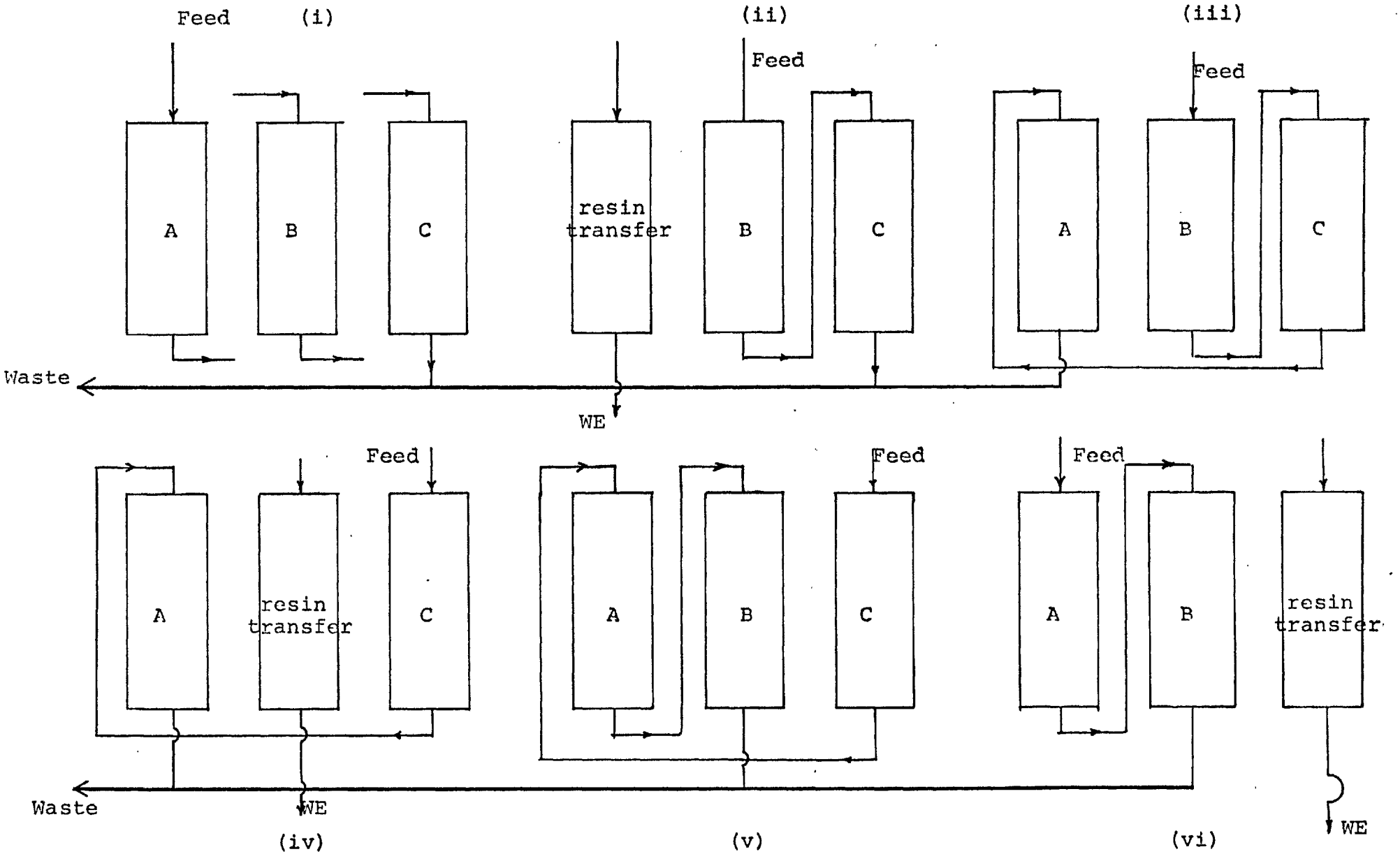

Figure 27. Porter-Arden moving bed continuous ion exchange contactor.
Sequence of steps in the operation
WE - to washing and to elution column
Feed - Leach liquor

freshly regenerated resin becomes the tail of this bank of three columns. The loaded resin, after back washing, is transferred into an elution column, which now becomes the tail end of the elution bank of three columns. A single set of three elution columns serve the whole plant. /for The process is continuous, except/a short interruption during the changeover of liquid flow. The resin moves in slugs throughout the circuit.

This technique reduces the inventory of resin in the process,though savings in respect of plant components is probably marginal when compared with the traditional fixed-bed column equipment. However, the Porter-Arden moving bed process was the earliest continuous ion exchange process applied on an industrial scale and is still in operation.

b. Partial Transfer of Resin Bed

In the Porter-Arden process, the whole of the resin bed is transferred between the columns after the exhaustion cycle. This can lead to long cycle times between the regeneration and exhaustion of the resin. More recently several contactors, the Asahi (1962), Higgins (1954) and others (e.g. Clayton 1969) have been developed, which reduce the cycle time by transferring only a part of the bed at any one time. These techniques are also cyclic but continuous and countercurrent with respect to both the adsorption and regeneration contactors. This ensures that the product stream retains virtually constant composition during the service cycle.

The latest version of the Higgins contactor employs a loop in which the resin is loaded, regenerated and washed in separate sections of the same equipment. It contains a number of automatic valves separating the sections. The countercurrent movement of the resin in the adsorption cycle is upflow which is induced by a hydraulic pulse in the wash section (see Figure 28). The main drawback to this contactor is the movement of the resin through the valves which can cause serious resin attrition. Several

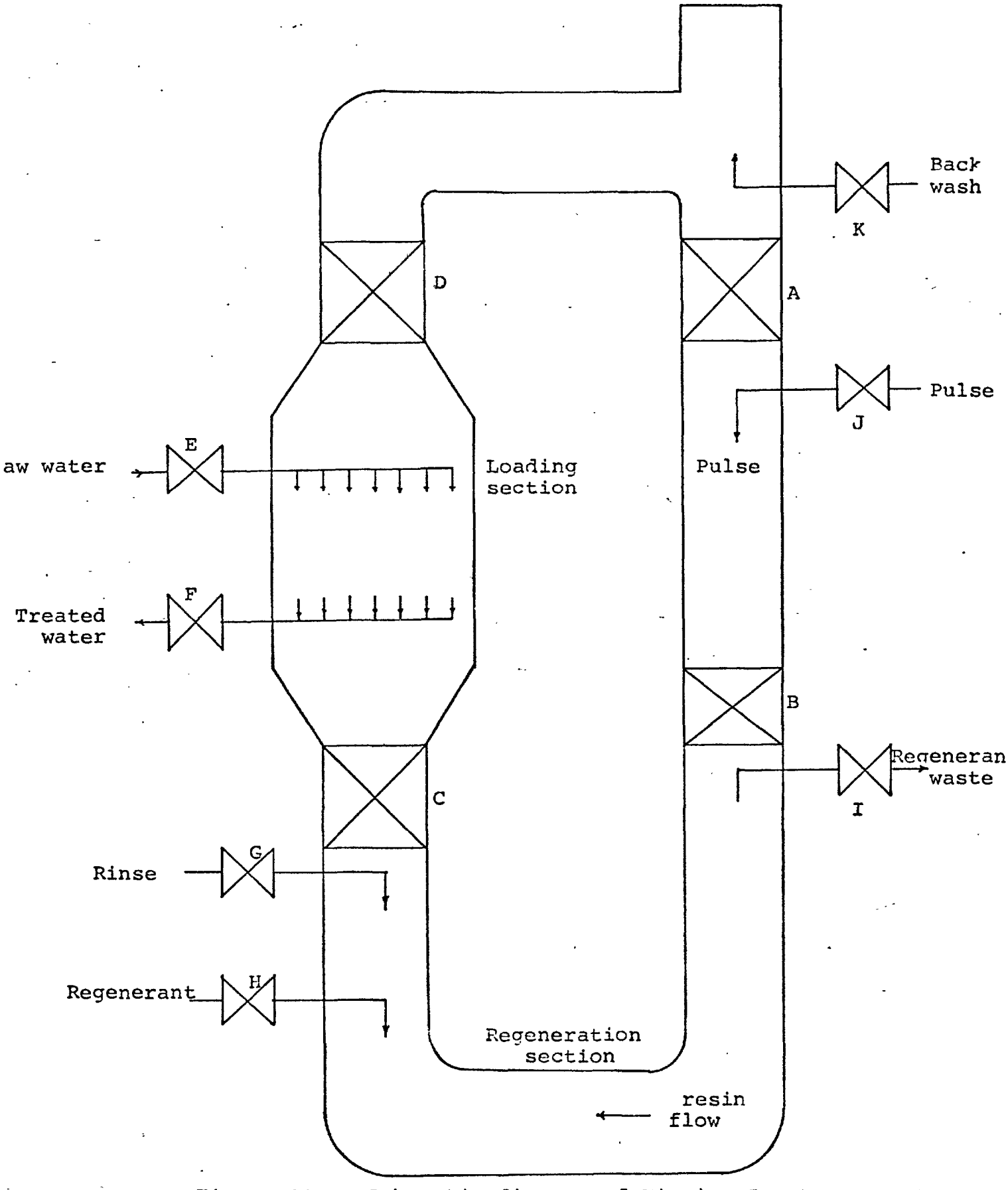

Figure 28. Schematic diagram of Higgins Countercurrent contactor

Position of valves	Service	Resin transfer
Valve close	B, C, D, J	A, I, E, F, G, H
Valve Open	A, I, E, F, G, H.	B, C, D, J

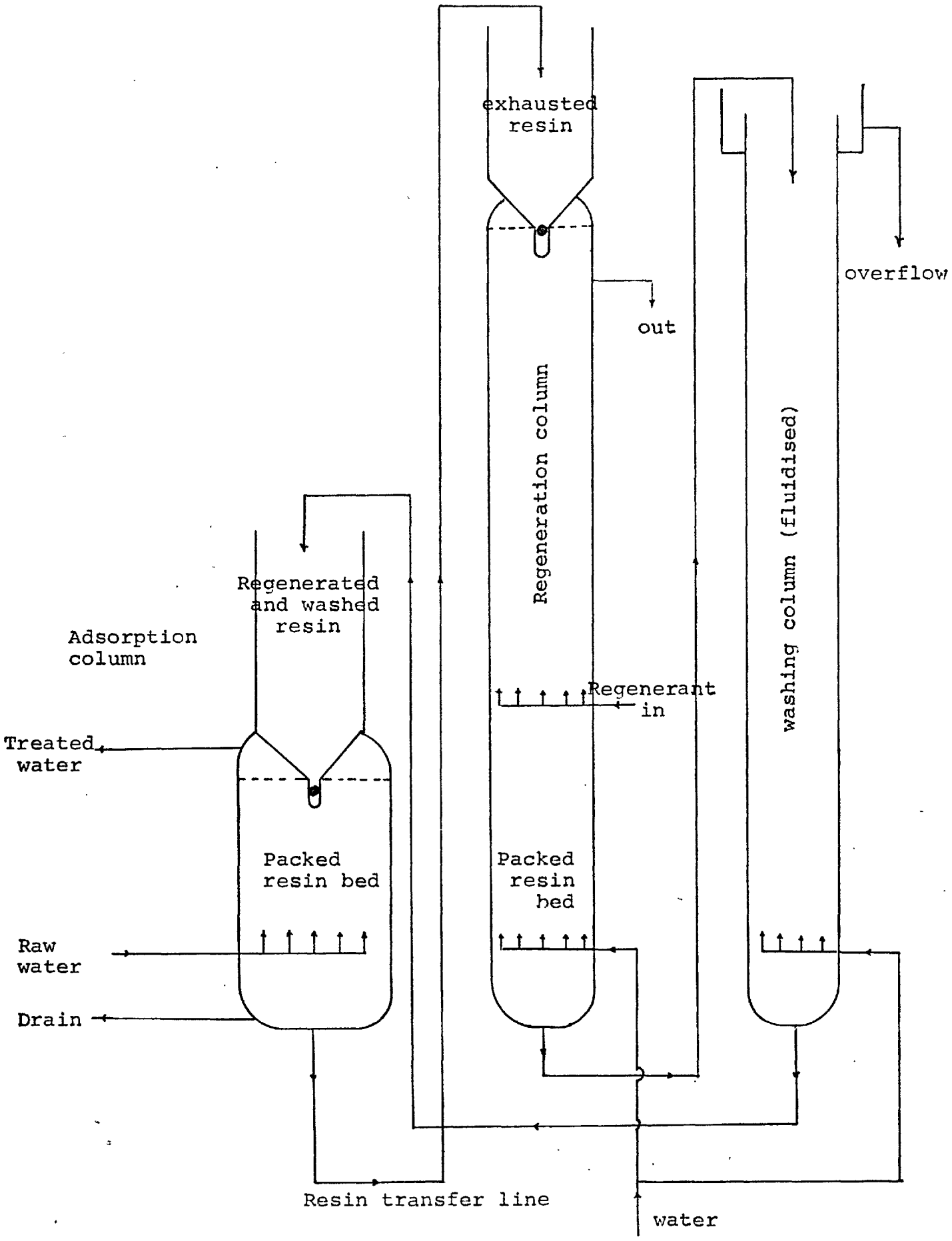

Figure 29 Asahi Co. countercurrent contactor

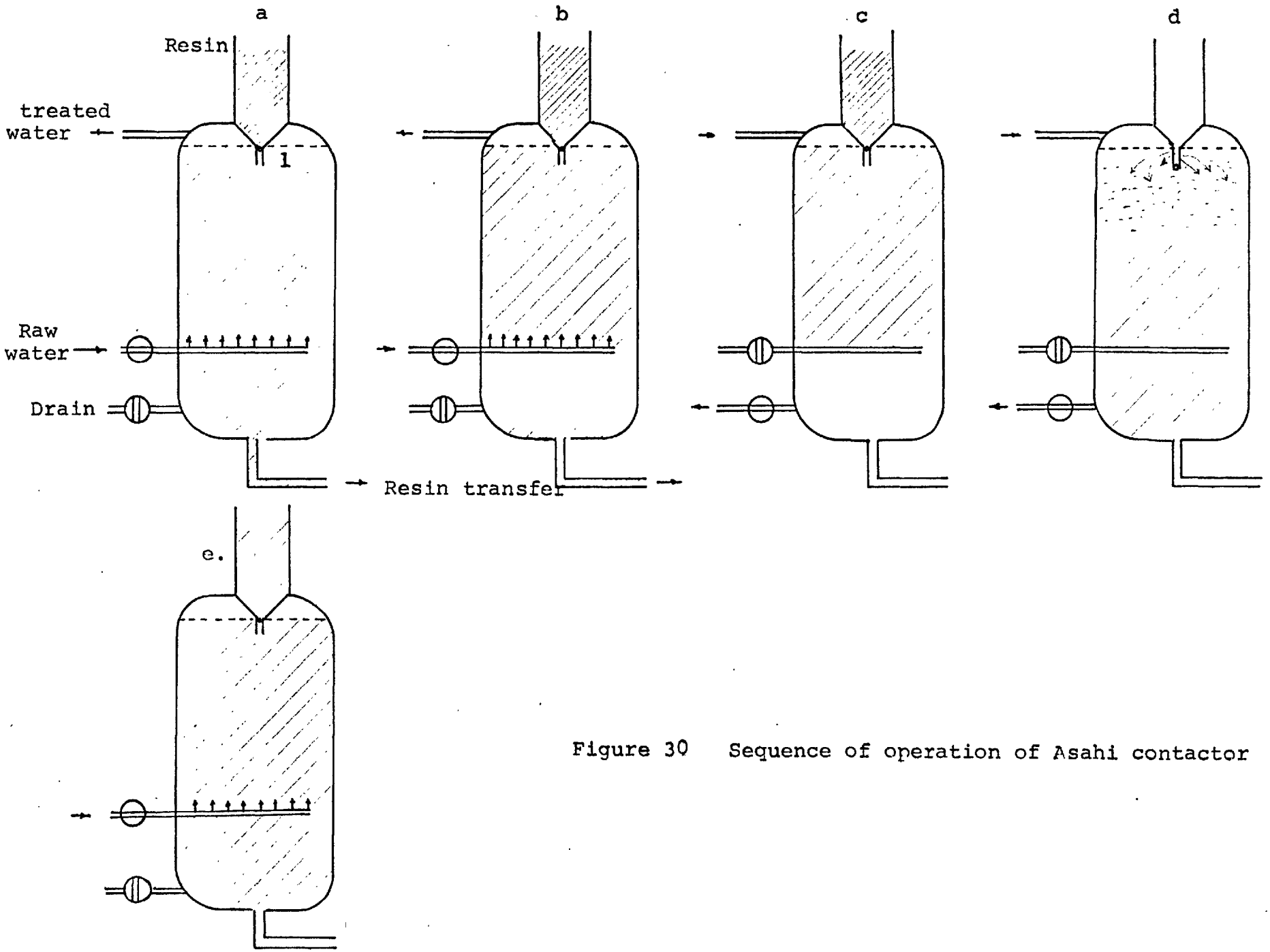

Figure 30 Sequence of operation of Asahi contactor

modifications have been suggested to avoid the use of valves.

In the Asahi process, the resin is loaded and regenerated in separate columns (see Figure 29). The resin in the adsorption columns is operated as a packed bed. The process is cyclic in operation. During the service cycle water passes in upflow through the adsorption column and the resin is retained in the column by a screen fitted at the top. Resin is transferred in down flow by the back pressure generated during the passage of water through the resin bed. This forces the resin lying below the water inlets at the bottom of the column through resin transfer pipes into the regeneration column, and creates a water void in the lower part of the column. During the discharge cycle, the liquid flow is stopped and the water discharge valve opens (see Figure 30). The whole packed bed of resin drops creating a suction head at the top of the column. Consequently, the resin feed valve (1) opens and allows freshly regenerated resin into the column and the service cycle is repeated. The regeneration column is hydraulically similar to the (service) adsorption column. The wash column is operated as a fluidised bed, though retaining countercurrent operation. The washed, fully regenerated resin is transferred to the adsorption column, by the difference in hydraulic head between the wash and the adsorption column.

Both of these processes are semi-continuous but have been most successful in the field of water treatment. The resin particles in both processes remain in contact and render these techniques less satisfactory for the processing of liquors containing suspended solids.

3.1.3. Pulsed bed technique

The idea of separating the resin particles became necessary in an attempt to develop a resin-in-pulp contactor

for the uranium industry. The earliest attempts involved the resin-in-basket principle (Hollis and McArther 1955) which is still in use in U.S.A. The technique employs mechanically shaken stainless steel baskets containing the resin. The resin particles are momentarily separated and allow the pulp to flow. A more sophisticated technique to handle liquors with suspended solids has been developed by Arden et al (1959). This employs single packed bed columns which are pulsed or jigged to induce momentary separation of the resin particles. The liquor passes through the resin bed continuously in upflow and the resin moves countercurrently in downflow. An air pulse or a mechanically vibrated diaphragm at the base of the column is used to jig the bed and exhausted resin is removed at the bottom together with some of the pulp liquor. Regenerated resin is introduced at the top of the column. The treated liquor overflows through a screen at the top of the column. The use of a screen is a drawback since it will tend to block and increase pressure drop.

More efficient than a single jigged bed is a cascade of jigged beds operated in series. This has been described by Heister (1954) and Swinton and Weiss (1953). Here the column is divided into separate compartments by a series of sieve plates. In the design by Heister the plates are vibrated to induce the flow of resin by gravity. Swinton and Weiss pulsed the liquid flow, retained stationary plates, which induced the resin to pass from plate to plate through downcomers. A similar technique has been described by Grimmett and Brown (1962). Again, the liquid is pulsed and the resin particles are suspended in the upflowing liquor and are transferred over downcomers. Mechanical vibration of the resin particles in these techniques may give rise to resin attrition problems. Bypassing of upflowing liquor through the downcomers will tend to make the process inefficient.

3.1.4. Continuous fluidised bed technique

The use of stagewise fluidised beds of resin particles for ion exchange is an extension of the earlier work of Swinton and Weiss. Resin particles are totally supported in an upward flow of process liquor and pass from stage to stage using downcomers without the need for mechanical agitation. A limiting factor is the terminal falling velocity of the resin particles which restricts the maximum superficial velocity of the process liquor. Generally, lower flow-rates than in packed beds can be tolerated and it is usual to grade the resin beads to a close size range, in the region of 0.8-1.0 mm diameter, to improve hydraulics and to avoid segregation. An early example of the use of fluidised resin beds in water softening is the Dorr Hydrosoftener (1954). In this contactor resin is transfered between stages using water ejectors. The unit was satisfactory when only few stages were required but became less attractive for large scale multicompartment applications.

Since resin transfer is the major problem a recent continuous countercurrent column with perforated plates has been described by Turner et al (1963). The resin particles are fluidised by the process liquor and transfer from stage to stage using downcomers. Such devices require a careful hydraulic balance between the pressure drop in the downcomer and across the distributor plate. Instabilities are known to occur during normal operation and start-up is particularly difficult. On a large scale, valves would be required in the downcomers to avoid bypassing of the process solution.

3.1.5. Cyclic fluidised bed technique

More sophisticated designs for fluidised beds avoid the use of downcomers or other techniques to promote resin flow, by allowing the resin particles to pass through the distributor plates.

The Cloete-Streat contactor (1963) is the first example of this type of design and was developed in this department. A vertical column consists of several stages separated by perforated distributor plates which allow the resin particles to pass in either upward or down ward flow (Figure 31). Normal fluid flow is upward and it fluidises the resin particles above each distributor plate and resin transfer is achieved by periodic reversal of fluid flow. The distributor plate has a free area of about 5% and is designed to retain the resin hold-up during a no-flow condition.. At each reversal of flow an increment of resin is transfered between adjacent stages countercurrent to the net fluid flow and an equal volume of regenerated resin is admitted to the top of the column. This mode of operation is simple and flexible and permits the flow rates and flow-rate ratio between resin and solution to be varied over a wide range. Also, of course this design can be successfully used for pulp solutions. Satisfactory operation of a pilot plant contactor has been reported by Stevenson (1969) for water softening handling 50,000 gal/day.

The cyclic nature of this technique does not allow it to be strictly termed as a steady state continuous counter-current contactor. However, product streams approach pseudo-steady state compositions. Normal operation is at atmospheric pressure, contrary to all forms of packed bed equipment, which involve a higher pressure drop, particularly at high flowrates and will thus necessiate more robust equipment. A fluidised contactor of this type does not have any valves, screens or other moving parts likely to cause resin attrition and experience suggests that resin damage is negligible.

George and Rosenbaum (1969) have operated a very similar contactor. This employs orifice plates which divide a column into a number of compartments. Countercurrent transfer of the resin is achieved by stopping the fluid flow for a short period and withdrawing resin from the bottom com-partment. Simultaneously equivalent volumes of resin

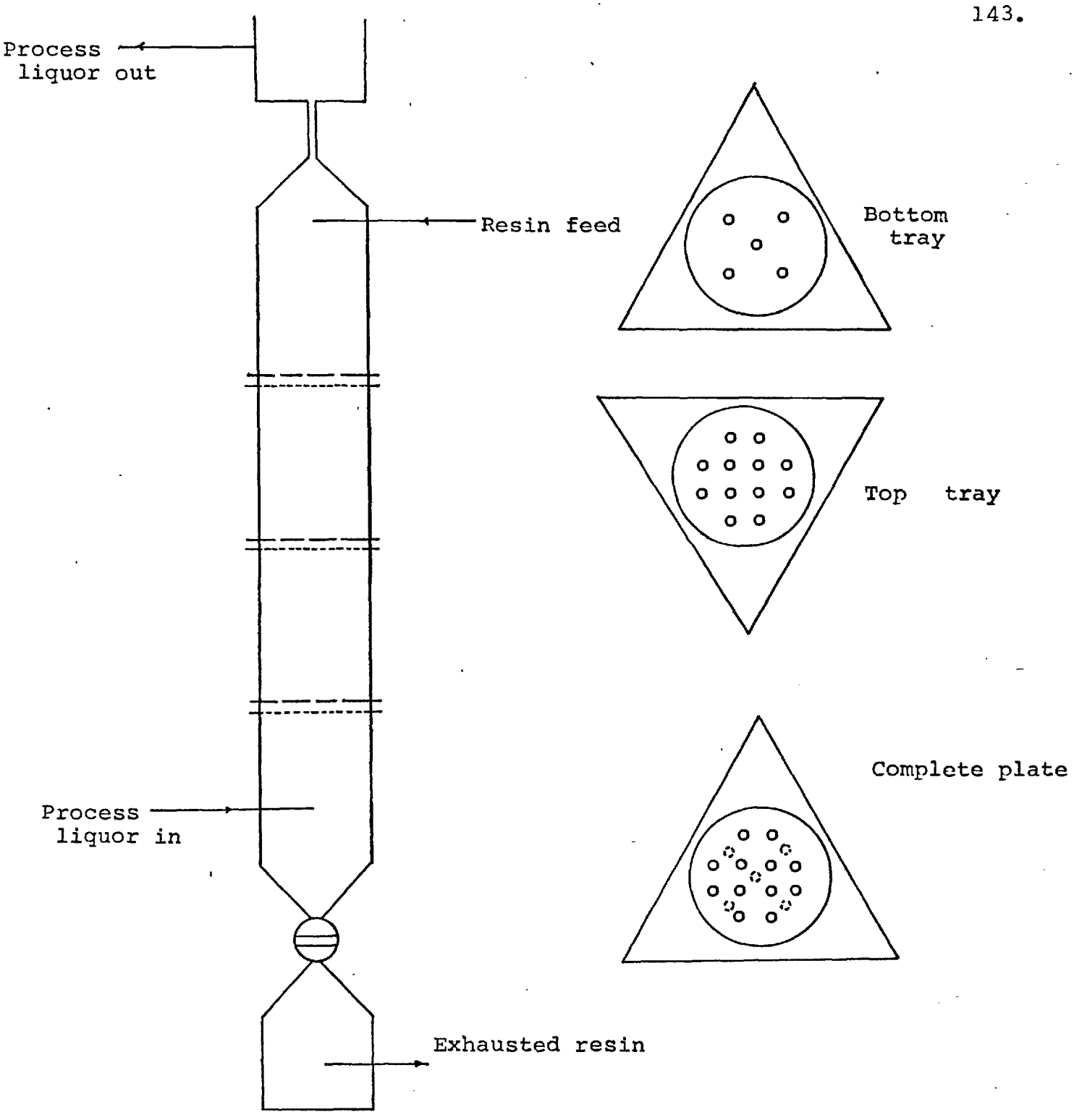

Figure 31 Cloete-Streat cyclic countercurrent column with details of perforated plate.

transfer rapidly down the column through the orifice plates between the stages. A small forward flow of solution is always required to retain the resin hold-up in each stage and to avoid drainage. This can be an undesirable feature in many applications involving a large number of stages, in the event of pump failure, since the concentration profile in the column is destroyed. Elaborate start-up procedures i.e. resin filling, will then be necessary.

In thelight of the foregoing discussion it may be concluded that the optimum technique should possess the following features:

a) Continuous operation
b) Countercurrent flow
c) Minimum resin inventory
d) High chemical efficiency
e) Low space requirements
f) Ability to handle a variety of process liquors.

Strictly speaking none of the present day contacting devices can completely satisfy all these requirements. Almost all the so-called continuous techniques are actually semi-continuous in operation and involve a short out-of-service period. They are in fact cyclic although the frequency and duration of the out-of service period may differ substantially in each case.

There is an intuiative feeling that cyclic operation is disadvantageous and that steady-state continuous operation is generally to be preferred. Certainly, this has been the aim in the design and operation of conventional chemical plant equipment. The objective of this section of research is to examine whether controlled cycling of the process streams is disadvantageous. The Cloete-Streat ion exchange contactor which is cyclic in operation has been employed for this study.

A typical process in water softening i.e. regeneration of the calcium form of a cation exchange resin by a concentrated solution of sodium chloride has been chosen for the study. Finally an attempt has been made to develop a theoretical model to analyse the performance of the cyclic contactor based on equilibrium and kinetic data which has been obtained during the course of this work.

3.2 Theory

3.2.1. Theoretical interpretation of a continuous countercurrent ion exchange process (steady-state)

A continuous countercurrent steady-state ion exchange process implies that the compositions of both phases at any point in a column are independent of time. This is true for both differential and stagewise contacting under completely hypothetical operating conditions. If equilibrium is attained between the two phases at every point in the column, then the performance could be represented by the usual graphical method employing a McCabe-Thiele construction. In fact, this approach is only valid if each real stage represents a theoretical stage, which is possible only in the case of a rapid reaction, efficient mixing and under highly favourable equilibrium conditions. In real systems, these conditions are unlikely to occur and it is necessary to determine a value of stage efficiency. This is difficult to predict from first principles and thus normally determined experimentally.

Another approach is to predict performance in terms of HTU (Height of a Transfer Unit). This assumes the validity of a mass transfer coefficient approach. This approach is acceptable for liquid film controlled exchange reactions since there is sufficient evidence to support the concept of a liquid film mass transfer coefficient. The HTU concept has been applied to a hypothetical continuous countercurrent plugflow ion exchange column by Baddour and Gilliland (1953) and Moison and O'Hern (1959).

In the more general case of non-equilibrium contact and where the reaction is strictly controlled by diffusion in one or the other phase then the McCabe-Thiele or HTU concept cannot be rigorously applied. The prediction of column performance for non-equilibrium exchange reactions controlled by a variable diffusion coefficient requires the simultaneous consideration of the relevant rate equation, equilibrium behaviour and mass balance from stage to stage. A knowledge of the mixing behaviour of the two phases in the contactor

is also necessary for a complete mathematical model. For reactions controlled by resin phase diffusion the mathematical model is complex.

A stagewise ion exchange column can be treated as a cascade of individual reaction vessels in series (Figure 32A, Figure 32B).

Consider the i^{th} stage with reference to Figure 33. If it may be assumed that the exchange of ions between the two phases is controlled by resin phase diffusion, then the rate of exchange, for a given value of inter-diffusion coefficient $\bar{D}_{AB}$, depends on the momentary driving force available (Figure 33). This is equal to the difference in the compositions between the average particle composition $\bar{x}_i$ (representing concentration profile within the resin particle) and the composition at the surface of the particle $\bar{x}_i^*$ in equilibrium with the solution composition x_i in the stage i. For a steady state contactor this driving force is constant and independent of time (Figure 33).

If the performance of an ion exchange column may be defined as the extent of resin conversion or regeneration in this case i.e. $\bar{x}_o - \bar{x}_n/\bar{x}_o$, then for a given process in a steady state continuous ion exchange contactor this will depend on the number of stages, resin hold up per stage and the flow rate ratio of the two phases.

3.2.2. Theoretical interpretation of a cyclic countercurrent ion exchange process (unsteady-state)

Controlled cycling describes the method of operating a countercurrent stagewise contactor such that only one of the phases flows at any instant in time and both the phases uses the same interstage flow passage during their respective flow periods. The concept introduced by Cannon (1952) has been used in the field of distillation (McWhirter and Lloyd 1963) and solvent extraction (Belter

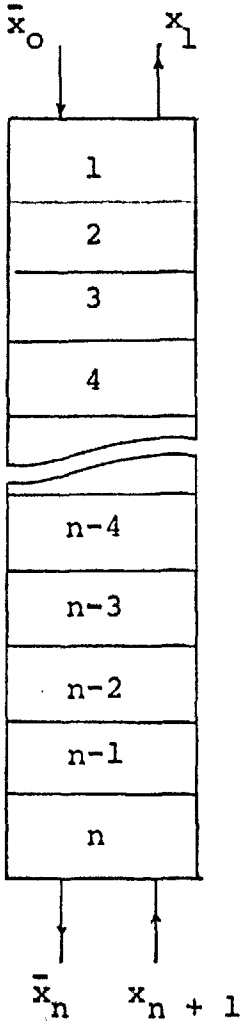

A.

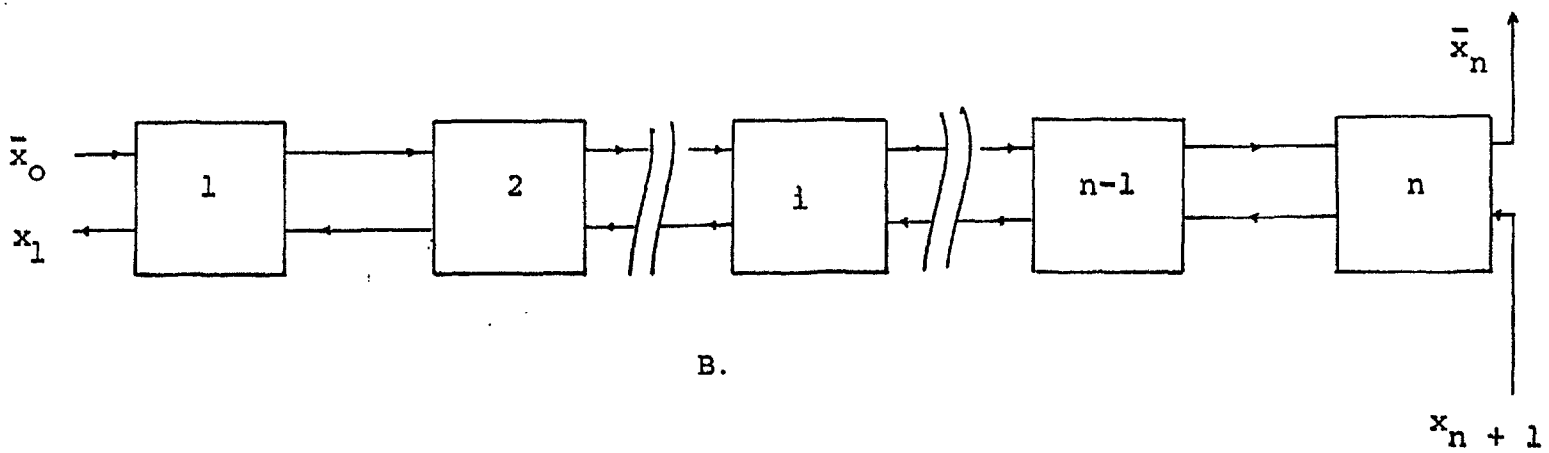

B.

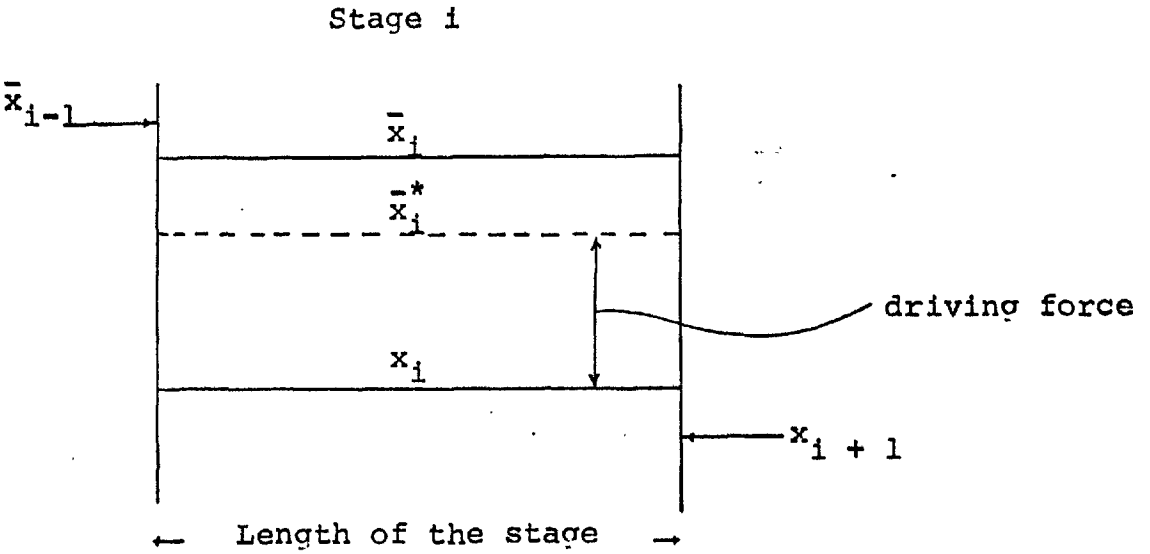

Figure 32. A Continuous countercurrent multistage column.
B Individual stages of the column

Figure 33. Driving force in stage i, both phases perfectly mixed

and Speaker 1967). The periodicity of fluid and resin flow in the Cloete-Streat contactor for ion exchange can be treated as controlled cycling operation.

Consider an ion exchange column divided into several separate stages by perforated plates. This can also be represented as a cascade of reaction vessels in series (see Figure 34). The controlled cycling of this system may be considered as a sequence of operations that repeat in a fixed period of time. Three cases may be considered.

i) Batch Reactor (Perfect Mixing)

Assume that each stage represents a batch reaction vessel isolated from the rest. The sequence of operations in the i^{th} stage during a complete cycle may be considered as follows:

a) Transfer the resin from stage (i-1) to stage i. At time (t) = 0 in i^{th} stage the resin composition is $\bar{x}_{i-1(T)}$ and equal to $\bar{x}_{i(0)}$. T represents the time of a complete cycle i.e. t_f+t_r, where t_f represents liquid flow period and t_r resin flow period.

b) Transfer the solution from stage (i+1) to stage i. At t=0 in stage i the solution composition is $x_{i+1\ (T)}$ and equal to $x_{i(0)}$.

c) The reaction proceeds in stage i for time 't_f' which corresponds with liquid flow period.

d) At time t_f, resin of composition $\bar{x}_{i(t_f)}$ is transfered to stage (i+1). This operation requires a time 't_r'. During the same period the solution of composition $x_{i(t_f)}$ is transfered to stage (i-1). At the completion of the resin and solution transfer step the compositions are $\bar{x}_{i(T)}$ and $x_{i(T)}$ respectively.

e) Repeat the cycle.

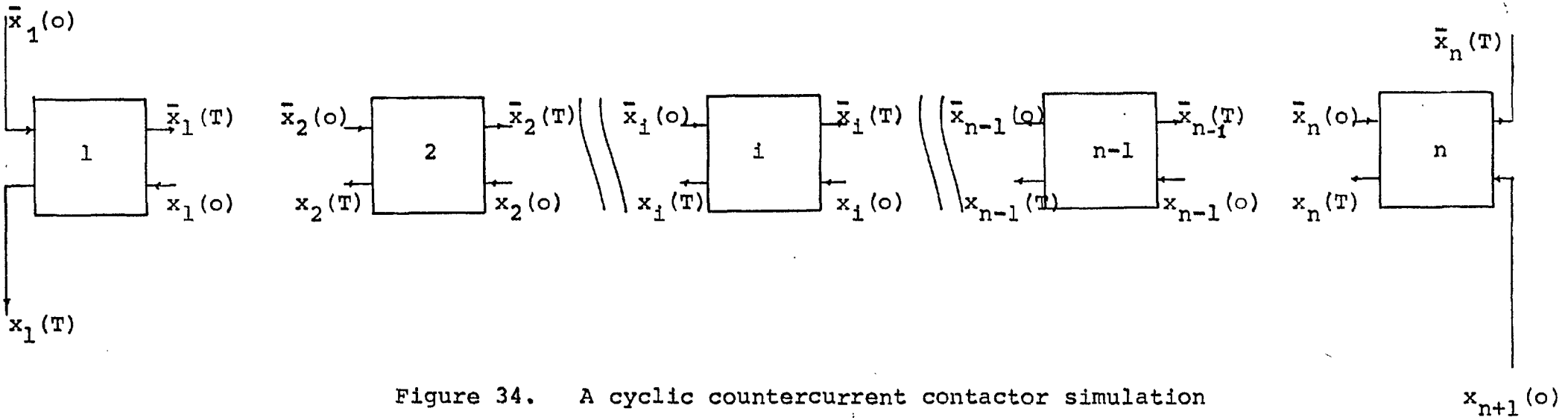

Figure 34. A cyclic countercurrent contactor simulation represented by perfectly mixed separate reaction vessels. Each stage is shown with its feed and product composition for a reaction time T.

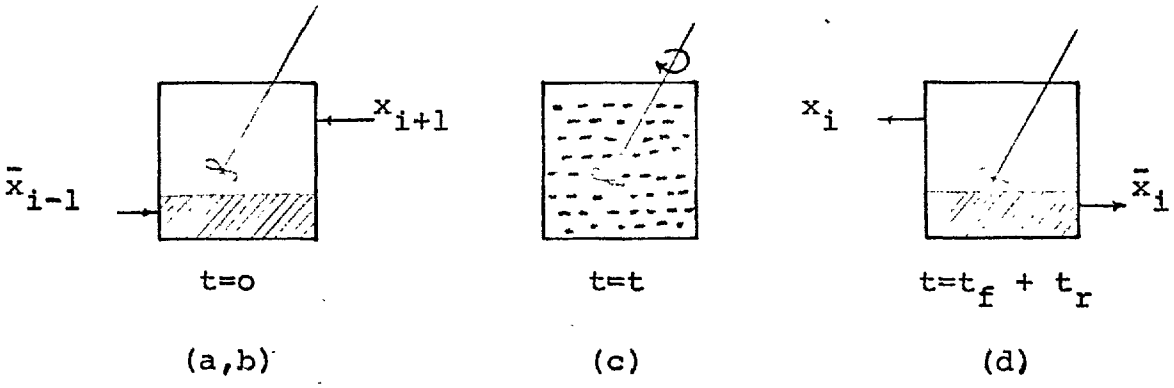

Figure 35. Sequence of operation in stage i of a cyclic countercurrent contactor as shown in Figure 34. (Stirrers are purely notional)

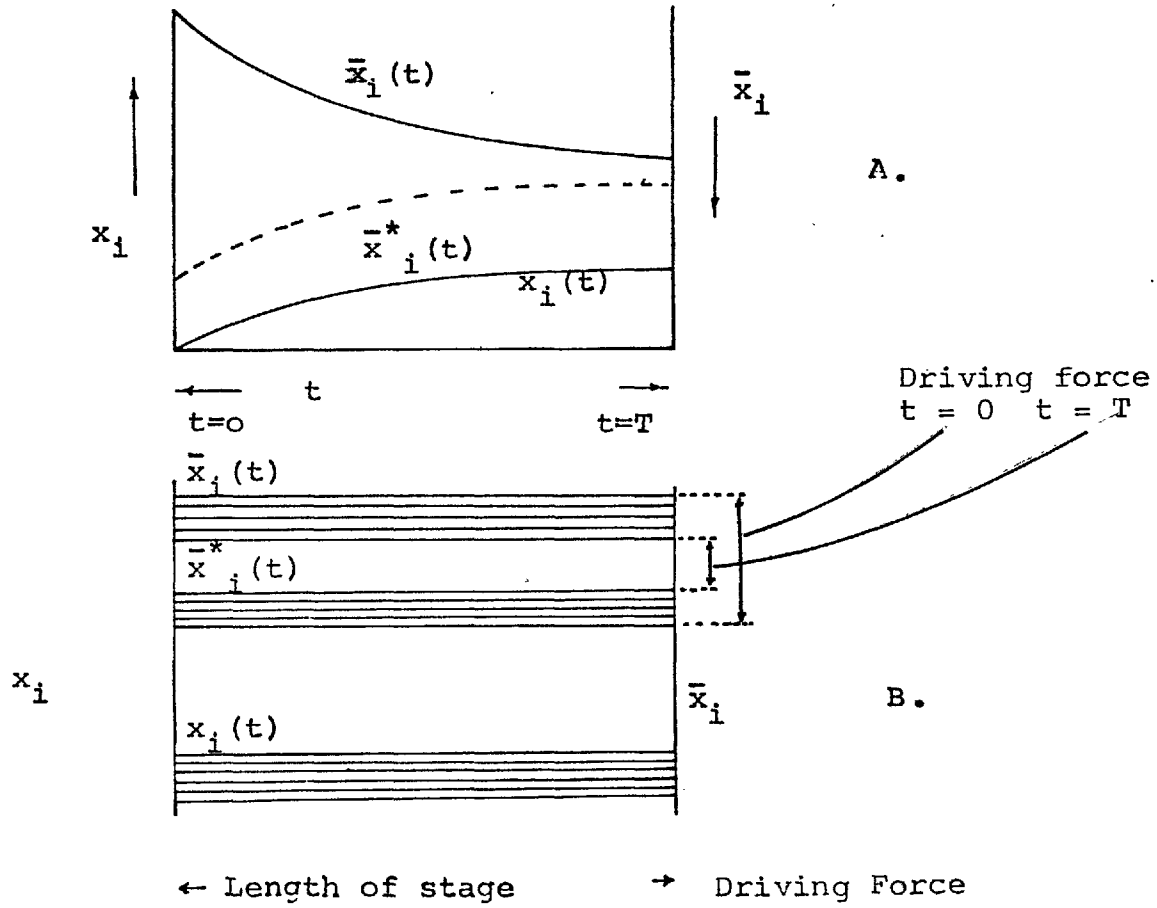

Figure 36 (A) Driving force variation with time in stage i
(B) Uniform composition throughout the stage at any time t.

Figure 35 is a schematic diagram of the controlled cycle operation showing individual steps.

The rate of ion exchange in the stage i will depend on the available momentary driving force (resin phase controlled reaction and perfectly mixed phases are assumed). Figure 36A shows the composition profile as a function of time in the stage. The corresponding driving forces are also shown in Figure 36B. For a long time period t_f, the process will attain equilibrium as shown in Figure 36A, with no further change in composition of both the phases. It may be noted that the composition of the liquid increases with time and is uniform throughout the stage. This implies that the feed solution transfered to the stage (i-1) at the end of a cycle will be of a fixed composition. The same will be true for the resin phase composition leaving stage i at t=T.

ii) Cyclic Flow Reactor (Perfectly Mixed)

Assume that each stage represents a perfectly mixed reaction vessel and solution flows from one stage to another during the liquid flow period t_f (Figure 37). The sequence of operations in the stage i during a complete cycle may be summarised as follows.

a) Transfer resin from stage (i-1) of composition $\bar{x}_{i-1\ (T)}$ to stage i at t=0.

b) Solution flow starts. The feed solution is of variable composition starting at $x_{i+1(0)}$ but rising continuously to $x_{i+1\ (t_f)}$ at the end of the liquid flow period. Within the stage i, the liquid composition x_i varies due to a time dependent feed and due to ion exchange from $x_{i(0)}$ to $x_{i(t_f)}$. Resin composition in stage i varies from $\bar{x}_{i(0)}$ to $\bar{x}_{i(t_f)}$ during the liquid flow period.

c) The liquid flow stops and resin of composition $\bar{x}_{i(t_f)}$ is transferred from stage i to stage (i+1). Assume that the resin transfer period is small compared to

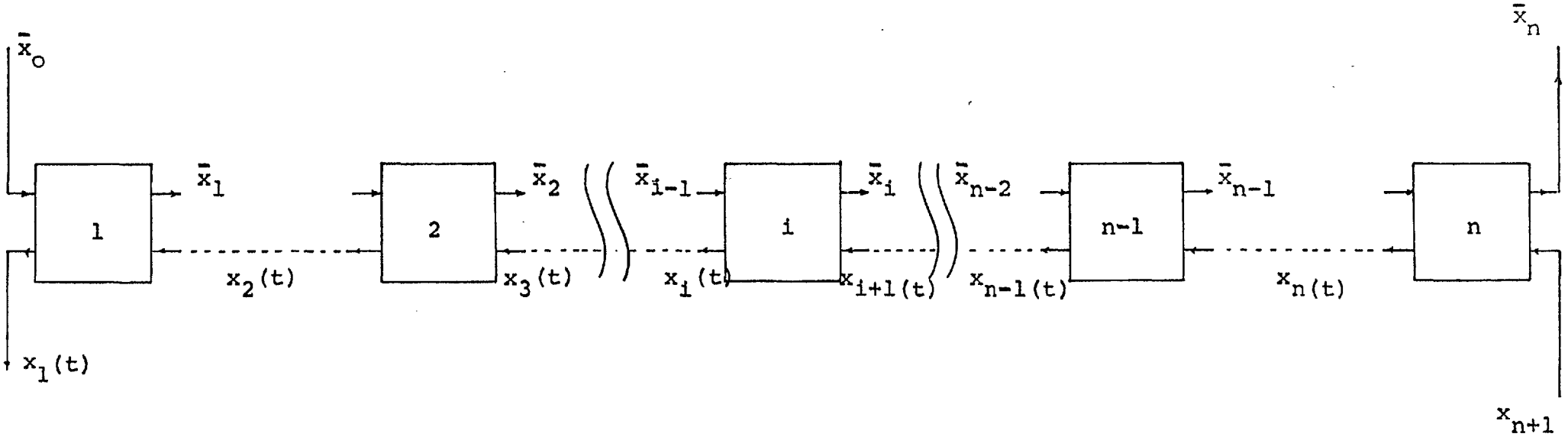

Figure 37 A cyclic countercurrent contactor simulation represented by perfectly mixed reaction vessels with fluid flow through them. Dotted lines show discontinuity of fluid flow during resin transfer period.

liquid flow period and thus any further exchange during t_r is negligible. Therefore the resin transferred to stage (i+1) will have composition $\bar{x}_{i\ (T)}$.

d) Repeat the cycle.

Figure 37A shows various steps of the controlled cycling operation. Figure 38A gives the composition-time profile of the liquid leaving as well as within the stage. Figure 38B shows the repetition of the time variant composition of the solution over each cycle.

It may be noted that the momentary driving force changes with time and is greatly enhanced at the start of the liquid flow period of the cycle (Figure 38C). This enhances the mass flux and despite the fact that the driving force decreases during the cycle the net effect is to greatly increase the performance. McWhirter and Lloyd (1963) have shown that controlled cycling in distillation may give stage efficiencies of as high as 200%. This is twice the performance of a single stage in a conventional column, since at steady-stae, 100% stage efficiency is the maximum attainable. Figure 38C shows the equilibrium isotherm and the momentary driving force within stage i during a complete cycle.

iii) Cyclic Reactor (Plug flow of liquid)

This type of operation assumes that the flow of liquid is plug flow throughout the contactor (Figure 39). The sequence of various operations is the same as in the case (ii).

Figure 39A shows the composition-time profile of the solution leaving the stage i at any moment in time. Figure 39D gives the repetition of the time-variant composition of the liquid leaving the stage i. During the liquid flow period, perfect resin mixing has been assumed. Plug flow of liquid is feasible in shallow fluidised beds but with deep fluidised beds the chances of mixing increase.

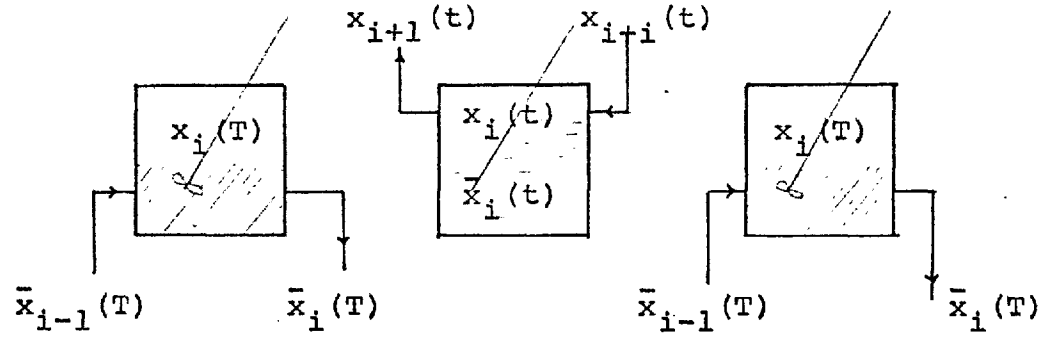

a) Resin transfer period (no flow)

b) Solution flow period

c) Resin transfer at the end of a cycle (no flow)

Figure 37 A. Sequence of operations in a cyclic countercurrent contactor.

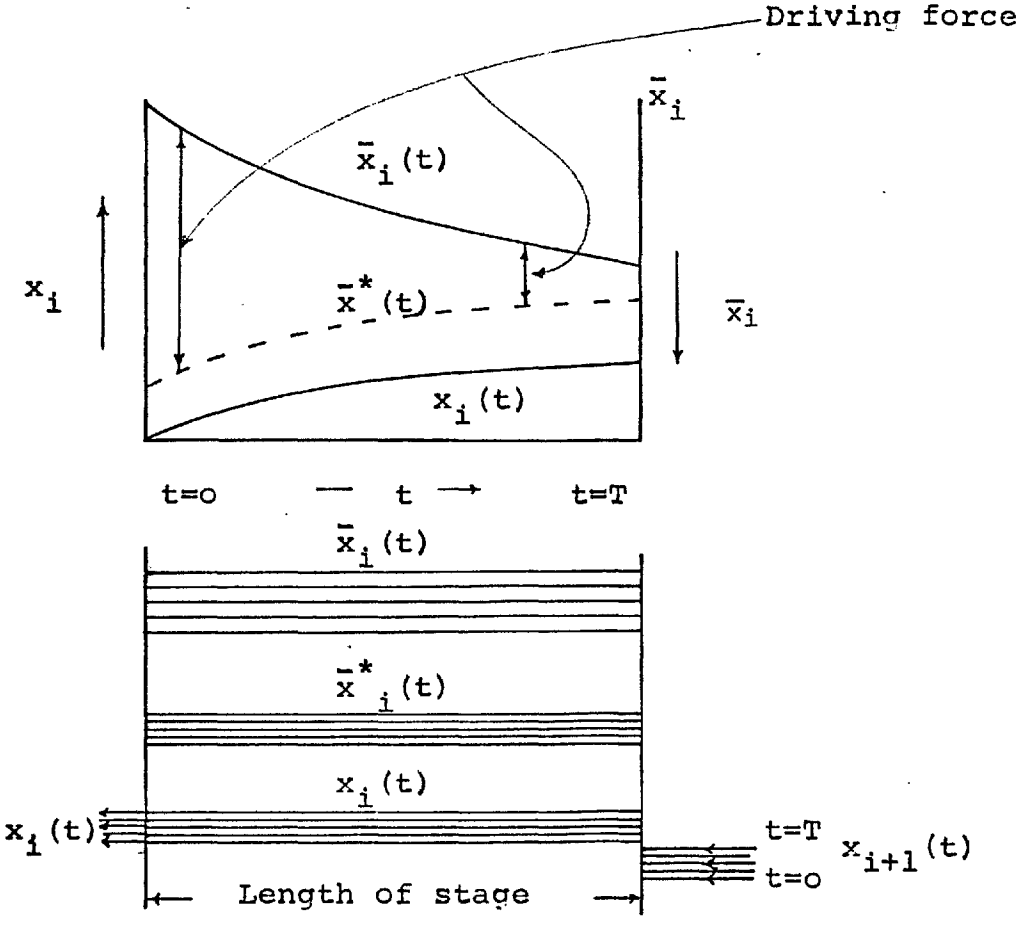

Figure 38.A (a) Time variant driving force in Stage i. $x_i(t)$ is solution composition in stage i as well as leaving it.

(b) . Uniform composition in stage i at time t. Note time variant composition of feed and product.

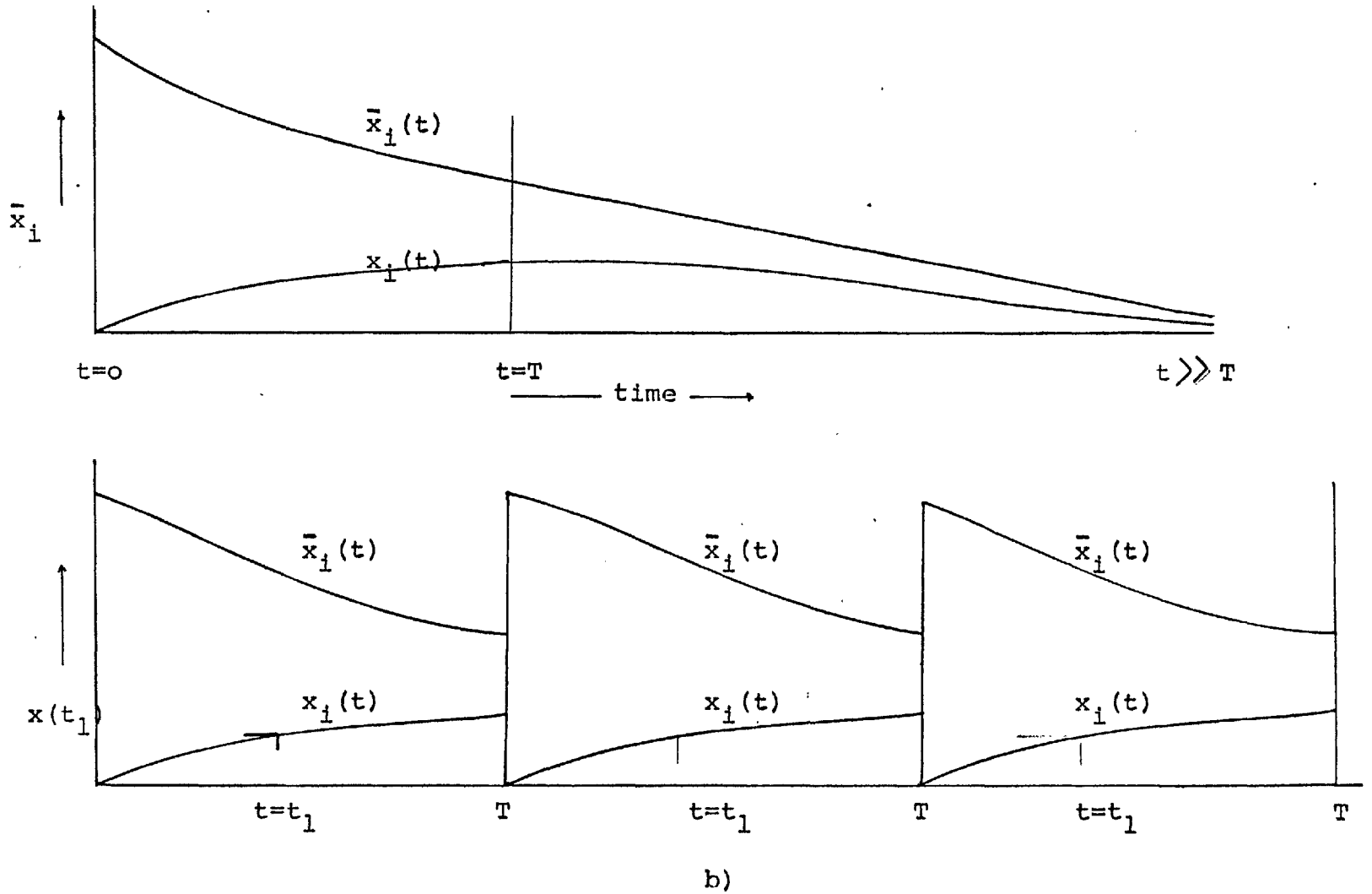

Figure 38 B. Composition profile of both phases as a function of fluid flow time (perfect mixing). Repetition of composition profile of both phases for a finite time cycle in stage i. $x_i(t)$ also represents composition time profile of solution leaving stage i.

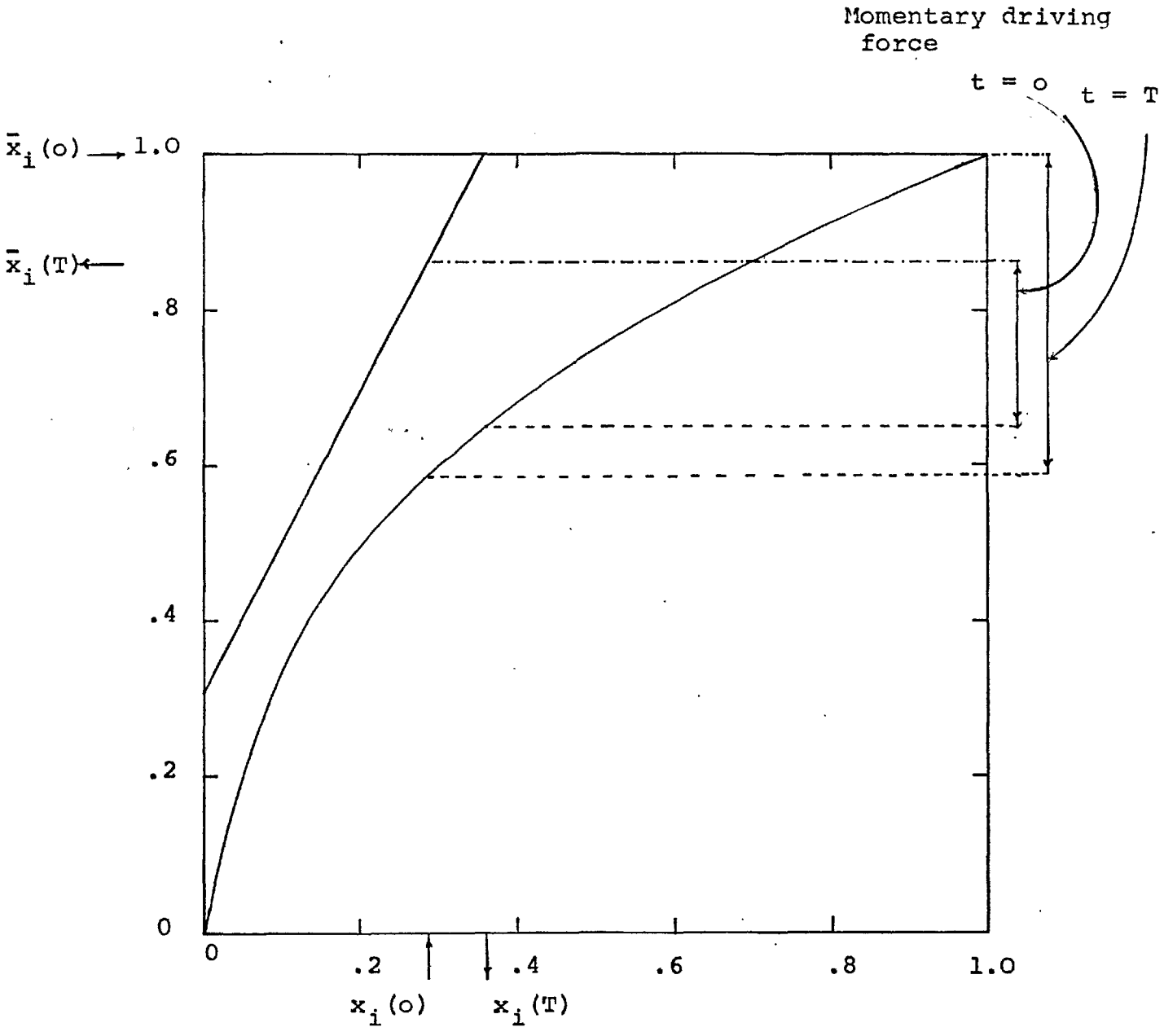

Figure 38 C. Variation of momentary driving force over a cycle in stage i.

As a result the concentration profile in the solution starts changing reaching the limiting condition of perfect mixing which corresponds to case (ii). Figure 39B shows the instantaneous driving force in stage i for various times during the liquid flow period. In this case, contrary to the previous one, the driving force increases during the cycle giving rise to higher flux. One would expect maximum advantage of the controlled cycling operation if the above conditions exist in the contactor.

The performance of the cyclic contactor will be strongly dependent on its frequency. Other important factors include the fractional transfer of hold-up of each phase during a cycle (the residence time distribution for each phase in the contactor). This may vary from zero to one.

Again consider stage i in a cascade of reaction vessels in series and assume that during the resin transfer period, complete resin hold up of the stage is transferred. If the rate of exchange is controlled by resin phase diffusion, the flux of ions at any instant in time may be assumed to depend on the apparent driving force between the average composition of the resin particle and the composition at the surface of the particle in equilibrium with the solution. This may be represented as

$$\bar{x}_{i(t)} - \bar{x}^{*}_{i(t)} \quad \text{(See Figure 40A)}$$

When only half of the resin hold up is transferred per cycle, the resin in the stage i at the start of the next cycle will consist of two fractions; half of the original hold up and half from stage (i-1). The average composition of the resin will thus be decreased resulting in a lower momentary driving force at the start of the cycle and reduced flux when compared with the case of complete transfer of resin i.e. $\bar{r} = 1.0$ (Figure 40B) This may be explained as follows:

Let the composition of resin holdup in the stage i at the start of a cycle, under the conditions of complete transfer

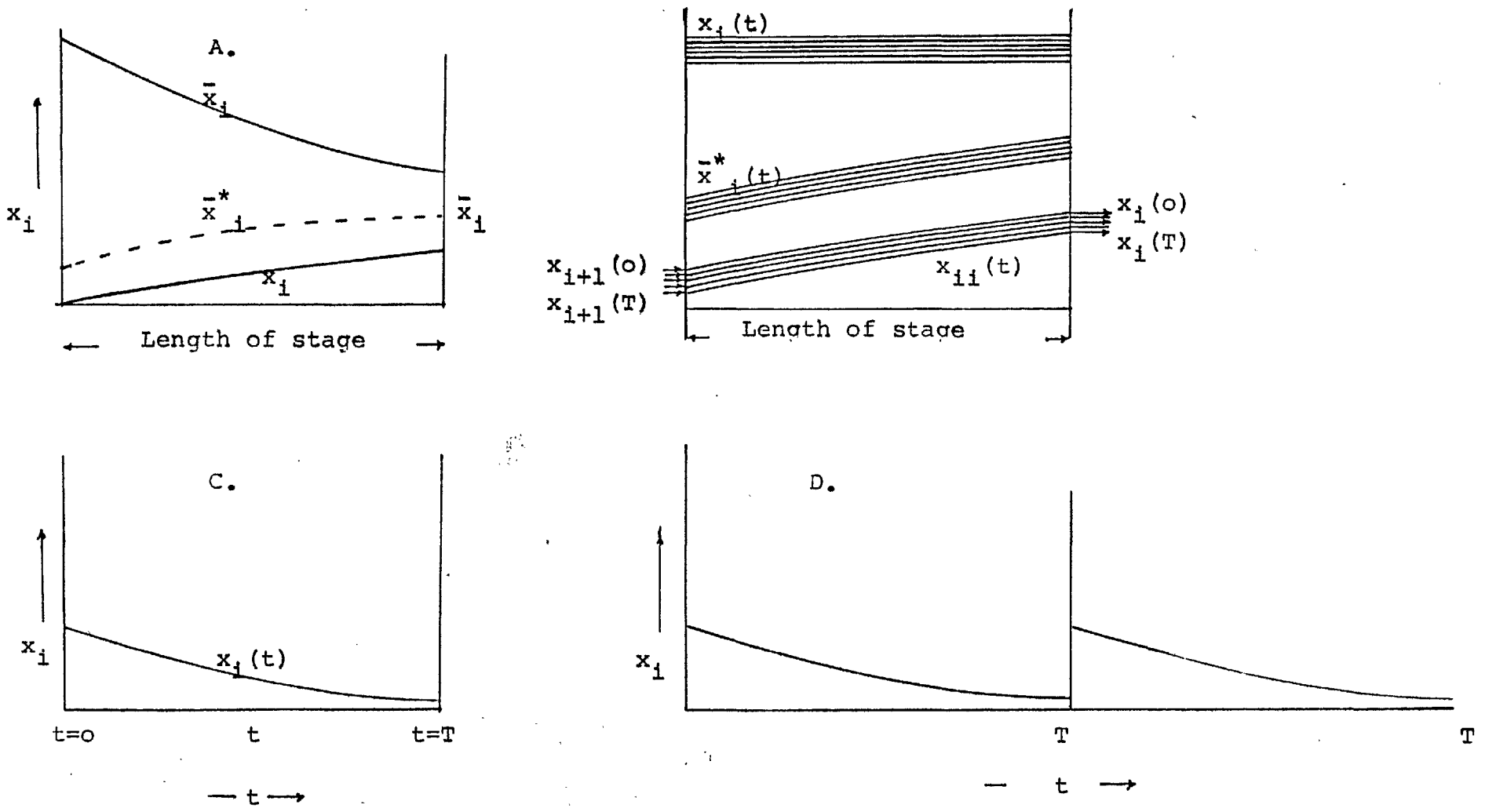

Figure 39.

A. Time variant driving force in stage i.

B. Composition profile of solution in stage at time t. Plug flow of liquid resin perfectly mixed.

C. Composition time profile of solution leaving stage i.

D. Repition of composition profile after each cycle time = T.

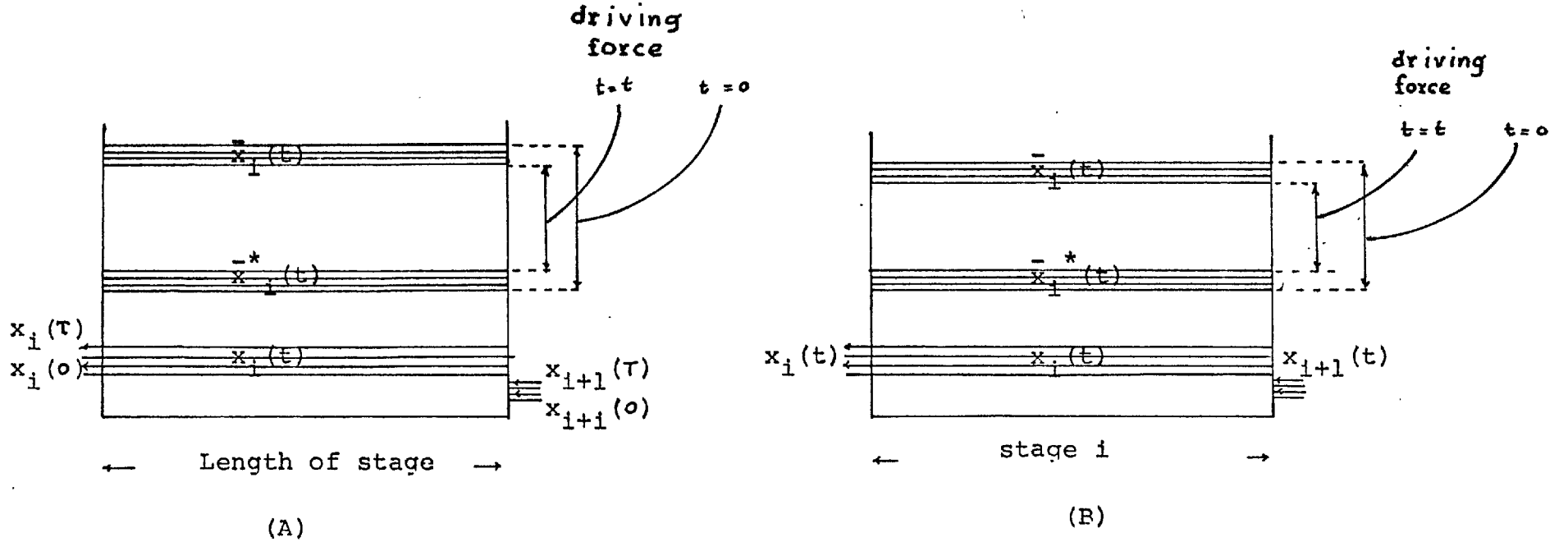

Figure 40.

A. Driving force in stage i with complete transfer of resin hold-up per stage per cycle.

B. Reduced driving force in the same stage with fractional ($\bar{r}$ = 0.5) transfer of resin hold-up per stage per cycle.

of resin per cycle, be represented by $\bar{x}_{i(O)}^{\bar{r}=1.0}$. At the end of a cycle, the resin composition decreases from $\bar{x}_{i(O)}^{\bar{r}=1.0}$ to $\bar{x}_{i(T)}^{r=1.0}$. Now, if only half of the resin hold up is transferred during the resin transfer period, stage i will be left with half of its original resin hold up of composition $\bar{x}_{i(T)}^{\bar{r}=1.0}$ and will recieve an equal volume of resin from the previous stage with composition of $\bar{x}_{i-1(T)}^{\bar{r}=0.5}$,

i.e.

Total resin hold up in stage i = half residual resin and half fresh resin from stage (i-1)

$$\text{Average } \bar{x}_{i(O)}^{\bar{r}=0.5} = \tfrac{1}{2}\, \bar{x}_{i(T)}^{\bar{r}=1.0} + \tfrac{1}{2}\, \bar{x}_{i-1(T)}^{\bar{r}=0.5} \qquad (74)$$

$$= \tfrac{1}{2}\, \bar{x}_{i(T)}^{\bar{r}=1.0} + \tfrac{1}{2}\, \bar{x}_{i(O)}^{\bar{r}=0.5} \qquad (75)$$

Since for a cycle, under complete transfer conditions

$$\bar{x}_{i(T)}^{\bar{r}=1.0} < \bar{x}_{i(O)}^{\bar{r}=1.0} \qquad (76)$$

Therefore from (75) and (76)

$$\text{Average } \bar{x}_{i(O)}^{\bar{r}=0.5} < \bar{x}_{i(O)}^{\bar{r}=1.0} \qquad (77)$$

A decrease in the resin composition results in lower driving force and flux and decreased performance (Figure 40B).

By a similar argument the solution entering the i^{th} stage will be of lower composition with respect to the ion stripped from the resin in stage (i+1) and will enhance the flux. Thus, these two effects oppose each other. The net result depends on the composition of the solution entering stage i.

Consider Figure 41 which shows three typical equilibrium isotherms for the system A-B. Curve 'a' is favourable for A, 'b' shows no preference for A and 'c' unfavourable for A. If the solution entering stage i is rich in ion A, a small

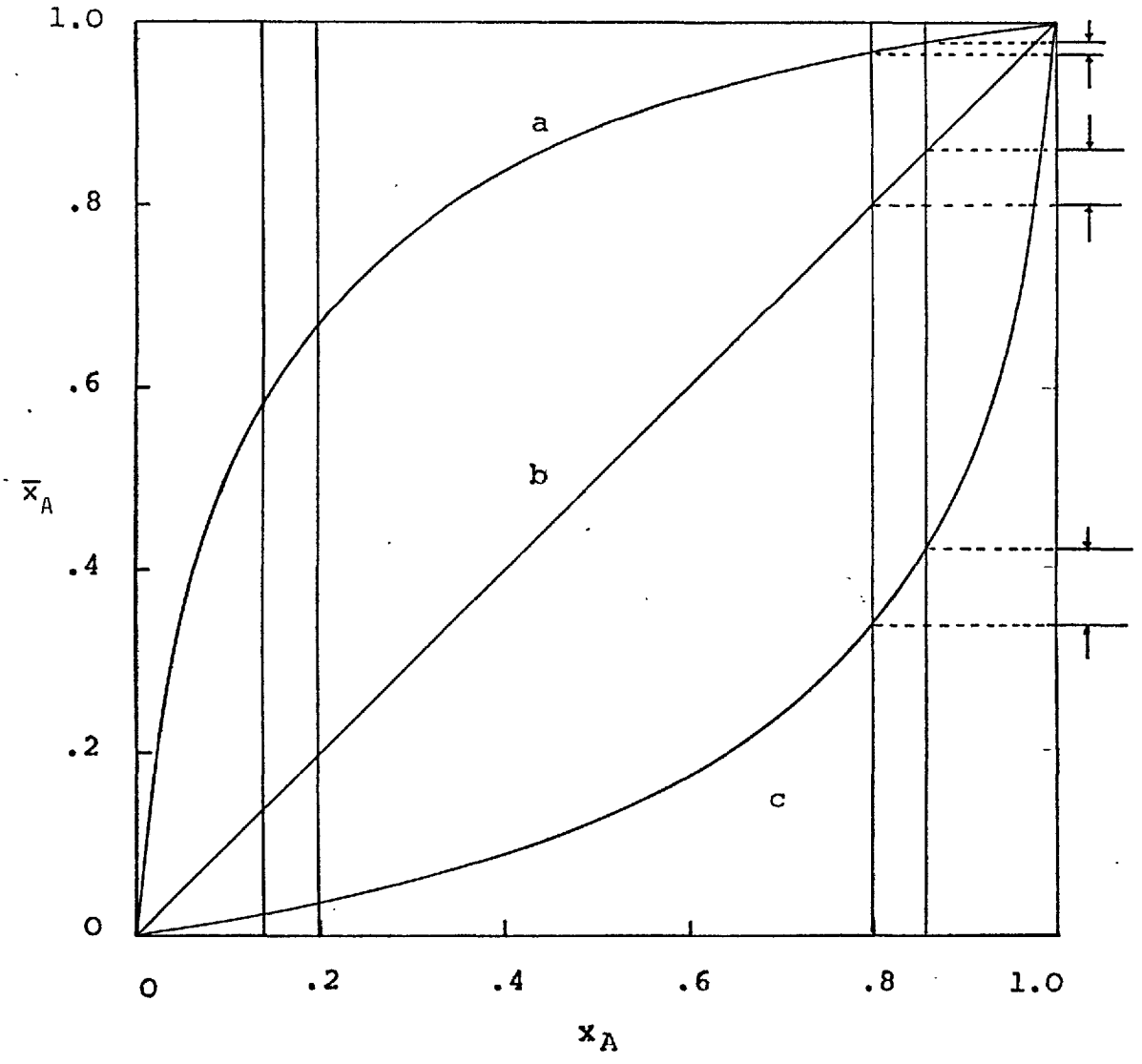

Figure 41. Typical equilibrium isotherm for a hypothetical system A-B.

a Favourable for A

b No preference

c Unfavourable for A

change in solution composition due to lower flux in the stage (i+1) will have a relatively small effect on the equilibrium composition $\bar{x}_i^*$ and the net result of the two opposite effects mentioned above will be a decrease in the flux in stage i and decreased performance. For curve b i.e. $x_{A_i} = \bar{x}_{A_i}$ the change in composition for both phases will be equal and thus the performance should be unaffected. For curve c a small change in the solution composition rich in A will have a substantial effect on the equilibrium composition of the resin phase and the net effect will be an enhancement of flux. Conversely, the effect of a small change in solution composition rich in B is far less significant and should not have a noticeable effect on the driving force and the flux.

It is also possible to operate with a fractional transfer of the liquid hold up per cycle and this will generally result in an increase in the ionic composition in the solution phase compared with complete transfer. This will result in a lower driving force and the net effect of controlled cycling will be decreased.

One may conclude from this discussion that it is likely that cyclic operation of a countercurrent stagewise process will give better performance than steady-state continuous operation particularly where the fractional transfer of resin between stages tends to one i.e. dumping of the complete resin hold-up per cycle.

3.3. Description of the Experimental Technique Used

A new multistage cyclic ion exchange contactor has been used in this study. The contactor designed by Cloete and Streat (1963) is semi-continuous and operates under fluidised bed conditions. The countercurrent movement of the resin from one stage to another is achieved by periodic reversal of the flow of fluid. A horizontal version of the Cloete-Streat contactor has been employed for all the experimental work.

A single stage consists of a contacting vessel and a transfer leg. Figure 42 shows a single stage with its segments, the contacting vessel (A), transfer leg (B) and the partitions (C). These segments when put together can be used to build up a multistage contactor.

The operation of the contactor consists of a cyclic flow of liquid into the contactor. A typical flow cycle is shown in Figure 43. The liquid passes through a series of stages fluidising the resin bed during the forward flow period (t_f). During the reverse flow period (t_r) equal amounts of resin are transferred between the adjacent stages in a direction countercurrent to the net flow of liquid. The transfer of resin takes place in dense phase flow. Resin feed is introduced using a separate pump at the beginning of a reverse cycle.

The average flow rate of liquid depends on the instantaneous flow rate (U) and the time periods for forward and reverse flow;

$$L = U\frac{(t_f - t_r)}{t_f + t_r}$$

where L is the average liquid flow rate. The average flow rate of resin (R) is

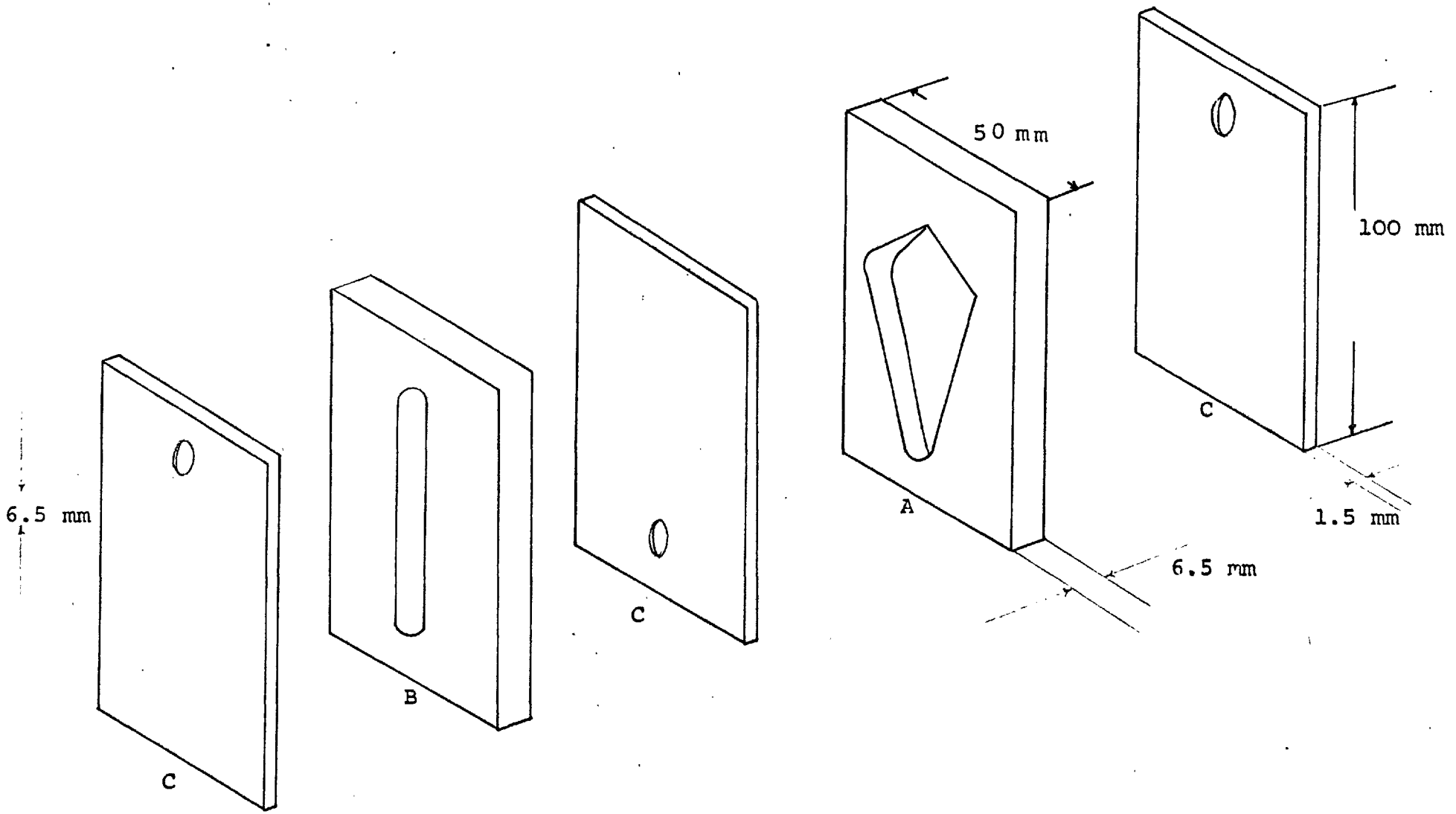

Figure 42. Various segments of a single stage.

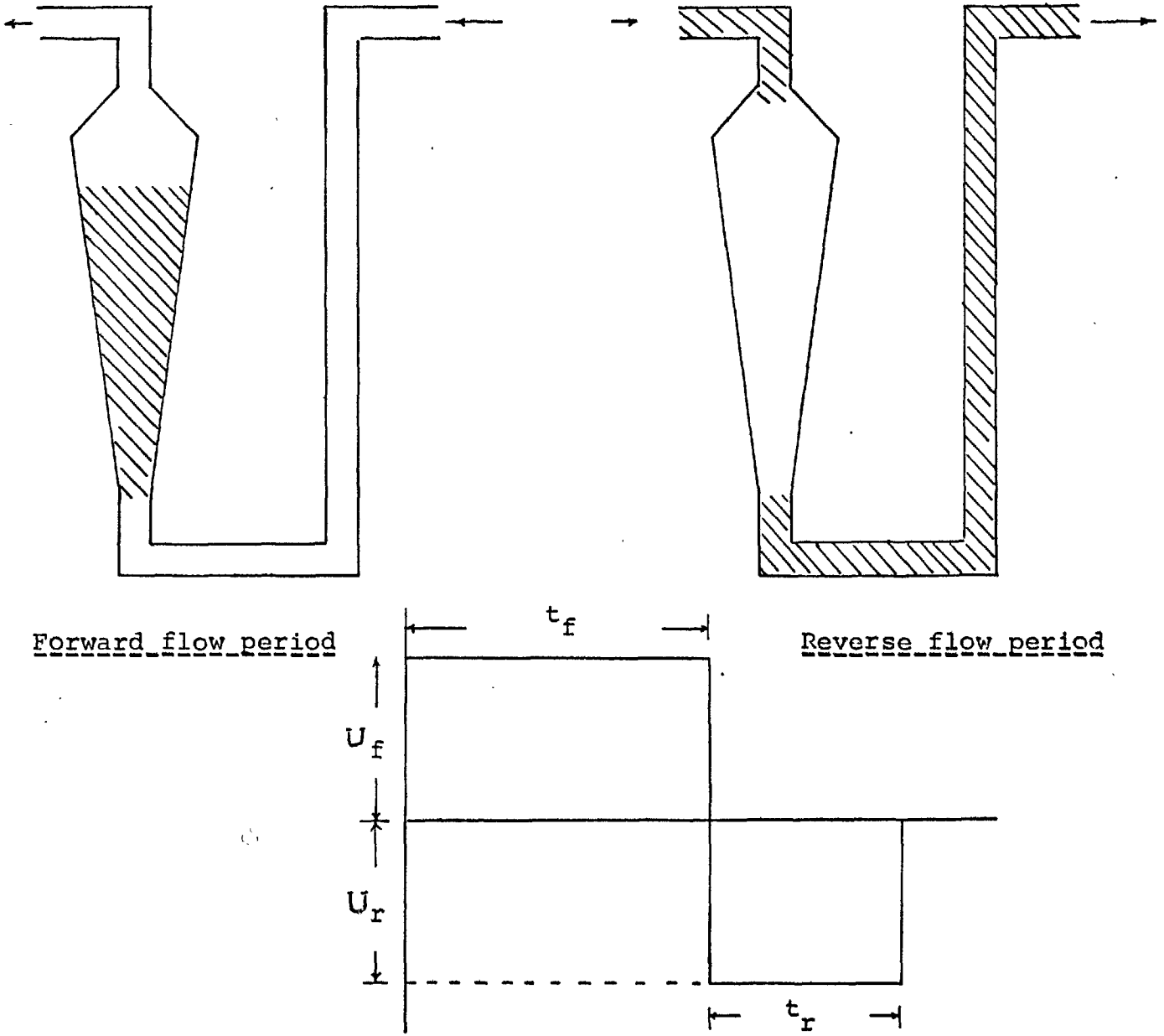

Figure 43. Typical flow cycle of the contactor.

$$R = \frac{W}{t_f + t_r}$$

where W is the volume of resin transferred every cycle.

The stages used in this study were designed by Frost (1968) and are made of perspex. Each stage holds about 10 ml of liquid. Details of other dimensions are given in Figure 42.

3.3.1. Hydrodynamics

In order to analyse the performance of a multistage countercurrent contactor from equilibrium and kinetic data of the system involved it is essential to have a knowledge of the average flow rates and average residence times of each phase in the contactor.

Previous work by Bennett et al (1969) on a horizontal contactor of 50mm internal diameter and of similar design has shown that each real stage may be considered as a perfectly mixed vessel with respect to the resin phase. Under such conditions the average residence time of resin in each stage may be calculated as the ratio of the resin hold-up per stage divided by the average resin flow rate.

The flow of the liquid through the contactor is rather complicated. Bennett et al (1969) using a pulse signal in the liquid phase showed that each real stage may be considered equivalent to two perfectly mixed vessels in series. In fact the mode of liquid flow depends on the ratio of the forward and reverse flow time periods. When the two time periods i.e. t_f and t_r are similar the flow of the liquid is close to perfectly mixed. On the other hand as the ratio t_f/t_r increases the liquid residence time distribution approaches plug flow.

In the small scale contactor used during this work, perfect mixing of both phases has been assumed. This is considered a reasonably valid assumption.

3.4. Experimental

A complete flowsheet of the equipment used in the present work is shown in Figure 44. The contactor consists of a horizontal assembly of ten perspex stages and a solution feed stage. Solution feed tank T_1 was of standard QVF glass-ware and could hold about 5 litres of process solution. Resin feed tank T_2 was a graduated burette of capacity 100 mls supplemented by a resin storage tank T_{10} of capacity 1 litre. Sodium chloride (1N) was used to regenerate the calcium form of the resin.

Dewrance solenoid three way valves V_1, V_2 and V_3 have been used to control the direction of flow of the solution. Their operation was controlled through a cycle timer. Three independent Crouzet timer units (Type 207, Valence, made in France) were employed to operate the cyclic contactor. A line diagram shows the sequence of various time periods in a complete cycle (Figure 43). For the delivery of the solution and resin into and outof the contactor DCL Series II Micropumps P_1 and P_2 were employed. The solution feed was displaced by kerosene pumped from tank T_3 into the top of the feed tank T_1. Odourless kerosene was used as a hydraulic transfer fluid to displace the feed solution since this avoided any possibility of contamination of the feed solution by corrosion of the pump and valves. Back pressure valves Y_1 and Y_2 were used at the outlet of both the pumps to prevent siphoning of liquid through the pumps from the feed tank. Sintered glass filters F_1 and F_2 of zero porosity were placed at the inlet to the pumps to prevent particles of dirt from interferring with the efficient working of the ball valves in the pumps and solenoid valves

The pipelines between V_1 and V_2 were 3/10" internal diameter copper tubing. The pipe between the pump P_1 and tank T_1 was of plasticised PVC (polyvinylchloride). Use of copper and plasticised PVC piping gave satisfactory operation. For all the other connections nylon tubing was used. Deionised water was used as a hydraulic transfer fluid for resin feed and nylon tubing between pump P_2 and T_2 through valve V_3 was found satisfactory throughout the work.

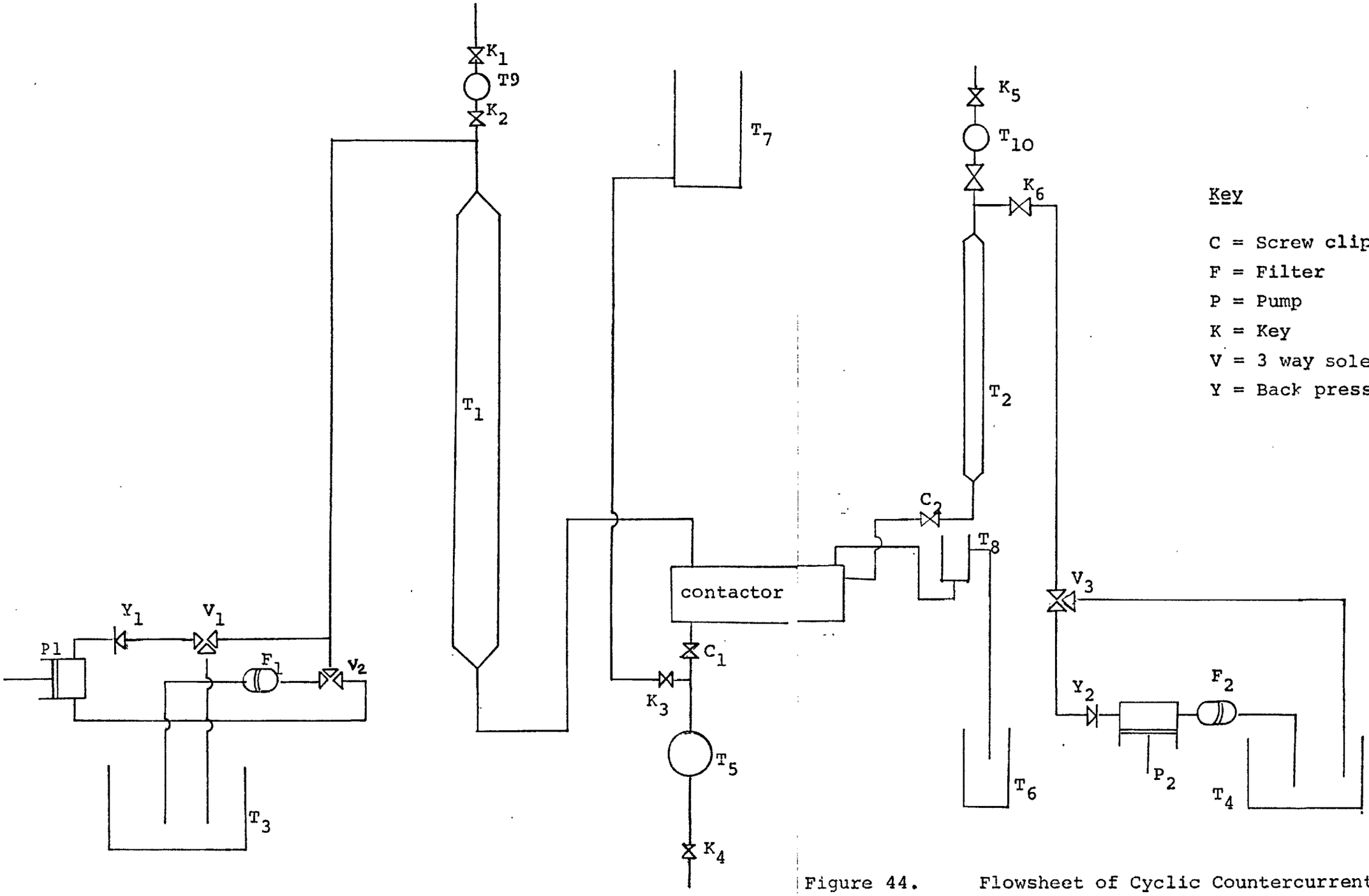

Key

C = Screw clip
F = Filter
P = Pump
K = Key
V = 3 way solenoid valve
Y = Back pressure value

Figure 44. Flowsheet of Cyclic Countercurrent ion exchange contactor used in this study.

The liquid outlet of the contactor must be open to atmosphere because liquid is pumped into and out-of the contactor during the forward flow and reverse flow periods respectively. A small tank T_8 was used at the liquid outlet to prevent air being sucked into the contactor during the reverse flow period. The liquid product together with the slip water entering with the resin feed overflowed into the measuring tank.

The resin product passes from the contactor into the resin product tank T_5 and displaces an equal volume of solution (feed solution in this case) back into the contactor. An arrangement of screwclips was set to remove the resin product from the tank T_5 by periodic flushing of resin by solution from tank T_7.

The progress of a run could be followed by regular analysis of the liquid product collected over ten or more complete cycles. Composition of the resin product was calculated from a mass balance. When the solution analysis at the product end was constant for three consective samples, a test run was commenced. Solution samples from the solution product end and from interstage sampling points were collected periodically at the same instant in a particular cycle and subsequently analysed using atomic absorption spectroscopy. In an assembly of 10 stages, samples were withdrawn from 4th, 6th, 8th and the 10th stage using a syringe inserted through silicon rubber bungs fitted at the outlet of these stages. All the solution samples were collected at the end of the forward flow period from each sampling point. A volume check was made on all feed and product streams at the beginning and the end of the run to check volume balance and to determine the average flow rates of the resin and solution phase through the contactor. The resin compositions were always calculated by mass balance.

3.5 RESULTS

Tables 22-27 give the details of operating conditions of the experimental runs. The first four runs represent the conditions where operation with fractional transfer of resin and solution holdups (~.25) between the stages were carried out. Runs 5 and 6 were carried out with increasing value of the fractional transfer of resin and solution phase.

An instantaneous solution flow rate of 26.6 ml/min was chosen since it was observed that the resin is gently fluidised in each stage. In all runs slip water with the resin feed was about 50%. Tables 22-27 show that an excellent volume balance was obtained for both phases.

The resin holdup of a stage was found from the total holdup of the ten stage contactor at the end of each run. The average flow rate of solution is the sum total of solution feed rate and the solution which is fed into the contactor by displacement in the resin product receiving tank.

The computed results of the compositions of both phases have been reproduced from the computer output.

The numbers 4, 6, 8 and 10 refer to the interstage compositions of solution and resin phases (Tables 22-27 and Figures 45-50, 52) and correspond to the composition at those points. For example, sample point 4 represents the composition of solution leaving the fourth stage (x_4) and that of the resin entering the fourth stage i.e., $\bar{x}_3$.

Table 22. Operating conditions and results of experimental runs on cyclic countercurrent contactor. Regeneration of calcium form resin with solution of sodium chloride

Run No: 1

Number of actual stages	10
Forward flow period (t_f) sec.	15.5
Reverse flow period (t_r) sec.	14.0
Liquid flow rate $U_f = U_r$ cm^3/min.	26.6
Average liquid flow rate (L) cm^3/min.	2.05
Average resin flow rate (R) cm^3/min.	0.85
Solution feed concentration mequiv./ml.	1.00
Resin exchange capacity mequiv./ml.	2.00
Solution volume fed into the contactor ml/90 min.	138.6
Water to the resin feed column ml/90 min.	136.0
Solution volume recovered after the run ml.	275.0
Resin volume fed into the contactor during the run (90 min.) ml.	76.5
Resin recovered after the run ml.	75.0
Resin holdup per stage ml.	1.70
Resin holdup fraction transferred per cycle	0.25
Liquid holdup per stage ml.	8.98
Liquid hold up fraction transferred per cycle	0.114
Ratio $LC_o/R\bar{C}_o$	1.207
Total time for the run	120.0
Total No.of computed stages	5

Analysis of interstage solution samples withdrawn at fixed times after the start of a run

Time (mins.)	Resin Feed End		4		6		8		10		Solution feed end	
	x_{Ca}	$\bar{x}_{Ca}$	x_{Ca}	$\bar{x}_{Ca}$	x_{Ca}	$\bar{x}_{Ca}$	x_{Ca}	$\bar{x}_{Ca}$	x_{Ca}	$\bar{x}_{Ca}$	x_{Ca}	$\bar{x}_{Ca}$
10	.258	1.00										
20	.396	1.00										
30	.440	1.00										
60	.442	1.00	.325	.860	.252	.772	.179	.685	.10	.59	0.00	.468
90	.452	1.00	.320	.855	.265	.790	.180	.685	.090	.578	0.00	.456
120	.440	1.00	.330	.870	.250	.770	.160	.660	.090	.578	0.00	.472

Computed interstage composition of resin and solution

	1	2	3	4	5	6	7	8	9	10
x_{Ca}	.441	.288	.207	.141	.0712					
$\bar{x}_{Ca}$	1.00	.849	.748	.665	.581					

	11	12	13	14	15	16	17	18	19	20
x_{Ca}										
$\bar{x}_{Ca}$										

Table 23. Operating conditions and results of experimental runs on cyclic countercurrent contactor. Regeneration of calcium form resin with solution of sodium chloride

Run No: 2

Number of actual stages	10
Forward flow period (t_f) sec.	15.75
Reverse flow period (t_r) sec.	14.00
Liquid flow rate $U_f = U_r$ cm^3/min.	26.60
Average liquid flow rate (L) cm^3/min.	2.10
Average resin flow rate (R) cm^3/min.	1.00
Solution feed concentration mequiv./ml.	1.00
Resin exchange capacity mequiv./ml.	2.00
Solution volume fed into the contactor ml/90 min.	135.00
Water to the resin feed column ml/90 min.	135.00
Solution volume recovered after the run ml.	272.00
Resin volume fed into the contactor during the run (90 min.) ml.	90.0
Resin recovered after the run ml.	91.5
Resin holdup per stage ml.	2.00
Resin holdup fraction transferred per cycle	0.25
Liquid holdup per stage ml.	8.80
Liquid hold up fraction transferred per cycle	0.119
Ratio $LC_o/R\bar{C}_o$	1.050
Total time for the run min.	120.0
Total No.of computed stages	9

Analysis of interstage solution samples withdrawn at fixed times after the start of a run

Time	Resin Feed End		4		6		8		10		Solution feed end	
(mins)	x_{Ca}	$\bar{x}_{Ca}$	x_{Ca}	$\bar{x}_{Ca}$	x_{Ca}	$\bar{x}_{Ca}$	x_{Ca}	$\bar{x}_{Ca}$	x_{Ca}	$\bar{x}_{Ca}$	x_{Ca}	$\bar{x}_{Ca}$
10	.220	1.00										
20	.480	1.00										
30	.550	1.00										
60	.550	1.00	.410	.854	.320	.760	.239	.675	.146	.580	0.00	.422
90	.544	1.00	.409	.851	.336	.775	.244	.680	.152	.585	0.00	.429
120	.548	1.00	.403	.846	.322	.762	.243	.680	.153	.585	0.00	.425

Computed interstage composition of resin and solution

	1	2	3	4	5	6	7	8	9	10
x_{Ca}	.548	.415	.342	.287	.240	.195	.151	.100	.035	
$\bar{x}_{Ca}$	1.00	.883	.805	.745	.693	.644	.595	.540	.471	

	11	12	13	14	15	16	17	18	19	20
x_{Ca}										
$\bar{x}_{Ca}$										

Table 24. Operating conditions and results of experimental runs on cyclic countercurrent contactor. Regeneration of calcium form resin with solution of sodium chloride

Run No: 3

Number of actual stages	10
Forward flow period (t_f) sec.	17.55
Reverse flow period (t_r) sec.	14.00
Liquid flow rate $U_f = U_r$ cm^3/min.	26.60
Average liquid flow rate (L) cm^3/min.	3.36
Average resin flow rate (R) cm^3/min.	0.875
Solution feed concentration mequiv./ml.	1.00
Resin exchange capacity mequiv./ml.	2.00
Solution volume fed into the contactor ml/90 min.	246.20
Water to the resin feed column ml/90 min.	120.00
Solution volume recovered after the run ml.	370.00
Resin volume fed into the contactor during the run (90 min.) ml.	78.75
Resin recovered after the run ml.	75.50
Resin holdup per stage ml.	1.75
Resin holdup fraction transferred per cycle	0.266
Liquid holdup per stage ml.	8.95
Liquid hold up fraction transferred per cycle	0.181
Ratio $LC_o/R\bar{C}_o$	1.925
Total time for the run	120.0
Total No.of computed stages	9

Analysis of interstage solution samples withdrawn at fixed times after the start of a run

Time (mins.)	Resin Feed End		4		6		8		10		Solution feed end	
	x_{Ca}	$\bar{x}_{Ca}$	x_{Ca}	$\bar{x}_{Ca}$	x_{Ca}	$\bar{x}_{Ca}$	x_{Ca}	$\bar{x}_{Ca}$	x_{Ca}	$\bar{x}_{Ca}$	x_{Ca}	$\bar{x}_{Ca}$
10	.280	1.00										
20	.300	1.00										
30	.360	1.00										
60	.360	1.00	.225	.735	.150	.590	.105	.510	.047	.395	0.00	.308
90	.358	1.00	.218	.722	.155	.600	.110	.514	.059	.415	0.00	.312
120	.361	1.00	.220	.725	.158	.616	.107	.510	.057	.410	0.00	.305

Computed interstage composition of resin and solution

	1	2	3	4	5	6	7	8	9	10
x_{Ca}	.361	.249	.202	.167	.137	.110	.085	.058	.0285	
$\bar{x}_{Ca}$	1.00	.824	.726	.656	.542	.542	.489	.436	.378	

	11	12	13	14	15	16	17	18	19	20
x_{Ca}										
$\bar{x}_{Ca}$										

Table 25. Operating conditions and results of experimental runs on cyclic countercurrent contactor. Regeneration of calcium form resin with solution of sodium chloride

Run No: 4

Number of actual stages	10
Forward flow period (t_f) sec.	19
Reverse flow period (t_r) sec.	14
Liquid flow rate $U_f = U_r$ cm^3/min.	26.60
Average liquid flow rate (L) cm^3/min.	4.50
Average resin flow rate (R) cm^3/min.	0.85
Solution feed concentration mequiv./ml.	1.00
Resin exchange capacity mequiv./ml.	2.00
Solution volume fed into the contactor ml/90 min.	357.0
Water to the resin feed column ml/90 min.	114.75
Solution volume recovered after the run ml.	470.0
Resin volume fed into the contactor during the run (90 min.) ml.	77.0
Resin recovered after the run ml.	75.0
Resin holdup per stage ml.	1.70
Resin holdup fraction transferred per cycle	0.25
Liquid holdup per stage ml.	8.98
Liquid hold up fraction transferred per cycle	0.275
Ratio $LC_o/R\bar{C}_o$	2.647
Total time for the run min.	120.0
Total No.of computed stages	11

Analysis of interstage solution samples withdrawn at fixed times after the start of a run

Time (min)	Resin Feed End		4		6		8		10		Solution feed end	
	x_{Ca}	$\bar{x}_{Ca}$	x_{Ca}	$\bar{x}_{Ca}$	x_{Ca}	$\bar{x}_{Ca}$	x_{Ca}	$\bar{x}_{Ca}$	x_{Ca}	$\bar{x}_{Ca}$	x_{Ca}	$\bar{x}_{Ca}$
10	.270	1.00										
20	.279	1.00										
30	.286	1.00										
60	.288	1.00	.189	.715	.134	.570	.103	.487	.044	.334	0.00	.237
90	.294	1.00	.186	.712	.135	.572	.106	.495	.046	.336	0.00	.220
120	.296	1.00	.188	.715	.134	.570	.105	.490	.045	.335	0.00	.215

Computed interstage composition of resin and solution

	1	2	3	4	5	6	7	8	9	10
x_{Ca}	.296	.208	.172	.147	.127	.110	.095	.082	.069	.057
$\bar{x}_{Ca}$	1.00	.802	.701	.630	.574	.525	.481	.441	.404	.368
	11	12	13	14	15	16	17	18	19	20
x_{Ca}	.045									
$\bar{x}_{Ca}$	.333									

Table 26 . Operating conditions and results of experimental runs on cyclic countercurrent contactor. Regeneration of calcium form resin with solution of sodium chloride

Run No: 5

Number of actual stages	10
Forward flow period (t_f) sec.	56
Reverse flow period (t_r) sec.	4
Liquid flow rate $U_f = U_r$ cm^3/min.	10
Average liquid flow rate (L) cm^3/min.	4.50
Average resin flow rate (R) cm^3/min.	0.85
Solution feed concentration mequiv./ml.	1.00
Resin exchange capacity mequiv./ml.	2.00
Solution volume fed into the contactor ml/90 min.	355.0
Water to the resin feed column ml/90 min.	114.75
Solution volume recovered after the run ml.	475.50
Resin volume fed into the contactor during the run (90 min.) ml.	76.5
Resin recovered after the run ml.	75.0
Resin holdup per stage ml.	1.70
Resin holdup fraction transferred per cycle	0.50
Liquid holdup per stage ml.	8.980
Liquid hold up fraction transferred per cycle	0.500
Ratio $LC_o/R\bar{C}_o$	2.647
Total time for the run min.	120.0
Total No.of computed stages	16

Analysis of interstage solution samples withdrawn at fixed times after the start of a run

Time (mins.)	Resin Feed End		4		6		8		10		Solution feed end	
	x_{Ca}	$\bar{x}_{Ca}$	x_{Ca}	$\bar{x}_{Ca}$	x_{Ca}	$\bar{x}_{Ca}$	x_{Ca}	$\bar{x}_{Ca}$	x_{Ca}	$\bar{x}_{Ca}$	x_{Ca}	$\bar{x}_{Ca}$
10	.250	1.00										
20	.279	1.00										
30	.296	1.00										
60	.298	1.00	.150	.570	.120	.490	.059	.325	.018	.225	0.00	.204
90	.311	1.00	.160	.595	.100	.440	.065	.345	.020	.230	0.00	.175
120	.312	1.00	.155	.580	.110	.465	.067	.350	.021	.232	0.00	.173

Computed interstage composition of resin and solution

	1	2	3	4	5	6	7	8	9	10
x_{Ca}	.312	.227	.193	.170	.151	.136	.124	.112	.102	.091
$\bar{x}_{Ca}$	1.00	.808	.712	.647	.595	.551	.513	.480	.450	.422
	11	12	13	14	15	16	17	18	19	20
x_{Ca}	.081	.071	.061	.051	.042	.032				
$\bar{x}_{Ca}$	.395	.369	.343	.316	.289	.262				

Table 27 . Operating conditions and results of experimental runs on cyclic countercurrent contactor. Regeneration of calcium form resin with solution of sodium chloride

Run No: 6

Number of actual stages	10
Forward flow period (t_f) sec.	114
Reverse flow period (t_r) sec.	6
Liquid flow rate $U_f = U_r$ cm^3/min.	10
Average liquid flow rate (L) cm^3/min.	5.29
Average resin flow rate (R) cm^3/min.	1.00
Solution feed concentration mequiv./ml.	1.00
Resin exchange capacity mequiv./ml.	2.00
Solution volume fed into the contactor ml/90 min.	423.00
Water to the resin feed column ml/90 min.	135.00
Solution volume recovered after the run ml.	550.00
Resin volume fed into the contactor during the run (90 min.) ml.	90.00
Resin recovered after the run ml.	85.00
Resin holdup per stage ml.	2.00
Resin holdup fraction transferred per cycle	1.00
Liquid holdup per stage ml.	8.80
Liquid hold up fraction transferred per cycle	1.20
Ratio $LC_o/R\bar{C}_o$	2.647
Total time for the run	120.00
Total No.of computed stages	16

Analysis of interstage solution samples withdrawn at fixed times after the start of a run

Time (mins.)	Resin Feed End		4		6		8		10		Solution feed end	
	x_{Ca}	$\bar{x}_{Ca}$	x_{Ca}	$\bar{x}_{Ca}$	x_{Ca}	$\bar{x}_{Ca}$	x_{Ca}	$\bar{x}_{Ca}$	x_{Ca}	$\bar{x}_{Ca}$	x_{Ca}	$\bar{x}_{Ca}$
10	.180	1.00										
20	.277	1.00										
30	.292	1.00										
60	.298	1.00	.125	.50	.085	0.40	.052	.30	.019	.22	0.00	.210
90	.300	1.00	.132	.52	.090	0.41	.057	.32	.021	.22	0.00	.205
120	.313	1.00	.140	.54	.086	0.40	.056	.32	.020	.22	0.00	.170

Computed interstage composition of resin and solution

	1	2	3	4	5	6	7	8	9	10
x_{Ca}	.313	.228	.195	.171	.153	.137	.125	.114	.103	.093
$\bar{x}_{Ca}$	1.00	.808	.713	.648	.595	.553	.515	.482	.453	.425
	11	12	13	14	15	16	17	18	19	20
x_{Ca}	.083	.073	.063	.053	.043	.033				
$\bar{x}_{Ca}$	.398	.372	.346	.320	.293	.266				

3.6. Interpretation of Results

A controlled cyclic stagewise process attains a pseudo-steady-state condition when considered over a large number of cycles. At any particular time in a cycle the composition of either/should be the same from cycle phase/ to cycle. However, during any one cycle the process is unsteady-state, since only one phase flows at a time. Thus conventional steady-state material balance equations and the use of a conventional operating line cannot rigo rously describe a controlled cyclic process. Nevertheless, a pseudo-operating line based on the average equivalent flow rates and the composition of both streams at a fixed time in a cycle can be used to represent the process. The pseudo-operating line will represent the locus of the momentary compositions of liquid and resin phase over a cycle in each stage. Several approaches exist for the theoretical analysis of controlled cyclic operations (for example Lewis 1936, McWhirter and Lloyd 1963 and Belter and Speaker 1967) for special cases.

In the present work a simplified theoretical model has been developed which analyses the performance of the experimental contactor (see section 3.3.). The following assumptions have been made for the development of the theoretical treatment.

1) It has been assumed that cyclic operation of the contactor can be represented by a cascade of reaction vessels separated from each other and operated with a batchwise transfer of solution and resin phase between the stages according to a pre-determined cycle.

2) It has been assumed that only resin phase diffusional resistance is rate determining in the exchange reaction. The assumption is reasonably satisfactory when concentrated solutions and large size particles are used.

3) It has been assumed that both phases are perfectly mixed and that the reaction time for the cycle and the residence time of resin in each reaction vessel are equal

to H/R, where R, the average resin flow rate is $H\ \bar{r}/t_f+t_r$. Here, $\bar{r}$ is the fraction of resin hold up(H) transferred per cycle and has been assumed to be unity.

4) It has been assumed that the ratio of the stoichiometric hold up of both phases in each stage is the same as that based on the average flow rates in the contactor i.e. $\frac{LC_o}{R\bar{C}_o} = \frac{VC_o}{\bar{V}\bar{C}_o}$

5) The sequence of the various operations in the controlled cycle are assumed to be identical to case (i) as described in Section 3.2.2.

6) A constant composition for resin, and solution feed to a stage at the start of each cycle has been assumed. This is an over-simplification of the actual operating conditions in the contactor. In fact the composition of resin feed may be taken as constant but the composition of the solution feed to each stage varies with time as has been described in case (ii) of Section 3.2.2.

Under these conditions, each stage is reduced to a batch reaction vessel for which the change in the resin and solution composition with time can be computed provided the rate law, equilibrium data and the stoichiometric ratio of the two phases are known (c.f. Section 2.5.)

A trial and error method is required to predict the number of stages required for a given process. The following procedure has been adopted.

Consider a cascade of n stages as shown in Figure 34. Generally, for a given process, the terminal compositions are known i.e. $\bar{x}_o$, $\bar{x}_{n(T)}$, $x_{1(T)}$, and x_{n+1}. The number of stages required to convert resin feed of composition $\bar{x}_o$ to a resin product of composition $\bar{x}_n$ can be computed if the change in the resin composition for each stage is known. This can be determined by a stagewise calculation starting at $\bar{x}_o$ if the intial and the appropriate boundary conditions for each stage are known. For stage 1, this requires a knowledge of $\bar{x}_o$, $x_{1(T)}$, and $x_{1(o)}$ and $LC_o/R\bar{C}_o$.

Since $x_{1(O)} \equiv x_{2(T)}$, this is not known and a trial value for $x_{1(O)}$ is used in order to start a computation. In reality, for a continuous flow contactor, it is necessary to make a guess at the time variant value of x_2 from $x_{2(O)}$ to $x_{2(T)}$. This in turn requires the solution of compositions in stage 2 prior to stagel. This is not possible since none of the initial conditions for stage 2 are known . Thus, the present treatment involves a guessed fixed value of x_2 at the end of the previous cycle and this enables the calculation of the time variant $\bar{x}_1$ and x_1 to commence.

The use of the diffusion equation with variable diffusion coefficient and equilibrium data along with the value of $LC_o/R\bar{C}_o$ gives the composition of each phase as a function of time. The computer programme which solves the diffusion equation numerically has been described in detail in Appendix 5 .

The computed value of $x_{1(T)}$ is then compared with the known value of $x_{1(T)}$ from the operating line. If the two values; $x_{1(T)}$ (computed) and $x_{1(T)}$ (fixed) are in close agreement then the guessed value of $x_{1(O)}$ is a correct one. A mass balance gives $\bar{x}_{1(T)}$. If there is a large divergence between the computed and the known values of $x_{1(T)}$ then a new value of $x_{1(O)}$ is tried and so on until convergence between the two is obtained. The above procedure is repeated from stage to stage along the cascade until the composition of the liquid stream becomes equal to the initial value i.e. x_{n+1}. The computation then provides the number of stages required for a given process.

Since a resin phase controlled reaction has been assumed a concentration profile within the resin particle always exists at times greater than zero. This is always considered in the present computation. For this reason the above calculations cannot be started from the liquid feed end of the process, since the concentration profile in the resin particles at the end of the process (stage n) is not known and would be extremely difficult to predict.

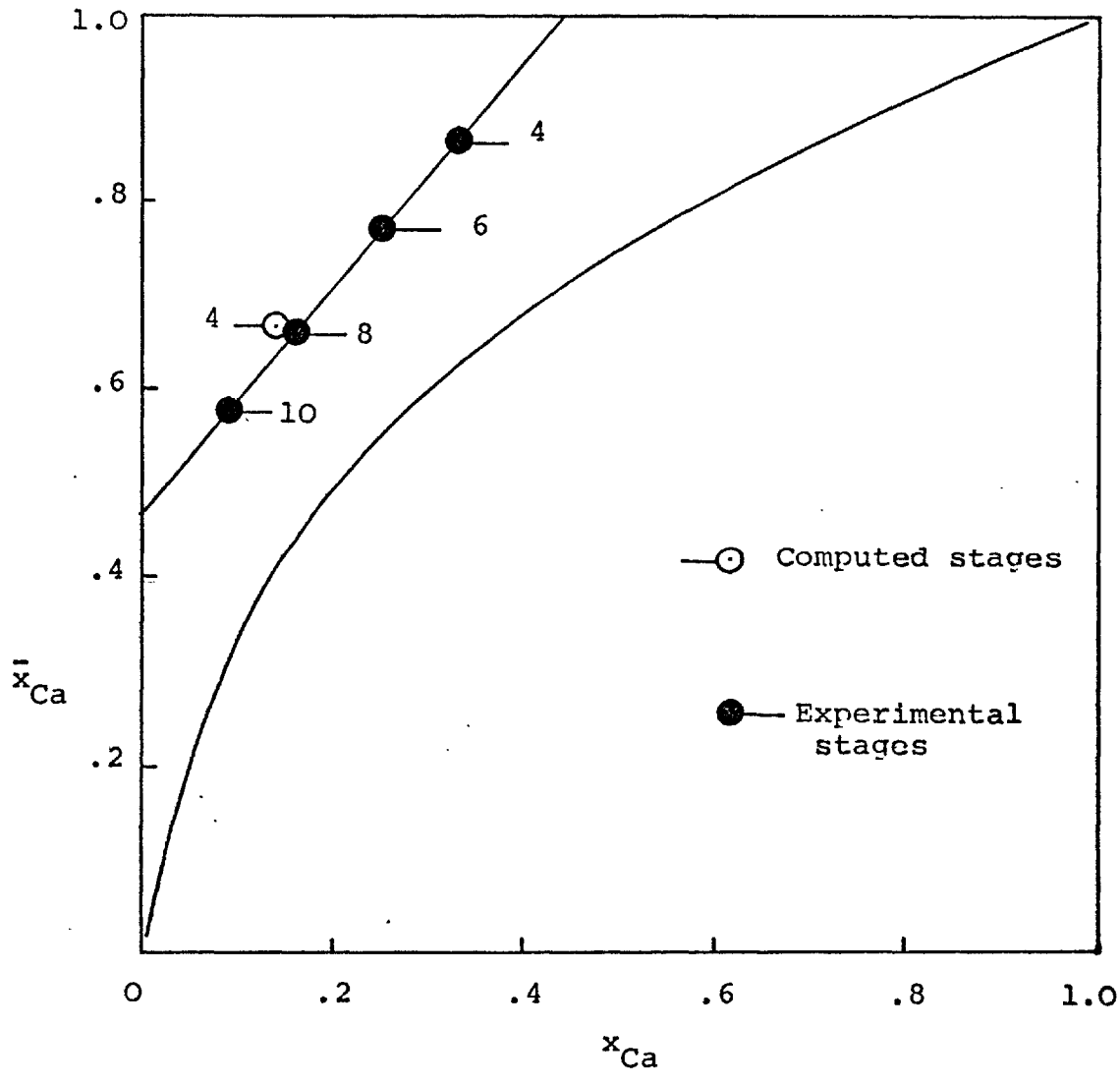

Figure 45.

Run no: 1
Operating line and interstage compositions.

$\frac{LC_o}{RC_o}$ = 1.207

r = .25

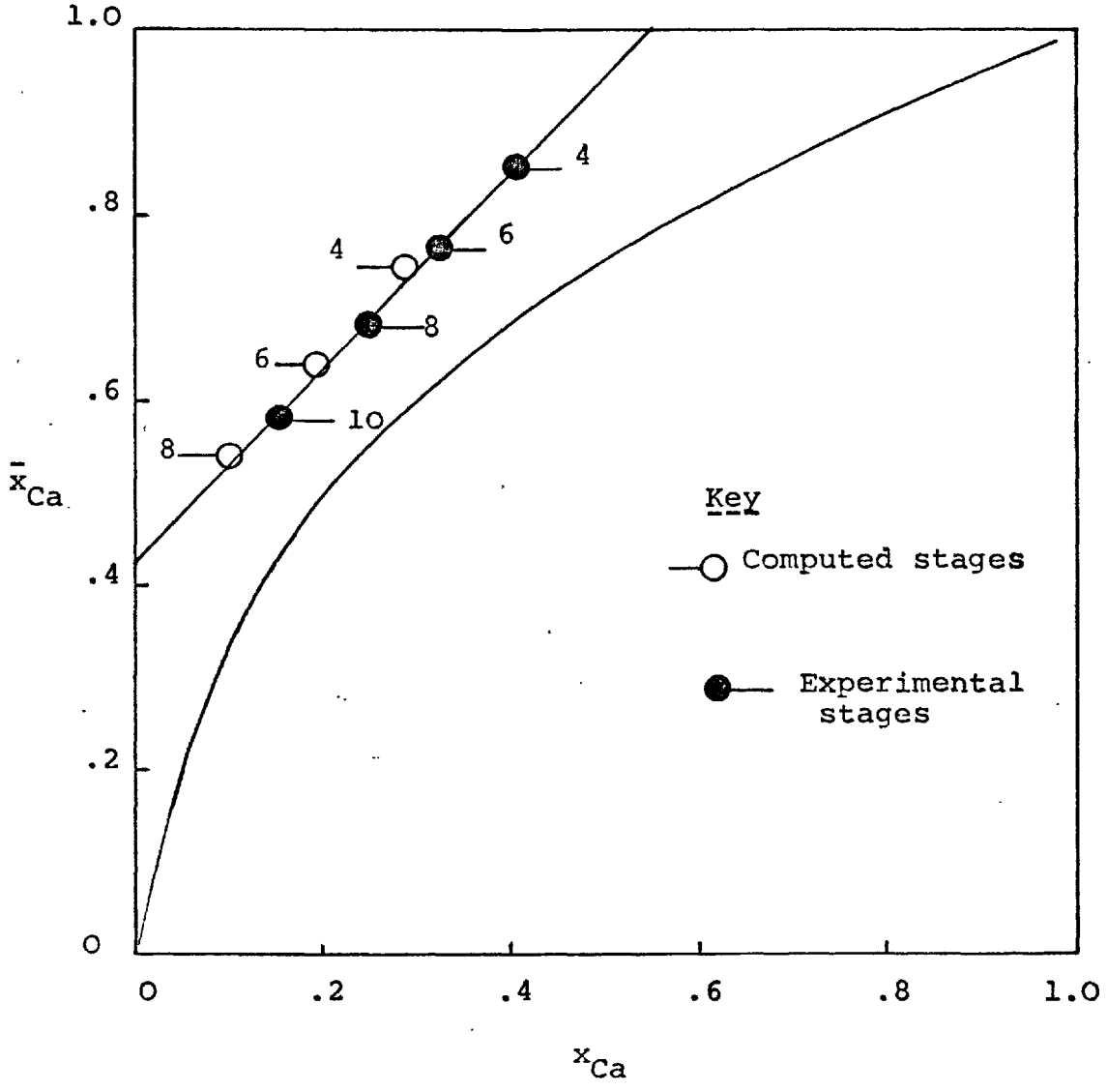

Figure 46. Run no. 2
Operating line and interstage compositions.

$\frac{LC_o}{R\bar{C}_o} = 1.05$

r = .25

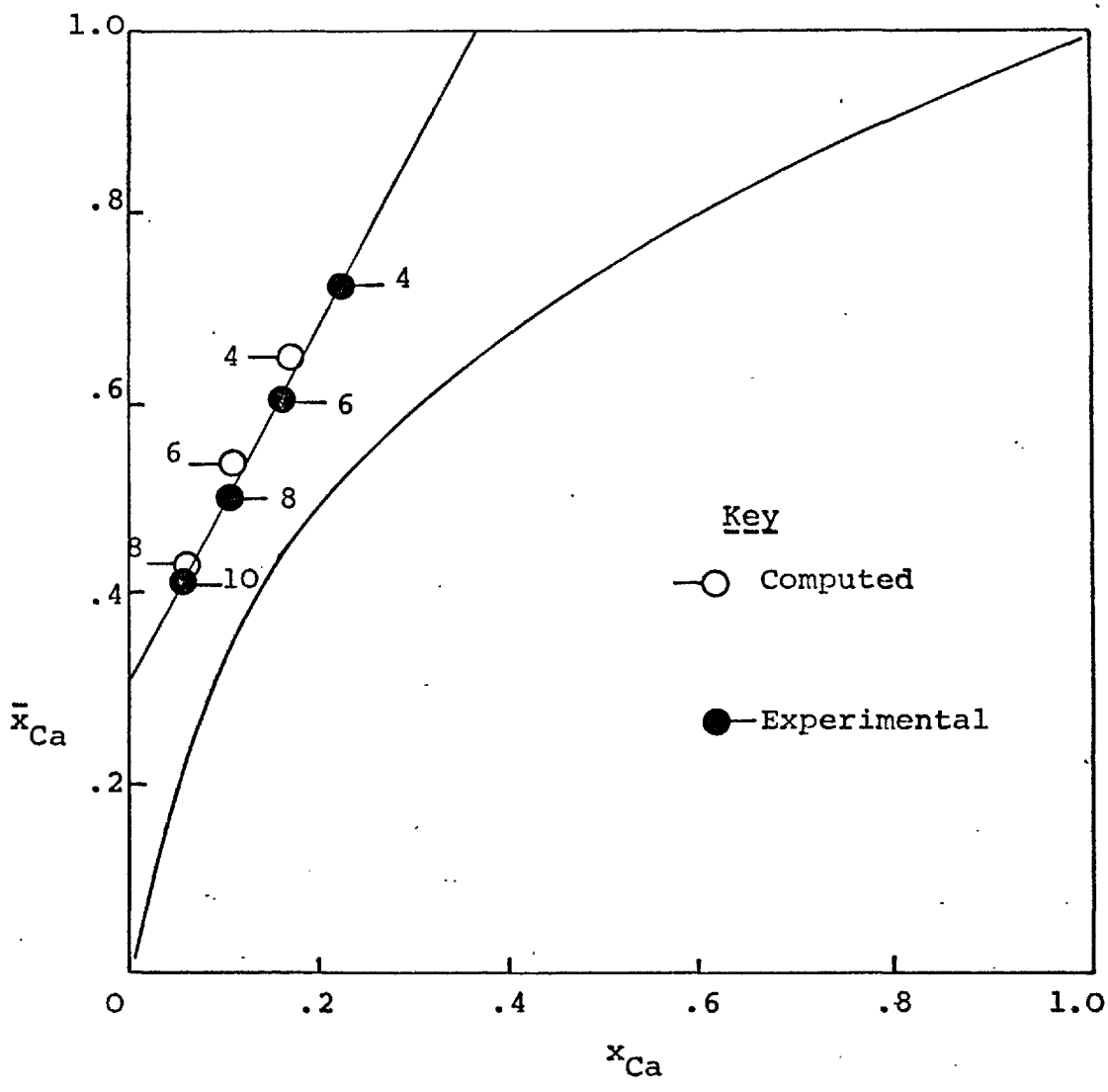

Figure 47. Run no. 3
Operating line and interstage composition

$\frac{LC_o}{R\bar{C}_o} = 1.925$

r = .266

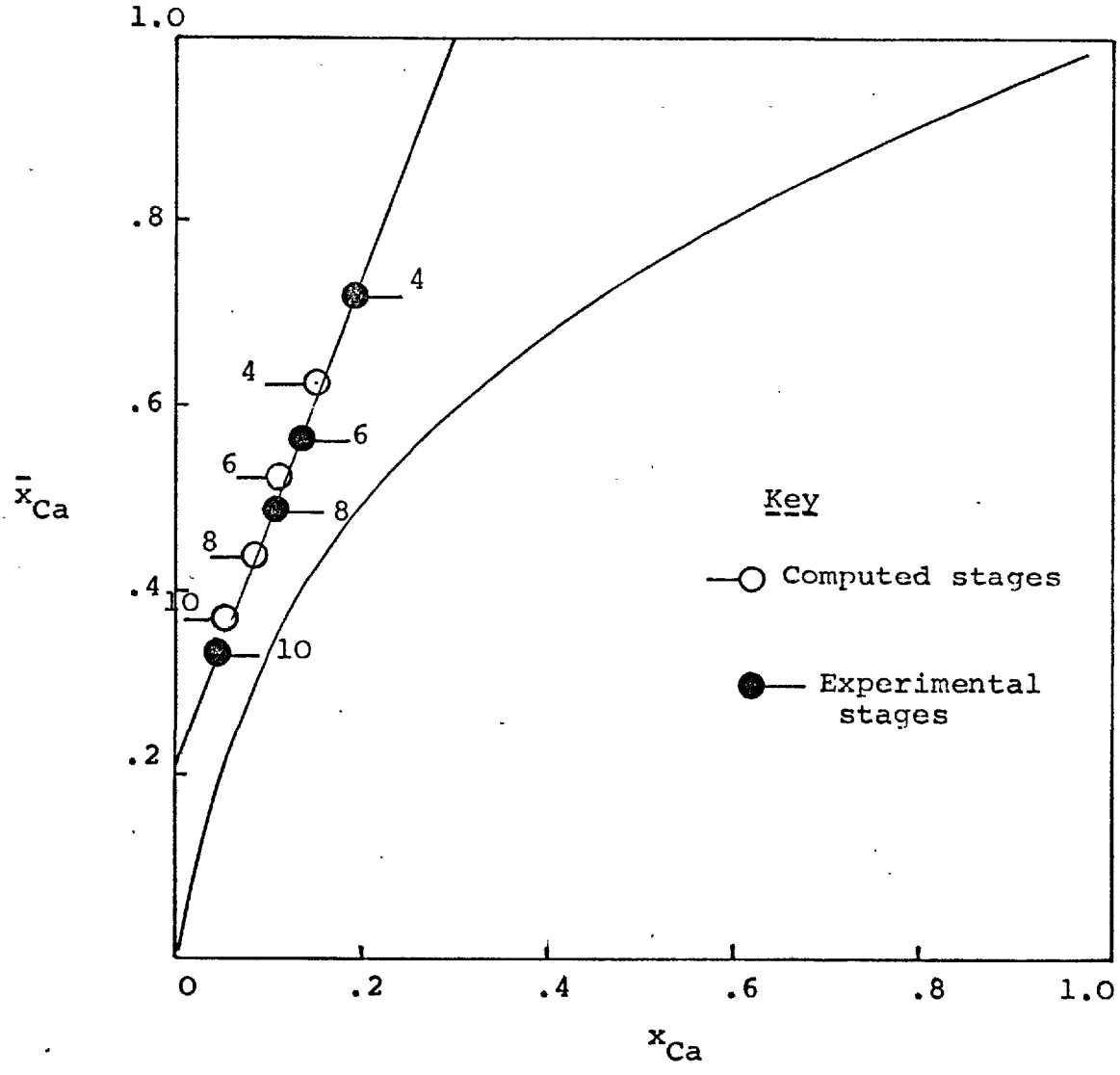

Figure 48

Run No. 4

Operating line and interstage compositions.

$\frac{LC_o}{R\bar{C}_o} = 2.647$

r = .25

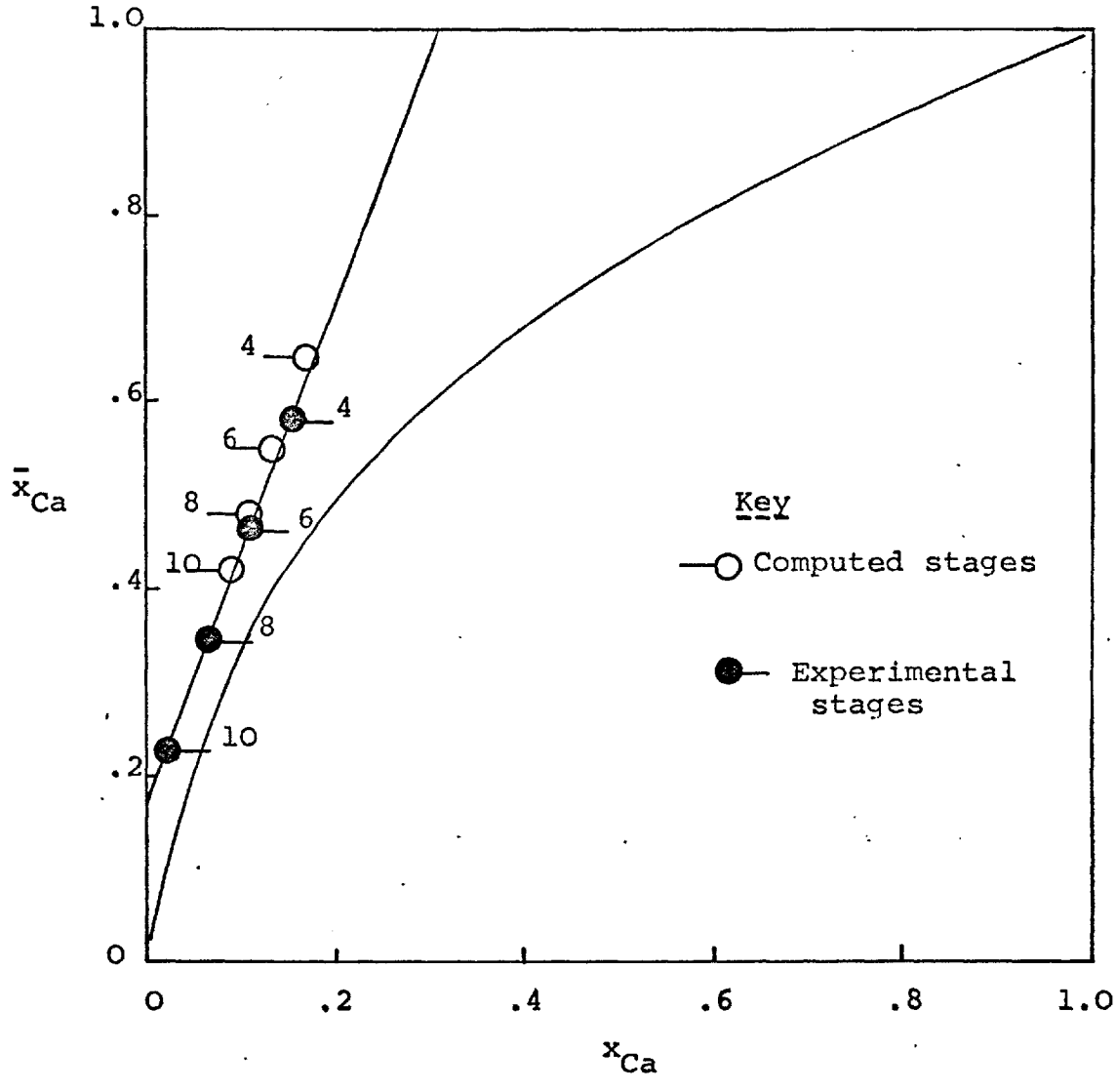

Figure 49 Run no. 5
Operating line and interstage compositions.

$\frac{LC_o}{R\bar{C}_o} = 2.647$

r = .50

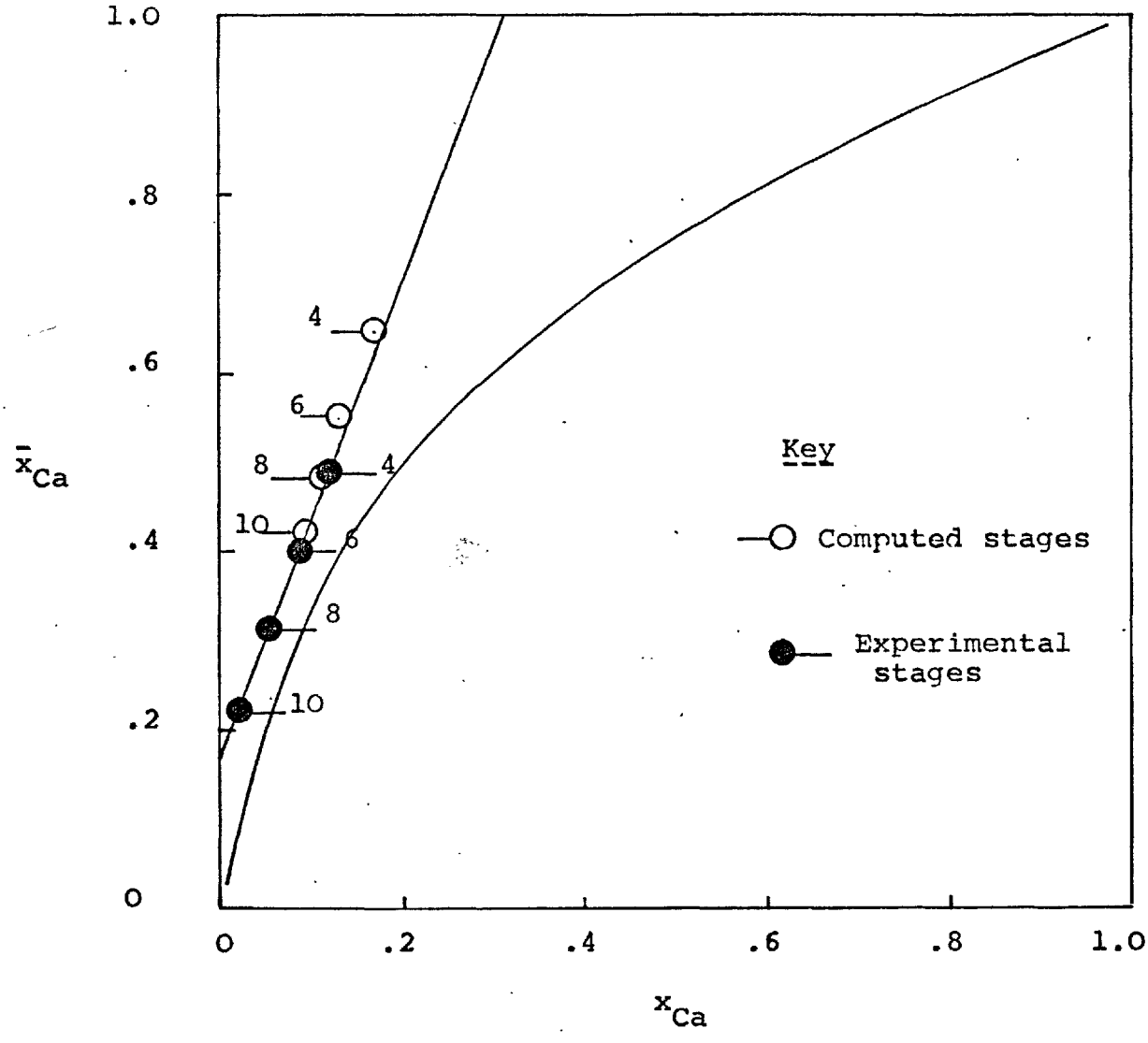

Figure 50 Run no. 6
Operating line and interstage compositions.

$\frac{LC_o}{RC_o} = 2.647$

r = 1.00

3.7. DISCUSSION

The results of the experimental runs have been shown in Tables 22 to 27 and Figures 45 to 50. Figure 51 shows the operating lines for Runs 1, 2, 3 and 4. As one would expect the conversion of resin from calcium to sodium form improves as the stoichiometric ratio of sodium chloride solution to resin flow is increased. However, this is at the expense of regenerant utilization which decreases as the slope of the operating line increases.

Runs 1,2,3 and 4 may be grouped together for comparison since they represent similar operating conditions i.e. the cycle times for all of them is about 30 seconds with t_r equal to about 15 seconds. The fractional transfer of resin hold up per cycle is about 0.25. The predicted number of stages required for each run are shown in Tables 22,23,24 and 25 along with stagewise composition of both phases. The number of predicted stages for each run are 5,9,9 and 11 respectively. It is interesting to note that on average about 10 stages are required for each run (except Run no. 1). The corresponding number of actual stages are 10.

The fact that the mathematical model predicts roughly the same number of stages actually required is gratifying. However, the theoretical model presented in this study for cyclic countercurrent operation cannot be considered an exact representation of the contactor. It is important to consider the basic differences in the simplified mathematical model and actual working of the cyclic contactor.

Consider the stage i of a cascade (Figure 36).

a) The simplified mathematical model presented here assumes that at the start of the cycle the resin hold-up has a concentration $\bar{x}_{i(O)}$ and solution $x_{i(O)}$. The solution composition $x_{i(O)}$ is taken equal to the final composition at the end of the cycle in the previous stage, i.e. $x_{i+1(T)}$. The computation commences by assuming an initial

/...

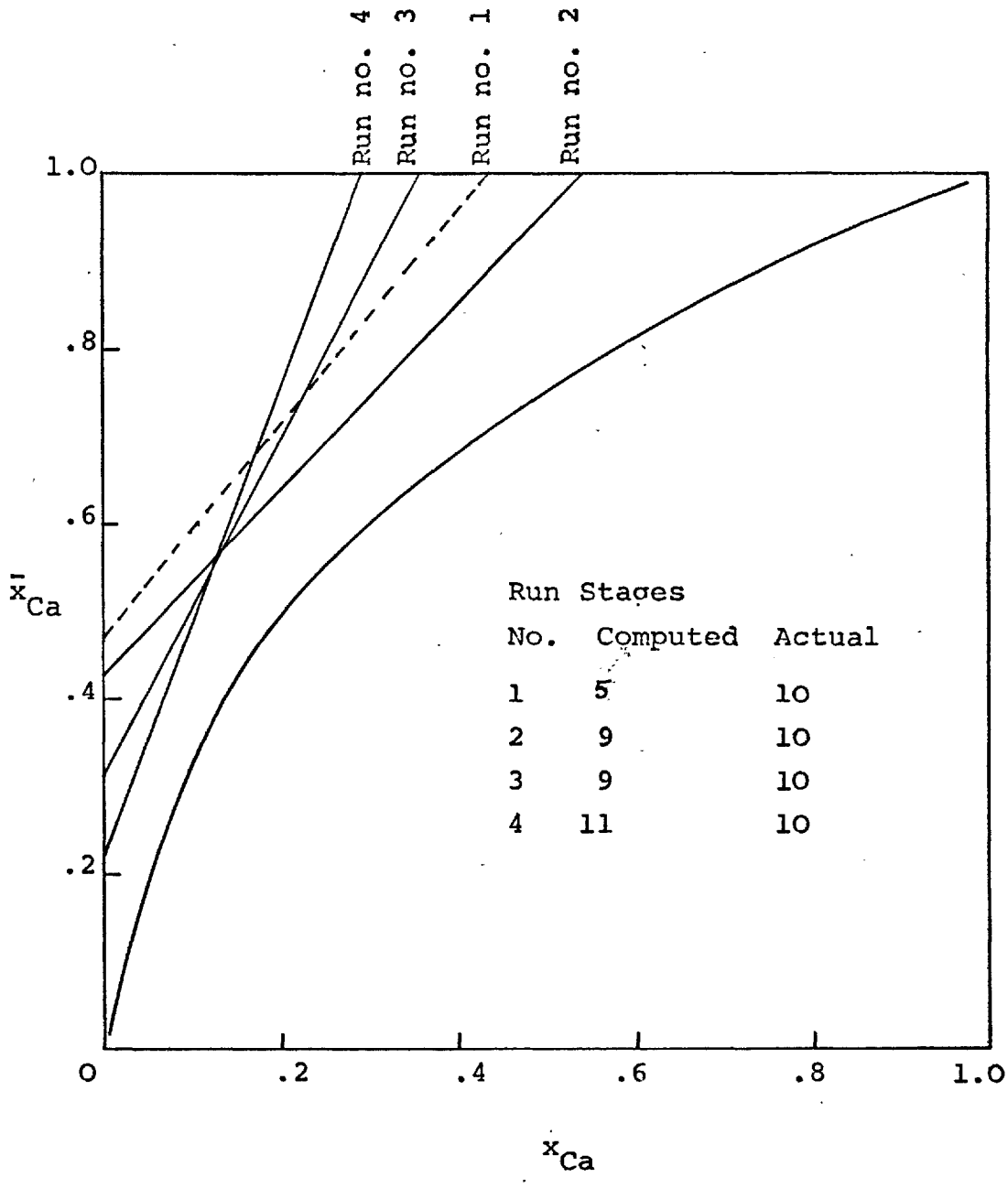

Figure 51. Operating lines of Run 1, 2, 3 and 4 and total number of computed stages.
Cycle time = 30 seconds.
Fractional transfer of resin ($\bar{r}$) = 0.25

driving force ($\bar{x}_{i(O)} - \bar{x}^{*}_{i(O)}$), where $x^{*}_{i(O)}$ is taken from the equilibrium diagram at value corresponding with $x_{i+1(T)}$.

b) In the actual contactor, continuous solution flow occurs during each cycle. At the start of the cycle, the resin phase composition will be $\bar{x}_{i(O)}$ as before, but the momentary concentration of the solution (Figure 38) is not $x_{i+1(T)}$. For a perfectly mixed cascade of reaction vessels it will vary from $x_{i+1(O)}$ to $x_{i+1(T)}$ during each cycle. Since $x_{i+1(O)}$ is clearly less than $x_{i+1(T)}$, the momentary driving force at the start of the cycle ($\bar{x}_{i(O)} - \bar{x}^{*}_{i(O)}$), where $\bar{x}^{*}_{i(O)}$ is based on $x_{i+1(O)}$, will be significantly enhanced.

c) The mathematical model assumes complete transfer of both the phases per cycle, whereas in the actual contactor runs 1,2,3 and 4 represent operation with fractional transfer of resin and solution hold ups ($\ll 0.25$). This will result in the retardation of flux and decreased performance of the contactor. The magnitude of retardation of flux would, of course, depend on the solution compositions existing in the contactor

In view of the above mentioned factors, a close agreement between the actual and the predicted number of stages, for a given conversion of resin, must be considered coincidental. It is most likely that under the operating conditions of these runs the opposing effects of the two factors is equal, i.e. enhancement of flux due to time variant composition of the feed to a stage is cancelled by the retardation due to fractional transfer of resin and solution hold up per cycle.

Figure 52 compares the operating lines for Runs 4,5 and 6. All these runs were carried out with the same $LC_o/R\bar{C}_o$ value but the fractional transfer of resin hold up per cycle has been varied form $\bar{r} = 0.25$ to $\bar{r} = 0.5$ and $\bar{r} = 1.0$ respectively. This results in better performance. More significant is the improvement in the performance of individual stages as shown by the experimental interstage compositions in the 4th stage for each run. The improved performance confirms the expected effect as outlined in

/...

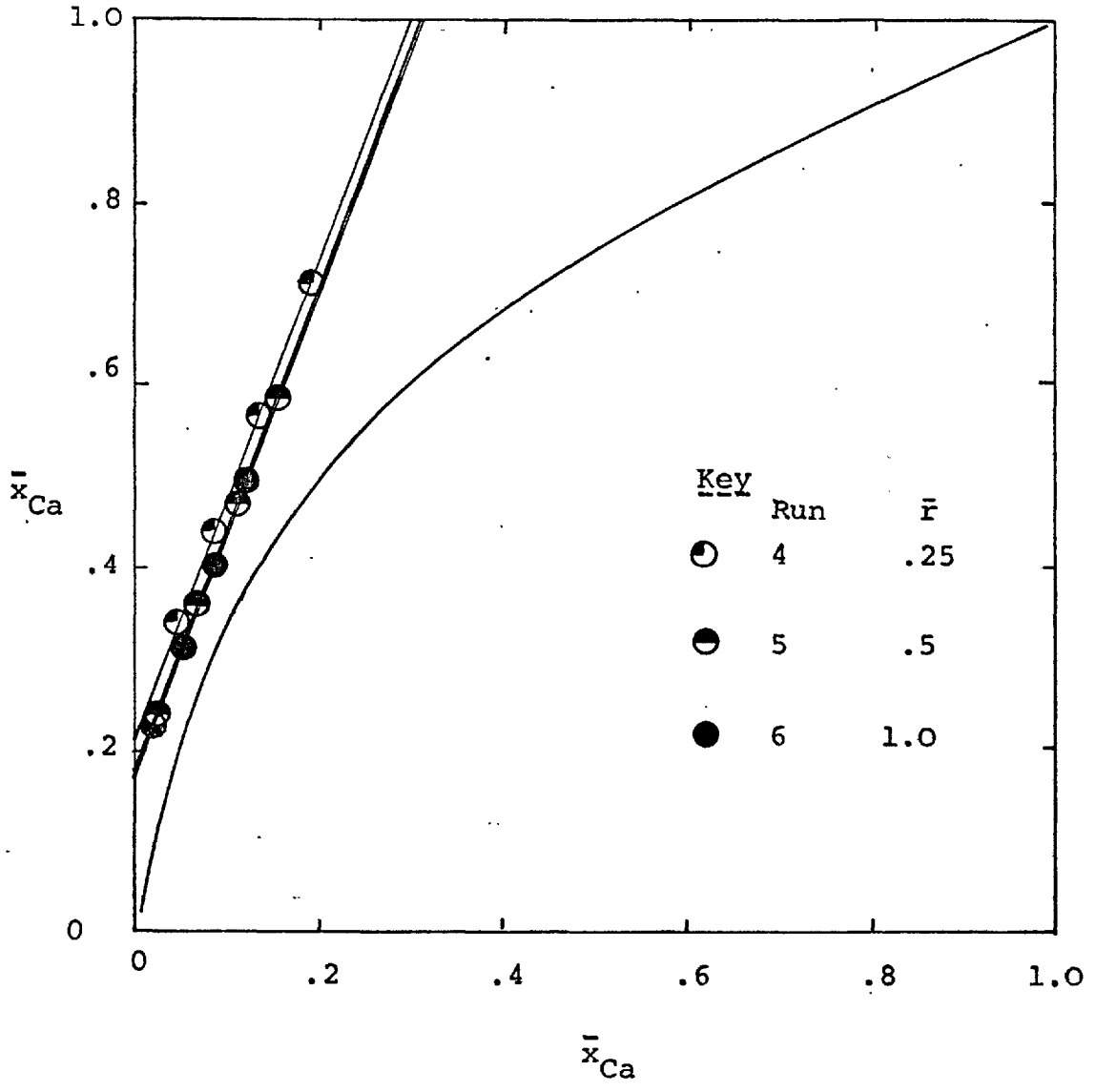

Figure 52. Operating lines of Run 4,5 and 6.

$\frac{LC_o}{RC_o} = 2.647$

Section 3.2.2. (ii). The mathematical model predicts about 16 stages for the same conversion of resin as has been achieved by 10 actual stages.

The improved performance confirms the expected effect. From Tables 26,27 and 28 it may be noted that longer forward flow periods have been employed for Runs no. 5 and 6. This type of hydrodynamics corresponds to plug flow of solution and will tend to give better flux due to time variant composition of solution flowing through the stages (See Section 3.2.2. (iii)). The opposite effect of fractional transfer of resin hold up, here, is very small because of the higher values of $\bar{r}$. ($\bar{r}$ = 0.5 and $\bar{r}$ = 1.0). The net result is better performance.

The desirability of approaching complete transfer of resin hold up for a given number of stages in a cyclic contactor is obvious (See Figure 52). This is consistant with observations in other two-phase mass transfer operations particularly distillation and solvent extraction (McWhirter and Lloyd (1963) and Belter and Speaker (1967)). The decreased effect of cycling at the tail end of the process (Figures 48,49 and 50) in each case may be due to the lower driving forces that exist with these particular operating lines. Controlled cycling is likely to produce greatest improvement in performance in cases where a large driving force exists throughout the length of the process.

3.7. CONCLUSION

The results obtained so far suggest that the simplified theoretical model for the prediction of the number of stages for a given ion exchange process with fractional transfer($\ll 0.25$) of resin and solution hold up in a cyclic contactor gives a good estimate. However, the present model is not exact. Further studies are required to provide an accurate knowledge of the hydrodynamics of the cyclic contactor. The present model should be modified to incorporate the time variant solution composition of feed to each stage during a cycle and also to include the effect of fractional transfer of resin and solution hold up.

The experimental results obtained here tend to confirm that cyclic operation is likely to produce a better performance than a conventional steady state process for the same system. The advantage of cycling is likely to be greatest when the entire resin hold up per stage is transferred each cycle, the effect of backmixing on the liquid composition profile in the stages is minimum, the equilibrium is favourable for the ion being removed and large driving forces exist during the process.

CHAPTER 4

THEORETICAL PERFORMANCE OF A CONTINUOUS ION EXCHANGE PROCESS

4. THEORETICAL PERFORMANCE OF A CONTINUOUS ION EXCHANGE PROCESS

4.1. Introduction

It has been claimed that a continuous countercurrent ion exchange process has many advantages over fixed bed techniques in many applications. It offers the advantage of lower resin inventory, increased chemical efficiency, lower capital cost and a continuous flow of processed liquor of constant composition.

For the design of a continuous ion exchange plant, it is necessary to have an exact knowledge of the kinetic and equilibrium behaviour of the particular system together with the hydrodynamics of the type of equipment to be employed. However, the feasibility of a particular process can be assessed from an analysis of the operating diagram in a similar manner to other continuous mass transfer processes e.g. distillation, absorption and solvent extraction. This requires an exact knowledge of the equilibrium behaviour for the system and the location of the operating line. A simple approach is here described to show the use of the operating diagram for a process design with reference to water softening.

4.2. Continuous Water Softening

Figure 53 shows a schematic flowsheet of a continuous countercurrent ion exchange water softening process. Raw water containing the salts of calcium, magnesium and sodium flows through the adsorption contactor countercurrent to a regenerated resin flow. The treated water composition will depend on the number of contacting stages and the flow rates of the two phases.

The exhausted resin leaves the adsorption contactor almost in equilibrium with the incoming water and is transferred to a regeneration contactor where it is treated with a concentrated solution of sodium chloride. The adsorbed ions are replaced by sodium ions. The regenerated resin is rinsed with either raw water or with softened water to remove sodium chloride and calcium chloride from the voids. It is then recycled to the adsorption contactor. In theory, only two continuous columns are required for this process.

4.2.1. Adsorption contactor

Consider the softening of raw water containing 100 ppm Ca^{++} (250 ppm $CaCO_3$ total hardness) with Zeo-Karb 225. Let the composition of the treated water be 2.0 ppm Ca^{++} (5 ppm Ca CO_3). Figure 54A shows an equilibrium isotherm for the sodium chloride-calcium chloride-Zeo-Karb 225 resin system at a total cationic solution concentration of 0.005 N (100 ppm Ca^{++}). This isotherm has been drawn by applying the expression

$$K_D = \frac{\bar{x}_{Ca}\,(1 - x_{Ca})^2}{x_{Ca}\,(1 - \bar{x}_{Ca})^2} \quad \frac{C_E}{\bar{C}_E}$$

where K_D, the Donnan equilibrium constant for this system has been determined experimentally and is taken as 1.30

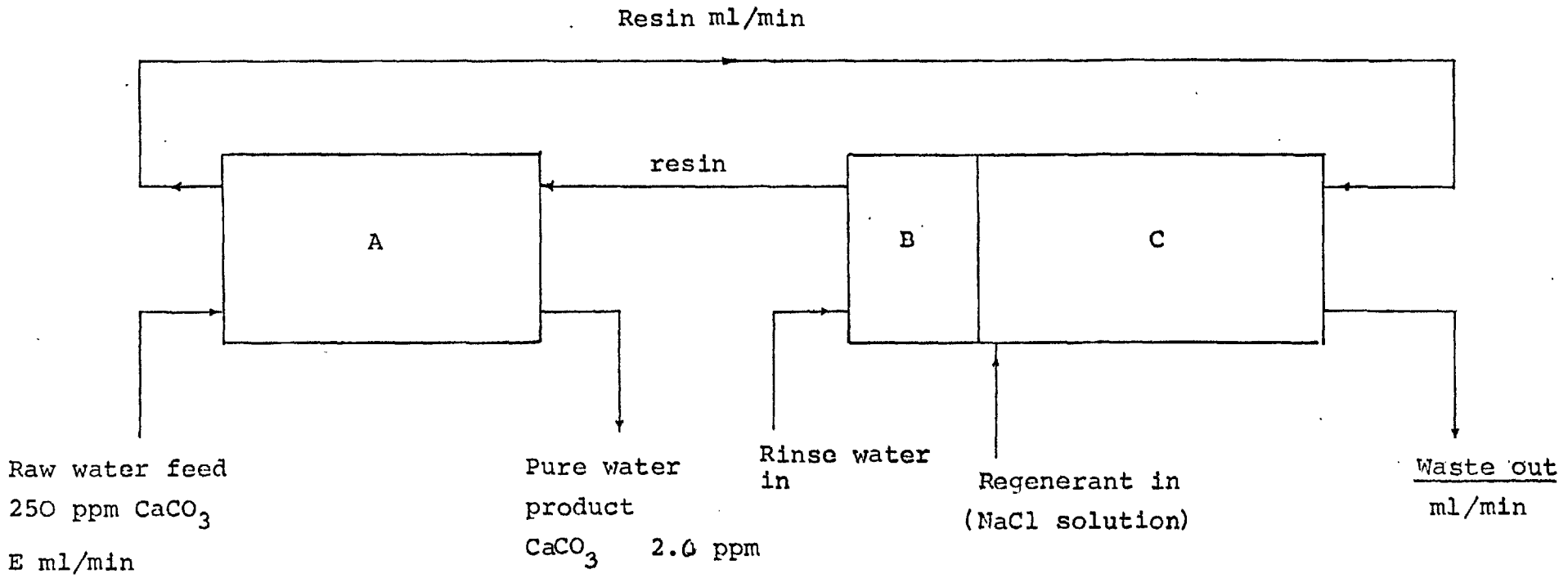

Figure 53 Flow sheet for softening of raw water

A Adsorption unit

B Resin washing unit

C Regeneration unit

(c.f. Section 1). It may be noted that the equilibrium isotherm is extremely non-linear which is a graphical representation of the fact that the resin is highly selective for the divalent calcium ion. At these concentrations the kinetics of the process is governed by liquid film diffusion (Boyd et al 1947). Suitable mathematical models exist for the prediction of performance of the contactor in this case, since a liquid film mass transfer coefficient can be evaluated and used in stagewise computations (e.g. see Stevenson 1969). Clearly, under such favourable conditions very few actual contacting stages will be required to achieve the desired treated water composition.

Assuming complete exhaustion of the resin, an operating line AA'may be drawn to represent the process (Figure 54A). The resin feed composition is determined by the quality of treated water desired. In this particular case (2.0 ppm Ca^{++} i.e. $x_{Ca} = 0.02$) a limiting pinch point, represented by point A where the operating line touches the equilibrium isotherm, fixes the resin feed composition $\bar{x}_F$ at 0.82. This represents a process with an infinite number of contacting stages. In practice, water quality slightly greater than 2.0 ppm can be obtained with a finite number of contacting stages.

In a continuous process, the treated effluent water is almost in equilibrium with the regenerated resin entering the adsorption contactor. This contactor can be run continuously in conjuction with a regeneration contactor which must produce resin of composition $\bar{x}_{Ca} = 0.82$.

4.2.2. Regeneration contactor

The exhausted resin is usually regenerated with concentrated brine. The corresponding operating line RR', representing the regeneration of completely exhausted resin with a solution of sodium chloride (1N), is shown in Figure 54B. This operating line represents a process with an

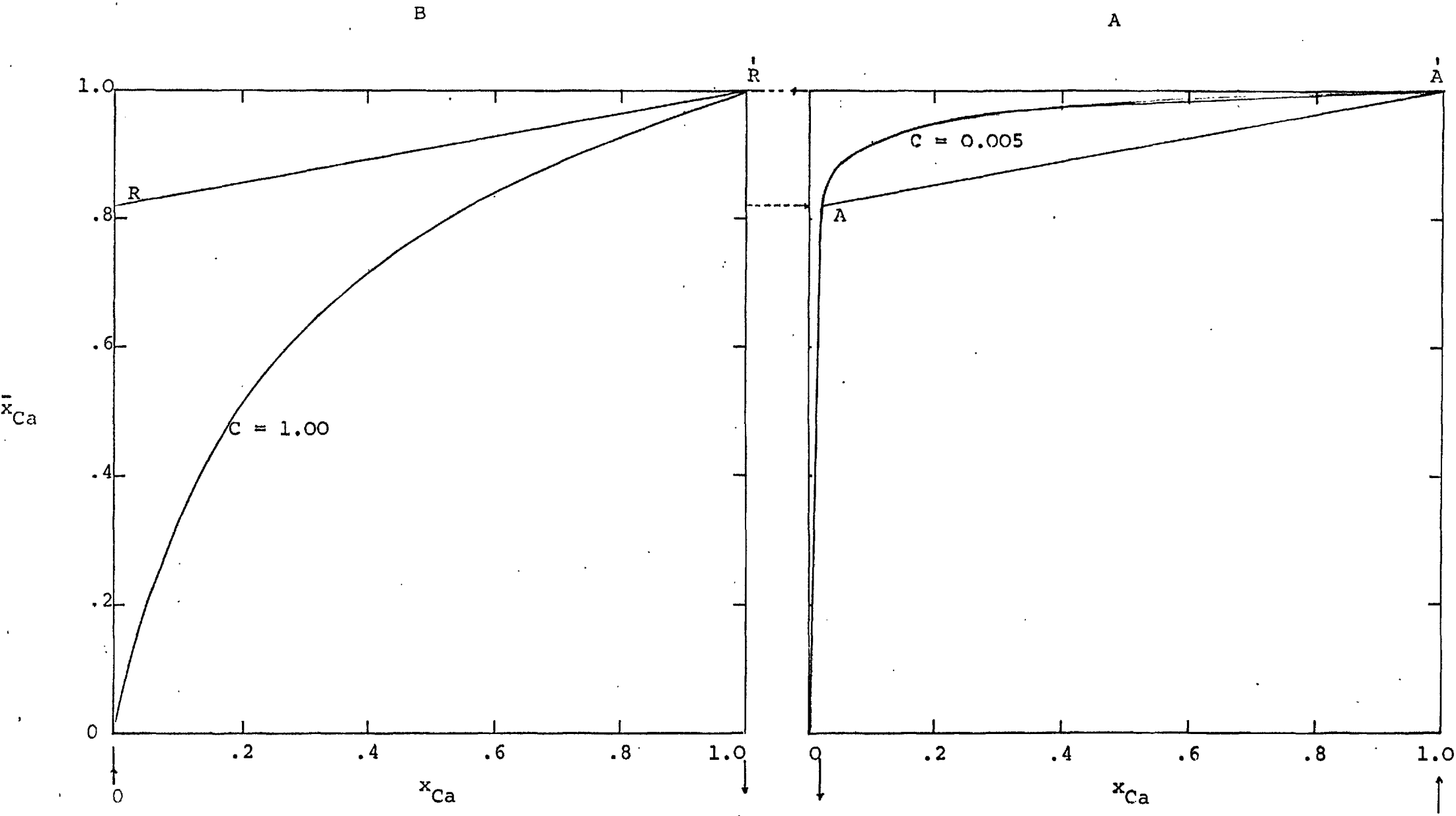

Figure 54 Operating diagram for water softening. Feed water 100 ppm Ca^{++}, treated water 2 ppm Ca^{++}.

infinite number of stages because of the pinch occuring near the pont R'. In practice, the pinching effect can be avoided by altering the flowrate of the regenerant solution such that the operating line representing the process is no longer a tangent to the equilibrium curve. Regenerant utilization of 95-98% can then be achieved with a finite number of contacting stages.

In the regeneration process, the kinetics is controlled by resin phase diffusion. The prediction of the actual number of contacting stages for a given resin conversion can be made by a theoretical analysis considering the kinetic, equilibrium and hydrodynamic behaviour involved. Nevertheless, the process performance can be represented on an operating diagram with the help of an equilibrium isotherm and the flow rates of the two phases.

4.3 Efficiency of a Softening Process

The operating cost of a water softening process depends chiefly on the cost of regenerant chemicals, usually brine. The efficiency of the softening process may be defined as the percentage utilization of the regenerant employed. A process with 100% efficiency represents a case where for every equivalent of regenerant supplied, one equivalent of calcium (representing total hardness) is removed from the raw water. This is theoretically possible but limits the degree of resin conversion that can be achieved.

In certain cases where treated water of very high quality is required the resin feed to the adsorption contactor has to be of a high sodium equivalent fraction. For example to obtain treated water of 0.10 ppm $CaCO_3$ (raw water total hardness 250 ppm $CaCO_3$), it is impossible to achieve an efficiency of more than 62% with sodium chloride (1N). The operating line QQ', a tangent to the equilibrium isotherm depicts this regeneration process in Figure 55. For the same conditions any improvement in the efficiency demands regenerant of higher concentration for which the equilibrium isotherm shifts towards the diagonal and allows better utilization of the regenerant. For example an operating line QS' in Figure 55 represents a process in which 2N solution of sodium chloride is employed for regeneration and corresponds to an efficiency of 80%. Thus for a particular process the efficiency is controlled by the quality of treated water required.

In practice, for softening a typical raw water containing 250 ppm $CaCO_3$ (total hardness) down to 1 ppm $CaCO_3$ in a continuous countercurrent contactor efficiencies up to 96% have been claimed (Clayton 1969). Whereas, the efficiencies reported by Bouchard (1969) for a raw water of slightly greater hardness (300-360 ppm $CaCO_3$) and for the same quality of treated water, using the Asahi contactor, range between 50-60%. In theory an efficiency as high as 100% can be achieved for the same process (operating line RR', Figure 54B), but would require a very large number of regeneration stages.

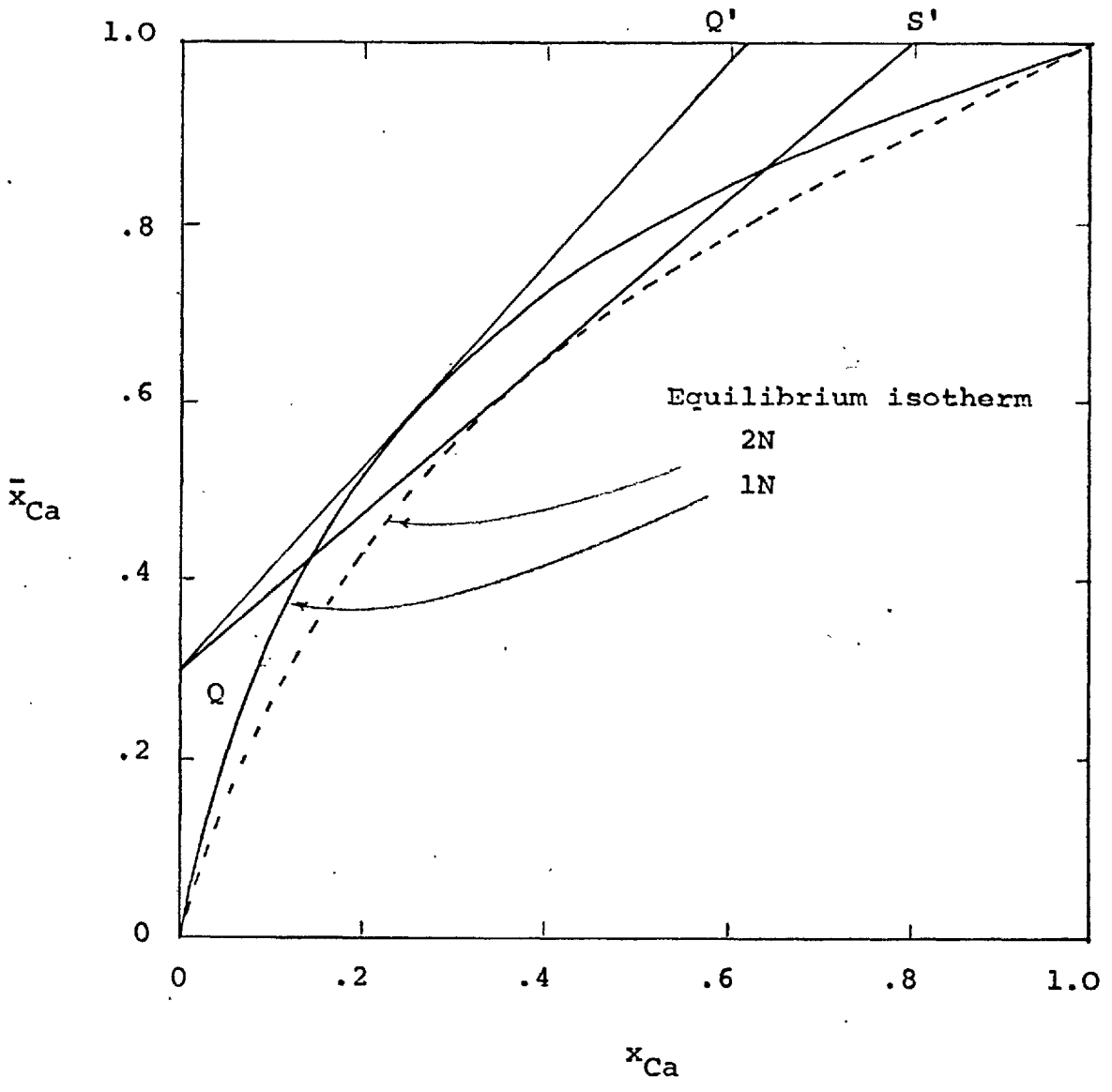

Figure 55 Improvement in regeneration utilization or efficiency with concentrated regenerant.

In view of the above discussion one may, therefore, conclude that it is possible to assess the feasibility and the theoretical performance of a continuous water softening process with the help of the operating diagrams.

4.4. Fixed Bed Water Softening Process

The theoretical performance of a water softening unit based on a fixed bed technique is more complex. In this case the process is basically batchwise, unlike continuous ion exchange, and thus cannot be represented by an operating diagram.

In a fixed bed adsorption contactor, raw water feed is introduced at the top and treated water leaves almost in equilibrium with the resin at the base of the bed. The raw water flow is continued until the quality of the treated water starts to deteriorate.(Leakage). At this point the resin bed is almost completely exhausted, except the lowest layer. The change in the resin composition during a complete adsorption cycle is depicted in Figure 56A.

At any time during the adsorption cycle, the resin bed has three distinctive zones. Zone A represents resin completely exhausted, zone B, resin being exhausted and zone C, the regenerated resin waiting to be exhausted. The water flow is stopped at a point when the lower end of zone B reaches the bottom of the resin bed (Breakthrough). Any further flow of water through the contactor will yield water with a gradually increasing hardness finally approaching the feed composition.

During theregeneration process the exhausted resin is converted to sodium form by an upflow of the regenerant solution. Here again, zones A and B and C develop and start moving upwards. The regenerant flow is continued until breakthrough point i.e. when sodium starts building up in the effluent. Figure 56B depicts the composition of resin in the column during the regeneration cycle.

It is clear from Figure 56 that a portion of the resin bed is not being effectively used during the adsorption and regeneration cycles. To overcome this a stoichiometric excess quantity of regenerant would be required but this effects the chemical efficiency of the process. It has been reported that the efficiency goes down as the

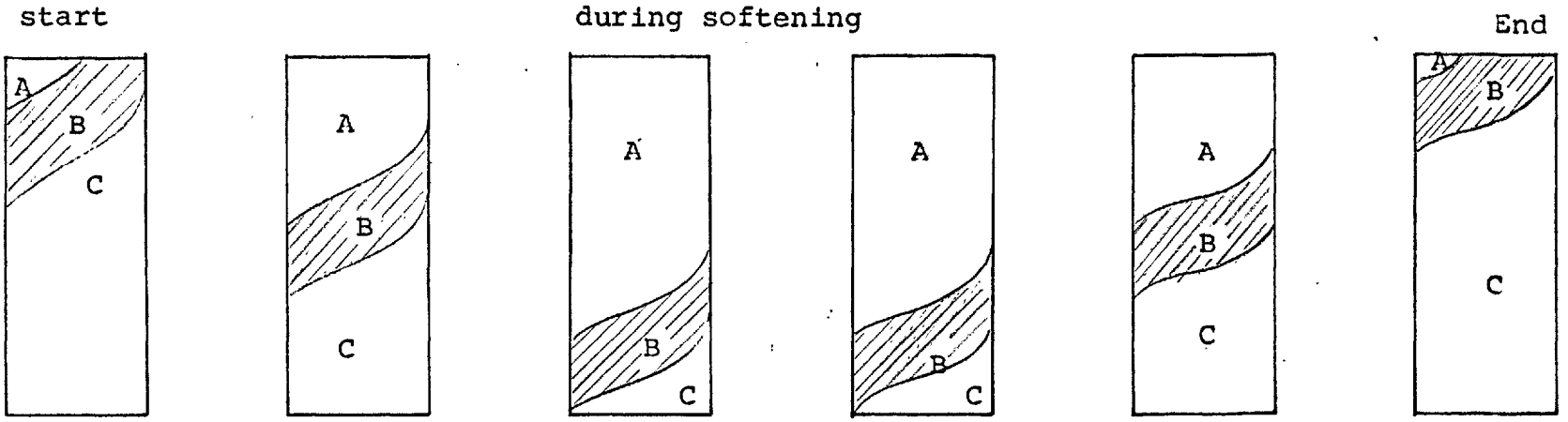

A.

Adsorption

B.

Regeneration

Figure 56

Composition of resin in fixed bed during a complete adsorption cycle. The regeneration (countercurrent) steps are represented from d to e to f.

regeneration level i.e. the quantity of salt required to regenerate a unit volume of resin is increased (Arden 1968). Clearly, the process will perform best with fully regenerated resin, but this is uneconomical. It is, nevertheless, quite possible to soften hard water utilizing resin that has been regenerated with an amount of sodium chloride which is insufficient to remove all the calcium from the resin (See Section 4.2.1.)

An increase in the total cationic concentration or the ratio of sodium ions in the raw water results in an early breakthrough point (Leakage) and thus the effective exchange capacity available is correspondingly reduced, and the resin requirement for a particular throughput increases. Although regeneration efficiency is of economic importance the quantity of resin and the capital cost of the equipment must also be considered. Efficiencies of 80-85% have been reported for fixed bed operation softening water of 250 ppm $CaCO_3$ total hardness down to 5 ppm $CaCO_3$ (Clayton 1969).

4.5. Salt requirements for continuous softening

Table 28 gives the salt requirements together with the efficiency for various operating conditions in a continuous softening process. These values are computed for the maximum efficiencies that are theoretically possible to achieve (See Appendix 6).

Table 28 shows that softening of raw water containing 250 ppm $CaCO_3$ can be achieved with almost 100% efficiency. The salt requirement increases with the quality of the treated water. In the case of raw water with greater hardness, the efficiency of the process can be improved by using a more concentrated regenerant.

Table 28 also indicates the necessary action required to overcome the irregularities in the continuous operation. For example, to maintain the quality of the treated water, a sudden increase in the total hardness of the raw water can be easily handled by increasing the regenerant flow rate in the regeneration contactor and the resin flow rate in the unit. Also, during continuous operation the quality of the water can be improved by simply increasing the flow rate of the regenerant and cutting down the resin flow rate.

Table 28

Salt requirement for softening 1 gallon of water per day in a continuous ion exchange process

Feed Quality of treated water (Ca^{++})	100 ppm (Ca^{++})			250 ppm (Ca^{++})				500 ppm (Ca^{++})				
	R	Salt*(1N) gm.	E	R	Salt(1N) gm.	E	Salt(2N) gm.	E	R	Salt(1N) gm.	E	Salt(2N) gm.	E
5 ppm	0.0934	1.265	100	0.1626	3.265	100	3.265	100	0.1202	7.215	91.5	6.640	100
4	0.0866	1.279	100	0.0917	3.278	100	3.278	100	0.1110	7.560	87.5	6.640	100
3	0.0750	1.292	100	0.0835	3.298	100	3.298	100	0.1010	8.280	80.0	6.750	98.0
2	0.0618	1.305	100	0.0710	3.361	98.5	3.310	100	0.0906	9.330	71.0	7.280	91.5
1	0.0418	1.320	100	0.0562	3.820	87.5	3.320	100	0.0773	11.680	57.0	8.470	78.5
0.5	0.0338	1.329	100	0.0439	4.82	69	3.738	89	0.0686	14.050	47.0	10.30	65.0

* Salt(N) Regenerant used as solution of normality N

R = Resin in litres/day

E = Efficiency of the process (%)

NOMENCLATURE

Nomenclature

A_i	Activity of species i
a_i	Thermodynamic activity of species i
$a_\pm$	Mean thermodynamic molal activity of an electrolyte
C_i	Concentration of species i (moles/L)
C_o	Concentration of species i (equiv./L)
C_E	Concentration of species i (mequiv./gm of solvent)
$\bar{D}_A$	Trace ionic diffusion coefficient of A in resin phase (cm^2/sec)
$\bar{D}_{AA}$	Self-diffusion (Isotopic) coefficient of A in resin phase (cm^2/sec)
$\bar{D}_{AB}$	Interdiffusion coefficient of counterions A and B (cm^2/sec.)
E_{Don}	Donnan potential
F	Fractional approach to equilibrium
f_i	Rational activity coefficient of species i
g	Moles of electrolyte
G	Gibbs free energy
h	Moles of solvent
I	Ionic strength
J_i	Flux of species i (moles/cm^2 sec)
$(J)_{diff}$	Diffusion flux of species i (moles/cm^2.sec.)
$(J)_{el}$	Electric transference of species i (moles/cm^2.sec.)

k	reaction rate constant
K	Equilibrium quotient
K_a	Thermodynamic equilibrium constant
K_D	Donnan membrane equilibrium constant
^nK_a	Rational thermodynamic equilibrium constant
L	Average flow rate of solution (mℓ/min)
m_i	Molality of species i (mol/gm)
n	Number of stage
P	Pressure (atmos)
Q_i	Amount of species i in resin
Q_r	Rational selectivity coefficient
Q_m	Molal selectivity coefficient
Q'_m	Corrected molal selectivity coefficient
r	Resin bead radius
$\bar{r}$	Fraction of resin bed transferred
R^o	Universal gas constant $(\frac{\text{atmos}}{\text{mole}^oK})$
R	Resin flow rate (mℓ/min)
SW	Swelling weight
t	Time sec.
t_f	Forward flow cycle time (sec)
t_r	Reverse flow cycle time (sec)
T	Total cycle time (sec)
u_i	Mobility of species i$(cm/_{volt.sec})$
U	Instantaneous fluid flow rate $(\frac{m\ell}{min})$
V	Volume (cm^3)
W	Resin transfer per cycle (mℓ)

x_i	Equivalent fraction of species i
z_i	Electrovalency of species i
α	Ratio of diffusion coefficients in resin phase
α_{ij}	Correction factor in Equation (49).
γ_i	Molal activity coefficient of species i
$\gamma\pm$	Mean molal activity coefficient of an electrolyte
η_i	Electrochemical potential of species i
μ	Chemical potential of species i
π	Swelling pressure atmos.
ρ	Density (gm/cm^3)
φ	Electric potential
τ	Time (dimensionless)
$\mathcal{F}$	Faraday's constant

Subscripts and Superscripts

A, B, Na, Ca	Counterionic species
Y	Coion
$\pm$	Cation and anion
*	Equilibrium

Quantities and symbols with overbars specify resin phase

Superscript $^{\circ}$ in thermodynamic functions refer to standard state.

DVB	Divinylbenzene
AAS	Atomic Absorption Spectrophotometer
p pm	Parts per million

REFERENCES

References

Arden, T. V. (1957)
The Institute of Mining and Metallurgy, London, P.119.

Arden, T. V., J. B. Davis, G. L. Herwig, R. M. Stewart, E. A. Swinton and D. E. Weiss (1959).
Proc. 2nd Intern. Conf. Peaceful Uses of Atomic Energy, Geneva, 1958. P.1096.

Arden, T. V. (1968)
Water Purification by Ion Exchange, Butterworths & Co. Ltd. (London).

Asahi Co. (1962)
British Patent 1023, 943.

Baddour, R. F., and E. R. Gilliland (1953)
I & EC., 45, 330.

Barrer, R. M. (1941)
Diffusion in and through solids, Cambridge University Press, N.Y.(1941).

Bauman, W. C., and J. Eichhorn (1947)
J. Am. Chem. Soc., 69, 2830.

Bauman, W. C., J. R. Skidmore and R. H. Osmun (1948)
I & EC., 40, 1350.

Belter, P.A., and S.M. Speaker (1967)
I & EC., Process Design Development, 6 (1), 36.

Bennett, B. A., F. L. D. Cloete and M. Streat (1969),
Ion Exchange in the Process Industries, Soc. Chem. Ind. (London), P.133.

Bonner, O. D., W. J. Argersinger Jr., and A. W. Davidson (1952)
J. Am. Chem. Soc., 74, 1044.

Bonner, O. D., and L. L. Smith (1957)
J. Phys. Chem., 61, 326.

Bouchard, J. (1969)
Ion Exchange in the Process Industries
Soc. Chem. Ind. (London), P.91.

Boyd, G.E., J. Schubert and A. W. Adamson (1947).
J. Am. Chem. Soc., 69, 2818.

Boyd, G. E., A. W. Adamson and L. S. Myers, Jr. (1947a)
J. Am. Chem. Soc., 69, 2836.

Boyd, G. E., and B. A. Soldano (1954)
J. Am. Chem. Soc., 75 (24), 6091.

Cannon, M. R. (1952)
Oil Gas J., 51, 268.

Clayton, R.C. (1969)
Ion Exchange in the Process Industries,
Soc. Chem. Ind. (London), P.98.

Cloete, F. L. D., and M. Streat (1963)
Nature (London), 200, 1199.

Dorr-Hydrosoftener (1954)
in Chemical Engineer's Handbook, by
J. H. Perry. P.16-21.

Duncan, J. F., and J. Lister (1949)
Diss. Faraday Soc., No. 7, 104.

Ekedaht, E., E. Hogfeldt and L. G. Silten (1950)
Acta. Chem. Scand., 4, 556, 829.

Elwell, W. T., and J. A. F. Gridley (1961)
Atomic Absorption Spectrophotometry.
Pergamon Press.

Frost, C. R. (1968)
Ph.D. Thesis, Univ. London.

Gaines, L. Jr. and H. C. Thomas (1953)
J. Chem. Phys., 21, 714..

George, D. R., and J. B. Rosenbaum (1969)
Ion Exchange in the Process Industries
Soc. Chem. Ind. (London).

Gregor, H. P., O. R. Abolafia and M. H. Gottlieb (1954).
J. Phys. Chem., 58, 984.

Grimmet, E.S., and B. Brown (1962),
I & EC., 54, 24.

Heister, N. K. (1954)
Chem. Eng. Prog., 50 (3), 139.

Helfferich, F., and M. S. Plesset (1958)
J. Chem. Phys., 28, 418.

Helfferich, F. (1962)
Ion Exchange
McGraw Hill, New York.

Helfferich, F. (1964)
IBM-SHARE
3187.

Hering, B., and H. Bliss (1963)
A.I. Chem. Eng. J., 9 (4), 495.

Higgins, I.R., and J. J. Robert (1954)
Chem. Engng. Prog. Symp. Series, 50 (14), 87.

Hollis, R. F., and C. K. McArther (1955)
Peaceful Uses of Atomic Energy,
Geneva (1955), P/526.

James, C. W. Kuo, and M. M. David (1963)
A.I. Chem. Eng. J., 9 (3), 365.

Kressman, R. R. E., and J. A. Kitchener (1949)
J. Chem. Soc., 1201.

Lewis, W. K. (1936)
I & EC, 26, 681.

Mackie, J. S., and P. Meares (1955)
Proc. Roy. Soc. (London) A232, 498.

McWhirter, J.R., and W. A. Lloyd (1963),
Chem. Eng. Prog., 69, 58.

Mickley, H. F., T. K. Sherwood and C. E. Reed (1957)
Mathematics in Chemical Engineering,
McGraw Hill, New York.

Moison, R. L., and H. A. O'Hern (1959)
Chem. Eng. Prog. Symp. Series, 55 (24), 71.

Moor, E. W., and J. W. Ross (1965)
J. App. Physiol, 20 (6),1332.

Morig, C. Rao., and Gopala Rao (1965)
Chem. Eng. Sci., 20, 889.

Parsons, R. (1951)
Handbook of Electrochemical Constants
Butterworths & Co. Ltd. (London).

Patterson, S. (1947)
Proc. Phys. Soc. (London) 59, 50.

Patterson, M. S., and R. C. Green (1965).,
Anal. Chem., 37, 854.

Porter, R. R., and R. V. Arden (1956)
in Water Purification by Ion Exchange,
Butterworths & Co. Ltd. (London), 1968.

Reichenberg, D. (1966)
Ion Exchange Vol. 1 by J. A. Marinsky,
Edward Arnold (London). P.235.

Robinson, R.A., and R.H. Stokes (1965)
Electrolyte Solutions
Butterworths & Co. Ltd. (London).

Soldano, B.A., and G.E. Boyd (1954)
J. Am. Chem. Soc., 75 (24), 6107.

Stevenson, D.G. (1969)
Ion Exchange in Process Industries
Soc. Chem. Ind. (London) P.114.

Subba Rao and M. M. David (1957)
Am. Inst. Chem. Eng. J., 3, 187.

Swinton, E. A., and D. E. Weiss (1953)
J. Aus. App. Sci., 4, 316.

Turner, J. C. R., and M. R. Church (1963)
Trans. Inst. Chem. Engrs., 41 (9), 283.

Turner, J. C. R., M. R. Church, A. S. W.
Johnson and C. B. Snowdon (1966).
Chem. Eng. Sci., 21, 317.

Wheeler, A. (1951).
Advances in Catalysis, 249.

APPENDICES

APPENDIX - 1

Determination of the cation exchange capacity of Zeo-Karb 225, 8% DVB resin.

A sample of about 10 ml of washed Zeo-Karb 225 resin, 8% DVB was placed in a glass column (2.5 cm internal diameter) and converted to the sodium ionic form with 1 litre of IN sodium chloride. The resin was subsequently washed free of excess salt with deionised water.

A portion (1-2 ml) of the resin, as prepared above, was centrifuged at 300 G until it attained a constant weight (W_H). It was then dried in air at 105°C. Ensuring that it had attained constant weight (W_D), the sample was transfered to a glass column and eluted with hydrochloric acid (1 N). A stoichiometric excess quantity of acid was used to completely elute the sodium ions from the resin. The eluant was then analysed by Atomic Spectroscopy for the concentration of sodium. This gave the number of equivalents of sodium eluted from a known weight (W_D) of resin, i.e. the sodium exchange capacity per unit weight of dry resin in sodium ionic form. A similar procedure was repeated for the calcium exchange capacity of Zeo-Karb 225.

Another portion (2.0 ml) of the prepared resin was transfered to a glass column and eluted with 250 ml of hydrochloric acid. The analysis of the eluant for sodium gave the sodium exchange capacity per unit volume of Zeo-Karb 225.

Swelling weight defined as the water content of resin per unit weight was computed as follows:

$$\text{Swelling weight} = \frac{W_H - W_D}{W_D}$$

The swelling weight of Zeo-Karb 225 8% DVB resin samples used

/...

in this study has been determined as 0.70 and 0.69 for the sodium and calcium ionic form respectively. For the calculation of molality of an ion within the resin phase a linear relationship between the resin composition and swelling weight has been assumed.

APPENDIX - 2A

SP-90 Atomic Absorption Spectrophotometer*

The instrument is designed for the determination of many metal ions in trace and high concentrations (1-100 ppm). The solution sample is accepted by the instrument in the form of droplets, sprayed through a capillary tube into an acetylene/air flame.

The instrument houses a Littrow prism monochromator, a plug-in electronic unit and interchangeable burner heads fed by pre-mixed fuel, air and sample. A hollow cathode lamp incorporates a cathode containing the element being determined so that it emits a line spectrum characteristic of that element. The lamp, supplied by a rectified current (up to 25 mA), provides a narrow bandwidth monochromatic source. Light from its cathode is focused at the centre of the flame. Light from the lamp (absorption spectroscopy) or from the flame (emission spectroscopy) is modulated on entering the monochromator. The monochromator is of the Littrow type and employs a 30° rear-aluminized silica prism. The dispersed light is refocussed onto the exit slit of the monochromator and then falls on the photomultiplier. The SP-90 employs an E.M.I. 9663B photomultiplier which covers a range from 200-770 μm. The signals from the photomultiplier are amplified, rectified in synchronism with the mains frequency and is then applied to the external potentiometric recorder.

*Manufactured by Unicam Instruments Ltd., Cambridge.

A P P E N D I X - 2 B

Analysis of sodium on SP-90, Atomic Absorption Spectrophotometer (Emission technique).

The instrument was switched on and set on emission. After about two hours an emission burner head was fitted and the air pump started. The air flow to the instrument was set at 5000 ml/min and the flame was lit. After another 15-20 minutes the folowing settings were made for the analysis of sodium:

Wave length = 589 mμ
Slit width = 0.08 mm

On introduction deionised water was automatically sucked into the flame and the corresponding reading on the recorder was set at zero. Standard solutions were introduced and their respective signals were recorded to obtain a calibration curve. Sample solutions were then introduced and their composition was determined by recording their signals and subsequently measuring the concentrations with the help of the calibration curve.

Deionised water was admitted to the instrument after each sample to check the zero setting and also to wash the capillary drawing the sample solution into the flame. Often slight changes in the operating conditions, as stated above, were necessary to optimize the output signals. A typical calibration curve of sodium in deionised water is given in Figure 57.

Calcium was analysed by the absorption technique. The following operating conditions were used as a guide line for its analysis:

Wave length = 422.7 mμ
Slit width = 0.08 mm

/...

Air flow rate = 5000 ml/min

Acetylene flow rate = 1500 ml/min

Cathode lamp current = 12 mA

A typical calibration curve for calcium in deionised water is shown in Figure 58.

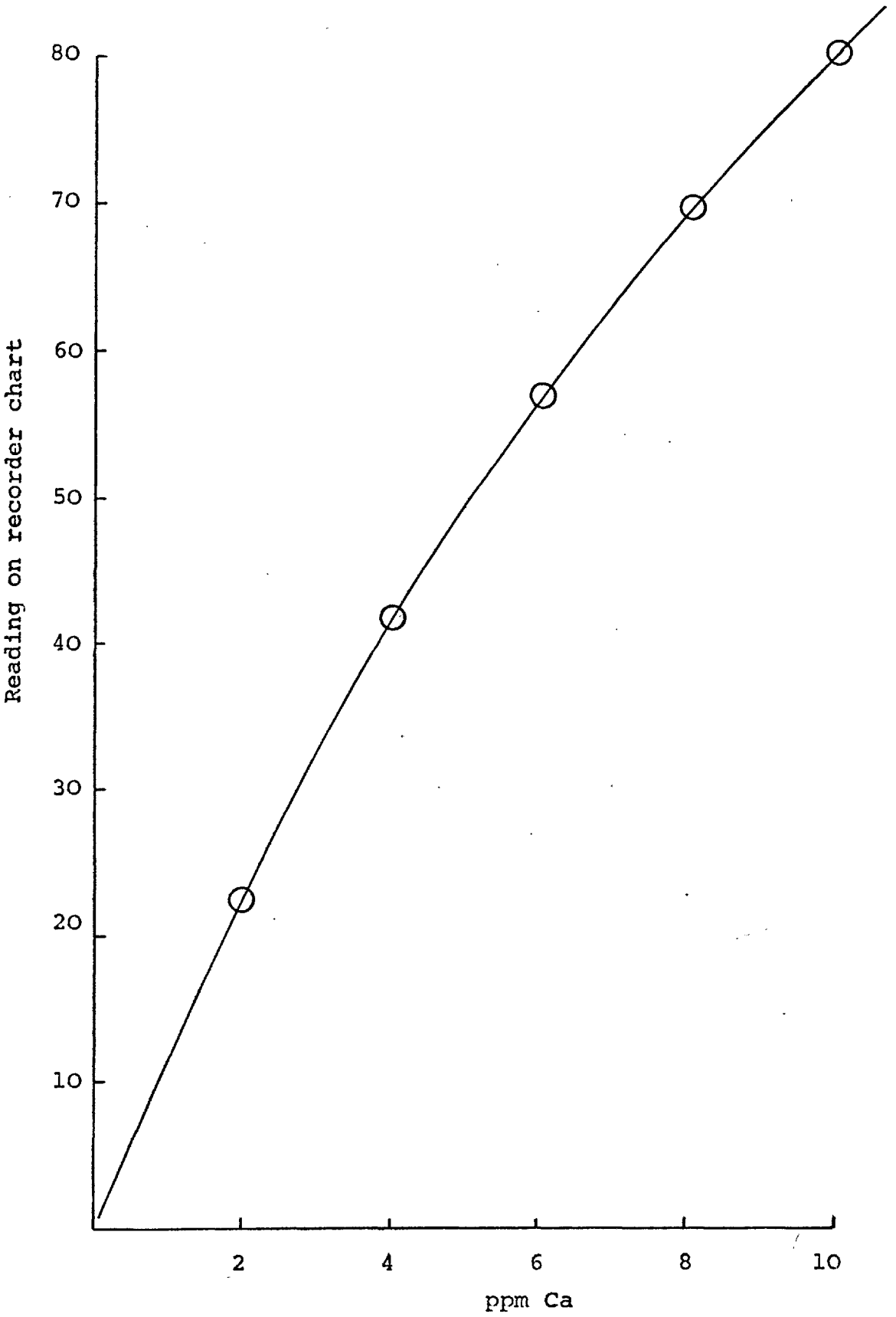

Figure 57 A typical calibration curve for calcium (AAS) Deionised water as blank.

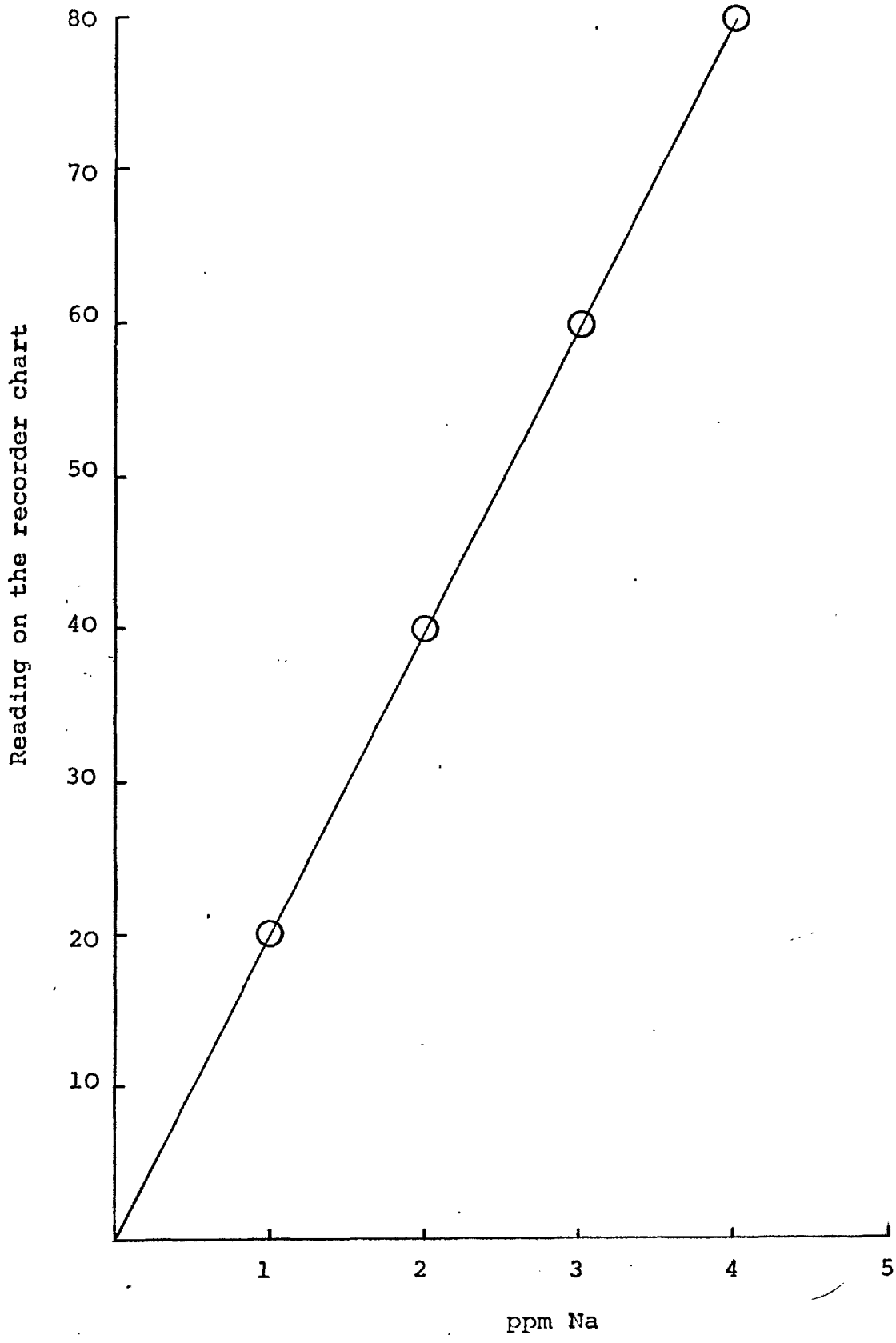

Figure 58. A typical calibration curve for sodium (AAS)
Deionised water as blank.

A P P E N D I X - 3

Calculation of Q_r and Q_m

Programme ONE

A computer programme listing is presented along with a short description and definitions of variables used.

Programme ONE calculates the value of Q_r and Q_m from the experimental data.
The rational selectivity coefficient Q_r and molal selectivity coefficient Q_m are computed from Equation 36 and 37.

$$Q_r = \frac{\bar{x}_{Ca}}{x_{Ca}} \left(\frac{x_{Na}}{\bar{x}_{Na}} \right)^2$$

and

$$Q_m = \frac{\bar{m}_{Ca}}{m_{Ca}} \left(\frac{m_{Na}}{\bar{m}_{Na}} \right)^2$$

Definition of the variables:

XA	Equivalent fraction of calcium in solution
YA	Equivalent fraction of calcium within resin phase
DCA, DNA	Densities of pure solutions of calcium chloride and sodium chloride respectively
A MOL LX	Molality of calcium in solution
A MOLLY	Molality of calcium within resin phase
A MOLES	Moles of calcium in solution
A MOLFX	Mole fraction of calcium in solution
AMOLFY	Mole fraction of calcium within resin phase
WTSOL	Weight of one litre of solution
WTSALT	Weight of salt in WTSOL
WATER	Weight of water in WTSOL
QRAT	Rational selectivity coefficient
QMOL	Molal selectivity coefficient

/...

AVQR	Average value of QRAT
AVQM	Average value of QMOL
DAV	Overall average value of AVQM
VARI	Variation of average value
STDEV	Standard deviation of DAV
AMDEV	Mean deviation of DAV

Sample calculation of molal selectivity coefficient Q_m.

The calculation of Q_m is shown in detail for one point on the equilibrium isotherm, e.g. $C_o = 1.0$. However, the results of the calculations for the other runs are given in Table 6. The calculation of Q_m requires molalities of the ions in both phases:

$$Q_m = \frac{\bar{m}_{Ca} \cdot m_{Na}^2}{m_{Ca} \cdot \bar{m}_{Na}^2}$$

Consider a case of Table 6, for $C_o = 1.0$ and $x_{Ca} = 0.1$. The corresponding value of $\bar{x}_{Ca}$ is 0.336.

Equivalent fraction of calcium in solution $x_{Ca} = 0.10$.

Normality of solution w.r.t. calcium = 0.10 x 1.0.

Molarity of solution w.r.t. calcium = $\frac{0.1}{2} = 0.05 \frac{\text{moles}}{\text{L}}$.

Weight of water in 1 litre of solution = weight of solution/L - weight of salts in solution/L.

Weight of solution/L = $1000 (x_{Ca} \times \rho_{Ca} + x_{Na} \times \rho_{Na})$

$1000 (0.1 \times 1.021 + 0.9 \times 1.024)$

$= 1043.4$ gm.

Weight of salt/L solution = $(x_{Ca} \times \text{Eq.Wt}(CaCl_2) + x_{Na} \times \text{Eq.Wt}(NaCl)) C_o$

$= 0.1 \times 55.5 + 0.9 \times 58.5$

$= 58.20$ gm.

Weight of water/L solution = $1043.4 - 58.20$

$= 985.20$ gm.

/...

Molality of solution w.r.t. calcium $= \frac{\text{Moles}}{1000 \text{ gm water}}$

$= \frac{0.05 \times 1000}{985.20}$

$m_{Ca} = 0.051$

Molality of solution w.r.t. sodium $= \frac{0.9 \times 1000}{985.2}$

$m_{Ca} = 0.914$

Calculation of molality of resin w.r.t. calcium and sodium:

Exchange capacity of resin containing calcium and sodium

$$\bar{C} = (\bar{x}_{Ca} \times 4.589 + \bar{x}_{Na} \times 4.524)$$

$$= (0.336 \times 4.589 + 0.664 \times 4.524)$$

$$= 4.546 \text{ equivalents/gm resin.}$$

Weight of water/gm resin $W = \bar{x}_{Ca} \times SW(Ca) + \bar{x}_{Na} \times SW(Na)$

$= 0.336 \times 0.69 + 0.664 \times .7$

$= 0.697$ gm.

Molality of resin w.r.t. calcium $= \frac{\bar{C}}{W} \frac{\bar{x}_{Ca}}{z_{Ca}}$

$= \frac{4.546}{0.697} \times \frac{0.336}{2}$

$\bar{m}_{Ca} = 1.096 \frac{\text{moles}}{1000 \text{ gm water}}$

Molality of resin w.r.t. sodium $= \frac{4.546 \times .664}{0.697}$

$\bar{m}_{Na} = 4.333$

$$Q_m = \frac{\bar{m}_{Ca} \cdot m_{Na}^2}{m_{Ca} \cdot \bar{m}_{Na}^2}$$

Molal selectivity coeff. $= \frac{1.096 \times (0.914)^2}{0.051 \times (4.33)^2} = 0.960$

PROGRAMME ONE

```
C       THIS SUB. CALCULATES THE QR AND QM FROM EXPT. DATA
        DIMENSION XA(63),XB(63),YA(63),YB(63),DCA(7),DNA(7),WTSOL(63),WTSA
       1LT(63),WATER(63),AMOLFS(63),AMOLLX(63),AMOLLY(63),BMOLLX(63),BMOLL
       2Y(63),CAPAC(63),SWT(63),QRAT(63),QMOL(63),AVQR(63),AVQM(63),C(7)
       3,BMOLES(63),AMOLFX(63),BMOLFX(63),AMOLFY(63),BMOLFY(63)

C      READ DATA CONCENTRATION AND DENSITIES OF PURE SOLUTIONS OF
C      SODIUM CHLORIDE AND CALCIUM CHLORIDE
        DATA C/0.025,0.11,0.20,0.60,1.00,2.00,1.00/,DNA/1.00,1.002,1.005,1
       1.024,1.044,1.092,1.044/,DCA/1.00,1.002,1.005,1.021,1.038,1.079,1.0
       238/
        NN=63
        DO 3 K=1,NN
C      READ EXPERIMENTAL DATA EQUIVALENT FRACTION OF CALCIUM IN SOLUTION
C      AND ON RESIN RESPECTIVELY
        READ(5,1)XCA,YCA
      1 FORMAT(2F6.4)
        XA(K)=XCA
        XB(K)=1.0-XCA
        YA(K)=YCA
        YB(K)=1.0-YCA
      3 CONTINUE
C       INITIALIZE VARIABLES
        EQA=55.5
        EQB=58.5
        NCOUNT=0
        SUMQR=0.0
        SUMQM=0.0
        DAV=0.0
        Y=0.0
        B=0.0
        TMDEV=0.0
        TSTDEV=0.0
        CAV=1.0
        ZA=2.0
        ZB=1.0
        N=1
        JCOUNT=1
        J=1
        WRITE(6,2)
      2 FORMAT(2X,8HSOLUTION,8H   RESIN,8HRATIOMAL,8HMOLES OF,8HMOLES OF,8
       1H   MOLE ,8HMOLES OF,8HMOLES OF,8H   MOLE ,8H   MOLAL,4X,8H WT. OF
       2 ,8H  WT. OF,8H  WT. OF,8H  RESIN ,8HSWELLING,2X,4HCASE/2X,8H
       3XCA,8H     YCA,8H   Q     ,7HCA IN S,7HNA IN S,8HFRACTION,8HCA IN
       4 R ,8HNA IN R ,9HFRACTION ,8H   Q     ,4X,8HSOLUTION,8H    SALT,8H
       5  WATER,9HCAPACITY,7H WEIGHT,2X,4H NO.////)
      5 WRITE(6,30)C(J)
     30 FORMAT(5X,5HTHIS  5HCASE 2HIS 20H     FOR ..........F8.3)
C       CALCULATION OF MOLALITY OF SOLUTION AND RESIN
        DO 6 I=N,NN
        N=N+1
        WTSOL(I)=1000.0*(XA(I)*DCA(J)+XB(I)*DNA(J))
        WTSALT(I)=(XA(I)*EQA+XB(I)*EQB)*C(J)
        WATER(I)=WTSOL(I)-WTSALT(I)
        AMOLES(I)=XA(I)*C(J)/ZA
        BMOLES(I)=XB(I)*C(J)/ZB
        AMOLLX(I)=(AMOLES(I)/WATER(I))*1000.0
        BMOLLX(I)=AMOLLX(I)*XB(I)*ZA/XA(I)
        CAPAC(I)=YA(I)*4.589+YB(I)*4.524
```

```
      SWT(I)=YA(I)*0.690+YB(I)*0.70
      AMOLLY(I)=YA(I)*CAPAC(I)/(ZA*SWT(I))
      BMOLLY(I)=YB(I)*CAPAC(I)/SWT(I)
      AMOLFX(I)=AMOLLX(I)/(AMOLLX(I)+BMOLLX(I))
      AMOLFY(I)=AMOLLY(I)/(AMOLLY(I)+BMOLLY(I))
C     CALCULATION OF RATIONAL AND MOLAL SELECTIVITY COEFFICIENT
      QRAT(I)=(YA(I)*XB(I)**2.0)/(XA(I)*YB(I)**2.0)
      QMOL(I)=(AMOLLY(I)*BMOLLX(I)**2.0)/(AMOLLX(I)*BMOLLY(I)**2.0)
      WRITE(6,40)WTSOL(I),WTSALT(I),WATER(I),CAPAC(I),SWT(I)
   40 FORMAT(86X,5F8.3)
      WRITE(6,10)XA(I),YA(I),QRAT(I),AMOLLX(I),BMOLLX(I),AMOLFX(I),AMOLL
     1Y(I),BMOLLY(I),AMOLFY(I),QMOL(I),I
   10 FORMAT(2X,10F8.3,46X,I4)
      SUMQR=SUMQR+QRAT(I)
      SUMQM=SUMQM+QMOL(I)
      NCOUNT=NCOUNT+1
      IF(NCOUNT.EQ.9)GO TO 4
    6 CONTINUE
    4 AVQR(JCOUNT)=SUMQR/9.0
      AVQM(JCOUNT)=SUMQM/9.0
      JCOUNT=JCOUNT+1
      NCOUNT=0
      WRITE(6,20)AVQR(J),AVQM(J)
      J=JCOUNT
   20 FORMAT(//10X,8H AVERAGE,F8.3,48X,F8.3////)
      SUMQR=0.0
      SUMQM=0.0
      IF(J.LT.8)GO TO 5
      DO 46 I=1,7
      WRITE(6,45)C(I),AVQR(I),AVQM(I)
   45 FORMAT(2X,3F10.3)
      DAV=DAV+AVQM(I)
   46 CONTINUE
      DAV=DAV/7.0
      WRITE(6,47)DAV
   47 FORMAT(2X,////F10.3)
      WRITE(6,52)
   52 FORMAT(2X,8HAV.QMOL ,8H  QMOL  ,9HVARIATION,10HSQ.OF VARI/////)
      DO 49 I=1,NN
C     CALCULATION OF STANDARD DEVIATION
      VARI=(DAV-QMOL(I))
      SQVARI=VARI*VARI
      TMDEV=TMDEV+ABS(VARI)
      TSTDEV=TSTDEV+SQVARI
      WRITE(6,51)DAV,QMOL(I),VARI,SQVARI
   51 FORMAT(2X,F5.3,5X,F5.3,3X,F5.3,5X,F5.3)
   49 CONTINUE
      AMDEV=TMDEV/63.0
      STDEV=TSTDEV/63.0
      WRITE(6,54)TMDEV,AMDEV,TSTDEV,STDEV
   54 FORMAT(2X,4F10.4)
   61 STOP
      END
```

A P P E N D I X — 4

Average radius of resin.

The average resin bead radius was determined by measuring the size of about 400 wet beads in both the ionic forms using a microscope. The resin beads were arranged on a glass slide which was covered with a very thin layer of grease to hold the beads. A magnification of x 50 enabled the size measurement to the nearest micron. The following table gives the size distribution for the batch of resin in sodium form:

Table. Resin Particle Size Distribution

Radius range cm.	No. of particles in Sodium form.
0.020 -- 0.030	10
0.030 -- 0.035	25
0.035 -- 0.040	22
0.040 -- 0.045	35
0.045 -- 0.050	180
0.050 -- 0.055	87
0.055 -- 0.060	37
	396

The arithmetic average radius of the resin sample in sodium ionic form has been computed to be 0.04702 cm by employing the following expression:

$$r = \frac{\Sigma N \times Y}{\Sigma N}$$

A similar size distribution analysis when applied to the resin batch in calcium form gave an average radius of resin bead as 0.050 cm.

A P P E N D I X - 5 .

Computer programme for the numerical solution of diffusion Equation (6).

The basis of the programme is the solution of the diffusion equation for systems having spherical symmetry, with a concentration dependent interdiffusion coefficient, $\bar{D}_{AB}$, under finite and infinite solution volume conditions.

The solution of the partial differential equation is accomplished by an explicit finite difference method. It gives a concentration profile, amount of ionic species left in the medium together with rate of exchange at an instant in time during the reaction. The amount of ions left in the medium is computed from radius integral of the concentration profile employing Simpson's rule. Application of mass balance gives solution phase composition in contact with resin in the case of finite solution conditions. The input data to the programme includes initial resin and solution concentrations, and boundary conditions.

The diffusion equation for spherical symmetry is:-

$$\frac{\partial \bar{C}_A}{\partial t} = \frac{1}{r^2} \frac{\partial}{\partial r}\left(r^2 \cdot \bar{D}_{AB} \cdot \frac{\partial \bar{C}_A}{\partial r}\right) \qquad (69)$$

or in dimensionless terms;

$$\frac{\partial \bar{x}_A}{\partial \tau} = \frac{1}{\rho^2} \frac{\partial}{\partial \rho}\left(\rho^2 \bar{D}_{max} \frac{\partial \bar{x}_A}{\partial \rho}\right) \qquad (78)$$

where

$$\bar{x}_A = \frac{z_A C_A}{z_A C_A + z_B C_B}, \qquad \rho = \frac{r}{r_o}$$

$$\bar{D}_{max} = \frac{\bar{D}_{AB}}{\bar{D}_A} = \frac{1 + b\bar{x}_A}{1 + a\bar{x}_A}$$

$$a = \frac{z_A \bar{D}_A}{z_B \bar{D}_B} - 1, \qquad b = \frac{z_A}{z_B} - 1$$

$$\tau = \frac{\bar{D}_A t}{r_o^2}$$

/...

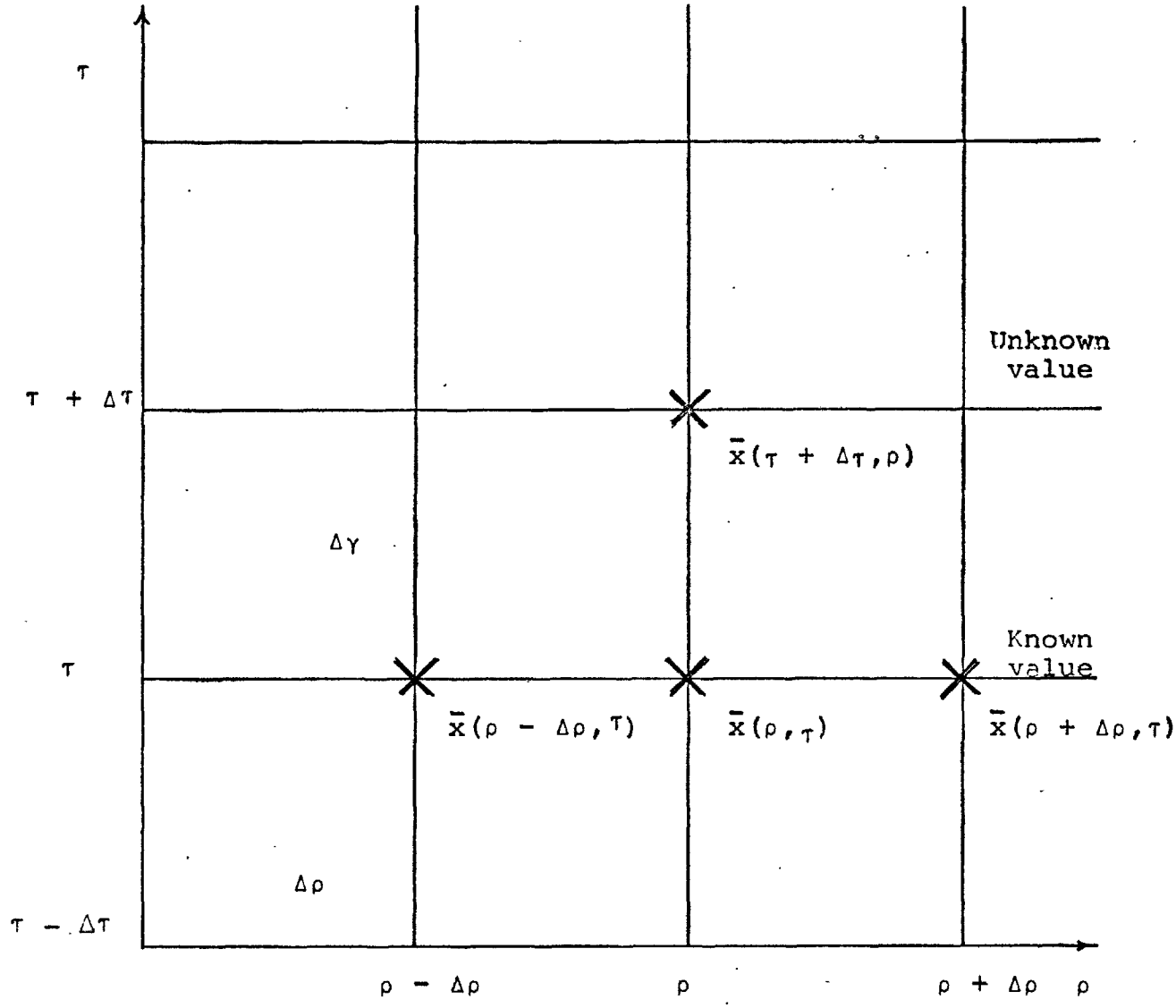

Figure 59. Arrangement of grid w.r.t. space and time employed in the finite difference method.

The above partial differential equation, when approximated to a difference equation by forward finite difference method, gives:-

L.H.S.

$$\frac{\partial \bar{x}_A}{\partial r} = \frac{\bar{x}_A(\rho, \tau + \Delta\tau) - \bar{x}_A(\rho, \tau)}{\Delta\tau} \qquad (79)$$

R.H.S.

$$\frac{1}{\rho^2} \cdot \frac{\partial}{\partial \rho}\left(\rho^2 \cdot \bar{D}_{max} \frac{\partial \bar{x}_A}{\partial \rho}\right)$$

$$= \frac{1}{\Delta\rho^2}\left\{\bar{D}_+ R_+\left[\bar{x}_A(\rho + \Delta\rho, \tau) - \bar{x}_A(\rho, \tau)\right] - \bar{D}_- R_-\left[\bar{x}_A(\rho, \tau) - \bar{x}_A(\rho - \Delta\rho, \tau)\right]\right\} \qquad (80)$$

where $\bar{D}_+(\tau) = \bar{D}_{max}(\tau)$ at $(\rho + \frac{1}{2}\Delta\rho)$

$\bar{D}_-(\tau) = \bar{D}_{max}(\tau)$ at $(\rho - \frac{1}{2}\Delta\rho)$

$$R_+(\rho) = \left(\frac{\rho + \frac{1}{2}\Delta\rho}{\rho}\right)^2$$

$$R_-(\rho) = \left(\frac{\rho - \frac{1}{2}\Delta\rho}{\rho}\right)^2$$

Figure 59 shows the formation of grid and various location w.r.t. time and space. Combining Equation (79) and (80), it becomes:-

$$\bar{x}_A(\rho, \tau + \Delta\tau) = \bar{x}_A(\rho, \tau) + \frac{\Delta\tau}{\Delta\rho^2}\left\{\bar{D}_+ R_+\left[\bar{x}_A(\rho + \Delta\rho, \tau) - \bar{x}_A(\rho, \tau)\right] - \bar{D}_- R_-\left[\bar{x}_A(\rho, \tau) - \bar{x}_A(\rho - \Delta\rho, \tau)\right]\right\} \qquad (81)$$

The L.H.S. of the Equation represents the unknown concentration of ionic species at a point in space as a function of time in terms of known concentrations existing in its neighbourhood. (See Figure 59). Application of Equation (81) gives a concentration profile in the resin bead at any instant in time. The total amount (dimensionless) of ionic species still left in the medium at time τ (dimensionless) may be obtained by integration of the concentration profile,

/...

$$\bar{Q}_A(\tau) = 3\int_0^1 \bar{x}_A\ (\rho,\tau)\ \rho^2.\partial\rho$$

This can be approximated by Simpson's rule, i.e.,

$$\bar{Q}_A(\tau) = \Delta\rho\ 4\sum_{1,3,5,\ldots}^{\frac{1}{\Delta\rho}-1} (\rho^2.\bar{x}_A(\rho,\tau) + 2\sum_{2,4,6,\ldots}^{\frac{1}{\Delta\rho}-2} \rho^2\ \bar{x}_A(\rho,\tau)$$

Rate of exchange may be computed from the change in the amount of ionic species over a time step, i.e.,

$$\text{Rate} = \frac{\bar{Q}_A(\tau + \Delta\tau) - \bar{Q}_A(\tau)}{\Delta\tau}$$

In the case of finite solution volume the change in the concentration of solution and thus the new boundary concentration can be obtained from material balance,

$$x'_A(\tau) = x'_{A(0)} + \frac{V_R\bar{C}_o}{V\ C_o}\ (\bar{Q}_{A(0)} - \bar{Q}_A(\tau))$$

where x'_A is dimensionless concentration of ionic species A in solution phase. V and C represent volume and concentrations respectively.

Outline of the programme

The flow of control of programme is simple. Following the input data and calculation of time step according to the stability criterion, procedure is entirely iterative.

The finite difference scheme produces a series of concentration values $\bar{x}_A(\tau)$ along the grid points. These values are then used for the computation of $\bar{Q}_A(\tau)$, rate and $x'(\tau)$. With the addition of a time step, the computation then enters into iteration and continues to calculate the profile, amount, rate and solution composition. These values can be printed out at prefixed values of either τ or $\bar{Q}_A(\tau)$. Figures 60 and 61 give the flow diagrams of the two computer programmes used in this study.

Each of the five subroutines and six functions are called by the main programme for specified purposes. A fully commented listing of the FORTRAN programme statements together with the important variables, their

/...

meaning and function is given at the end of this appendix. The modified programmes have been adapted from the general programme (Helfferich 1964). It has been translated into FORTRAN IV and reduced in size to solve the specific problem of diffusion in a solid spherical bead with initial uniform concentration of the diffusing ion. For any variation, the reader is advised to consult the above cited reference.

Facility of APP.

The optional subroutine APP can be used to give higher accuracy of the finite difference approximation in the neighbourhood of initial concentration steps near the front boundary. The high accuracy is achieved by calculating $\bar{x}_A(\rho,\tau)$ with a small grid spacing, $\Delta\rho$.

Facility of TELESCOPING.

The time for computation may be saved by increasing the grid spacing and time step during computations. This may be applied when relatively flat concentration profiles exist in the bead. The device operates by eliminating from the current row $\bar{x}_A(\rho,\tau)$ every other value and using only the remaining values for further calculations.

The decision when to telescope is made by a function NTEL. Five constants can be specified by input to fix the time (τ) or amount $\bar{Q}_A(\tau)$ in medium at which to telescope.

Preparation of the data Cards

The input data and flags are punched on five consecutive cards.

Card one*: The first 30 fields are for alphameric identification. The next 36 fields contain values for A,B and DIFM each of format F 12.7.

Card two: The first 36 fields contain values of SCOUTT, CINIT and WFRONT each of format F 12.7.

Card three: The first five fields contain values of integer variables NBOUND, NAPPR, NTELE, NINIT and NDCT for the corresponding run. The next six fields contain the value of IBLOCK followed by values of STTIME, JFREE, XFREE

*For meanings of variable names see listing of the programmes at the end of this appendix.

/...

and NFREE of formats F 12.7, I1, 2F 12.7, respectively.

Card four: The first 55 fields contain values of telescoping parameter Q(I), each of format F 11.9. The next 24 fields contain values of PTOL and TTOL each of format F 12.7.

Card five: This card (only for programme ~~THREE~~ TWO) contains values of COEFF, RADIUS, RATER, TCONCS, TCONCR and STEP with formats F 12.9 and 5 F 7.5, respectively.

COMPUTER PROGRAMME LISTING

THE NAMES OF THE VARIABLES, TOGETHER WITH THEIR FUNCTION AND MEANING ARE ENUMERATED BELOW. THESE NAMES ARE PASSED BETWEEN THE SUBROUTINES AND THEREFORE APPEAR IN THE COMMON STATEMENT.

QOLD	INITIAL AMOUNT IN THE RESIN PHASE
C	CONCENTRATION ELEMENTS FOR PROFILE AND INTEGRATION
STEPL	GRID WIDTH FOR CALCULATION
CINIT	INITIAL CONCENTRATION IN MEDIUM
FBLOCK,NBLOCK	SPECIFIES GRID SPACING AN EVEN NUMBER BETWEEN 640 AND 4
R	WEIGHT FACTOR USED IN SIMPSONS RULE FOR INTEGRATION
RPLUS,RMIN	FACTOR USED IN FINITE DIFFERENCE EQUATION
STEPT	TIME INCREMENT AFTER EACH ITERATION
CFRONT	INITIAL FRONT BOUNDARY CONCENTRATION
FLIN	RATE OF EXCHANGE AT A KNOWN TIME
NBOUND	SPECIFIES FRONT BOUNDARY CONDITION 1 FOR CONSTANT 2 FOR VARIABLE, CLOSED SYSTEM
TIME	TIME FOR EXCHANGE REACTION
IEND	LAST POINT ON A GRID
Q2	AMOUNT LEFT IN THE MEDIUM
FACTOR	FACTOR USED IN THE SETTING OF TIME INCREMENT
NAPPR	SPECIFIES NUMBER OF TELESCOPINGS IN APP UP TO 5
A,B	PARAMETERS FOR FUNCTION DIF A=(ZA*DA/ZB*DB)-1 B=(ZA/ZB)-1
Q1	STORE FOR PREVIOUS AMOUNT IN THE MEDIUM
WFRONT	RESIN TO SOLUTION (EQUIVALENTS) RATIO
XFREE	FREE INPUT CONSTANT
SC	SOLUTION PHASE CONCENTRATION
NTELE	NUMBER OF TELESCOPINGS IN THE MAIN PROGRAMME UP TO 5
NINIT	FLAG FOR INITIAL DISTRIBUTION 1 FOR UNIFORM, AND 2 FOR NON-UNIFORM
DIFM	MAXIMUM VALUE OF DIFFUSION COEFFICIENT
TTOL	TIME LIMIT
PTOL	TIME LIMIT SPECIFIES PRINTOUT OF RESULTS
Q	TELESCOPING PARAMETER
NDCT	FLAG FOR THE DEPENDENCE OF DIFFUSION COEFFICIENT ON CONCENTRATION
STP	GRID WIDTH FOR CALCULATION IN SUBROUTINE APP
JREPET	INDICATES NUMBER OF TRIALS FOR THE CALCULATION OF A STAGE
S	CONCENTRATION ELEMENTS FOR THE STIRAGE OF PROFILE
STEP	FIRST TRIAL VALUE FOR STAGE CALCULATION
STTIME	STARTING TIME FOR A NEW CALCULATION
SCTARG	SPECIFIES FIXED VALUE OF SOLUTION LEAVING A STAGE
RATES	VOLUME OF SOLUTION IN A STAGE
RATER	RESIN VOLUME IN A STAGE
TCONC	TOTAL SOUTION CONCENTRATION
TCONR	TOTAL EXCHANGE CAPACITY OF RESIN 2 MEQ./ML.
SCOUTT	SOLUTION CONCENTRATION LEAVING THE FIRST STAGE
SCINIT	STARTING CONCENTRATION OF SOLUTION WITH A NEW GUESS
SCPOS	STARTING CONCENTRATION OF SOLUTION WHICH RESULTED IN AN OVERESTIMATE
SCNEG	STARTING CONCENTRATION OF SOLUTION WHICH RESULTED IN AN UNDERESTIMATE
ERRPOS	DIVERGENCE OF THE COMPUTED VALUE OF SOLUTION

	CONCENTRATION LEAVING A STAGE
ERRNEG	SAME AS ERRPOS
GUESS	A GUESS FOR THE CONCENTRATION OF SOLUTION AT THE START OF A REACTION
ERRORX	ERROR IN THE COMPUTED SOLUTION PHASE CONCENTRATION AGAINST SOLUTION CONCENTRATION DETERMINED BY MASS BALANCE
ERRORY	SAME AS ABOVE FOR RESIN PHASE
EQUIB	FRACTIONAL APPROACH TO EQUILIBRIUM
FRACT	FRACTION OF IONIC SPECIES THAT DIFFUSED OUT OF THE MEDIUM AT A KNOWN TIME
DCA	DIFFUSION COEFFICIENT OF CALCIUM
DNA	DIFFUSION COEFFICIENT OF SODIUM
DADB	RATIO OF DNA AND DCA
FX1,TY1	DATA FOR AN EXCHANGE CURVE
DCAV	AVERAGE DIFFUSION COEFFICIENT FOR A GIVEN VALUE OF DNA/DCA
JKL	FLAG SPECIFIES THE DIRECTION OF EXCHANGE REACTION
F	STABILITY CRITERION FACTOR FOR THE SETTING OF TIME INCREMENT 0.38 FOR SPHERES

```
C       PROGRAMME NUMBER TWO CALCULATES THE NUMBER OF STAGES REQUIRED
C       FOR A GIVEN ION EXCHANGE PROCESS

        COMMON QOLD,C,STEPL,CINIT,FBLOCK,R,RPLUS,RMIN,STEPT,CFRONT,FLIN,NB
       1OUND,NBLOCK,TIME,IEND,Q2,RATE,FACTOR,NAPPR,A,B,Q1,WFRONT,XFREE,NFR
       2EE,JFREE,NTELE,NINIT,DIFM,TTOL,PTOL,Q,NDCT,STP,JREPET,STEP,STTIME,
       3SCTARG,RATES,RATER,TCONCS,TCONCR,SCINIT,SCPOS,SCNEG,ERRPOS,ERRNEG,
       4SC,GUESS,RADIUS,JKL
C       'READ' READS IN AND PRINTS OUT INPUT DATA
     1  CALL READ
        CALL SECOND(T1)
C       INITIALISING VARIABLES
        NSTAGE=0
        ERRPOS=0.0
        JREPET=1
        SCOUT=SC
        SCPOS=SC
C       SCINIT IS FIRST GUESS FOR SOLUTION CONCENTRATION ENTERING STAGE  1
        SCINIT=STEP/2.0
        SC=SCINIT
        JFREE=1
        CFRONT=BOUND(WFRONT,SC,JKL,JFREE)
        CSTART=CFRONT
        C(1,1)=CFRONT
        TIME=STTIME
        NT=NTELE
        F=0.38
        FACTOR=F/DIFM
        FLIN=0.0
     3  GO TO (4,8),NINIT
     4  CONTINUE
C       'APP' SMOOTHES OUT INITIAL SINGULARITIES
     5  CALL APP
C       SETTING UP OF INITIAL VALUE FOR UNIFORM INITIAL COMPOSITION
     6  Q1=CINIT
        DO 7 I=2,NBLOCK
     7  C(I,1)=CINIT
        GO TO 9
     8  Q1=Q2
C       SET QOLD EQUAL TO INITIAL AMOUNT
     9  QOLD=Q1
C       CALCULATE TIME INCREMENT
        STEPT=FACTOR*STEPL*STEPL
C       'K' IS SUBSCRIPT OF TELESCOPING VARIABLE
        K=1
C       'GEO 1 ' CALCULATES GEOMETRICAL FACTORS FOR SPHERE
    10  CALL GEO1
        FACTOR=STEPT/(STEPL*STEPL)
        ASSIGN 11 TO NBACK
C       NORMAL RE-ENTRY
C       CALCULATION OF DMIN FOR FIRST GRID INTERVAL
    11  DMIN=DIF(0.5*(C(2,1)+C(1,1)),A,B)
```

```
C       ITRATIVE CALCULATION OF CONCENTRATIONS BY FINITE DIFFERENCE EQUATION
        DO 13 I=2,NBLOCK
C       TIME SAVER TRANSFER TO 14 WHEN CALCULATION OF FURTHER VALUES
C       UNNECESSARY
        IF(C(I-1,1)-CINIT)12,14,12
C       CALCULATION OF CONCENTRATION DEPENDENT DIFFUSION COEFFICIENT
   12   DPLUS=DIF(0.5*(C(I+1,1)+C(I,1)),A,B)
        DPL=DPLUS
        DPLUS=DPLUS*RPLUS(I-1)
        DMIN=DMIN*RMIN(I-1)
C       FINITE DIFFERENCE EQUATION FOR CONCENTRATION VALUES
        CALL DIFEQ(I,FACTOR,DPLUS,DMIN,C)
   13   DMIN=DPL
        IEND=NBLOCK+1
C       STEP UP TIME VARIABLE
        TIME=TIME+STEPT
        C(IEND,1)=C(NBLOCK,2)
        GO TO 15
   14   IEND=I
        TIME=TIME+STEPT
   15   C(1,1)=BOUND(WFRONT,SC,JKL,JFREE)
        SCOUTT=SC
C       TRANSFER ROW OF NEWLY CALCULATED CONCENTRATION VALUES
        DO 16 I=3,IEND
   16   C(I-1,1)=C(I-1,2)
C       'AMOUNT'  CALCULATES TOTAL AMOUNT IN IN RESIN PARTICLE
        Q2=AMOUNT(NBLOCK)
        RATE=(Q2-Q1)/STEPT
        FLIN=RATE
C       TEST FOR PRINTOUT
        NPRIN=NPRINT(C,TIME,PTOL,SCTARG,SCPOS,SCNEG,SCINIT,SCOUTT,ERRPOS,E
       1RRNEG,GUESS)
        JREPET=JREPET+1
        GO TO (21,17,26,20),NPRIN
C       CORRECT GUESS CALCULATION FOR THE STAGE COMLETE PRINTOUT
C       COMPOSITIONS OF RESIN AND SOLUTION LEAVING THE BATCH REACTOR
   18   CALL SECOND(T2)
   17   NSTAGE=NSTAGE+1
        ABCUM=((RATES*TCONCS*(SCOUT-SCINIT))-(RATER*TCONCR*(CINIT-Q2)))*10
       10.0
        ABST=((RATES*TCONCS*(SC-SCINIT))-(RATER*TCONCR*(SQ2-Q2)))*100.0
        ERRORX=ABCUM/RATES*TCONCS
        ERRORY=((CINIT-Q2)-((SCOUT-SCINIT)/WFRONT))*100.0
        ITRT=PTOL/STEPT
        COMTIM=T2-T1
        JREPET=JREPET/ITRT
C       PRINTOUT RESULTS
        WRITE(6,34)NSTAGE,SC,Q2,ITRT,COMTIM,TIME,SCINIT,SCPOS,SCNEG,GUESS,
       1SCTARG,C(1,1),ERRORX,ERRORY,ERRPOS,ERRNEG,JREPET
        JREPET=0
        NINIT=2
C       STORE  COMPOSITION PROFILE AND AMOUNT
        SSC=SC
        SQ2=Q2
        SCTARG=SCINIT
        DO 19 I=1,IEND
   19   S(I,1)=C(I,1)
C       GUESS FOR THE SOLUTION ENTERING THE NEXT STAGE
        SCINIT=SCINIT-STEP
```

```
      GO TO 21
C     '20' ON RETURN FROM 'NPRINT' MAKES A NEW GUESS
   20 SCINIT=SCPOS
C     '21' ON RETURN FROM 'NPRINT' WITH A NEW GUESS
   21 SC=SCINIT
C     CHECK IF CALCULATION TO BE STOPPED
      IF(SCINIT-0.005)31,31,22
   22 JFREE=I
      CFRONT=BOUND(WFRONT,SC,JKL,JFREE)
      C(1,1)=CFRONT
C     SET TIME EQUAL TO ZERO
      TIME=STTIME
      GO TO (25,23),NINIT
   23 DO 24 I=1,IEND
   24 C(I,1)=S(I,1)
      QI=SQ2
   25 GO TO 3
C     TEST FOR TELESCOPING
   26 IF(NT)31,31,27
C     TELESCOPING
   27 O=Q(K)
      NTE=NTEL(O,Q1,Q2,TIME)
      GO TO(28,30,31),NTE
   28 K=K+1
      NBLOCK=NBLOCK/2
      FBLOCK=NBLOCK
      STEPL=2.0*STEPL
      STEPT=4.0*STEPT
      NT=NT-1
      ASSIGN 10 TO NBACK
      DO 29 I=1,NBLOCK
   29 C(I+1,1)=C(2*I+1,1)
C     TRANSFER OF NEWLY CALCULATED TOTAL AMOUNT
   30 Q1=Q2
C     RE-ENTRY FOR CALCATION
      GO TO NBACK,(10,11)
C     '31' PRINTS OUT VALUES OF VARIABLES IN CASE OF ERROR
   31 WRITE(6,32)SCINIT,SCPOS,SCNEG,SC,GUESS,JREPET
   32 FORMAT(2X,50H1ERROR NEGATIVE SOLUTION CONCENTRATION APPROACHING,2X
     1,5(2X,F10.4),I5)
   33 GO TO 1
   34 FORMAT(1X,I5,2F7.3,I5,2H *,12F8.4,I5)
      END



      FUNCTION NPRINT(C,TIME,PTOL,SCTARG,SCPOS,SCNEG,SCINIT,SCOUTT,ERRPO
     1S,ERRNEG,GUESS)
C     TRIGGERS PRINTOUT IF THE GUESSED VALUE MATCHES WITH THE FIXED
      DIMENSION C(641,2)
C     TEST FOR END OF CALCULATIONS
      IF(TIME-PTOL)1,2,2
    1 NPRINT=3
      GO TO 9
    2 IF(ABS(SCOUTT-SCTARG)-0.0050)3,3,4
    3 NPRINT=2
      GO TO 9
C     CHECK FOR DIVERGENCE BETWEEN GUESSED AND THE FIXED VALUE
```

```
    4 IF(SCOUTT-SCTARG)5,3,7
C     PREVIUOS GUESS IS AN UNDERESTIMATE
    5 SCNEG=SCINIT
      ERRNEG=SCOUTT-SCTARG
      IF(ERRPOS)6,6,8
    6 NPRINT=4
      GO TO 9
C     PREVIUOS GUESS IS AN OVERESTIMATE
    7 SCPOS=SCINIT
      ERRPOS=SCOUTT-SCTARG
C     'GUESS' CALCULATES A NEW VALUE BY INTERPOLATION
    8 GUESS=(SCNEG*ERRPOS-SCPOS*ERRNEG)/(ERRPOS-ERRNEG)
      SCINIT=GUESS
      NPRINT=1
    9 RETURN
      END
```

```
C       PROGRAMME THREE CALCULATES DIFFUSION COEFFICIENT WITHIN THE RESIN
C       PHASE FROM EXPERIMENTAL DATA EMPLOYING DIFFUSION EQUATION



        COMMON QOLD,C,STEPL,CINIT,FBLOCK,R,RPLUS,RMIN,STEPT,CFRONT,FLIN,NB
       1OUND,NBLOCK,TIME,IEND,Q2,RATE,FACTOR,NAPPR,A,B,Q1,WFRONT,XFREE,NFR
       2EE,JFREE,NTELE,NINIT,DIFM,TTOL,PTOL,Q,NDCT,STP,JREPET,STEP,STTIME,
       3SCTARG,RATES,RATFR,TCONCS,TCONCR,SCINIT,SCPOS,SCNEG,ERRPOS,ERRNEG,
       4SC,GUESS,RADIUS,JKL
        DIMENSION C(641,2),R(641),RPLUS(639),RMIN(639),Q(5),S(641,2)
       1,RESIN(100),EQLB(100),FRACT(100)
       2,DCA(100),DADB(100),DNAV(100),FX1(16),FX2(16),TY1(16),TY2(16)
       4,AA(101),BB(10),STIME(100),DBDA(100),DCAV(100)
        DATA FX1/0.05,0.10,0.15,0.2,0.25,0.3,0.35,0.4,0.5,0.6,0.7,0.8,0.85
       1,0.9,0.95,1.00/,TY1/4.0,8.5,14.0,20.0,27.0,35.0,45.0,55.0,88.0,130
       2.0,205.5,330.75,427.5,575.2,755.5,1000.0/,FX2/0.05,0.1,0.15,0.2,0.
       325,0.3,0.35,0.4,0.5,0.6,0.7,0.8,0.85,0.9,0.95,1.00/,TY2/3.5,7.0,10
       4.0,17.5,25.0,35.0,47.0,60.0,102.0,160.0,240.0,360.0,465.0,600.0,87
       55.0,1300.0/
        RADIUS=0.0470
C       'READ' READS IN AND PRINTS OUT INPUT DATA
      1 CALL READ
C       INITIALISING VARIABLES
        JKL=0
        XFREE=0.0
        WRITE(6,6)
      6 FORMAT(////96H0                    RATE                    RESIN COMPOSITION
       1      SOLUTION COMPOSITION                TIME    //////)
        LL=1
        ALPHA=A
        BETA=B
        TIME=STTIME
        NT=NTELE
        F=0.38
        FACTOR=F/DIFM
        FLIN=0.0
C       '3' IS RE-ENTRY FOR CALCULATION OF NEXT STAGE
C       UNIFORM OR NON-UNIFORM COMPOSITION OF RESIN PARTICLE
      3 GO TO (4,8),NINIT
      4 CONTINUE
        IF(NAPPR)6,6,5
C       'APP' SMOOTHES OUT INITIAL SINGULARITIES
      5 CALL APP
      6 Q1=CINIT
        DO 7 I=2,NBLOCK
      7 C(I,1)=CINIT
        GO TO 9
C       SET QOLD EQUAL TO INITIAL AMOUNT
      8 Q1=Q2
      9 QOLD=Q1
C       CALCULATE TIME INCREMENT
        STEPT=FACTOR*STEPL*STEPL
C       'K' IS SUBSCRIPT OF TELESCOPING VARIABLE
        K=1
```

```
C       'GEO 1 ' CALCULATES GEOMETRICAL FACTORS FOR SPHERE
   10   CALL GEO1
        FACTOR=STEPT/(STEPL*STEPL)
        ASSIGN 11 TO NBACK
C     . NORMAL RE-ENTRY
C       CALCULATION OF DMIN FOR FIRST GRID INTERVAL
   11   DMIN=DIF(0.5*(C(2,1)+C(1,1)),A,B)
C       ITRATIVE CALCULATION OF CONCENTRATIONS BY FINITE DIFFERENCE EQUATION
        DO 13 I=2,NBLOCK
C       TIME SAVER TRANSFER TO 14 WHEN CALCULATION OF FURTHER VALUES
C       UNNECESSARY
        IF(C(I-1,1)-CINIT)12,14,12
C       CALCULATION OF CONCENTRATION DEPENDENT DIFFUSION COEFFICIENT
   12   DPLUS=DIF(0.5*(C(I+1,1)+C(I,1)),A,B)
        DPL=DPLUS
        DPLUS=DPLUS*RPLUS(I-1)
        DMIN=DMIN*RMIN(I-1)
C       FINITE DIFFERENCE EQUATION FOR CONCENTRATION VALUES
        CALL DIFEQ(I,FACTOR,DPLUS,DMIN,C)
   13   DMIN=DPL
        IEND=NBLOCK+1
C       STEP UP TIME VARIABLE
        TIME=TIME+STEPT
        C(IEND,1)=C(NBLOCK,2)
        GO TO 150
   14   IEND=I
        TIME=TIME+STEPT
C       CALCULATE FRONT BOUNDARY CONCENTRATION
  150   GO TO(16,15),NBOUND
   15   C(1,1)=BOUND(WFRONT,SC,JKL,JFREE)
        DO 16 I=3,IEND
C       TRANSFER ROW OF NEWLY CALCULATED CONCENTRATION VALUES
   16   C(I-1,1)=C(I-1,2)
C       'AMOUNT'  CALCULATES TOTAL AMOUNT IN IN RESIN PARTICLE
        Q2=AMOUNT(NBLOCK)
        RATE=(Q2-Q1)/STEPT
        FLIN=RATE
C       TEST FOR PRINTOUT
        NPRIN=NPRINT(STEPT,TIME,PTOL)
        GO TO (34,17,35,35),NPRIN
   17   WRITE(6,36)RATE,Q2,SC,TIME
        STIME(LL)=TIME
        LL=LL+1
        IF(Q2-0.001C)19,19,18
   18   NEN=NEND(RATE)
        GO TO (19,29,35),NEN
   19   LL=LL-1
        DO 20 MM=1,LL
        FINISH=1.0-Q2
        FRACT(MM)=1.0-RESIN(MM)
C       CALCULATES THE VALUE OF FRACTIONAL APPROACH TO EQUILIBRIUM
   21   EQLB(MM)=FRACT(MM)/FINISH
        IF(JKL.EQ.1) GO TO 24
C       'CROSPLOT' CALCULATES VALUES OF AVERAGE  DIFFUSION COEFFICIENT AS A
C       FUNCTION OF DA/DB
        CALL CRSPLOT(STIME,FX1,TY1,LL,DCAV,DADB,DIFM,NFREE,ND,EQLB,RADIUS,
       1BETA,ALPHA,LAST)
        IF(NFREE)1,1,21
C       TEST FOR THE COMPLETION OF CASES OF FIRST GROUP
```

```
   21 DO 22 I=1,ND
   22 DCAV(I)=DCAV(I)*(10.**7.0)
C     PRINT OUT DA AND DA/DB
      WRITE(6,23)(DCAV(L),DADB(L),L=1,ND)
      JKL=1
      RADIUS=0.050
      GO TO 1
      CALL CRSPLOT(STIME,FX1,TY1,LL,DCAV,DADB,DIFM,NFREE,ND,EQLB,RADIUS,
     1BETA,ALPHA,LAST)
      IF(NFREE)1,1,25
   25 DO 26 L=1,ND
   26 DNAV(L)=DNAV(L)*(10.**7.)
      DO 27 L=1,ND
   27 DBDA(L)=1.0/DBDA(L)
C     PRINT OUT DB AND DA/DB
      WRITE(6,28)(DNAV(L),DBDA(L),L=1,ND)
   28 FORMAT(51H       AV.DIFF.COEFFICIENT                          ALPHA    /15X,
     1F10.5,15X,F10.5)
      GO TO 1
   29 IF(NT)34,34,30
   30 O=Q(K)
      NTE=NTEL(O,Q1,Q2,TIME)
      GO TO (32,34,35),NTE
   32 K=K+1
      NBLOCK=NBLOCK/2
      FBLOCK=NBLOCK
      STEPL=2.0*STEPL
      STEPT=4.0*STEPT
      NT=NT-1
      ASSIGN 10 TO NBACK
      DO 33 I=1,NBLOCK
   33 C(I+1,1)=C(2*I+1,1)
   34 Q1=Q2
      GO TO NBACK,(10,11)
   3N WRITE(6,36)DPLUS,DMIN
   36 FORMAT(4(10X,F15.8))
      GO TO 1
      END



      FUNCTION NPRINT(STEPT,TIME,PTOL)
C     TRIGGER OUT PRINT AT PREFIXED TIME INTERVALS
      FREQUENCY 1(1,0,0),31(1,0,1)
      IF(TIME-PTOL)2,2,3
    2 NPRINT = 1
C     NO PRINT
      GO TO 6
    3 NPRINT = 2
C     PRINT
    6 RETURN
      END



      FUNCTION NEND (RATE)
      IF(RATE+0.00010)3,2,2
```

```
    2 NEND = 1
C     END
      GO TO 4
    3 NEND = 2
C     NO END
    4 RETURN
      END



      SUBROUTINE CRSPLOT(T,FX1,TY1,LL,DCAV,DADB,DIFM,NFREE,ND,F,RADIUS,B
     1ETA,ALPHA,LAST)
C     SUBROUTINE CROSPLOT CALCULATES DIFFUSION COEFFICIENT FROM EXPERIMENTAL
C     DATA AND THEORETICAL 'F' VS 'TAW' CURVE  AS A FUNCTION OF DA/DB
      DIMENSION FX1(14),TY1(14),PLYV(100),T(LL),DCA(100),DCAV(11),DADB(1
     11),A(10),F(LL)
      DIMENSION TPDICT(100),DELTA(100)
      DATA A/10*0.0/,INDEX/0/
    1 SUM=0.0
      INDEX=INDEX+1
      IF(INDEX.EQ.1)
C     POLYFIT CALCULATES POLYNOMIAL FOR EQUILIBRIUM ISOTHERM
     1CALL POLYFIT(FX1,TY1,A,M)
      M=M+1
      DO 2 L=1,M
    2 C(L)=A(L)
      N=M-1
      DO 3 L=1,LL
      XXR(L)=F(L)
      XXI=0.0
      VI=0.0
C     POLYEV CALCULATES TIME FOR GIVEN VALUES OF 'F'
      CALL POLYEV(N,XXR(L),XXI,C,PLYV(L),VI)
      IF(F(L+1)-0.950)3,3,4
    3 CONTINUE
    4 LL=L
      DO 5 LE=1,LL
C     CALCULATE DIFFUSION COEFFICIENT
      DCA(LE)=(T(LE)*RADIUS*RADIUS)/PLYV(LE)
    5 SUM=SUM+DCA(LE)
      DCAV(INDEX)=SUM/FLOAT(LL)
      TPDICT(LE)=(T(LE)*RADIUS*RADIUS)/DCAV(INDEX)
C     CALCULATE ERROR IN PREDICTED TIME FOR GIVEN VALUE OF 'F' BASED ON
C     COMPUTED VALUE OF DIFFUSION COEFFICIENT
    6 DELTA(LE)=((PLYV(LE)-TPDICT(LE))/PLYV(LE))*100.0
      WRITE(6,7)
    7 FORMAT(1X//35X,5H *F* ,15X,4HTAW ,15X,5H TIME,15X,12H DIFF.COEFF/)
C     PRINTOUT 'F',TAW,TIME,DIFFUSION COEFFICIENT,PREDICTED TIME,ERROR
      WRITE(6,8)(F(L),T(L),PLYV(L),DCA(L),TPDICT(L),DELTA(L),L=1,LL)
    8 FORMAT(10X,F10.5,10X,F10.5,10X,F10.5,10X,F15.10,10X,F10.5,10X,F10.
     15)
      WRITE(6,9)DCAV(INDEX)
    9 FORMAT(1X//10H DAVERAGE=//F20.10)
      IF(BETA)10,10,11
   10 DADB(INDEX)=(ALPHA+1.0)*2.0
      GO TO 12
   11 DADB(INDEX)=(ALPHA+1.0)/2.0
C     CALCULATE AVERAGE VALUE OF DIFFUSION COEFFICIENT
```

```
      DCAV(INDEX)=DCAV(INDEX)/DADB(INDEX)
   12 ND=INDEX
      IF(NTEST.EQ.1)INDFX=0
      RETURN
      END



      SUBROUTINE POLYEV(N,XXR,XXI,C,VR,VI)                              00000
C     SUBROUTINE TO FIND THE VALUE, V, OF AN N DEGREE POLYNOMIAL        00000
      DIMENSION C(100)
      ZERO = 0.0                                                        00000
      TP13 = ZERO                                                       POLYO
      TP14 = ZERO                                                       POLYO
      M = N + 2                                                         POLYO
C     COMMENCE ITERATION                                                00000
   10 M = M - 1                                                         POLYO
      TP13 = C(M) + TP13                                                POLYO
      TP15 = XXR * TP13 - XXI * TP14                                    POLYO
      TP14 = XXR * TP14 + XXI * TP13                                    POLYO
      TP13 = TP15                                                       POLYO
      IF(M-2) 20,20,10                                                  POLYO
C     COMPLETE CALCULATION                                              00000
   20 TP13 = C(1) + TP13                                                POLYO
      VR = TP13                                                         POLYO
      VI = TP14                                                         POLYO
      RETURN                                                            POLYO
      END                                                               POLYO
```

```
C      THE FOLLOWING SUBROUTINES ARE COMMON TO PROGRAMME TWO AND THREE


       SUBROUTINE READ
       COMMON QOLD,C,STEPL,CINIT,FBLOCK,R,RPLUS,RMIN,STEPT,CFRONT,FLIN,NB
      1OUND,NBLOCK,TIME,IEND,Q2,RATE,FACTOR,NAPPR,A,B,Q1,WFRONT,XFREE,YFR
      2EE,JFREE,NTELE,NINIT,DIFM,TTOL,PTOL,Q,NDCT,STP,JREPET,STEP,STTIME,
      3SCTARG,RATES,RATER,TCONCS,TCONCR,SCINIT,SCPOS,SCNEG,ERRPOS,ERRNEG,
      4SC,GUESS,JKL
       DIMENSION C(641,2),R(641),RPLUS(639),RMIN(639),Q(5),S(641,2),IDENT
      11(3),IDENT2(2)
C      WRITE TITLE
       WRITE(6,7)
C      READ IN DATA
     1 READ(5,8)(IDENT1(I),I=1,3),(IDENT2(I),I=1,2),A,B,DIFM
       WRITE(6,9)(IDENT1(I),I=1,3),(IDENT2(I),I=1,2)
     3 READ(5,10)SCOUTT,CINIT,WFRONT
     4 READ(5,11)NBOUND,NAPPR,NTELE,NINIT,NDCT,IBLOCK,STTIME,JFREE,XFREE,
      1YFREE,(Q(K),K=1,5),PTOL,TTOL
       READ(5,12)COEFF,RADIUS,RATER,TCONCS,TCONCR,STEP
C      SETTING UP OF FLAGS AND VARIABLES
       JKL=0
       NTE=0
       NBLOCK=IBLOCK
       FBLOCK=IBLOCK
       TIME=STTIME
       STEPL=1.0/FBLOCK
       FDENOM=NBLOCK*2**NAPPR
       STP=1.0/FDENOM
       SC=SCOUTT
       SCTARG=SC
       JFREE=1
       CFRONT=BOUND(WFRONT,SC,JKL,JFREE)
       CTARG=CFRONT
       C(1,1)=CFRONT
       C(NBLOCK+1,1)=CREAR
       CALL LIST
       RATES=(TCONCR*RATER)/(TCONCS*WFRONT)
C      PRINTOUT OF DATA AND FLAGS
       WRITE(6,13)IBLOCK,WFRONT,Q(2),NTELE,SCOUTT,Q(2),NBOUND,CINIT,Q(3),
      1NAPPR,PTOL,Q(4),JFREE,TTOL,Q(5),A,B,DIFM,XFREE,NFREE
     6 RETURN
     7 FORMAT(56H1          CALCULATION  OF THE NUMBER OF STAGES REQUIRED
      1/10X,42HFOR A GIVEN ION EXCHANGE PROCESS IN A      /10X,42HCYCLIC
      2 COUNTERCURRENT CONTACTOR(WITH VAR/10X,42HIABLE RESIN PHASE DIFFUS
      3ION CONTROLLED     /10X,14HREACTION       ////)
     8 FORMAT(3A6,2A6,3F12.7)
     9 FORMAT (10X,3A6/10X,2A6)
    10 FORMAT(3F12.9)
    11 FORMAT(5I1,I6,F12.7,2I1,2F12.7/5F11.9,2F12.7)
    12 FORMAT(F12.9,5F7.5)
    13 FORMAT(1H0//9X,15H FLAGS AND DATA //10X,7HIBLOCK I4,4X,6HCFRONTF12
      1.4,4X,8HQ(1)     F12.4//10X,7HNTELE  I4,4X,6HSCOUTTF12.4,4X,8HQ(2)
      2   F12.4//10X,7HNBOUND I4,4X,6HCINIT F12.4,4X,8HQ(3)     F12.4//10X
      3,7HNAPPR  I4,4X,6HPTOL  F12.4,4X,8HQ(4)     F12.4//10X,7HJFREE  I4,
      44X,7HTTOL   F12.4,4X,8HQ(5)     F12.4//10X,4HA   F7.4,4X,6HB      F1
```

```
     52.4.4X.8HDIFM     F4.1///10X.7HXFREE  F12.4.4X.6HNFREE I12)
 6666 CALL EXIT
 7777 CALL DUMP
      END



      SUBROUTINE LIST
C     FOR DETAILED TEXT DESCRIBING SYSTEM
      COMMON QOLD.C.STEPL.CINIT.FBLOCK.R.RPLUS.RMIN.STEPT.CFRONT.FLIN.NB
     1OUND.NBLOCK.TIME.IEND.Q2.RATE.FACTOR.NAPPR.A.B.Q1.WFRONT.XFREE.NFR
     2EE.JFREE.NTELE.NINIT.DIFM.TTOL.PTOL.Q.NDCT.STP
      DIMENSION C(641.2).R(641).RPLUS(639).RMIN(639).Q(5)
      WRITE(6.11)
      WRITE(6.12)
      GO TO (1.2).NBOUND
    1 WRITE(6.13)CFRONT
    2 WRITE(6.14)WFRONT
      WRITE(6.16)DIFM.A.B
      WRITE(6.17)
      WRITE(6.18)STEPL
      IF (NAPPR)7777.4.3
    3 WRITE(6.19)STP
    4 IF (NTELE)7777.5.6
    5 WRITE(6.20)
      GO TO 9
    6 WRITE(6.21)Q(1)
      IF(NTELE-1)7777.9.7
    7 DO 8 I=2.NTELE
    8 WRITE(6.22)Q(I)
    9 WRITE(6.23)PTOL.TIME
      WRITE(6.24)CINIT.CFRONT
      RETURN
   11 FORMAT (1H0//9X.13H SOLID SPHERE)
   12 FORMAT (29H0          BOUNDARY CONDITIONS)
   13 FORMAT (14X.28H FRONT BOUNDARY     CONSTANT/33X.16H CONCENTRATION
     1 F14.8)
   14 FORMAT (14X.43H FRONT BOUNDARY     VARIABLE. CLOSED SYSTEM/33X.14H
     1 VOLUME RATIO F15.7)
   16 FORMAT (31H0          DIFFUSION COEFFICIENT/14X.24H MAXIMUM VALUE
     1         F12.7/14X.24H PARAMETER VALUES      A F12.7/35X.3H B F12.7)
   17 FORMAT (14X.42H MONOTONICAL FUNCTION OF CONCENTRATION AND/27X.29H
     1DOES NOT INCREASE WITH TIME.)
   18 FORMAT (23H0          GRID SPACING .18X. F10.8)
   19 FORMAT (14X.27H INITIAL GRID SPACING      F10.8)
   20 FORMAT (14X.16H NO TELESCOPING.)
   21 FORMAT (14X.16H TELESCOPING AT .7X. F13.7)
   22 FORMAT (38X.F12.7)
   23 FORMAT (35H0          AVERAGE RESIDENCE TIME OF/10X.15HRESIN PER ST
     6AGE.14X. F12.7//9X.19H TIME SET AT START .10X. F12.7//9X.18H INITI
     2AL CONDITION)
   24 FORMAT (14X.35H UNIFORM DISTRIBUTION                F12.7/14X.35H FR
     1ONT-BOUNDARY CONCENTRATION      F12.7//)
 7777 CALL DUMP
      END
```

```
      FUNCTION BOUND (WFRONT,SC,JKL,JFREE)
C     CALCULATES FRONT BOUNDARY CONCENTRATION IN EQUILIBRIUM WITH SOLUTION
      COMMON QOLD,C,STEPL,CINIT,FBLOCK,R,RPLUS,RMIN,STEPT,CFRONT,FLIN
      DIMENSION C(641,2),R(641),RPLUS(639),RMIN(639)
      IF(JFREE)1,1,3
    1 XF=0.0
      XF=STEPT*FLIN*WFRONT
      SC=SC-XF
      IF(JKL-1)2,3,3
    2 SC=1.0-SC
C     POLYNOMIAL FOR EQUILIBRIUM ISOTHERM
    3 BOUND=(((((-8.3897*SC+30.721)*SC-45.541)*SC+35.245)*SC-15.516)*SC+
     14.4733)*SC+0.0061711
      JFREE=0
      IF(JKL-1)4,5,5
    4 BOUND=1.0-BOUND
    5 RETURN
      END


      SUBROUTINE DIFEQ(I,FACTOR,DPLUS,DMIN,C)
C     FINITE DIFFERENCE EQUTION FOR CONCENTRATION IN RESIN PARTICLE
      COMMON NERR
      DIMENSION C(641,2)
      C(I,2)=C(I,1)+FACTOR*(DPLUS*(C(I+1,1)-C(I,1))-DMIN*(C(I,1)-C(I-1,1
     1)))
      RETURN
      END


      FUNCTION DIF(C,A,B)
C     CALCULATES VARIABLE DIFFUSION COEFFICIENT
      DIMENSION C(641,2),R(641),RPLUS(639),RMIN(639),Q(5)
      DIF=(1.0+B*C)/(1.0+A*C)
      RETURN
      END


      FUNCTION AMOUNT(NBLOCK)
C     CALCULATES TOTAL AMOUNT IN RESIN BY SIMPSON'S RULE
      COMMON QOLD,C,STEPL,CINIT,FBLOCK,R
      DIMENSION C(641,2),R(641)
      AMOUNT=C(1,1)*R(1)+C(NBLOCK+1,1)*R(NBLOCK+1)
      DO 1 I=2,NBLOCK,2
    1 AMOUNT=AMOUNT+4.0*C(I,1)*R(I)
      DO 2 I=3,NBLOCK,2
    2 AMOUNT=AMOUNT+2.0*C(I,1)*R(I)
      AMOUNT=AMOUNT*STEPL
C     SENSE LIGHT'1' INDICATES CALL FROM APP
      IF(SENSE LIGHT 1) 3,4
      A1=(1.0-STEPL*FBLOCK)**2.0
      AMOUNT=AMOUNT+CINIT*A1
```

```
    4 RETURN
      END



      FUNCTION NTEL(O,Q1,Q2,TIME)
C     TRIGGERS TELESCOPING WHEN AMOUNT HAS DECREASED FROM A PREFIXED VALU
      IF(O-Q2)1,2,2
    1 NTEL=2
      GO TO 3
    2 NTEL=1
    3 RETURN
      END



      SUBROUTINE GEO 1
C     CALCULATES GEOMETRICAL FACTORS FOR SPHERE
      COMMON QOLD,C,STEPL,CINIT,FBLOCK,R,RPLUS,RMIN,STEPT,CFRONT,FLIN,NB
     1OUND,NBLOCK,TIME,IEND
      DIMENSION C(641,2),R(641),RPLUS(639),RMIN(639)
      A2=2.0-STEPL
      A1=1.0
      DENOM = A2 - STEPL
C     'RPLUS' AND 'RMIN' ARE MODIFICATION FACTORS IN FINITE-DIFFERENCE
C     EQUATION
    2 DO 3 I=2,NBLOCK
      RMIN(I-1)=(A2/DENOM)**2.0
      A2 = A2 - 2.0*STEPL
      RPLUS(I-1)=(A2/DENOM)**2.0
    3 DENOM = DENOM - 2.0*STEPL
      IEND = NBLOCK + 1
C     R-FACTORS ARE WEIGHT FACTORS FOR CONCENTRATIONS IN CALCULATION
C     OF TOTAL AMOUNT IN MEDIUM BY 'AMOUNT'
    4 DO 5 I=1,IEND
      R(I)=A1**2.0
    5 A1 = A1 - STEPL
    8 RETURN
      END



      SUBROUTINE APP
C     SMOOTHES OUT INITIAL SINGULARITIES AT FRONT BOUNDARY
      COMMON QOLD,C,STEPL,CINIT,FBLOCK,R,RPLUS,RMIN,STEPT,CFRONT,FLIN,NB
     1OUND,NBLOCK,TIME,IEND,Q2,RATE,FACTOR,NAPPR,A,B,Q1,WFRONT,XFREE,NFR
     2EE,JFREE,NTELE,NINIT,DIFM,TTOL,PTOL,Q,NDCT,STP,JREPET,STEP,STTIME,
     3SCTARG,RATES,RATER,TCONCS,TCONCR,SCINIT,SCPOS,SCNEG,ERRPOS,ERRNEG,
     4SC,GUESS
      DIMENSION C(641,2),R(641),RPLUS(639),RMIN(639),Q(5),S(641,2)
C     CALCULATES INITIAL GRID SPACING AND TIME INCREMENT AND SETS UP
C     INITIAN CONDITIONS
      DO 1 I=1,NAPPR
    1 STEPL=0.5*STEPL
      DO 2 I=1,NBLOCK
    2 C(I+1,1)=CINIT
```

```
      Q1=CINIT
      MBLOCK=NBLOCK
      QOLD=CINIT
      STEPT=FACTOR*STEPL*STEPL
      GO TO (3,4,4),NBOUND
    3 ASSIGN 11 TO NBOUN1
      GO TO 5
    4 ASSIGN 10 TO NBOUN1
C     N-LOOP FOR NUMBER OF TELESCOPINGS IN APP
    5 DO 16 N=1,NAPPR
      CALL GEO1
C     M-LOOP FOR NUMBER OF CONCENTRATION ROWS BETWEEN TELESCOPING
      DO 13 M=2,MBLOCK
      DMIN=DIF(0.5*(C(2,1)+C(1,1)),A,B)
C     I- LOOP FOR NUMBER OF CONCENTRATION VALUES IN ROW
      DO 7 I=2,NBLOCK
      IF(C(I-1,1)-CINIT)6,18,6
    6 DPLUS=DIF(0.5*(C(I+1,1)+C(I,1)),A,B)
      DPL=DPLUS
      DPLUS=DPLUS*RPLUS(I-1)
      DMIN=DMIN*RMIN(I-1)
      CALL DIFEQ(I,FACTOR,DPLUS,DMIN,C)
    7 DMIN=DPL
      IEND=NBLOCK+1
      GO TO 8
   18 IEND=I
    8 DO 9 I=3,IEND
      C(I-1,1)=C(I-1,2)
    9 CONTINUE
      TIME=TIME+STEPT
      GO TO NBOUN1,(10,11)
   10 C(1,1)=BOUND(WFRONT,SC,JKL,JFREE)
C     SENSE LIGHT 1 IS PICKED UP BY FUNCTION AMOUNT SIGNIFIES CALL FROM
C     APP
   11 SENSE LIGHT 1
      Q2=AMOUNT(NBLOCK)
      RATE=(Q2-Q1)/STEPT
      FLIN=RATE
      NPRIN=NPRINT(C,TIME,PTOL,SCTARG,SCPOS,SCNEG,SCINIT,SCOUTT,ERRPOS,E
     1RRNEG,GUESS)
      GO TO (12,13,13),NPRIN
   12 JREPET=JREPET+1
   13 Q1=Q2
      IHALF=(IEND-2)/2
      DO 14 I=1,IHALF
   14 C(I+1,1)=C(2*I+1,1)
      IHALF=IHALF+3
      DO 15 I=IHALF,IEND
   15 C(I-1,1)=CINIT
      STEPL=2.0*STEPL
      STEPT=4.0*STEPT
   16 MBLOCK=NBLOCK-IHALF+3
      RETURN
      END
```

Figure 60
Programme 2.
Flow diagram

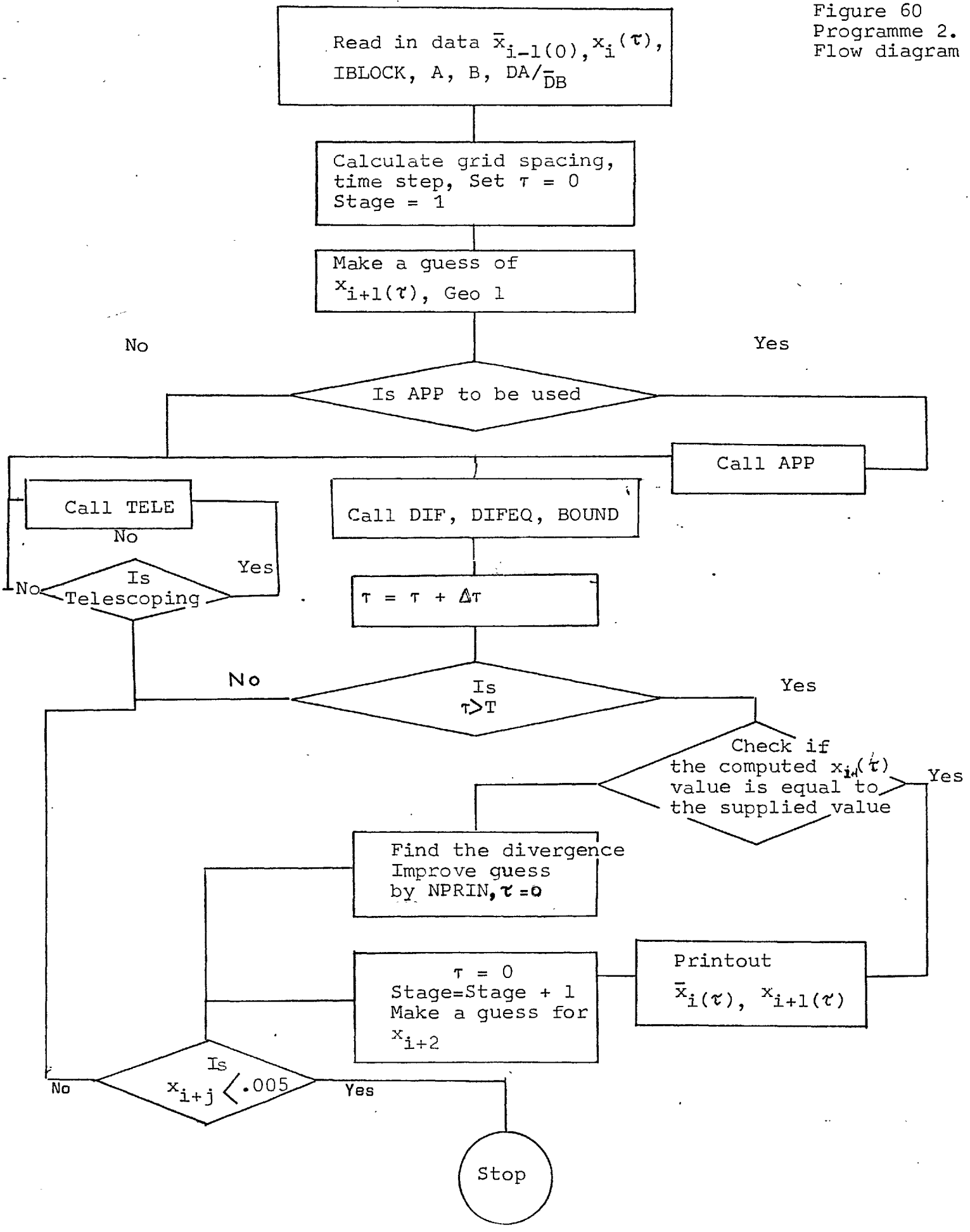

Figure 61
Flow diagram of Programme 3.

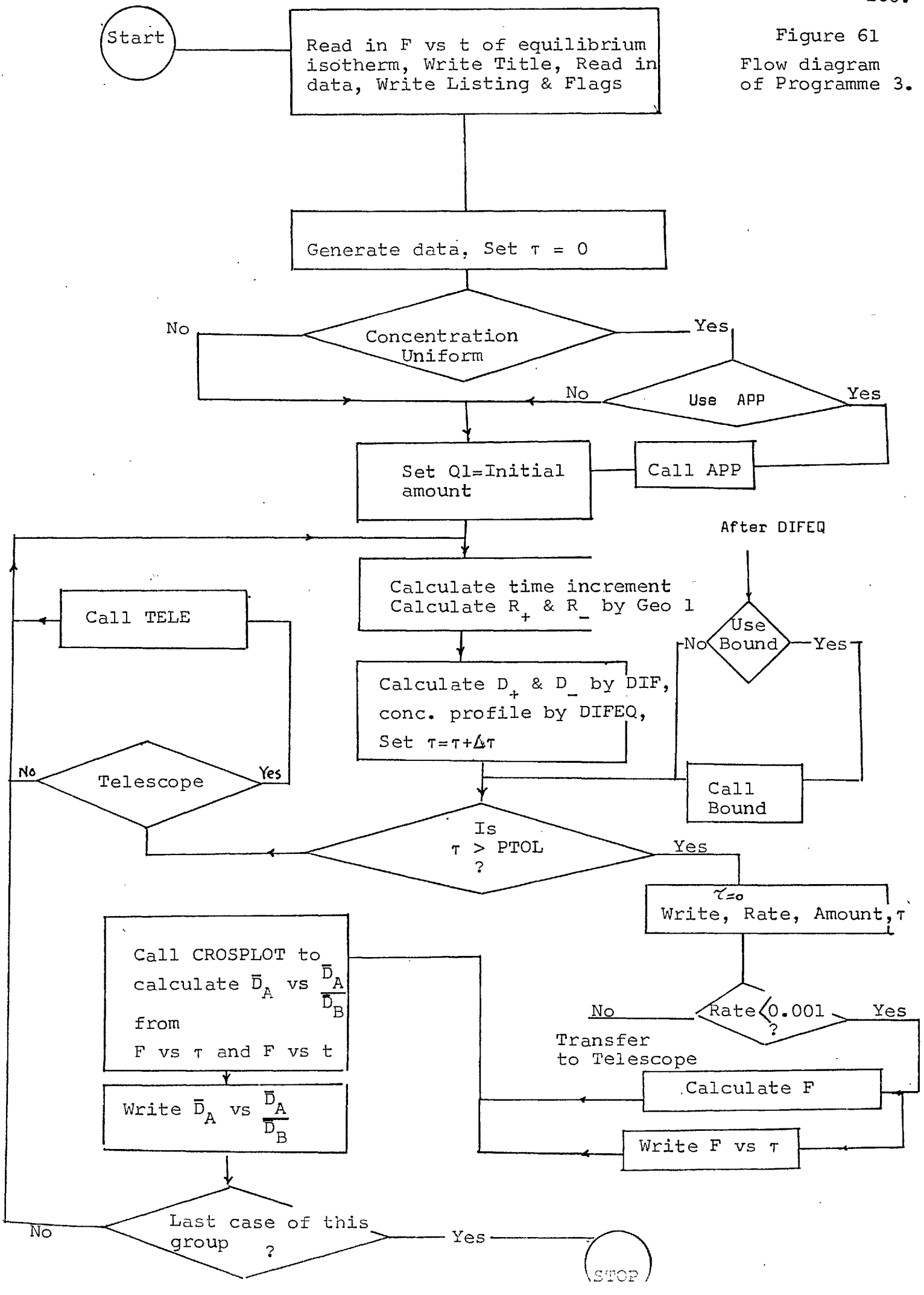

APPENDIX - 6

Sample Calculation for salt requirements for a continuous softening process.

Let us assume a throughput of 1 gallon of water/day. Other information available is:

Raw water composition $x_{Ca} = x_F$

Concentration $= C_F$

Flow rate $= L_F$

Treated water composition $= x_P$

The regenerant composition $x_R = 1.00$

Concentration $= C_R$

Flow rate $= L_R$

Let the two processes, i.e. adsorption and regeneration, be represented by Figures 54 A and B.

The material balance in the adsorption contactor gives:

$$C_F L_F (x_P - x_F) = R\bar{C} (\bar{x}_F - \bar{x}_P)$$

$$R = \frac{L_F C_F}{\bar{C}} \times \frac{x_P - x_F}{\bar{x}_F - \bar{x}_P}$$

$$= \frac{L_F C_F}{\bar{C}} \times \frac{1}{\text{Slope of Adsorption of line}}$$

$$\text{Resin/day} = \frac{L_F C_F \times 4.55}{\bar{C} \frac{(L_F C_F)}{R\bar{C}}} \quad \text{Litres/day}$$

Salt requirement/day:

Slope of the regeneration Op. line $= \frac{L_R C_R}{R\bar{C}}$

Equivalent of salt/Equiv. of resin per day $= \frac{L_R C_R}{R\bar{C}}$

/...

$$\text{Grams of salt/Equiv. of resin per day} = \frac{L_R C_R \times 58.55}{R\bar{C}}$$

$$\text{Gm. of salt/Litre per day} = \frac{L_R C_R \bar{C} \times 58.55}{R\bar{C}}$$

$$\text{Total salt required} = 4.55 \frac{L_R C_R}{R\bar{C}} \bar{C} \frac{L_F C_F}{\bar{C}} \frac{58.55}{\frac{L_F C_F}{R\bar{C}}}$$

$$= 267.41 \frac{L_F C_F}{} \frac{(\text{Slope of reg. op. line})}{\text{Slope of adsorp. op. line})}$$

The salt requirements tabulated in Table 28 are for one gallon of water/day. For L gallons/day multiply the values by L.